

COMPRESSION FIELD THEORY FOR
STRUCTURAL CONCRETE SUBJECTED TO
FLEXURE AND SHEAR //

BY

STANLEY MUSE SHITOTE

THIS THESIS HAS BEEN ACCEPTED FOR
THE DEGREE OF M.Sc.
AND A COPY MAY BE PLACED IN THE
UNIVERSITY LIBRARY.

A thesis submitted in fulfilment for the degree
of Master of Science in the University of Nairobi.

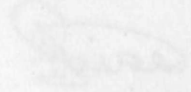
1984



UNIVERSITY OF NAIROBI
LIBRARY

DECLARATION

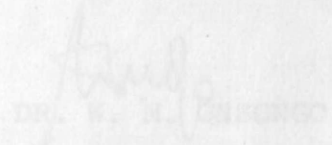
This is my original work and has not been presented for a degree in any other university.



S. N. MISRA

TO MY PARENTS

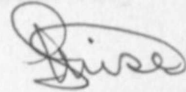
This thesis has been submitted for examination with my approval as University Supervisor.



DR. N. N. MISRA

DECLARATION

I wish to thank my supervisor, Dr. W. M. Onsongo for his guidance and assistance throughout the preparation of this thesis. This is my original work and has not been presented for a degree in any other university.



S. M. SHITOTE

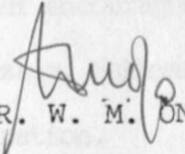
I am also indebted to the technicians in the Engineering Department, in particular Phillip Mwaia and James Thairu for their assistance in the laboratory work. My special thanks also go to my friends whose encouragement and direct involvement ensured the successful completion of the experimental program. I feel obliged to at least mention Messrs Mwangi, Mutitu, Mutitu, Mwangi, Mwangi and Mwangi for their help in the preparation of the test specimens and collection of data.

The work done by the Print Bureau, under the leadership of Mrs. Mwaia, in typing the manuscript is also

This thesis has been submitted for examination with my approval as University Supervisor.

for his assistance in stenciling the figures.

I also thank my wife, Gladys, for her encouragement throughout the project. My children, Mwangi and Mwangi were also a great source of inspiration.



DR. W. M. ONSONGO

Finally, I wish to thank the German Academic Exchange Service (D.A.A.D.) for the direct sponsorship of the project and also acknowledge the financial assistance received from the National Council of Science and Technology of the Republic of Kenya.

ACKNOWLEDGEMENTS

I wish to thank my supervisor, Dr. W. M. Onsongo for his guidance and suggestions throughout the preparation of this work. Indeed, without his keen supervision and interest, the successful completion of this work would have been very difficult.

I am also indebted to the technicians of the Civil Engineering Department, in particular Philip Maina and James Thairu for their assistance in the laboratory work. My special thanks also go to my friends whose encouragement and direct involvement ensured the successful completion of the experimental program. I feel obliged to at least mention Messrs Ndinika, Mulli, Atibu, Mwandau, Nyangaga and Amulyoto for their help in the preparation of the test specimens and collection of data.

The work done by the Print Bureau, under the leadership of Mrs. Mutiso, in typing the manuscript is also gratefully acknowledged. I also wish to acknowledge Mr. Okoth for his assistance in stencilling the figures.

I also thank my wife, Clasina, for her encouragement throughout the project. My children, Nanzala, Mukhwana and Mulongo were also a great source of inspiration.

Finally, I wish to thank the German Academic Exchange Service (D.A.A.D.) for the direct sponsorship of the project and also acknowledge the financial assistance received from the National Council of Science and Technology of the Republic of Kenya.

TABLE OF CONTENTS

TITLE.....	i
DECLARATION.....	iii
ACKNOWLEDGEMENTS	iv
TABLE OF CONTENTS.....	v
LIST OF FIGURES.....	viii
LIST OF TABLES.....	x
LIST OF PLATES.....	xi
SUMMARY.....	xii
NOTATION.....	xiv
CHAPTER 1 INTRODUCTION	1
CHAPTER 2 LITERATURE REVIEW.....	4
2.1 Early Design	
Procedures	5
2.2 Performance	
of the Truss.....	
Analogy.....	6
2.3 Modifications of	
of the Truss	
Analogy and	
Development of the	
Compression Field	
Theory	9
CHAPTER 3 COMPRESSION FIELD THEORY FOR	
COMBINED FLEXURE AND SHEAR	
LOADING.....	13
3.1 Assumptions.....	14
3.2 Equilibrium	
Considerations.....	16
3.2.1 Concrete Stress.	16
3.2.2 Transverse	
Equilibrium....	19
3.2.3 Longitudinal	
Equilibrium....	19

CHAPTER 3	COMPRESSION FIELD THEORY FOR COMBINED FLEXURE AND SHEAR LOADING (Cont.)	
3.3	Geometrical Considerations.....	21
3.4	Stress-Strain Relationships for Materials.....	22
3.4.1	Concrete.....	22
3.4.2	Steel	24
3.5	Direction of Principal Strains.....	25
3.6	Solution Technique	25
3.7	Theoretical Study Using Computer.....	28
3.8	Application of Theory to Prestressed Concrete Sections.....	29
CHAPTER 4	DATA COLLECTION.....	38
4.1	Objectives and choice of Test Specimens.....	38
4.2	Test Specimens.....	39
4.2.1	Materials.....	39
4.2.1.1	Concrete.....	39
4.2.1.2	Steel	40
4.2.2	Preparation of Test Specimens.....	40
4.3	Parameters of Test Program.....	41
4.4	Test Rig.....	41
4.5	Calibration of Testing Machines.....	42
4.6	Instrumentation.....	43
4.7	Testing Procedure.....	43

CHAPTER 5	ANALYSIS AND DISCUSSION.....	64
	5.1 Behaviour of Test Specimens.....	64
	5.2 Limitations of Test Specimens and Testing Equipment.....	66
	5.3 Transverse Strains Profiles and Principal Compression Strains Profiles.....	68
	5.4 Longitudinal Strains Profiles.....	70
	5.5 Shear Force-Shear Strain Relationships.....	71
	5.6 Shear Force-Angles of Principal Compression Relationships.....	72
	5.7 Moment-Curvature Relationships.....	73
	5.8 Response with Varying Material Properties and Loading Condition	73
CHAPTER 6	CONCLUSIONS AND RECOMMENDATIONS....	94
	6.1 Conclusions.....	94
	6.2 Recommendations.....	95
REFERENCES	97
APPENDIX A	EQUATIONS FOR USE IN SOLUTION TECHNIQUE AND EXAMPLE CALCULATIONS.....	99
APPENDIX B	COMPUTER PROGRAM.....	113
APPENDIX C	EXPERIMENTAL DATA AND PLOTS.....	137
APPENDIX D	EVALUATION OF SHEAR FLOW AT COMPRESSION STEEL LEVEL.....	191

LIST OF FIGURES

Figure 2.1	Distribution of Forces in Classical Truss Analogy.....	12
Figure 2.2	Forces Acting at an Inclined Crack.....	12
Figure 3.1	Concrete Beam Model.....	31
Figure 3.2	Distribution of Stresses on Section	32
Figure 3.3	Material Stress-strain characteristics	33
Figure 3.4	Equilibrium Considerations.....	34
Figure 3.5	Mohr's Circle of Strains	35
Figure 3.6	Comparison of Responses	35
Figure 3.7	Variation of Longitudinal Steel Content.....	36
Figure 3.8	Variation of Transverse Steel Content.....	36
Figure 3.9	Variation of Concrete Strength	36
Figure 3.10	Prediction Model for Prestressed Concrete	37
Figure 4.1	Loading Arrangement	46
Figure 4.2	Concrete stress-strain curves	47
Figure 4.3	Steel stress-strain curves	52
Figure 4.4	Typical Reinforcing Details.....	56
Figure 4.5	Calibration Curve for Beam Loading Machine	57
Figure 4.6	Calibration Curve for Cylinder Loading Machine.....	57
Figure 4.7	Target Patterns.....	58
Figure 5.1	Stress Concentrations	76
Figure 5.2	Transverse Strains Profiles.....	77
Figure 5.3	Principal Compression Strains Profiles	78

Figure 5.4	Longitudinal Strains Profiles (8" gauge length)	79
Figure 5.5	Longitudinal Strains Profiles (4" gauge length)	80
Figure 5.6	Shear Force-Shear Strain Relationship	81
Figure 5.7	Variation of shear strains	82
Figure 5.8	Shear Force-Principal Angles of compression relationships	83
Figure 5.9	Moment-Curvature Relationships	84
Figure 5.10	Comparison of Moment-Curvature Relationships	87
Figure B.1	Flow charts for computer program	131
Figure C.1	Target Arrangements	137
Figure C.2	Mohr's Circle for Measured Strains	141
Figure C.3	Transverse Strains Profiles	175
Figure C.4	Principal Compression Strains Profiles ...	177
Figure C.5	Longitudinal Strains Profiles	179
Figure C.6	Variation of Shear Strain	181
Figure C.7	Shear Force-Principal Angles of Compression Relationships	182
Figure C.8	Moment-Curvature Relationships	184
Figure D.1	Determination of Shear Flow	194
Figure D.2	Shear Flow Distribution	194

LIST OF TABLES

Table 4.1	Summary of Test Program	61
Table A.1	Iteration Process	112
Plate 4.1	Anchorage of Support	51
Plate 5.1	Beam CFT-TB4 at Flexural Cracking Capacity	84
Plate 5.2	Beam CFT-TB4 at start of Inclined Cracks	85
Plate 5.3	Beam CFT-TB4 at about $\frac{1}{2}$ capacity	89
Plate 5.4	Beam CFT-TB4 at near capacity Loading	90
Plate 5.5	Beam CFT-TB4 at Capacity Loading	90
Plate 5.6	Beam CFT-TB4 After Failure	90
Plate 5.7	Beam CFT-TB1 at start of test	91
Plate 5.8	Beam CFT-TB1 at about $\frac{1}{2}$ capacity	91
Plate 5.9	Beam CFT-TB1 at near capacity load	92
Plate 5.10	Beam CFT-TB1 at failure	92
Plate 5.11	Beam CFT-TB1 at failure	92
Plate 5.12	Beam CFT-TB6 at failure	92
Plate C.1	Failure, Beam CFT-TB2	188
Plate C.2	Failure Beam CFT-TB3	188
Plate C.3	Failure, beam CFT-TB7	189
Plate C.4	Failure, beam CFT-TB8	189
Plate C.5	Failure, Beam CFT-TB5	190

LIST OF PLATES

Plate 4.1	Initial set up of Test Rig	62
Plate 4.2	Revised set up of Test Rig	62
Plate 4.3	Anchorage of Support	63
Plate 5.1	Beam CFT-TB4 at Flexural Cracking Capacity	88
Plate 5.2	Beam CFT-TB4 at start of Inclined Cracks	88
Plate 5.3	Beam CFT-TB4 at about $\frac{1}{4}$ capacity	89
Plate 5.4	Beam CFT-TB4 at near capacity Loading	89
Plate 5.5	Beam CFT-TB4 at Capacity Loading	90
Plate 5.6	Beam CFT-TB4 After Failure	90
Plate 5.7	Beam CFT-TB1 at start of test.....	91
Plate 5.8	Beam CFT-TB1 at about $\frac{1}{2}$ capacity	91
Plate 5.9	Beam CFT-TB1 at near capacity load ...	92
Plate 5.10	Beam CFT-TB1 at failure.....	92
Plate 5.11	Beam CFT-TB1 at failure.....	93
Plate 5.12	Beam CFT-TB6 at failure.....	93
Plate C.1	Failure, Beam CFT-TB2	188
Plate C.2	Failure Beam CFT-TB3	188
Plate C.3	Failure, Beam CFT-TB7	189
Plate C.4	Failure, Beam CFT-TB8	189
Plate C.5	Failure, Beam CFT-TB5	190

SUMMARY

In structural design, a rational model enables the engineer to develop a better understanding of actual structural behaviour and leads to simple general methods of design. For structural members subjected to structural actions involving shear, such a model is absent.

In this thesis, a rational model called the compression field theory is applied to the case of structural concrete subjected to combined flexure and shear. The compression field theory is a recently developed method of analysis which involves a consideration of equilibrium compatibility and the stress-strain characteristics of the concrete and the reinforcing steel.

The thesis shows how the complete response of a given section under flexure and shear can be predicted using the equations developed from the compression field theory. A program has also been written to enable a computer aided solution.

Further to the theoretical predictions, the thesis also presents a test programme in which experimental data is collected in order to verify the trends established from the theoretical model.

A comparative study is then carried out between the theoretical and experimental trends to assess the

capability of the model. It is established that within the assumptions of the theoretical model and the limitations of the experimental program, the trends predicted by the compression field theory model and those from the laboratory test data are in good agreement.

NOTATION

A_l	Area of bottom longitudinal steel
A'_l	Area of top longitudinal steel
A_v	Area of transverse steel (2 legs)
a	Shear span
b	Width of section
C_1	Compression force in concrete above neutral axis
C_2	Compression force in concrete below neutral axis
C_s	Compression force in top longitudinal steel
c	The ratio $\frac{t_v f_{vy}}{q}$
d	Depth from extreme compression fibre to centre of mass of bottom longitudinal steel
d'	Depth from extreme compression fibre to centre of mass of top longitudinal steel
E	Modulus of elasticity for steel
f'_c	Peak concrete cylinder stress
f_{cp}	Principal stress in concrete
f_l	Stress in bottom longitudinal steel (f_{ly} = yield stress)
f'_l	Stress in top longitudinal steel (f'_{ly} = yield stress)
f_v	Stress in transverse steel (f_{vy} = yield stress)
f_y	General yield stress value for steel
h_l	Distance between centres of mass of top and bottom longitudinal steel
j	Lever arm factor
M_p	Pure moment value
M	Moment in section for combined case

q	Shear flow
s_v	Spacing of transverse steel
T	Tension force in bottom longitudinal steel
t_v	The ratio $\frac{A_v}{s_v}$
V	Shear force in section
\bar{x}_2	Distance from bottom longitudinal steel to point of action of C_2
y	Depth of any fibre in section measured from extreme compression fibre
y_n	Depth to neutral surface measured from extreme compression fibre for combined flexure and shear case
α, β	Equivalent rectangular stress block factors defined by equations (A.1) and (A.2)
γ_{lt}	Shear strain
ϵ_{co}	Concrete strain corresponding to peak concrete stress
ϵ_{cp}	Principal compressive strain in concrete
ϵ_{ct}	Extreme top fibre compression strain
$\epsilon_{d1}, \epsilon_{d2}$	Measured diagonal strains
ϵ_l	Strain in bottom longitudinal steel ($\epsilon_{ly} =$ yield strain)
ϵ'_l	Strain in top longitudinal steel ($\epsilon'_{ly} =$ yield strain)
ϵ_v	Strain in transverse steel ($\epsilon_{vy} =$ yield strain)
ϵ_t	Principal tensile strain in concrete
η	The ratio $\frac{\epsilon_v}{\epsilon_{vy}}$
ϕ	Curvature
θ	Principal angle of compression measured with respect to the beam longitudinal axis

CHAPTER 1

INTRODUCTION

- σ_{cl} Stress in concrete in longitudinal direction
- σ_{ct} Stress in concrete in vertical direction
- τ Shear stress in concrete
- λ Effective peak concrete stress in beam
- $\Omega_{cp}, \Omega_t, \Omega_\ell, \Omega_{vy}$ Ratios defined as $\frac{\epsilon_{cp}}{\epsilon_{co}}, \frac{\epsilon_t}{\epsilon_{co}}$ and $\frac{\epsilon_\ell}{\epsilon_{co}}$ and $\frac{\epsilon_{vy}}{\epsilon_{co}}$ respectively
- that due to the presence of such a ratio for shear, and combinations of flexure and shear, procedures for design are quite unsatisfactory compared to those for flexure and axial load. Thus although safe designs are possible, there is still a lack of understandable central philosophy resulting in complaints about design codes that are unworlably complicated". In this thesis, the behavioral response of structural concrete loaded in flexure and shear is predicted using a rational model called the compression field theory. The work is aimed at contributing to the present effort being undertaken to increase our understanding of the behaviour of members loaded in flexure and shear. The thesis also presents an experimental program conducted to test the performance of the theory.

The compression field theory is a recently developed method of analysis which has been successfully used to reliably explain the behaviour of structural concrete in pure torsion (Ghobaril, 9).

CHAPTER 1

INTRODUCTION

The role of rational models in enabling the engineer to develop a better understanding of actual structural behaviour has been pointed out by Collins, M.P. and Mitchell, D. (1980). They have also noted that due to the absence of such a model for shear, and combinations of loading including shear, procedures for design are quite unsatisfactory compared to those for flexure and axial load. Thus although safe designs are possible, "there is still a lack of understandable central philosophy resulting in complaints about design codes that are unworkably complicated". In this thesis, the behavioral response of structural concrete loaded in flexure and shear is predicted using a rational model called the compression field theory. The work is aimed at contributing to the present effort being undertaken to increase our understanding of the behaviour of members loaded in flexure and shear. The thesis also presents an experimental program conducted to test the performance of the theory.

The compression field theory is a recently developed method of analysis which has been successfully used to rationally explain the behaviour of structural concrete in pure torsion (Mitchell, D.

and Collins, M.P. 1974) and for the case of combined torsion, flexure and axial load (Onsongo, W.M. 1978). The full approach, as in the case of the well known theory for pure flexure, involves a consideration of equilibrium, compatibility and the stress-strain characteristics of the concrete and reinforcing steel.

The thesis first discusses the development of the compression field theory model from early design procedures. Basic equations for a proposed reinforced concrete beam model are then derived. Predictions of behavioral response for a series of beams are then done with material properties and loading conditions as the main parameters. The predicted behavioral responses are plotted on suitable graphs.

The experimental program designed to test the validity of the theory is also described. The test program contained eight reinforced concrete beams which were heavily instrumented to enable adequate data acquisition to validate or otherwise the various trends predicted by theory, in particular those involving strains.

For the beams tested, the actual material properties and loading condition are used to obtain theoretical predictions. The theoretical predictions are then plotted side by side with the experimental responses obtained from the laboratory test specimens. A comparative study is then done to assess agreement

between theoretical and experimental behaviour of the beams by observing trends of predicted and experimental responses.

The paper by Collins, M.P. and Mitchell, D (1980) includes a design procedure for a case of combined shear and flexure loading using the compression field theory. The design method proposes superposition of effects of shear and flexure in the elastic range and the imposition of various limiting factors in the non elastic range. The model in this thesis uses the equilibrium and compatibility relationships in an iterative scheme both in the elastic and non-elastic range to predict the response under combined flexure and shear.

It is, however, noted that a full understanding of the behaviour of structures subjected to shear does not yet exist.

As already noted, the present research utilizes the compression field theory model for prediction of structural concrete response in flexure and shear. In this chapter, the work accomplished by researchers in the development of this theory from early design procedures is discussed. As much as possible the review is restricted to the area of shear since the behaviour in flexure is already well understood.

CHAPTER 2

LITERATURE REVIEW

From about the turn of the century when Ritter and Mörsch proposed design procedures for shear, active research has been going on with the aim of developing a rational model for structural concrete members under not only shear loading but also its interaction with other structural actions. This is evident from the long lists of selective research papers available on this subject, for example in the Joint ASCE-ACI Task Committee 426 (1973), Joint ASCE-ACI Task Committee 426 (1974) and others. The research includes work on shear transfer mechanisms, factors affecting shear and serviceability of beams, methods of analysis for shear, modes of shear failure and distress and design procedures. It is, however, noted that a full understanding of the behaviour of structures subjected to shear does not yet exist.

As already noted, the present research utilizes the compression field theory model for prediction of structural concrete response in flexure and shear. In this chapter, the work accomplished by researchers in the development of this theory from early design procedures is discussed. As much as possible the review is restricted to the area of shear since the behaviour in flexure is already well understood.

2.1 Early Design Procedures

Early design procedures for shear were by the truss analogy introduced by Ritter and by Mörsh at the turn of the century. The method assumes that a reinforced concrete beam can be replaced by a pin jointed truss (Figure 2.1) in which transverse steel acts as ties and cracked concrete as struts. A problem, however, lies in the determination of the angle of inclination of concrete struts. As quoted by Collins, M.P. and Mitchel, D. (1980), Mörsh in 1922 made the following statement regarding this problem; "we have to comment with regards to practical application that it is absolutely impossible to mathematically determine the slope of the secondary inclined cracks according to which one can design the stirrups. For practical purposes one has to make a possibly unfavourable assumption for the slope, θ , and therefore, with $\tan 2\theta = \infty$, we arrive at our usual calculation for stirrups which presumes $\theta = 45$ degrees. Originally this was derived from the initial shear cracks which actually exhibit this slope."

Cracking is assumed to occur in directions mutually perpendicular to the principal tensile stresses, that is, parallel to the direction of principal compression stresses. The above statement by Mörsh indicates that it is impossible to calculate

the direction of principal compression stresses in cracked concrete. As will be shown in Chapter 3, this is no longer the case as the compression field theory model predicts the angles of principal compression from considerations of compatibility of strains in cracked concrete.

2.2 Performance of the Truss Analogy

In addition to the difficulty in choice of inclination of compression, the truss analogy model has been found to be extremely over-simplified in that it does not attempt to satisfy compatibility and it ignores some of the mechanisms of shear transfer proposed in the Joint ASCE-ACI Shear Committee 426 (1973).

The mechanisms of shear transfer proposed in the above report are indicated in Figure 2.2. These mechanisms are such that the total shear carried, V_T , is given by:

$$V_T = V_s + V_{cz} + V_d + V_{ay} \dots \dots \dots (2.1)$$

where V_s = Shear carried by transverse steel

V_{cz} = Shear carried by compression zone

V_d = dowel shear carried by longitudinal steel

V_{ay} = Vertical component due to interface shear

The truss analogy ignores the components V_{cz} , V_d

and V_{ay} . It is, however, noted that there is still disagreement as to the presence and roles of these components of shear and the subject of shear transfer mechanisms is not yet well understood. Extensive research by several researchers has been devoted to establishing the contributions of these various transfer mechanisms. Notable work done on this subject includes that by Leonhardt, F. and Walther, R. (1964), Leonhardt, F. (1965), Fenwick, R.C. and Paulay, T. (1968). Gergely, P. (1969), Hofbeck, J.A., Ibrahim, I.A., and Mattock, A.H. (1969) and more recently Jimenez, R., White, R.N., and Gergely, P. (1982).

Further, the mode of failure has been linked to the failure in one or a combination of the mechanisms of shear transfer. The failure of these mechanisms is deemed to be affected by the manner in which inclined cracks develop and grow, which in turn depend on the relative magnitudes of the shearing stress, v and the flexural stress, f_x . For beams with concentrated loads, the following expression (Joint ASCE-ACI Shear Committee 426(1973) has been deduced:

$$\frac{f_x}{v} = \alpha_3 \frac{(a)(bw)}{(d)(b)} \dots\dots\dots (2.2)$$

where α_3 is a coefficient depending on variables like geometry of beam, type of loading, amount and arrangement of reinforcement,

type of steel and interaction between steel and concrete. b , b_w are respectively the flange and web width of the beam.

From the above relationship, the variations in the inclined cracking load and shear capacity of rectangular beams are considered a function of varying $\frac{a}{d}$ (Bresler, B. and Macgregor, J.G. (1967)). For rectangular cross section beams, inclined cracks will normally occur in the range $2.0 < \frac{a}{d} < 6.0$.

The compression field theory assumes that the concrete and reinforcing steel act together and proceeds to rationally explain the behaviour of a cracked concrete beam by proposing that a redistribution of stresses occurs such that there is equilibrium of forces and compatibility of strains. It is of interest to note that the original truss analogy by Ritter and Morsch did not satisfy compatibility of deformations.

In spite of the simplifications of the truss analogy it must be noted that the model has been found to be an excellent conceptual tool in study of the beams with web reinforcement and to indicate the presence of tensile stresses in stirrups and compression stresses in concrete between inclined crack. In addition, the model correctly shows effects of variations of stirrup angle

to these stresses and thus may derive basic equations for design of web reinforcement. It also clearly shows that stresses in the longitudinal tensile reinforcement are larger than predicted from beam theory. These advantages are also revealed by the compression field theory.

2.3 Modifications to the Truss Analogy and Development of the Compression Field Theory

The truss analogy yields typically conservative results. In view of this and the other limitations already noted, attempts have been made to modify the approach for use in design for shear. In fact most design codes have developed modified forms of this model for handling design of structures subjected to shear. Modifications considered by the American Concrete Institute and the European Concrete Committee design procedures are mentioned by Collins, M.P. and Mitchell, D. (1980).

The compression field theory utilizes a different concept from the truss analogy as already noted in section 2.2. Most significant is the fact that the requirements of compatibility are not overlooked. The inclination of principal compression stresses is determined from these requirements.

The problem of determining the inclination of principal compression in concrete is analogous to the

problem investigated by Wagner in 1929 in studying buckling shear resistance of thin webbed metal girders (Collins, M.P. and Mitchel, D. 1980). Wagner assumed that after buckling, shear resistance of thin webbed metal girders cannot resist compression and that shear would be carried by a field of diagonal tension. By considering the deformation of the system, he assumed that the angle of inclination of the diagonal tensile stresses would coincide with the angle of inclination of principal tensile strains in order to determine the inclination of diagonal tension.

Wagner was dealing with material which after buckling could be considered to have no compression strength but resisted further loading in a tension field. Structural concrete can also be considered to have no tensile strength after cracking and further loading in the post-cracking range is resisted in a field of principal compression by the concrete while the reinforcing steel is assumed to take up the tension forces. Recognizing the analogy between this and the problem of Wagner, it has been shown (Onsongo, W.M. 1978) that the angle of principal compression strain in concrete with respect to the beam longitudinal axis is given by:-

$$\frac{\epsilon_l + \epsilon_{cp}}{\epsilon_v + \epsilon_{cp}} = \tan^2 \theta \dots \dots \dots (2.3)$$

This relationship which is used to establish

the compatibility requirements of the compression field theory links the strains in concrete, the longitudinal steel and the transverse steel. The full geometrical interpretation of equation (2.3) was, however, not done until the work of Onsongo (1978).

Basic equations for shear using the compression field theory have been derived by Collins, M.P. (1978). The model has been further discussed by Collins, M.P. and Mitchell, D. (1980) in a paper in which additional behavioral aspects have been proposed. The paper also includes design examples. From the design examples, it has been shown that the amount of reinforcement required by the compression field theory is in general comparable to amounts required by existing empirical design procedures. This presents hope of moving towards a rational model. In the next chapter, the model is applied to beams loaded in flexure and shear.

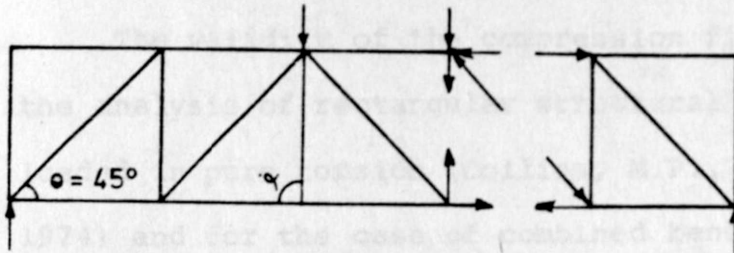


Fig.2.1: Distribution of force in classical Truss Analogy

(Joint ASCE-ACI Task committee 426(1973))

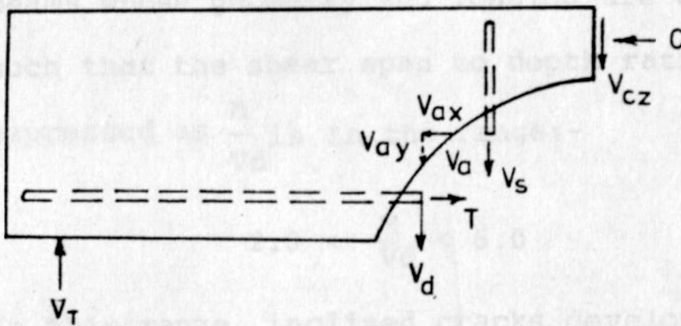


Fig.2.2: Forces Acting at an Inclined crack

(Joint ASCE-ACI Task committee 426(1973))

- | | |
|------------------|---|
| V_{ay}, V_{ax} | Components due to interface shear, V_a |
| V_d | dowel shear carried by longitudinal steel |
| V_{cz} | Shear carried by the compression zone |
| V_s | Shear carried by the shear reinforcement |

CHAPTER 3

COMPRESSION FIELD THEORY FOR COMBINED
FLEXURE AND SHEAR LOADING

The validity of the compression field theory for the analysis of rectangular structural concrete beams loaded in pure torsion (Collins, M.P., and Mitchel, D. 1974) and for the case of combined bending, axial load and torsion (Onsongo 1978) has already been established. In this chapter the theory is further developed for analysis of structural concrete subjected to combined flexure and shear. The theory is developed using rectangular reinforced concrete beams whose geometry and loading are assumed to be such that the shear span to depth ratio, which can be expressed as $\frac{M}{Vd}$ is in the range:-

$$2.0 < \frac{M}{Vd} < 6.0$$

In this range, inclined cracks develop due to a combination of shear and flexural stresses and the mode of failure could be due to either shear or flexure.

Figure 3.1 shows the assumed cracked beam model together with the loading condition. In Figure 3.2, the assumed distribution of stresses across the section is shown.

3.1 Assumptions

For the development of the theoretical model, the following basic assumptions were made:

- (i) Under the applied loads, the beam is fully cracked in the region below the neutral axis.
- (ii) The longitudinal strains along any line in a section vary linearly (Bernouli-Navier hypothesis).
- (iii) All strains at a point in a plane are compatible.
- (iv) The direction of principal compression strain evaluated from a set of compatible strains at a point in a plane of loading is coincident with the direction of principal compression stress at that point in the plane.
- (v) The resultant concrete compression force above the neutral axis can be evaluated using the well known rectangular stress-block theory used for pure flexure.

- (vi) Transverse steel content is the same in all faces.
- (vii) In the fully cracked region concrete resists load in principal compression and the tensile strength of concrete can be ignored.
- (viii) The stress-strain relationships for reinforcing steel are bilinear (Figure 3.3 (a)).

3.2 Equilibrium Considerations

- (ix) The stress-strain relationships for a standard concrete cylinder tested under compression may be taken to be parabolic (Figure 3.3 (b)).

3.2.1 Concrete Stresses

- (x) The principal compression stress in the structural concrete beam, f_{cp} , is assumed to be related to the principal compression strain ϵ_{cp} and the principal tensile strain ϵ_t as follows:

$$f_{cp} = \frac{f'_c}{0.8 + 0.34 \left(\frac{\epsilon_t}{\epsilon_{co}} \right)} \left(2 \frac{\epsilon_{cp}}{\epsilon_{co}} - \left(\frac{\epsilon_{cp}}{\epsilon_{co}} \right)^2 \right) \leq f'_c$$

- (xi) The shear flow variation down the section is assumed to be linear with a change of slope at the neutral surface (Figure 3.1).

These assumptions are necessary for the purpose of setting up of equilibrium and compatibility relationships. Assumptions (i) to (ix) are the usual accepted ones in the well established flexural theory of concrete. Assumption (x) has resulted from recent tests by Vecchio and Collins (1982) while assumption (xi) is a reasonable new one required to enable the setting up of the relevant equations of equilibrium.

3.2 Equilibrium Considerations

3.2.1 Concrete Stresses

Figure 3.1 shows the assumed cracked beam model subjected to a shear force, V , and a flexural moment, M . A typical element, A , which is assumed to be in the plane of shear flow will be subjected to a shear stress τ longitudinal stress, σ_{cl} and a transverse stress, σ_{ct} for the combined loading case. Assuming concrete has no tensile strength, the stresses can be considered equivalent to a field of principal compression in the cracked concrete, at an inclination, θ , with respect to the beam longitudinal axis which is determined by the equilibrium requirements and requirements of compatibility of deformations (see also Onsongo 1978).

Consider the typical element, A , just described. The stresses at equilibrium can be resolved using Mohr's circle of stresses as illustrated in Figure

3.4 (a). This leads to the following relationships:-

$$\tau = \frac{1}{2} f_{cp} \sin 2\theta \dots\dots\dots(3.1)$$

$$\sigma_{ct} = \tau \tan \theta \dots\dots\dots(3.2)$$

$$\sigma_{cl} = \frac{\tau}{\tan \theta} \dots\dots\dots(3.3)$$

The assumed shear flow distribution is shown in Figure 3.1. Now, at any given level of section, the shear stress, τ , when integrated across the width b results in the shear flow q . For the section shown in Figure 3.1, it is reasonable to assume that the shear stress, τ , is constant across the width b at any level. Hence,

$$q = \tau b \dots\dots\dots(3.4)$$

The determination of shear flow at the level of tension steel in the bottom face, q_b , is possible by considering the element shown in Figure 3.4 (d). In general, the applied moment, M , is related to the internal tension force, T , and the lever arm jd , as:-

$$M = Tjd \dots\dots\dots(3.5)$$

For the type of section and reinforcement details shown,

$$T = A_\ell f_\ell \quad f_\ell \leq f_{ly}$$

Differentiating equation (3.5),

$$\frac{\partial M}{\partial x} = \frac{\partial T}{\partial x} jd + Td \frac{\partial j}{\partial x}$$

But $\frac{\partial M}{\partial x} = V$ by definition

From Figure 3.4 (d) we deduce that

$$\frac{\partial T}{\partial x} = q_b$$

hence $V = q_b j d + T d \frac{\partial j}{\partial x}$

Assuming that $\frac{\partial j}{\partial x}$ is negligible, we deduce that

$$q_b = \frac{V}{j d} \dots \dots \dots (3.6)$$

From the assumed distribution, the shear flow at the neutral axis, q_n , is determined by recognizing that the shear flow equilibrates the applied shear, V , and hence:- $q_n = \frac{2}{d} (V + \frac{q_b y_n}{2}) - q_b \dots \dots \dots (3.7)$

It has been assumed that the amount of compression longitudinal steel in the top face, A'_s , is nominal and hence will not significantly affect the shear flow distribution. When a high content of top longitudinal steel is used, a value for the shear flow at the top compression steel, q_t , can be computed in a similar manner as for q_b . For such a case, the expected distribution and equations are presented in Appendix D. For simplicity, only cases with nominal top face longitudinal steel content are considered in the present analysis.

The components of the principal compression stress set up in concrete are resisted by the longitudinal and transverse reinforcing steel. The compressive stresses in concrete can be related to the steel stresses by considering the equilibrium of the

appropriate free body diagrams.

3.2.2 Transverse Equilibrium

Consider the free body diagram of Figure 3.4 (b).

Assuming that the transverse steel is placed perpendicular to the longitudinal axis and that within the spacing, s_v , the applied shear and the internal compression stresses in concrete are uniform, the following relationship is deduced:-

$$A_v f_v = \sigma_{ct} dA;$$

and using equation (3.2) this equation becomes

$$\frac{A_v f_v}{s_v} = \tau \tan \theta b \dots\dots\dots (3.8)$$

where the area of integration equals to $s_v b$.

Using equation (3.4), equation (3.8) becomes

$$\frac{A_v f_v}{s_v} = q \tan \theta \dots\dots\dots (3.9)$$

3.2.3 Longitudinal Equilibrium

Consider the free body diagram of Figure 3.4 (c). The distribution of equivalent stresses is included. For no axial load, equilibrium requires that the tension force in the reinforcing steel in the section be balanced by the resultant compression force in the concrete. Further, equilibrium requires that the external moments applied be balanced by the internal moment due to these resultant forces at the section.

From Figure 3.4 (c), the following relationship is deduced.

$$A_{\ell} f_{\ell} - A'_{\ell} f'_{\ell} = \alpha \beta f'_{c} b y_n + \int_{y_n}^d \frac{\tau}{\tan \theta} b dy$$

and hence
$$A_{\ell} f_{\ell} - A'_{\ell} f'_{\ell} = \alpha \beta f'_{c} b y_n + \int_{y_n}^d \frac{q dy}{\tan \theta} \dots (3.10)$$

The values of the shear flow, q , can be determined at a number of points (see Figure 3.1) and using these, the integral in equation (3.10) can be approximately evaluated using Simpson's rule. For three ordinates; at the neutral surface, at the bottom level and in the middle of these two points and if q_n , q_b and q_m are the respective shear flows and θ_n , θ_b and θ_m the corresponding angles of principal compression, the compressive force, C_2 , can be approximated as:-

$$C_2 = \frac{d-y_n}{6} (q_n \cot \theta_n + 4q_m \cot \theta_m + q_b \cot \theta_b) \quad (3.11).$$

Further, if \bar{x}_2 is the resultant of the above force measured from the tension steel in the bottom face, then, also by Simpson's integration rule:-

$$\bar{x}_2 = (d-y_n) \left(\frac{q_n \cot \theta_n + 2q_m \cot \theta_m}{q_n \cot \theta_n + 4q_m \cot \theta_m + q_b \cot \theta_b} \right) \dots (3.12)$$

The internal forces constitute a couple which equilibrates the applied moment, M, so that:-

$$M = C_2 \bar{x}_2 + \alpha \beta f'_c b y_n \left(d - \frac{\beta y_n}{2} \right) + A'_s f'_s \ell \dots (3.13)$$

3.3 Geometrical Considerations

The compression field theory links the strains in the concrete diagonal to the strains in the longitudinal and transverse directions to realise a compatible displacement. While the local strains of the cracked beam may exhibit discontinuities, the average strains in the various directions are related to one another by this requirement of compatibility (Onsongo 1978). Considering Mohr's circle of strains shown in Figure 3.5, the following relationships are deduced.

$$\frac{\epsilon_{cp} + \epsilon_\ell}{\frac{\gamma_{\ell t}}{2}} = \tan \theta \dots (3.14)$$

$$\frac{\frac{\gamma_{\ell t}}{2}}{\epsilon_{cp} + \epsilon_v} = \tan \theta \dots (3.15)$$

3.4 Strain Relationships for Materials

3.4.1 Concrete

where the longitudinal strain, ϵ_ℓ , and the transverse strain, ϵ_v , are considered positive when tensile and the principal compression strain ϵ_{cp} is considered positive when compressive. Combination of equations

This relationship is plotted in Figure 3.3 (b).

(3.14) and (3.15) yields the geometric relationship

$$\tan^2 \theta = \frac{\epsilon_l + \epsilon_{cp}}{\epsilon_v + \epsilon_{cp}} \dots \dots \dots (3.16)$$

and the shear strain $\gamma_{lt} = 2\sqrt{(\epsilon_l + \epsilon_{cp})(\epsilon_v + \epsilon_{cp})} \dots (3.17)$

Equation (3.16) represent the compatibility condition of strains and shows that given the three strains ϵ_l , ϵ_v and ϵ_{cp} , the direction of the average principal compressive strain, θ , can be determined. The geometric interpretation of this equation was developed by Onsongo (1978).

It should be noted that the diameter of the circle is a measure of the maximum shear strain, γ_m , which can be expressed as:

$$\gamma_m = \epsilon_l + \epsilon_v + 2\epsilon_{cp} \dots \dots \dots (3.18)$$

3.4 Stress-Strain Relationships for Materials

3.4.1 Concrete

From assumption (ix), the cylinder concrete stress-strain relationship is represented by:

$$f_{cp} = f'_c (2\Omega_{cp} - \Omega_{cp}^2) \dots \dots \dots (3.19)$$

This relationship is plotted in Figure 3.3 (b).

If it is assumed that the stress-strain relationship for concrete in a beam is identical to that of a standard cylinder test, then,

$$q = \frac{1}{2} f_{cp} \sin 2\theta b$$

(see equation (3.1))

and hence $f_{cp} = \frac{2q}{b \sin 2\theta}$ (3.20)

From equation (3.19), it can be deduced that

$$\Omega_{cp} = 1 \pm \sqrt{1 - \frac{f_{cp}}{f'_c}} \text{ (3.21)}$$

From equation (3.21), the principal compression strain can be calculated.

In the development of the compression field theory for concrete subjected to pure torsion (Mitchell, D. and Collins, M.P. 1974) and combined flexure, torsion and axial load (Onsongo 1978), the concrete stress-strain relationship was taken to be identical to the stress-strain response obtained from a standard concrete cylinder test. Thus equation (3.19) was equally applicable to a concrete beam as to a standard concrete cylinder. However, recent tests (Vecchio, F. and Collins, M.P. 1982) have shown that the principal compressive stress in a cracked reinforced concrete panel subjected to uniform biaxial strain is a function not only of the principal compressive strain ϵ_{cp} but also of the co-existing

principal tensile strain, ϵ_t . Collins, M.P. (1983) has suggested the following stress-strain relationship:

$$f_{cp} = \frac{f_c}{0.8 + 0.34\Omega_t} (2\Omega_{cp} - \Omega_{cp}^2) \dots\dots\dots (3.22)$$

The effect of equation (3.22) to the cylinder concrete stress-strain relationship is shown in Figure (3.6).

In the current development, equation (3.22) is used in the form

$$f_{cp} = \lambda (2\Omega_{cp} - \Omega_{cp}^2)$$

where $\lambda = f'_c / (0.8 + 0.34\Omega_t)$

This enables the use of the equation in an iterative scheme so that equations (3.19), (3.20) and (3.21) still apply.

3.4.2 Steel

For reinforcing steel, the following relationship is used:-

$$f = E\epsilon \leq f_y$$

where f , f_y are the respective steel stresses and ϵ , the strain

reinforcing steel are given, then for a specified extreme compression fibre strain, ϵ_{ct} , and a moment to shear ratio of loading, α , the following solution procedure is proposed.

3.5 Direction of Principal Strains

Strains, computed from the stress-strain relationships just discussed enable determination of the angle of principal compression using equation (3.16). It will be assumed that for the cracked beam the direction of the average principal compressive stress, f_{cp} , is coincident with the direction of the average principal compressive strain calculated from equation (3.16). In fact, recent tests at the University of Toronto (Vecchio, F. and Collins, M.P. 1982) indicate that this assumption is reasonable. The tests showed a difference in the angles for principal stress and principal strain to a magnitude of about $\pm 5^\circ$. For simplicity of analysis, this difference can be ignored.

3.6 Solution Technique

The equilibrium and geometric equations which have been derived are adequate to enable the prediction of a cracked structural concrete beam subjected to flexure and shear loading. Assuming that the beam cross section, the stress-strain characteristics of the concrete and reinforcing steel are given, then for a specified extreme compression fibre strain, ϵ_{ct} , and a moment to shear ratio of loading, a , the following solution procedure is proposed.

Step 1

Assume pure flexure case. Using the well established flexural theory, calculate the depth to the neutral surface, y_p , corresponding to the top fibre strain, ϵ_{ct} . Hence, calculate the pure moment value, M_p .

Step 5

Step 2

Recognising that the neutral surface depth, y_n , for the combined case of flexure and shear will be less than that for the pure flexure case, guess y_n ; say $y_n = 0.75 y_p$. Hence calculate curvature $\phi = \frac{\epsilon_{ct}}{y_n}$. With ϕ , determine the longitudinal steel strains and in turn the corresponding stresses using the given stress-strain characteristics. Also, determine the internal forces.

Step 3

With the internal forces obtained in step 2, evaluate the internal moment, M , and the internal moment lever arm $jd = \frac{M}{A_s f_s}$. Determine the shear force in section from the moment shear ratio and hence using equations (3.6) and (3.7) establish the shear flow distribution.

Step 4

Determine the angles and strains with the established shear flows and hence calculate the longitudinal compression forces in cracked concrete using equation (3.11).

Step 5

Check equilibrium (equation 3.10). If equilibrium is not satisfied, repeat steps 2, 3, and 4 using the latest evaluated value of jd for each new iteration thus:-

$$M = Tjd$$

and $V = \frac{M}{a}$

Step 6

When equilibrium is satisfied, solution results are recorded. A new extreme compression fibre strain can be selected and the process repeated until the required complete response is obtained.

The equations involved in the various steps of the solution process together with a sample calculation are presented in Appendix A.

3.7 Theoretical Study Using Computer

The solution technique just presented has been programmed to enable a computer aided solution in predicting the behavioral response of rectangular reinforced concrete beams loaded in flexure and shear. The steps of the program and the full listing are given in Appendix B

Beams with varying material properties and loading conditions have been studied. The cases considered include behaviour with changing longitudinal steel content, transverse steel content, concrete strength and moment-shear ratio. The predicted moment-curvature responses are plotted in Figures 3.7, 3.8 and 3.9.

Figures 3.7 (a), (b) and (c) show that the effect of increasing the longitudinal steel content ρ_l for a fixed $\frac{M}{Vd}$ ratio while keeping all other parameters constant is to decrease the section ductility and increase the moment capacity.

Figures 3.8 (a), (b) and (c) show that the effect of increasing the transverse steel content, ρ_{sv} , for a fixed $\frac{M}{Vd}$ ratio while keeping all other parameters constant is to decrease the section ductility and increase the moment capacity. However, the effect is not as dramatic as that due to variation of the longitudinal steel content particularly for large $\frac{M}{Vd}$ ratios.

Figures 3.9 (a), (b) and (c) show that the effect of increasing the concrete strength, f'_c , for a fixed $\frac{M}{Vd}$ ratio while keeping all other parameters constant is to increase section ductility and also increase the moment capacity. The increase in moment capacity for this particular section under study is small for concrete strengths above 30N/mm^2 .

Figures 3.7, 3.8 and 3.9 indicate that the effect of increasing the $\frac{M}{Vd}$ ratio for fixed ρ_l , ρ_{sv} and f'_c is to slightly decrease the ductility for slightly increased moment capacity.

The model prediction trends described above formed a useful basis for the design of an experimental program presented in Chapter 4.

3.8 Application of Theory to Prestressed Concrete Sections

The beam section shown in figure 3.10 was used in applying the theory to prestressed concrete sections. Apart from the main prestressing steel, nominal bars are used at corners for tying transverse steel. The basic equations for solving the combined flexure and shear case remain the same as those for reinforced concrete, effect of strain difference in the longitudinal direction due to prestressing operation being considered. The computer program is capable of

handling cases of prestressed concrete. Prediction of trends similar to those of Figures 3.7, 3.8 and 3.9 are possible.

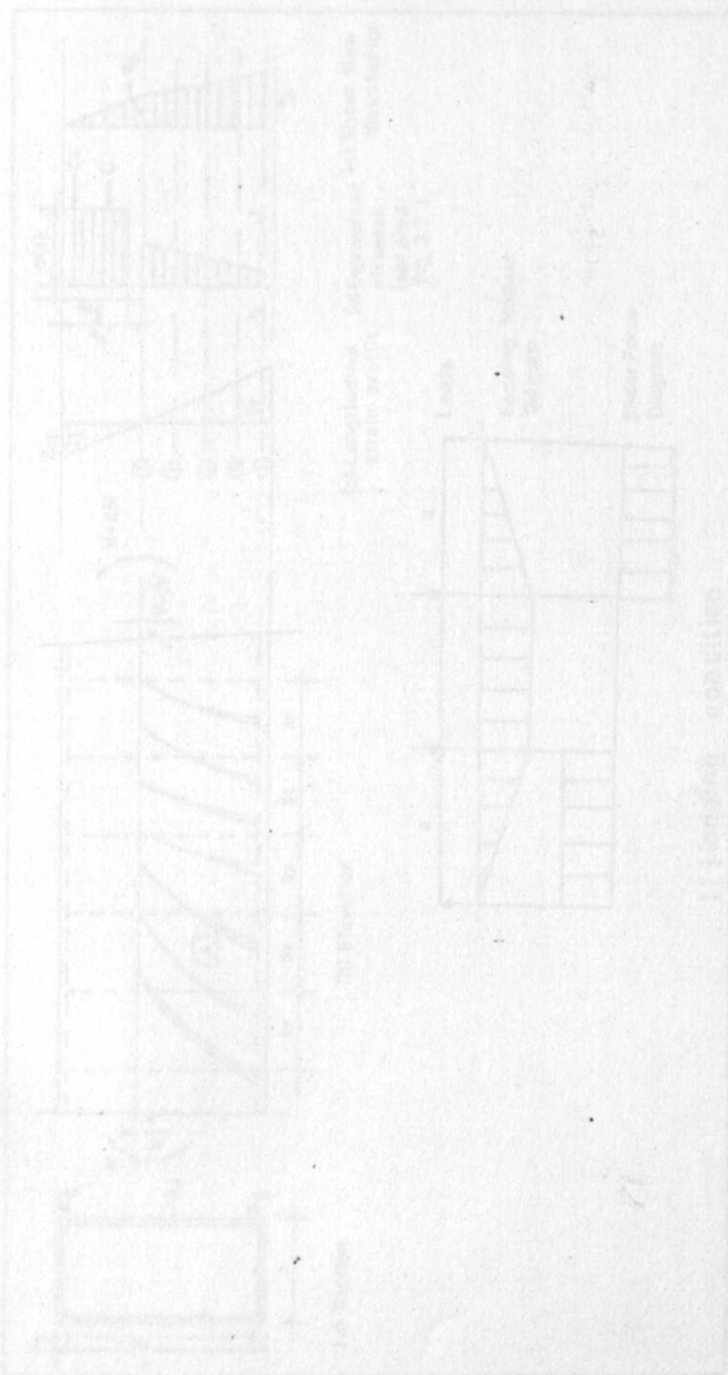


Fig 3.1 Concrete Beam Model

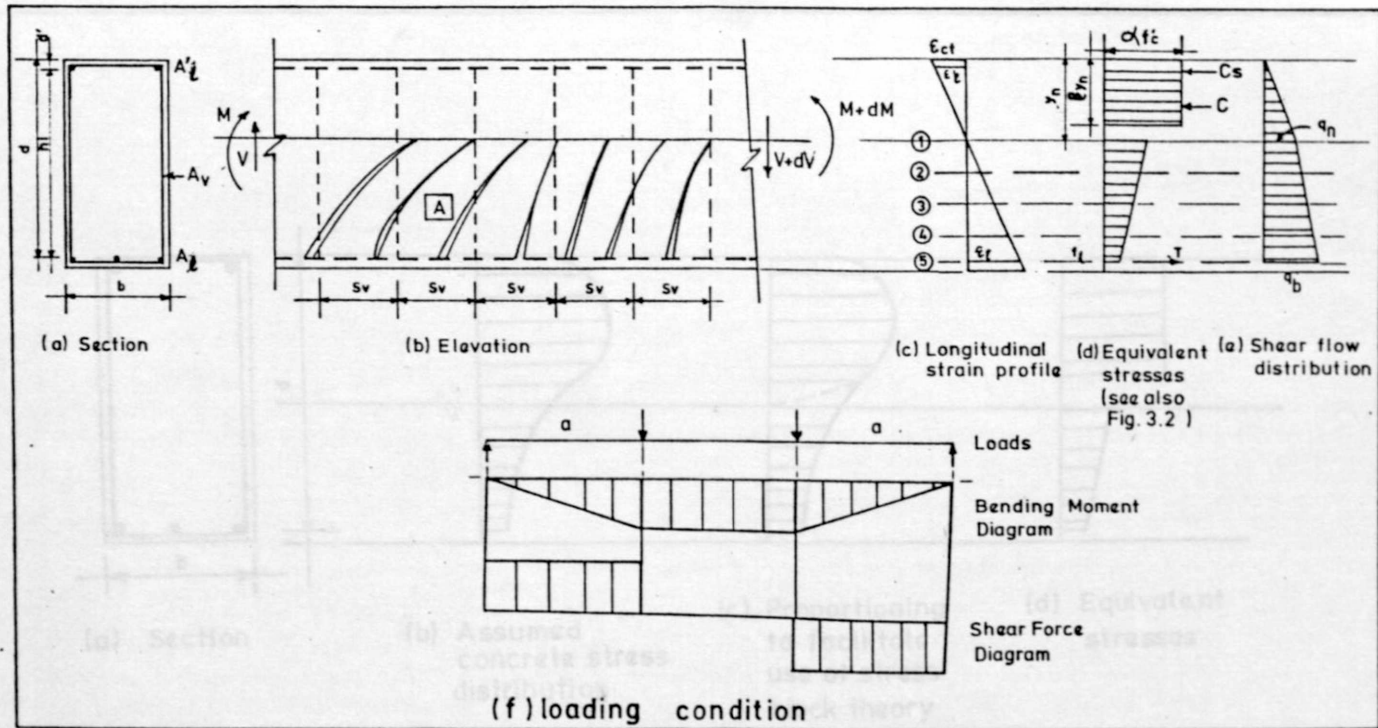


Fig. 3.1: Concrete Beam Model

Fig. 3.2: Distribution of stress on section

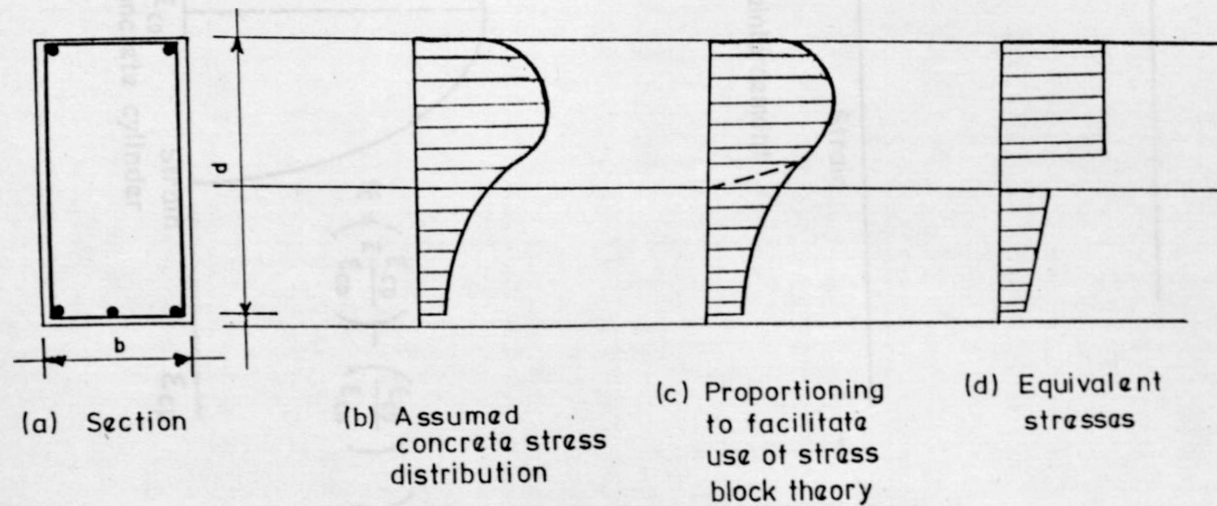
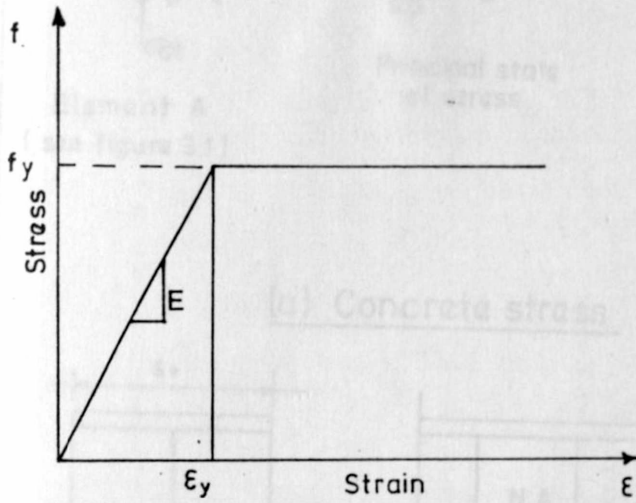
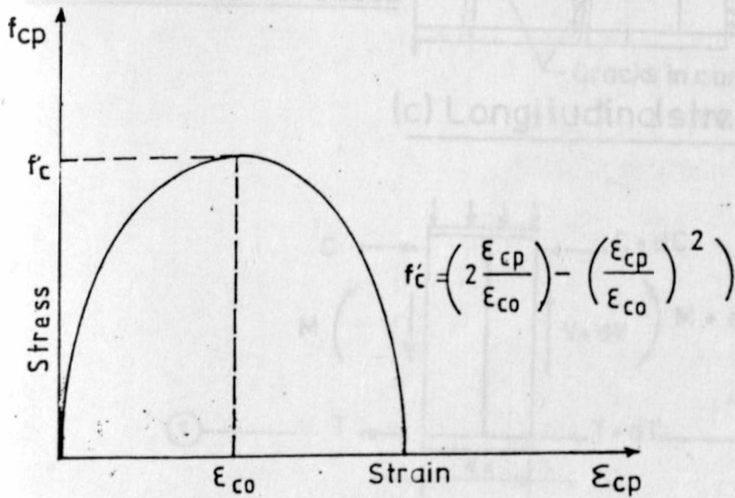


Fig. 3.2: Distribution of stress on section

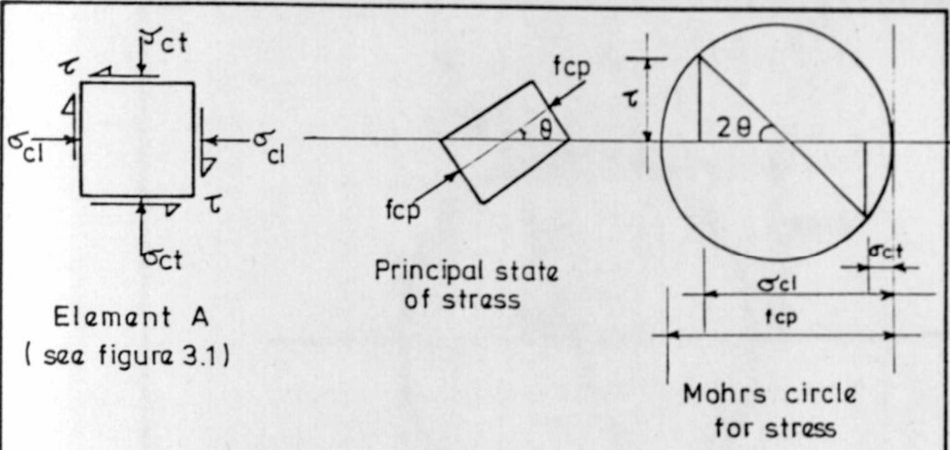


(a) reinforcement



(b) Concrete cylinder

Fig. 3.3 : Material idealised stress-strain characteristics



(a) Concrete stress

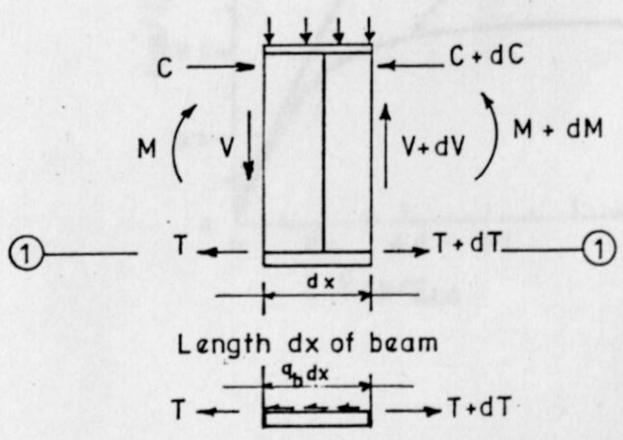
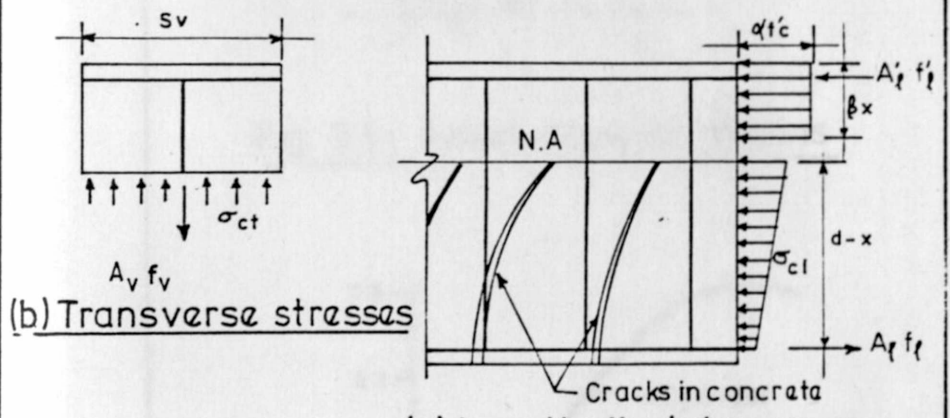


Fig. 3.4: Equilibrium considerations

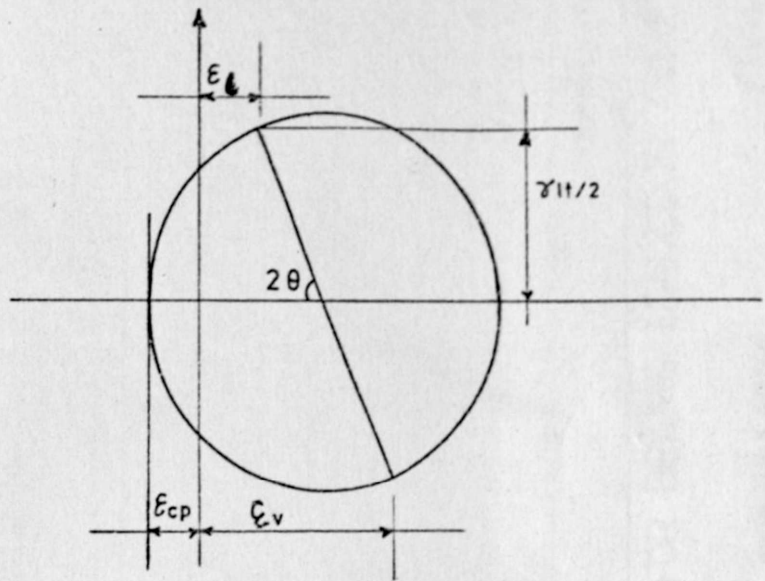


Fig. 3.5: Mohr's circle of strains

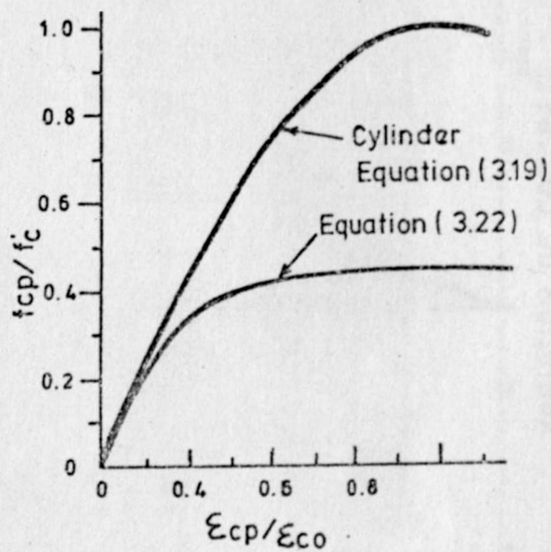
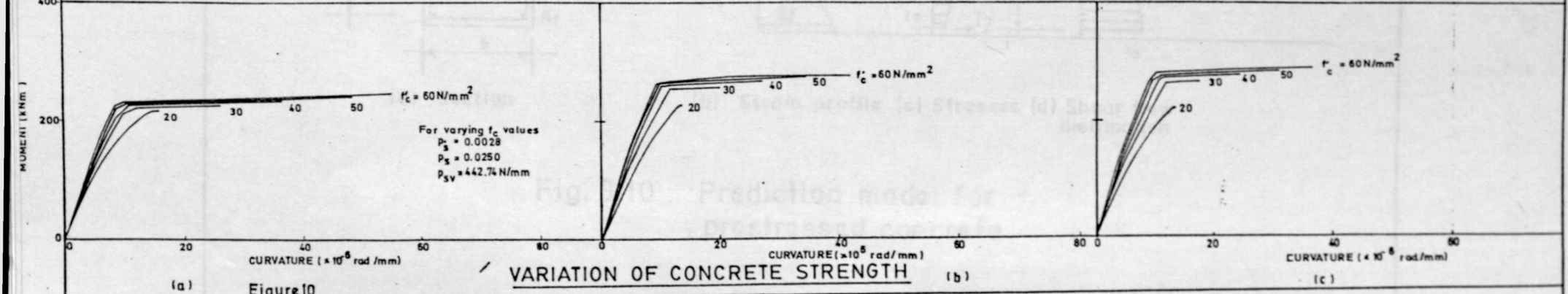
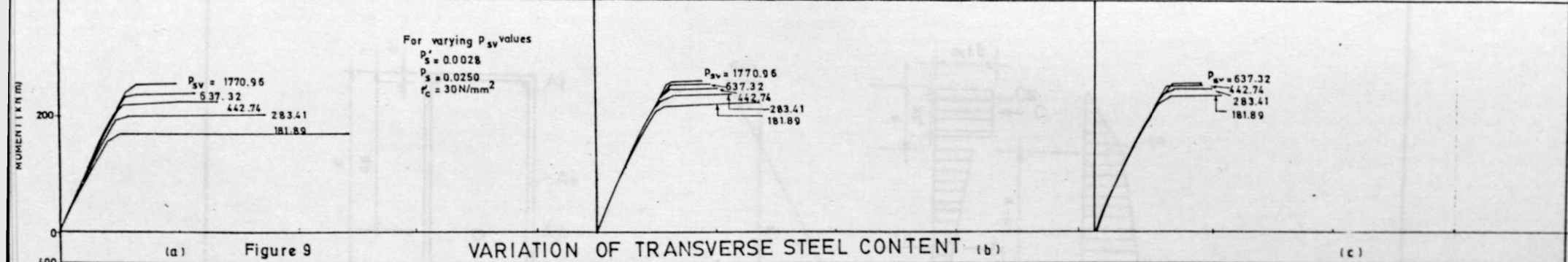
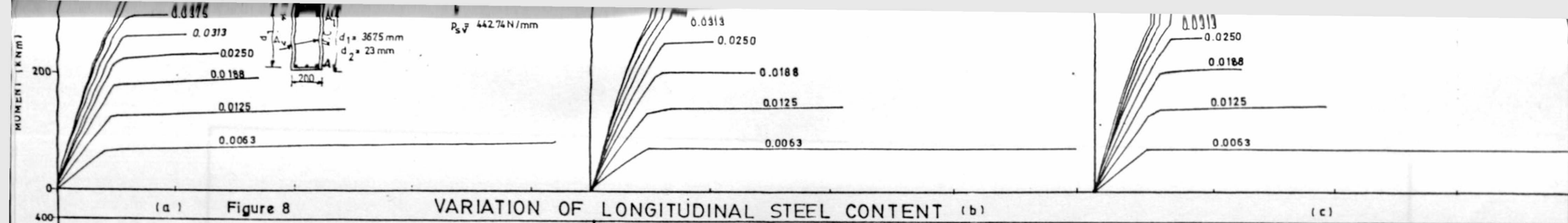
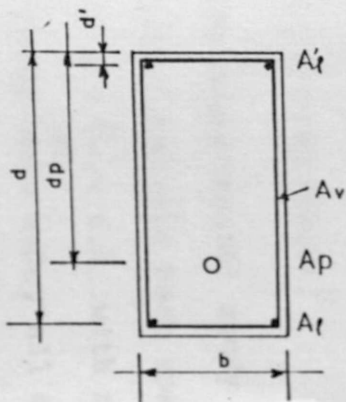


Fig. 3.6: Comparison of responses as predicted by equation (3.19) and (3.22) (Collins 1983)



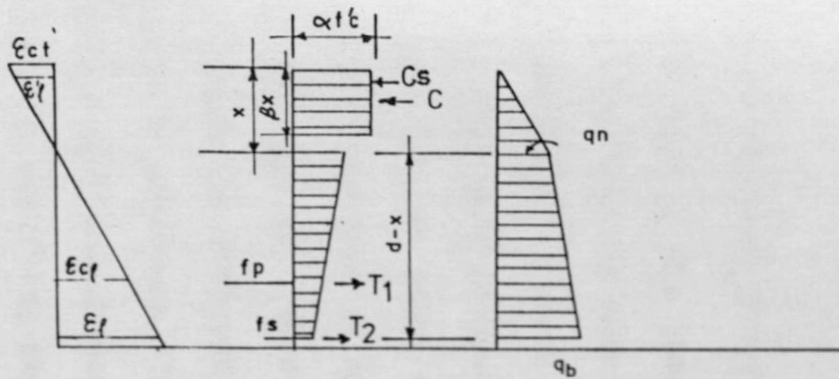
THEORETICAL PLOTS BASED ON COMPRESSION FIELD THEORY FOR BEAMS LOADED IN COMBINED MOMENT AND SHEAR

Note. In the derivation of these plots, the effect of equation 322 is not considered. However for the trends discussed in chapter 5, equation (3.22) is considered.



(a) Section

Fig. 3.10 :



(b) Strain profile (c) Stresses (d) Shear flow distribution

Prediction model for prestressed concrete

CHAPTER 4

DATA COLLECTION

4.1 Objectives and Choice of Test Specimens

In Chapter 3, the compression field theory model was developed for the case of combined loading in flexure and shear. It was noted that this rational model has been used to predict the response of reinforced concrete beams subjected to pure torsion and also for the case of combined bending, axial loading and torsion. This chapter describes a test program which was designed to test the validity of the trends of behaviour illustrated in Figures 3.7, 3.8 and 3.9 with the observations noted. The program also aimed at verifying the various other response characteristics predicted by the compression field theory model for the case of combined flexure and shear, in particular, the strains and angles of principal compression.

The experimental study was limited to rectangular reinforced concrete beam specimens in the loading range $2.0 < \frac{M}{vd} < 6.0$ with rectangular solid sections. Eight beams were made, all of the same section size (200mm x 400mm). Six of the beams had the same length of 2700mm, the other two having lengths of 2600mm and 4000mm. The properties of the beams were varied so as to obtain the desirable variables as summarised in Table 4.1.

Specimens were loaded symmetrically about the centre with two point loads to provide regions for pure flexure and combined flexure and shear, Figure 4.1. The shear span, a , was chosen such that the desired $\frac{M}{Vd}$ ratio was satisfied. Except for beam CFT - TB8, the value of the shear span was kept at 1m and for CFT - TB8 the shear span was 1.65m.

4.2 Test Specimens

4.2.1 Materials

4.2.1.1 Concrete

All concrete mix design was according to a method outlined by Neville, A.M. (1973), the aggregates grading having been approximated to one of the four type curves in Road Note No. 4 (1968). The standard cylinder strength was taken as that obtained from a cylinder made from actual batches used in casting the beam. Recognising that the loading durations on the actual beam were much longer than the normal 5-minute test for a cylinder, some test cylinders were tested taking into account duration of load on the beam. It was noticed that whereas the peak concrete stress remained about the same in both cases, the concrete strain corresponding to the peak concrete stress was much larger in the later case than the former. In Figures 4.2(a)-(h), the concrete stress-strain relationships for all the beams, obtained from the

cylinder tests are presented. The parabolic equation assumed to approximate the stress-strain relationships for standard cylinder is also shown.

4.2.1.2 Steel

Test specimens were cut from the actual steel used. These were tested for stress-strain characteristics in tension. Figure 4.3(a)-(i) gives a summary of the steel test results. For simplicity, approximate bilinear relationships were deduced from these curves for use in predicting behavioral response of the test beams.

4.2.2 Preparation of Test Specimens

The general reinforcement details of the test specimens are given in Figure 4.4. The steel cage, carefully tied to shape and as rigid as possible was lowered into a timber mould which was set on a vibrating table and secured into position by 10mm thick cover blocks. Batching was then started and owing to the small capacity of the mixer, casting was done in five equal batches to fill the mould. It took about one hour to complete the casting for one beam. Cylinder moulds were also filled and proper vibration of the table done at each of these casting stages to prevent honey-combing of the beam and cylinders. Stripping was done after about forty eight hours and curing

done in wet conditions for a sufficient number of days to obtain the desirable strength after which instrumentation was done in readiness for testing.

4.3 Parameters of the Test Program

Longitudinal steel content, transverse steel content, concrete strength and the $\frac{M}{Vd}$ ratio were the basic parameters varied in the tests as identified in the theoretical study and as revealed in Figures 3.7, 3.8 and 3.9.

Beam CFT-TB8 had a different $\frac{M}{Vd}$ ratio from the other beams but with other parameters approximating those of beam CFT-TB2 to enable study the effect of changing $\frac{M}{Vd}$ ratio while holding other parameters constant. In beams CFT-TB2, CFT-TB4 and CFT-TB6, the longitudinal steel content was varied. Beam CFT-TB1, CFT-TB3, CFT-TB5 and CFT-TB7 considered transverse steel variation while in beams CFT-TB2 and CFT-TB7 the parameter varied was the concrete strength. The details of the test program are summarised in Table 4.1.

4.4 Test Rig

Plate 4.2 shows the test rig in which the beams were tested. A schematic representation of the test set up is given in Figure 4.1.

Beams CFT-TB1, CFT-TB2 and CFT-TB4 were tested when the test rig arrangement was as shown in Plate 4.1.

In this arrangement, the left hand side support was secured in position using wedges and the jacks were not fixed to the vertical position using steel rods. This arrangement was however found unsuitable for the high loads required to fail the beams. At high loads the test rig tended to become unstable resulting in sudden unloading of the test specimen. Beams CFT-TB1 and CFT-TB2 were affected by this problem.

The test rig was revised so as to fully fix the line of the loading jacks as shown in Plate 4.2. One of the supports was rigidly fixed to steel columns using a trussed steel member. The jacks were held in the vertical position by an arrangement of steel plates and rods. It was necessary, as a further revision, to change the size of anchoring rods from 12mm diameter bars to 16mm bars to achieve stability of the test rig.

4.5 Calibration of Testing Machines

The machines used in transmitting load to the beam and for the crushing of test cylinders were calibrated against a spring type load sensor of 200 tons capacity to yield calibration curves of machine reading against the transmitted load. The curve for the two jacks that were used in loading the beams is presented in Figure 4.5 while Figure 4.6 gives the calibration curve for the compression machine used in cylinder crushing tests.

4.6 Instrumentation

For the measurement of the strains in the longitudinal, transverse and diagonal directions, targets were placed on the beam faces appropriately using durofix adhesive and left to dry for more than twelve hours. As in the case of Onsongo (1978), heavy instrumentation of the specimens was necessary for the purpose of obtaining enough strain measurements to give reasonable representative strain patterns to enable a comparison with the corresponding patterns predicted by the model. The Bernoulli-Navier hypothesis was also to be verified for the case of flexure and shear.

The target patterns varied from beam to beam as presented in Figures 4.7 (a) - (i). Before mounting the beam into the test rig, the positions of the targets were checked to ensure they were as close as possible to the desired gauge lengths. After proper positioning, the deflection gauges were set below the beam as shown in Plates 4.1 and 4.2 for monitoring of the central deflection of the beam.

4.7 Testing Procedure

Using approximate material properties, the theoretical model was used to predict behaviour of the test specimen before the test. Approximate load levels were then decided at which loading would be

stopped and held for the purpose of strain readings.

All the initial strain readings were taken before loading was started. As a necessary check that these strains were correct, each of the strain readings was taken again before commencement of loading. The specimen was then loaded in steps guided by the predetermined intervals. After the longitudinal steel yielded, deformation of the beam as recorded by the deflection gauges was used as a criterion for the interval of reading of strains. This was continued until the beam failed.

A period of 30 to 40 minutes was spent at every load stage taking readings. The load was observed to fall slightly during this period. If the load fell by more than 10%, reading was stopped and the load adjusted back to the desired level before proceeding. However, in the post yield range, where the tendency was for the beam to continue deforming at a sustained load, the load was allowed to fall until a condition of equilibrium was achieved, by observing no further change in the deflection gauges. Appendix C gives a summary of the measured strains for all the beams. The moments are reported in kNm. It is useful to note here that the instruments available for measurement of loads and strains were calibrated in English units but the measured results are reported in metric units after the appropriate conversion. The loading

machine was calibrated in pounds per square inch while the demec meters were in inches per division.

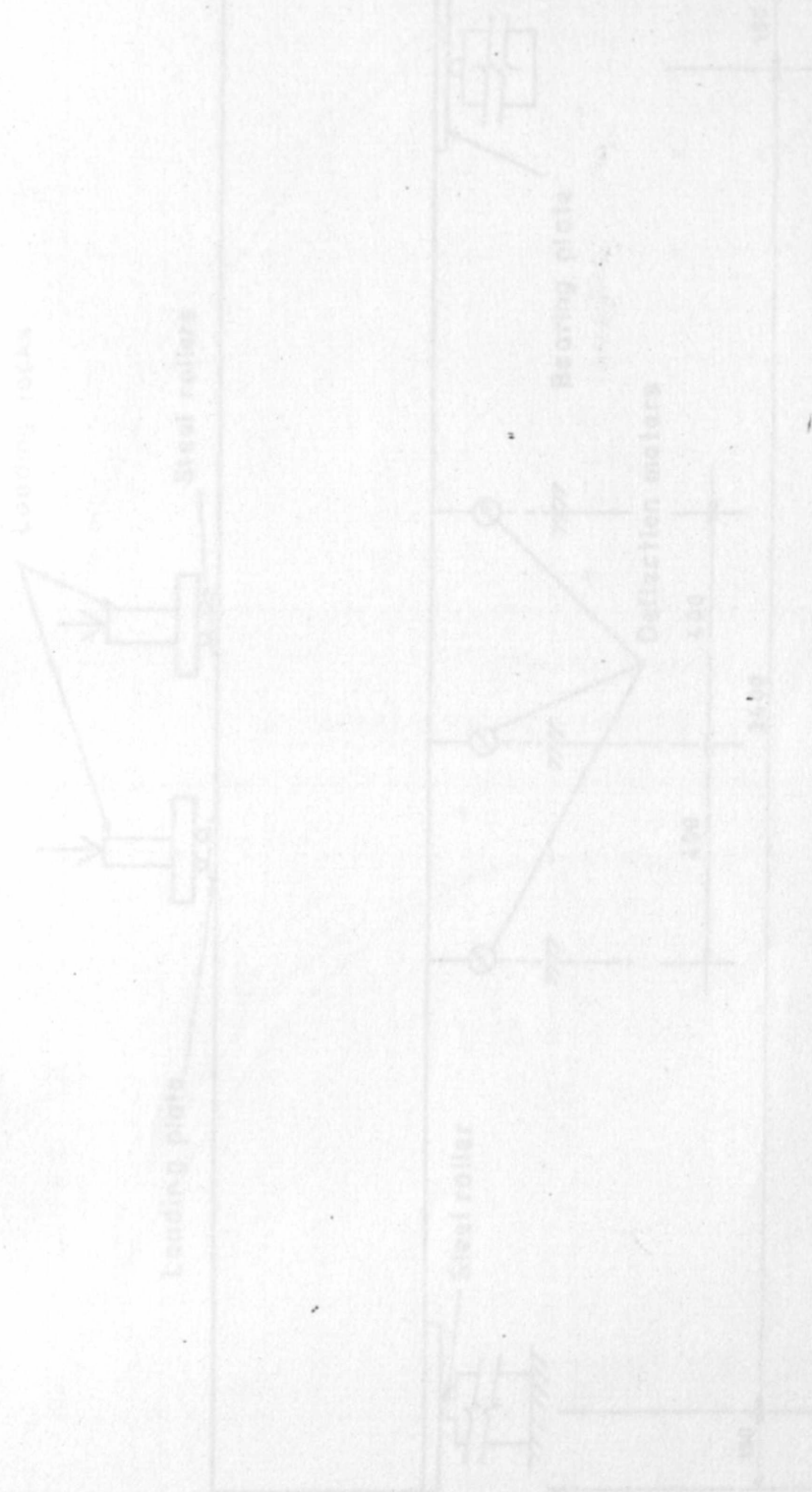


Fig 5.1 - Loading Arrangement.

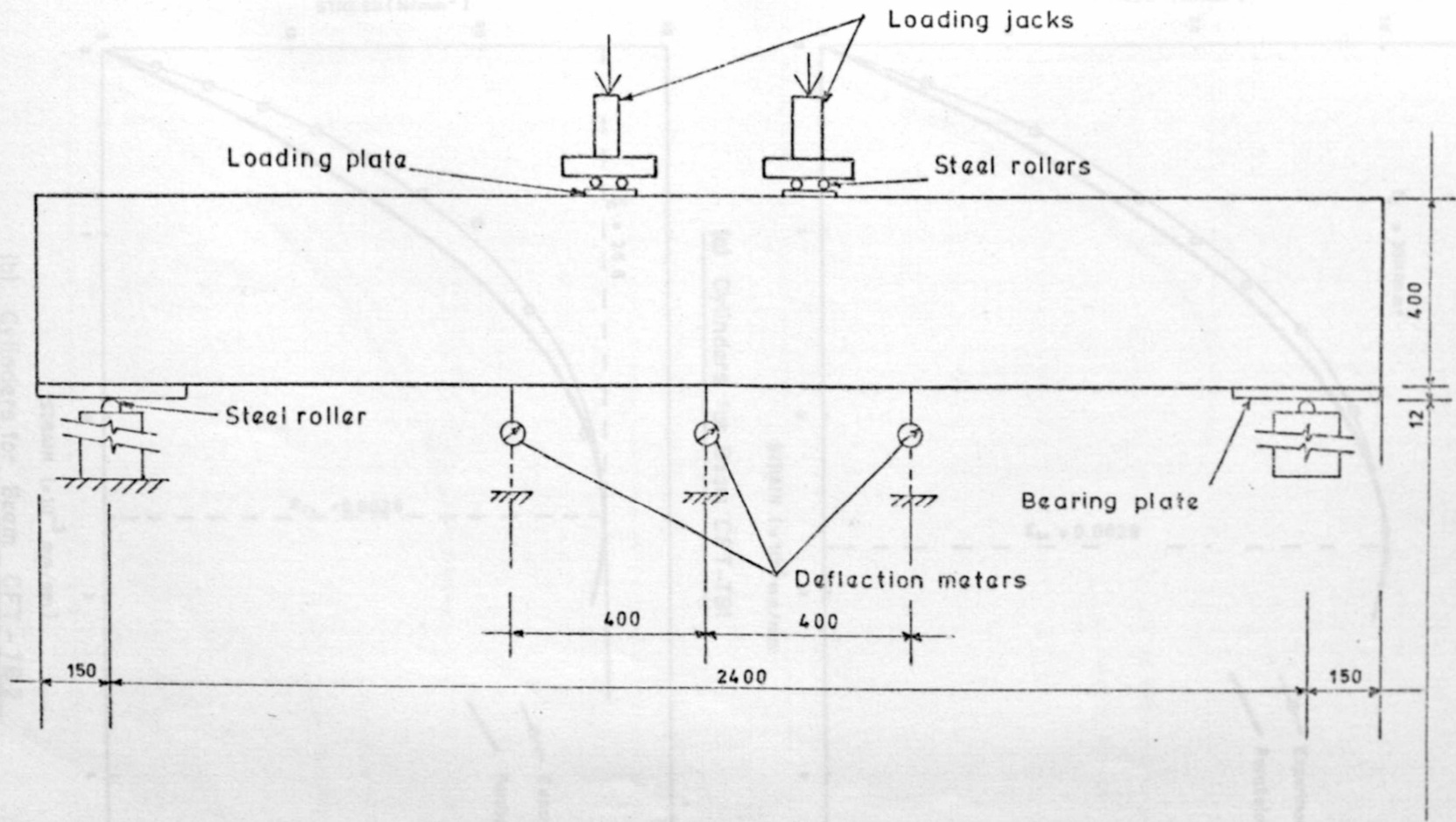
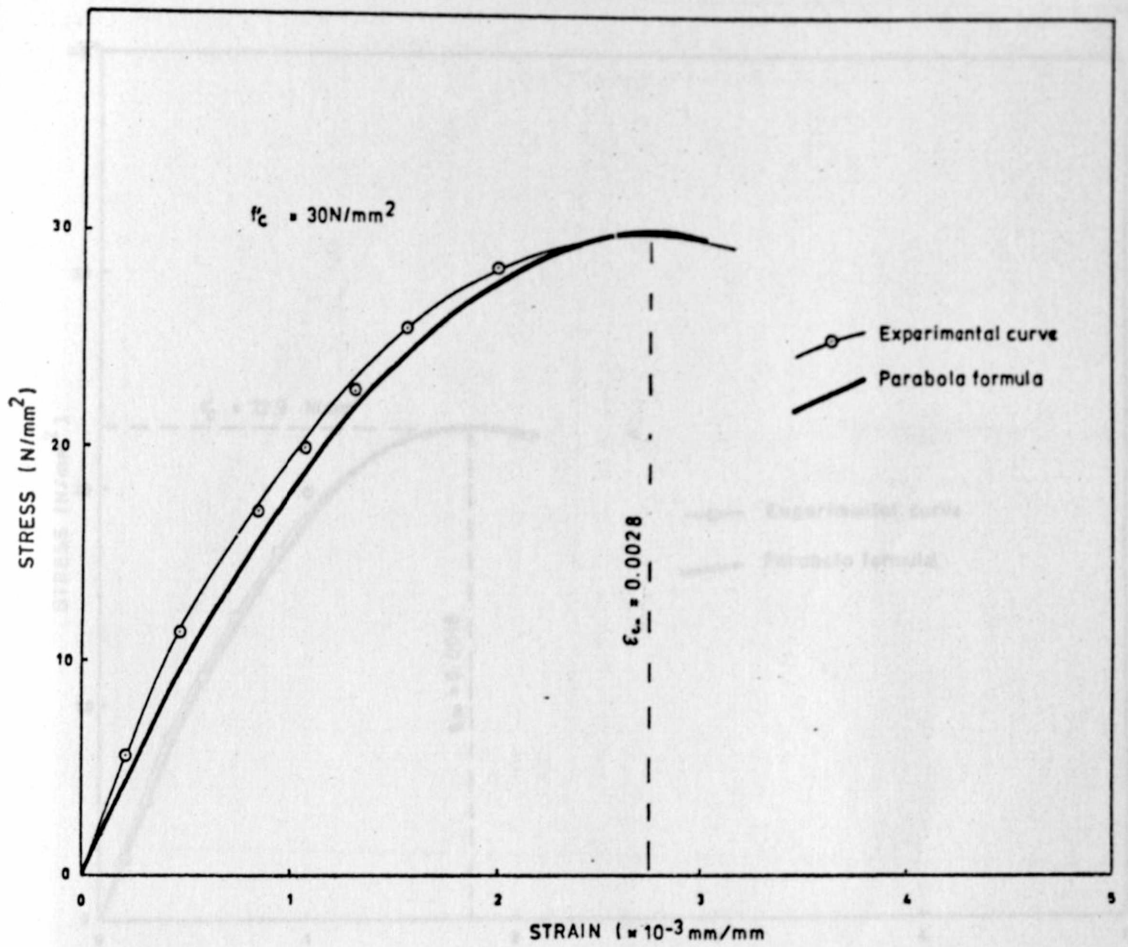
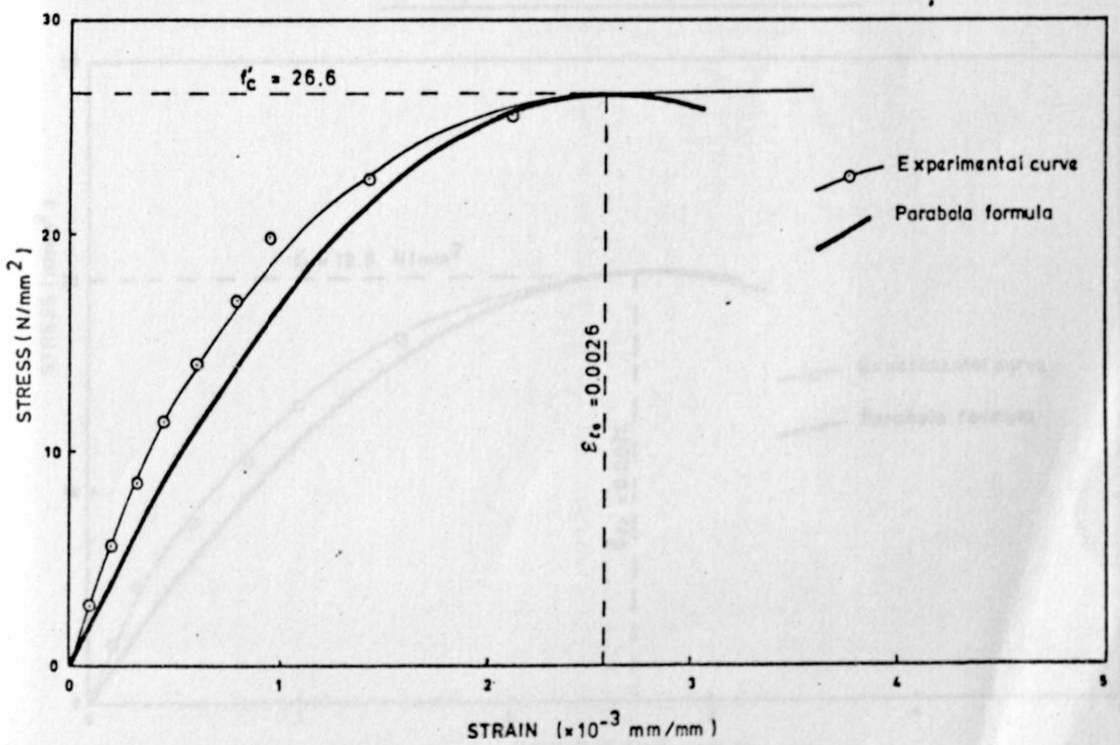


Fig. 4.1 : Loading Arrangement

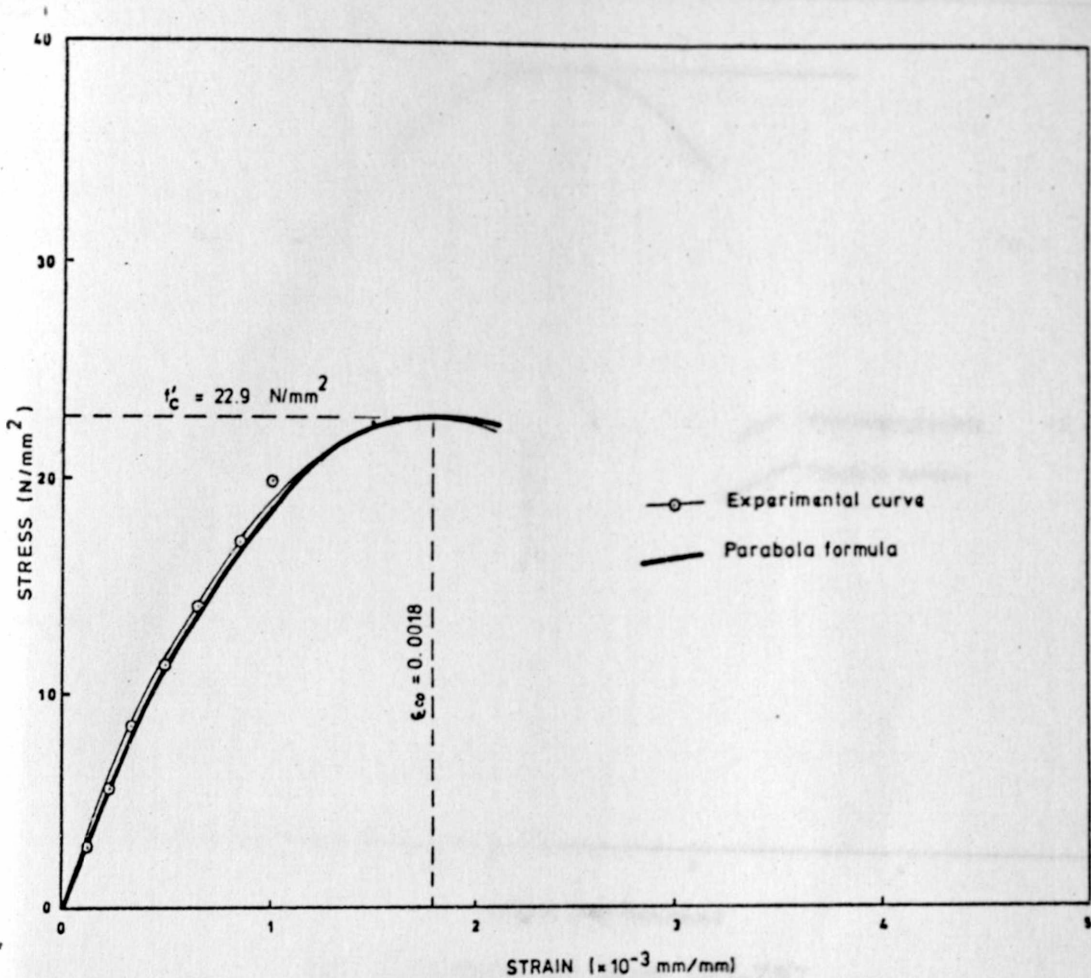


(a) Cylinders for Beam CFT-TB1

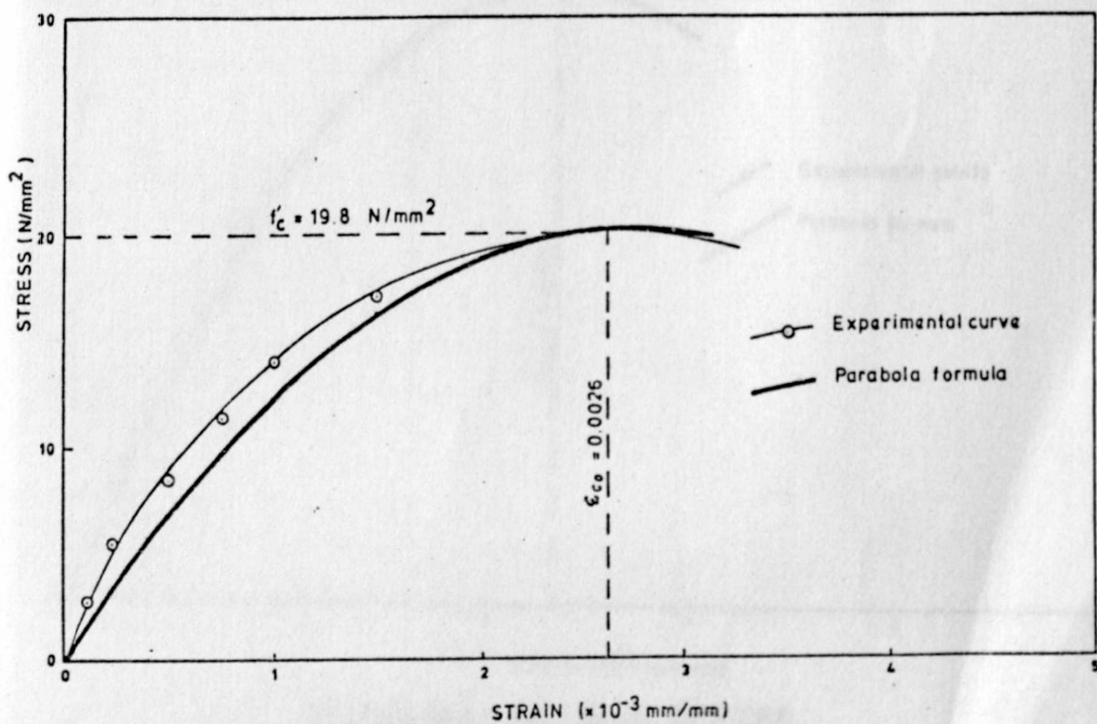


(b) Cylinders for Beam CFT-TB2

Fig. 4.2 : Concrete stress-strain Relationships

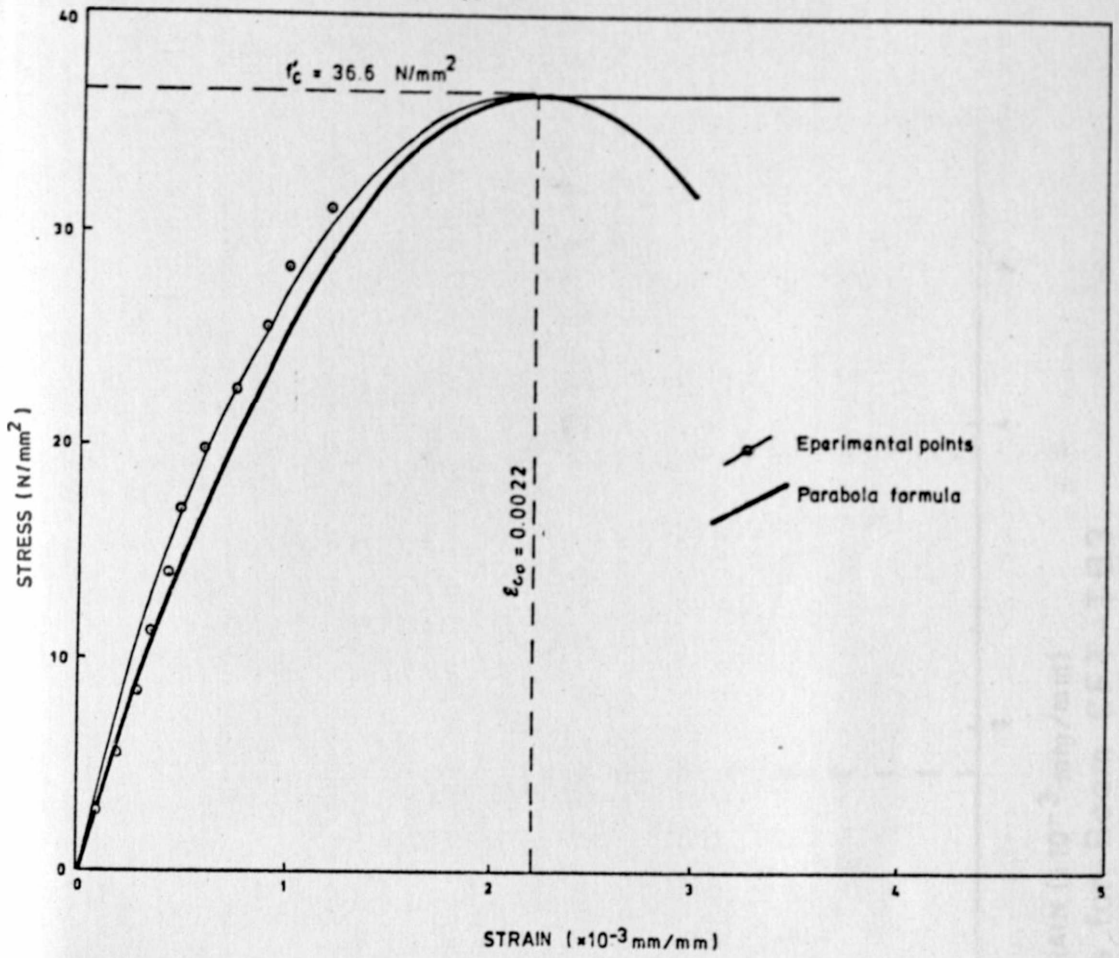


(c) Cylinders for Beam CFT-TB4

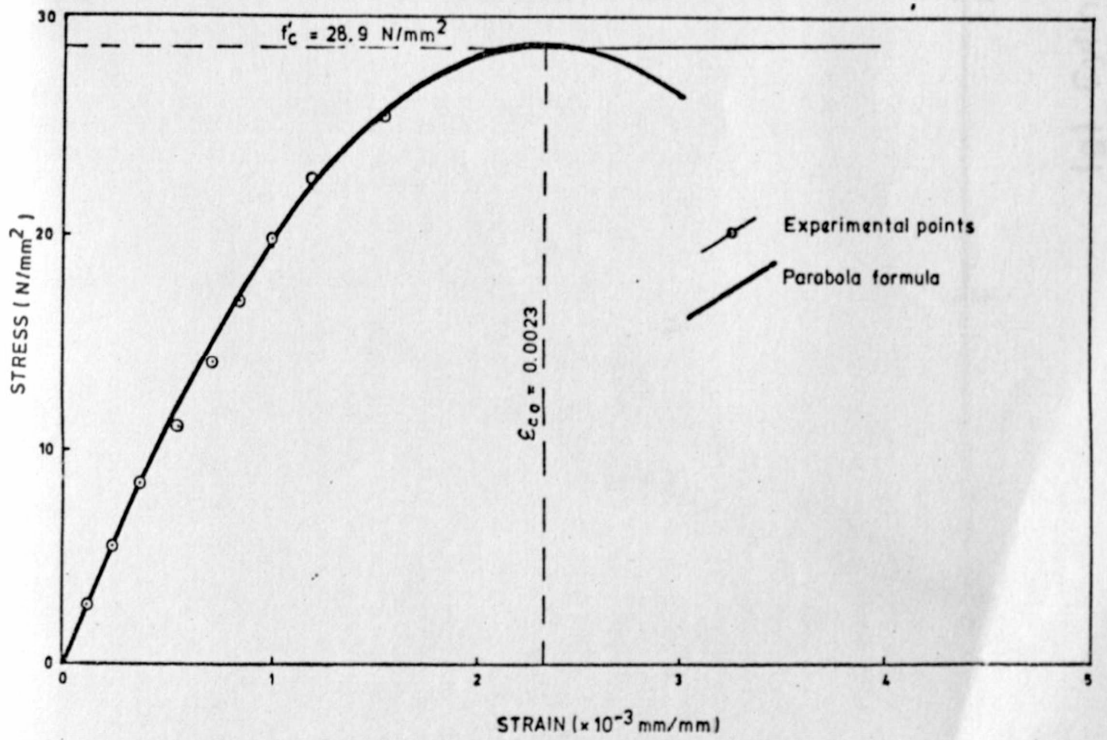


(d) Cylinders for Beam CFT-TB6

Fig. 4.2 : Concrete stress-strain Relationships

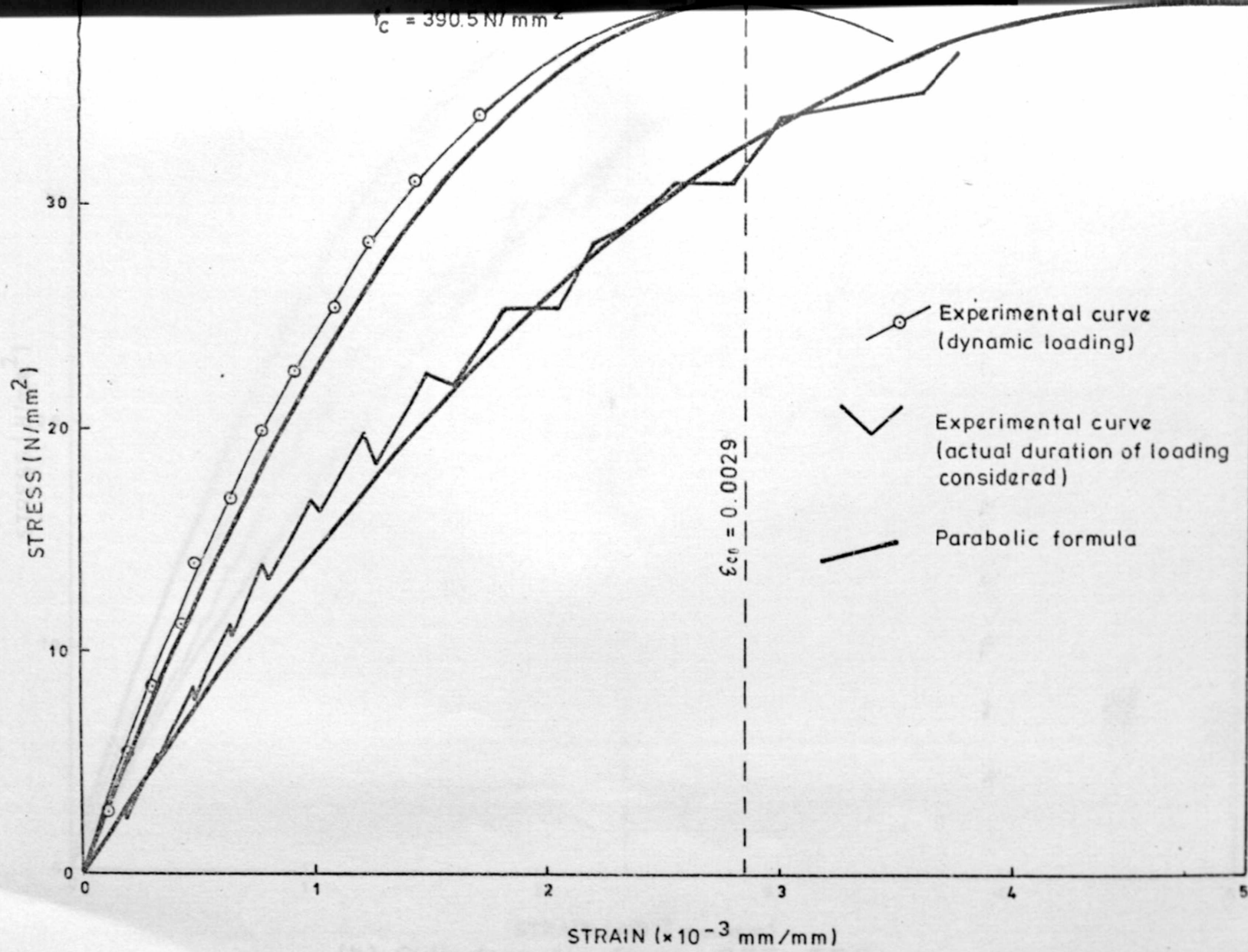


(e) Cylinders for Beam CFT-TB7



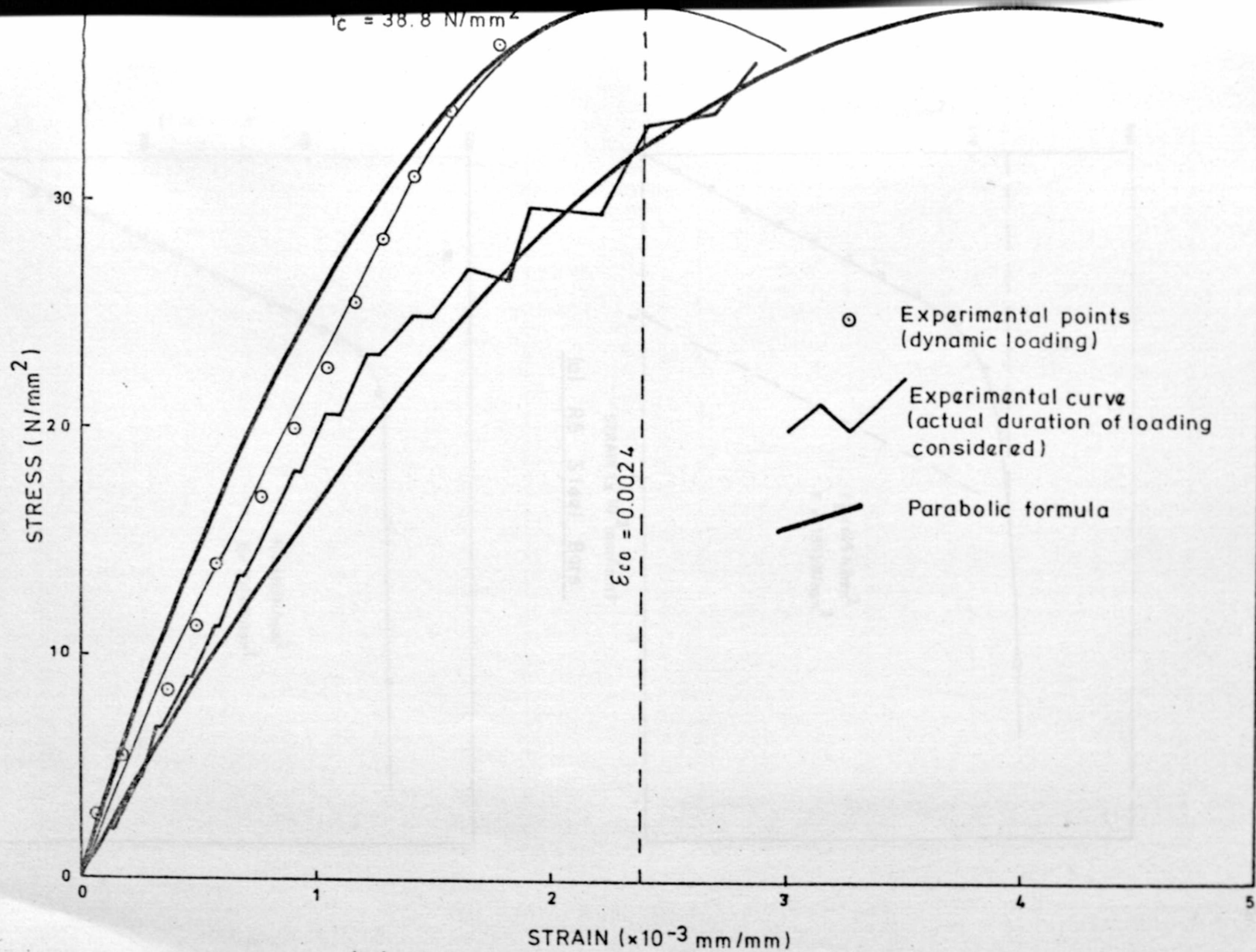
(f) Cylinders for Beam CFT-TB8

Fig.4.2: Concrete Stress-Strain Relationships

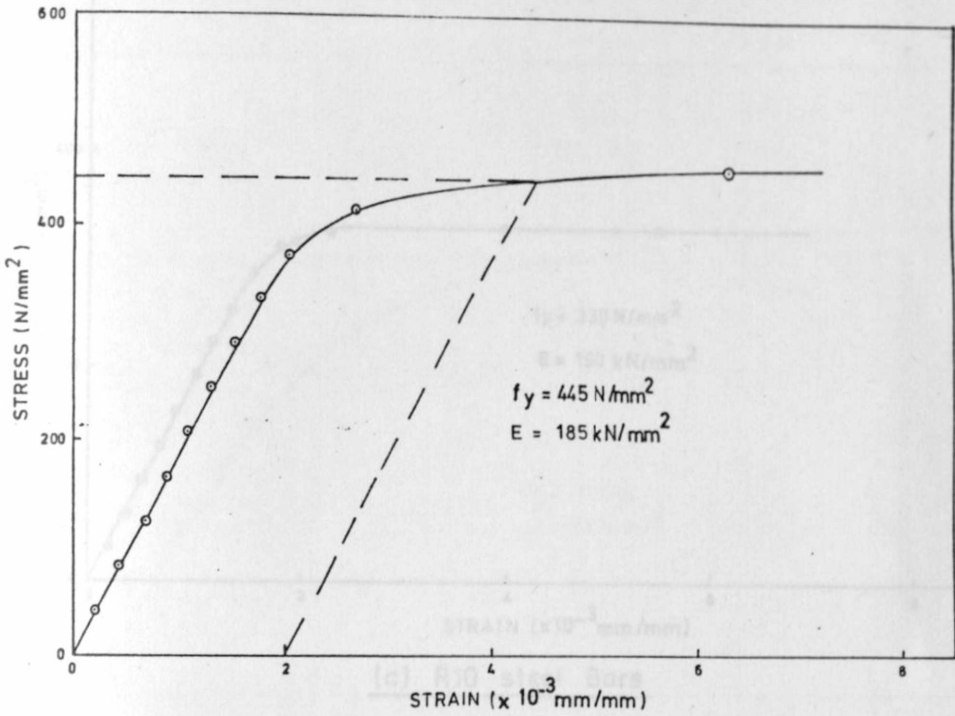


(g) Cylinders for Beam CFT-TB3

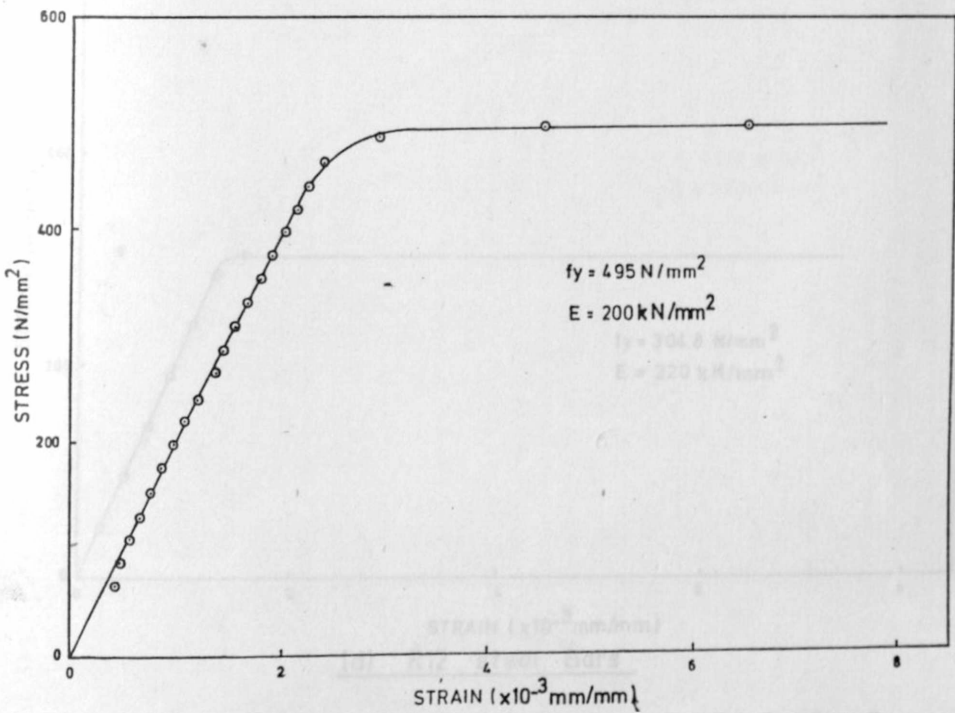
Fig.4.2 : Concrete stress - strain Relationships



(h) Cylinders for Beam CFT-TB5
 Fig. 4.2: Concrete stress-strain relationships



(a) R6 Steel Bars



(b) R8 Steel Bars

Fig. 4.3 : Stress-Strain-Relationships for Reinforcing Bars

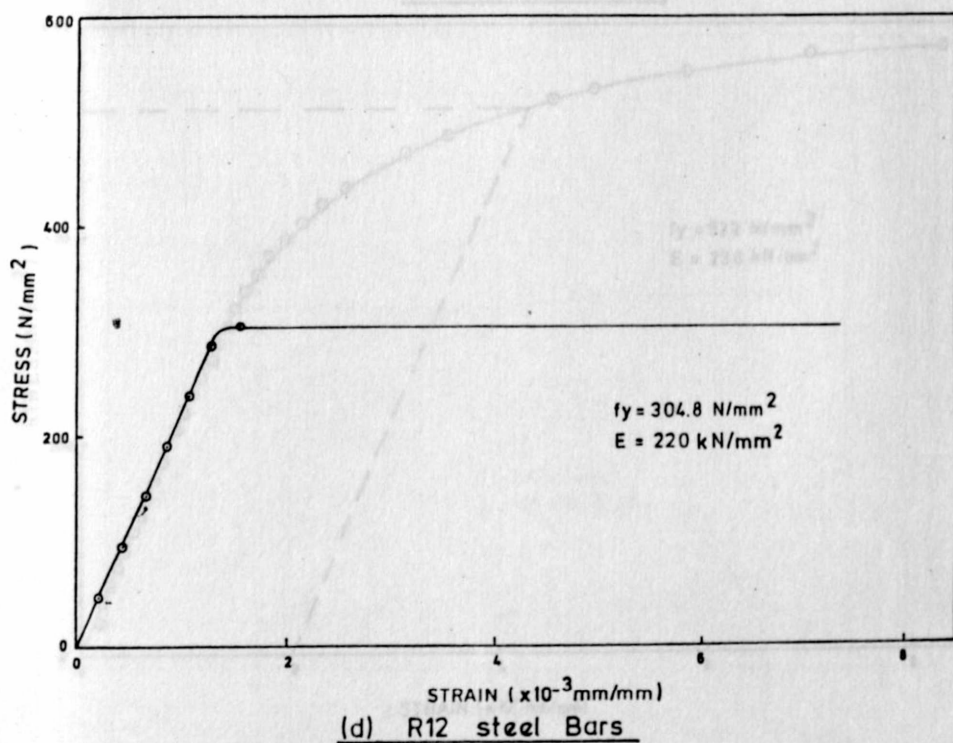
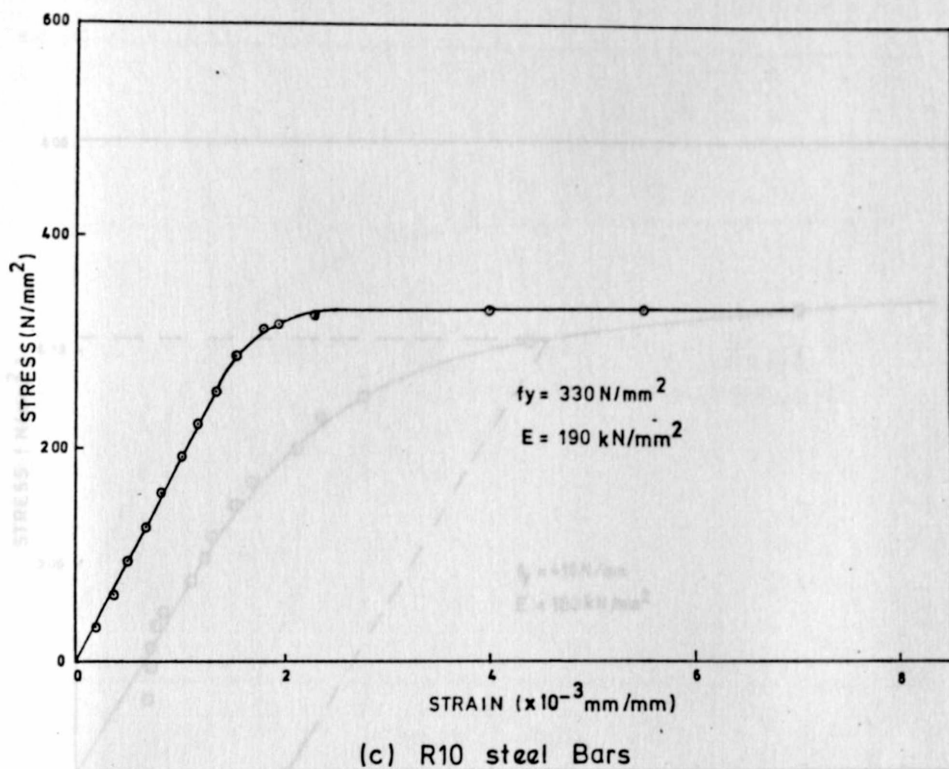
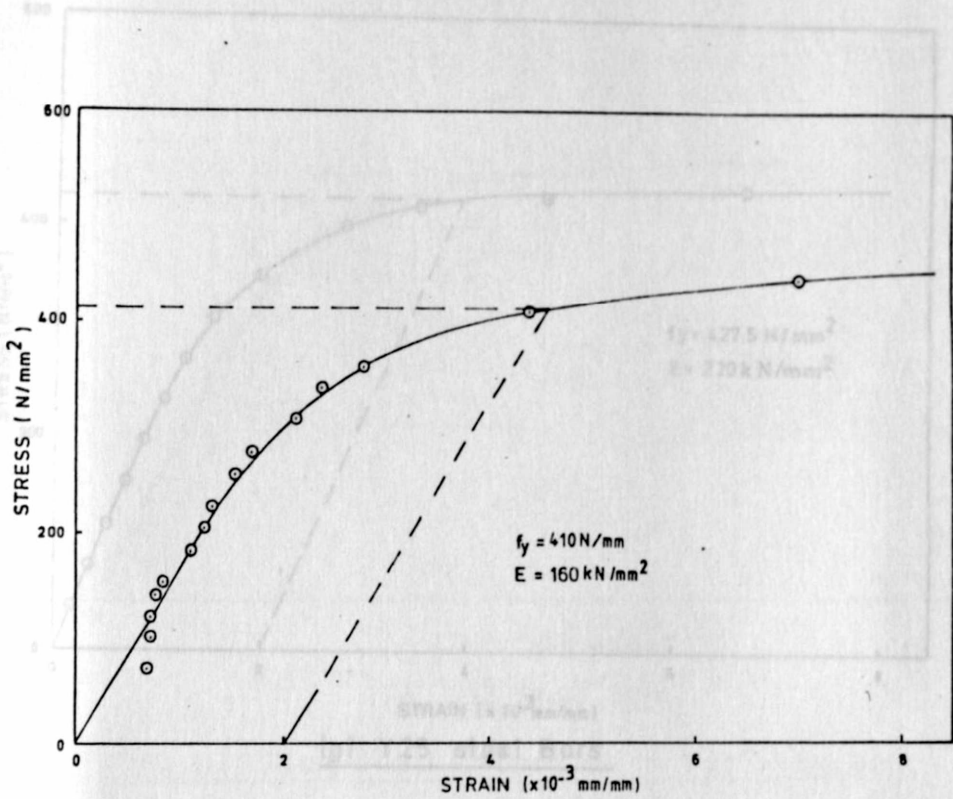
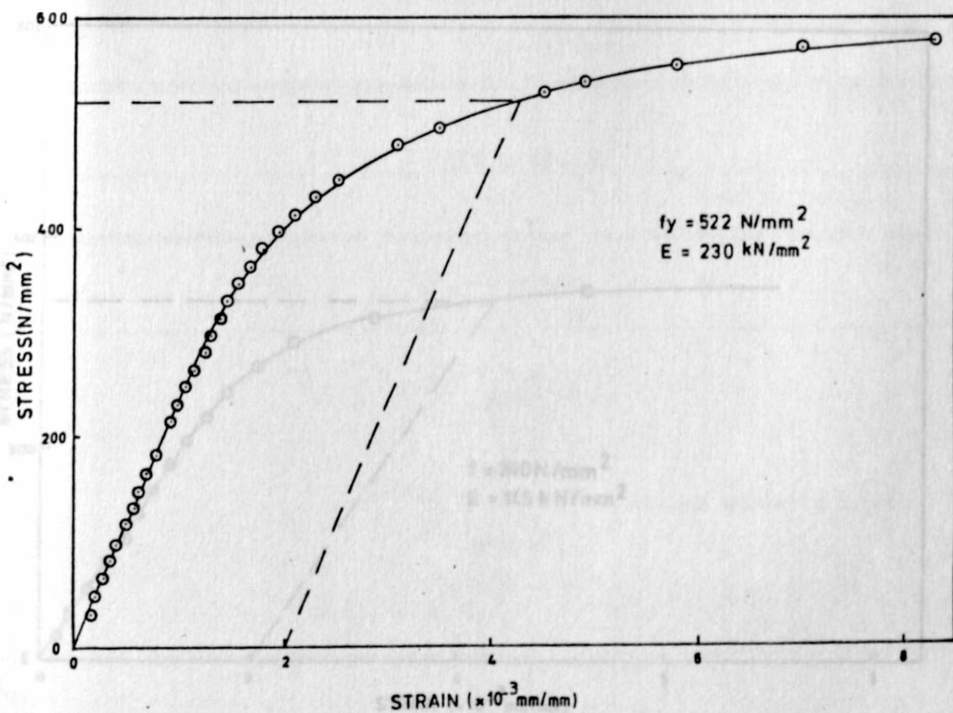


Fig. 4.3: Stress-Strain Relationships for Reinforcing Bars

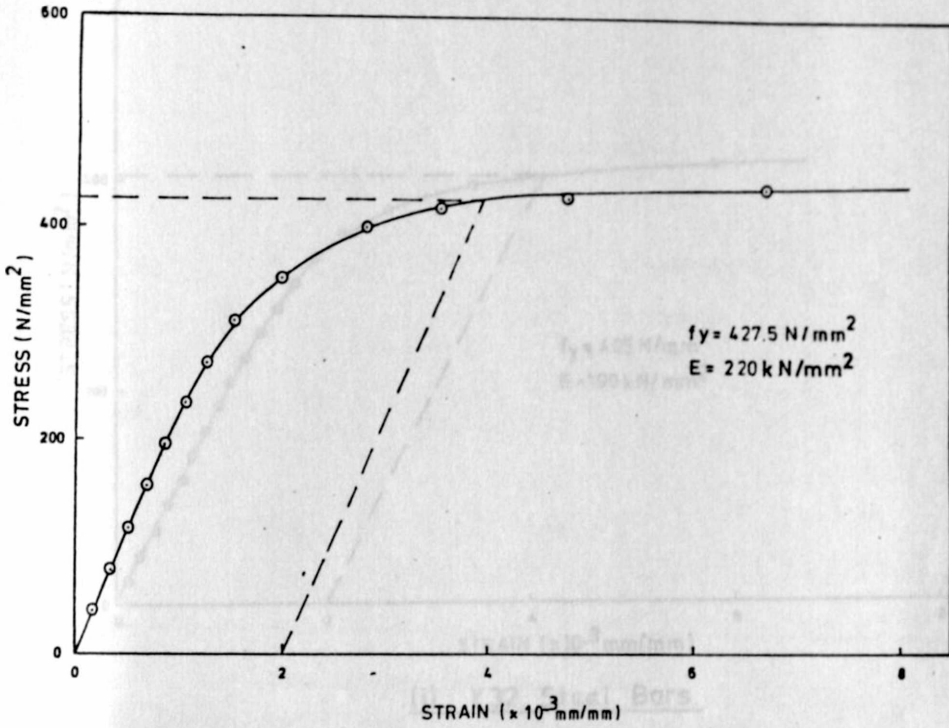


(e) Y10 steel Bars

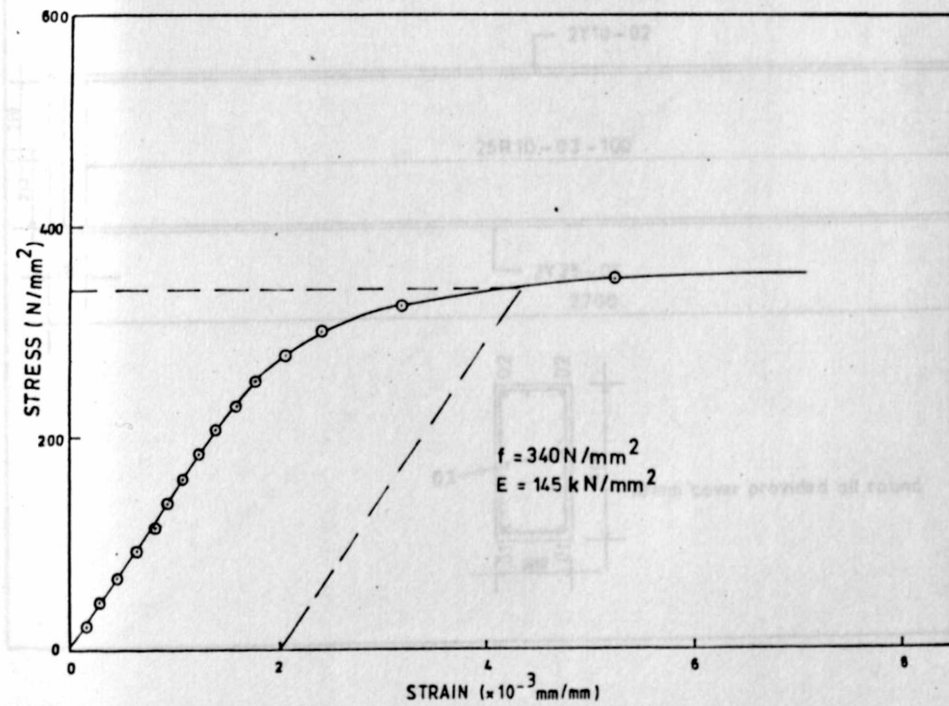


(f) Y12 steel Bars

Fig.4.3 : Stress-Strain Relationships for Reinforcing Bars

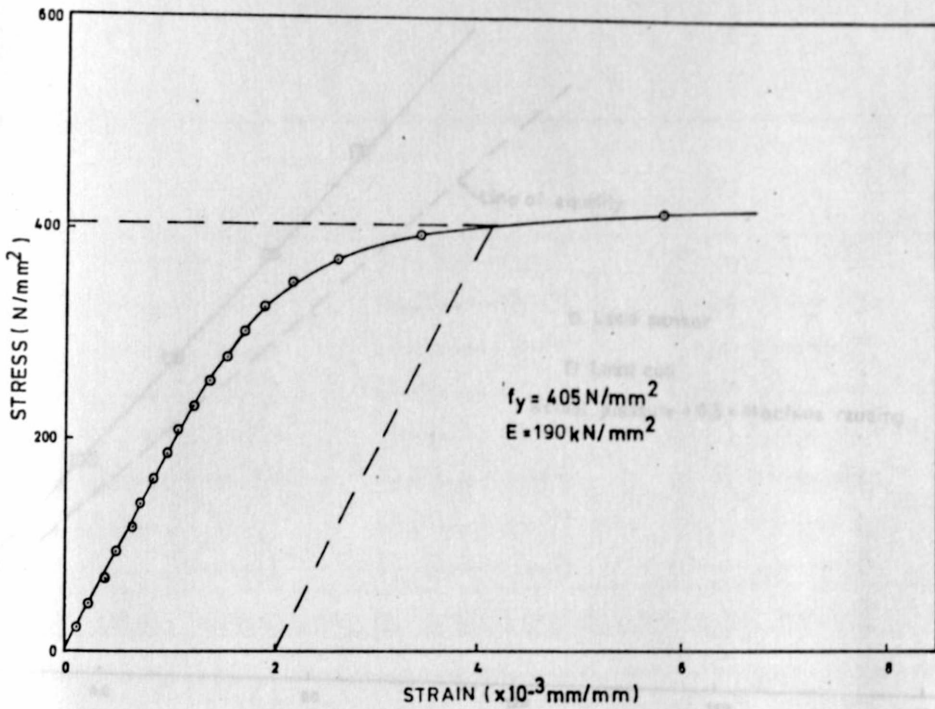


(g) Y25 steel Bars



(h) Y32A steel Bars

Fig. 4.3 : Stress - Strain Relationships for Reinforcing Bars



(i) Y32 Steel Bars

Fig. 4.3 : Stress-Strain Relationships for Reinforcing Bars

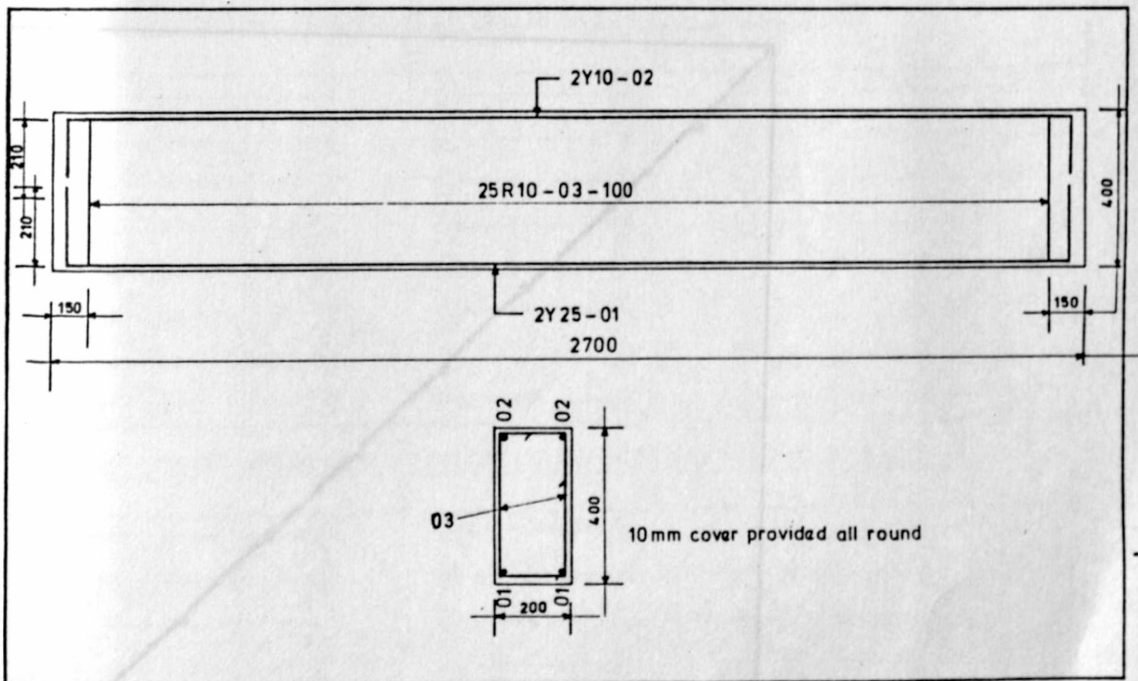


Fig. 4.4 : Typical Reinforcing Detail

(Bar sizes were varied for the various test specimens as shown in Table 4.1)

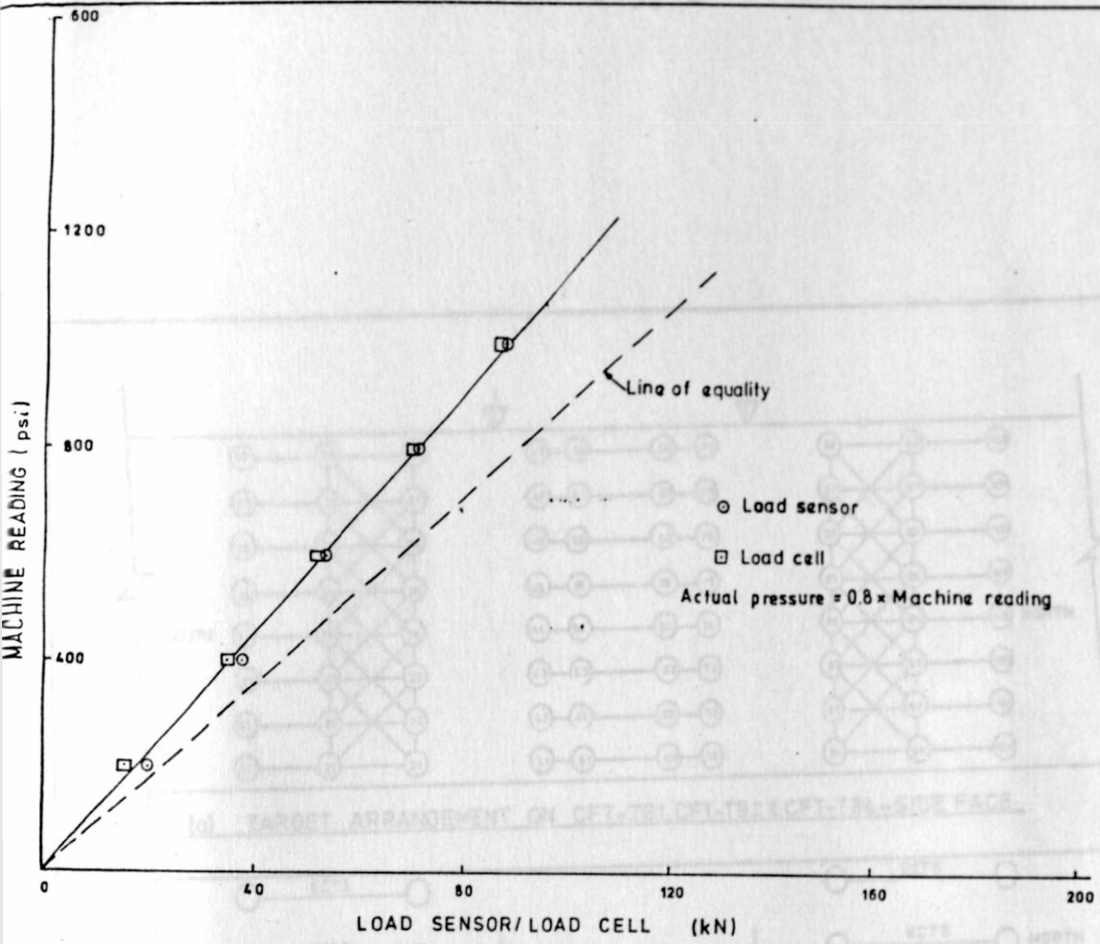


Fig. 4.5: Calibration of the Beam loading machine

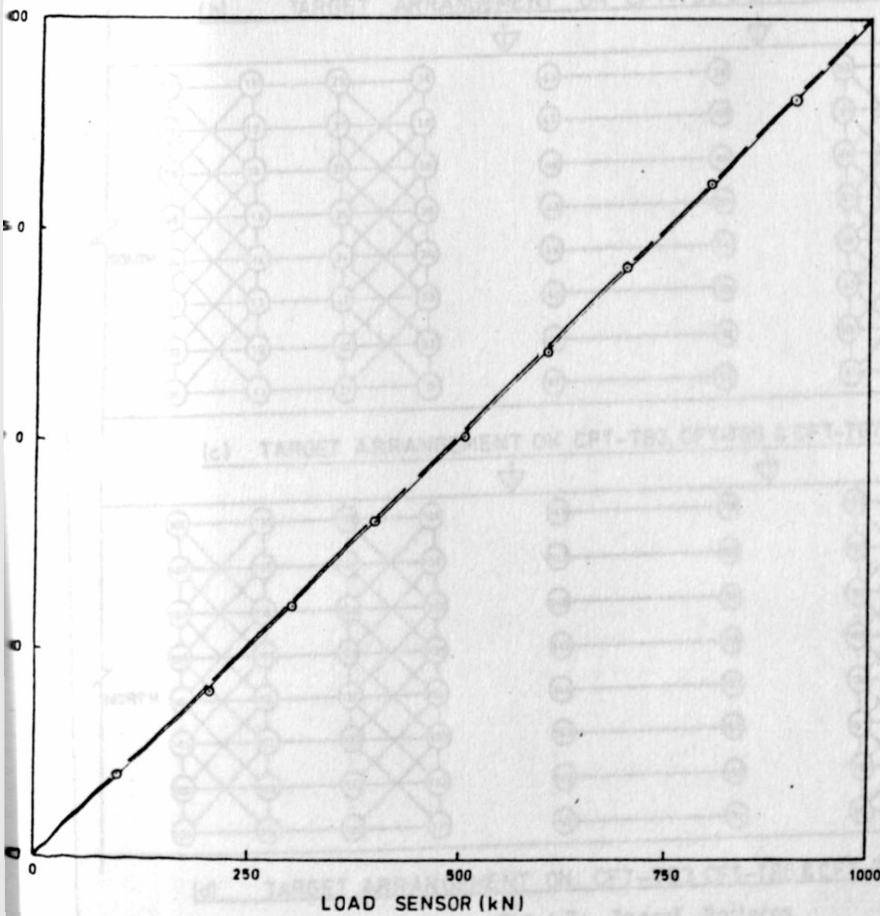
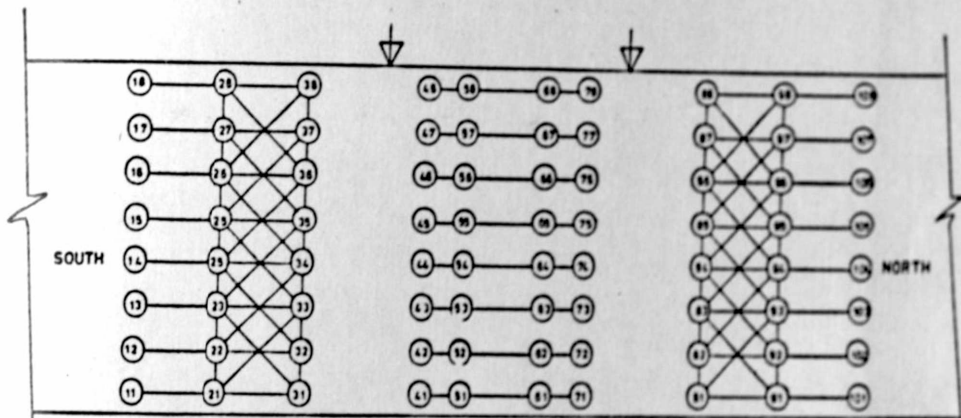
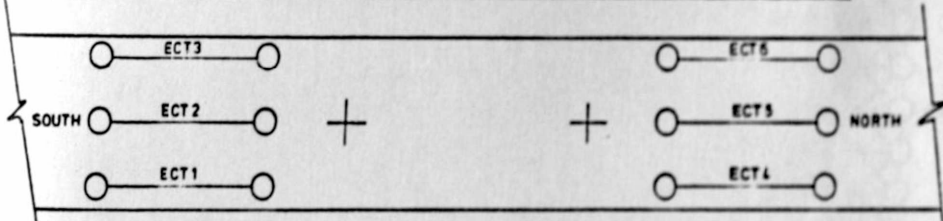


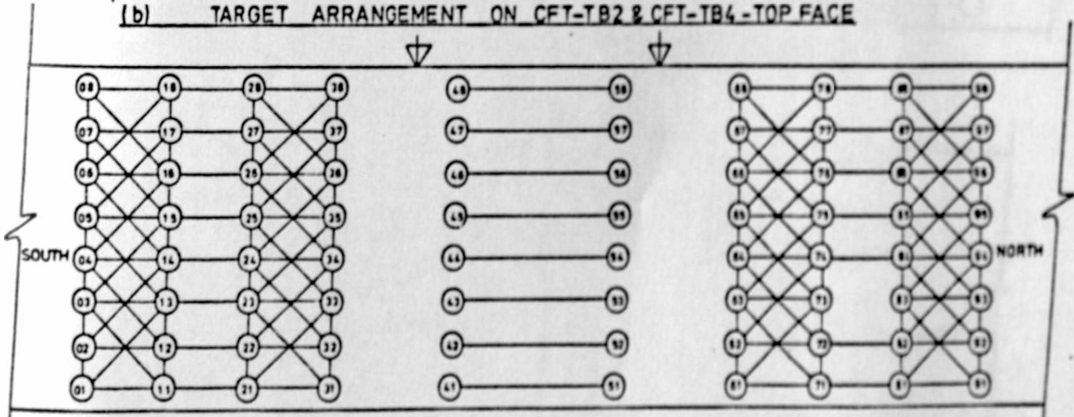
Fig. 4.6 Calibration of cylinder crushing Machine



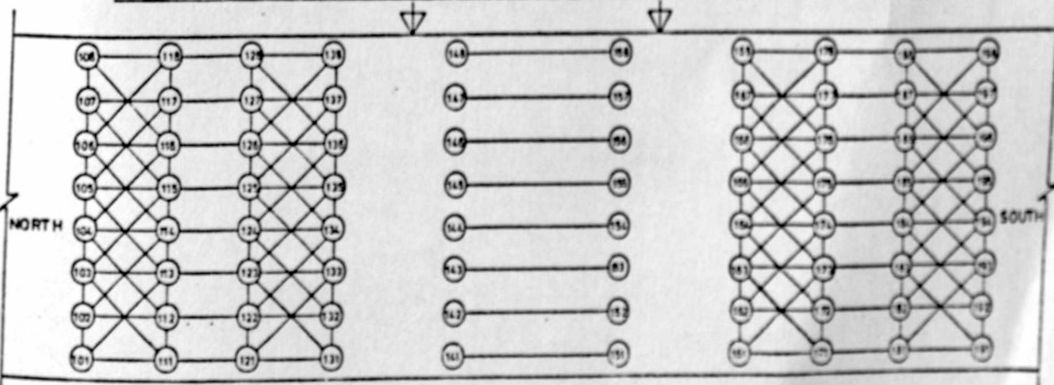
(a) TARGET ARRANGEMENT ON CFT-TB1, CFT-TB2 & CFT-TB4 - SIDE FACE



(b) TARGET ARRANGEMENT ON CFT-TB2 & CFT-TB4 - TOP FACE



(c) TARGET ARRANGEMENT ON CFT-TB3, CFT-TB6 & CFT-TB7 - SIDE FACE (A)



(d) TARGET ARRANGEMENT ON CFT-TB3, CFT-TB6 & CFT-TB7 - SIDE FACE (B)

Fig. 4.7: Target Patterns

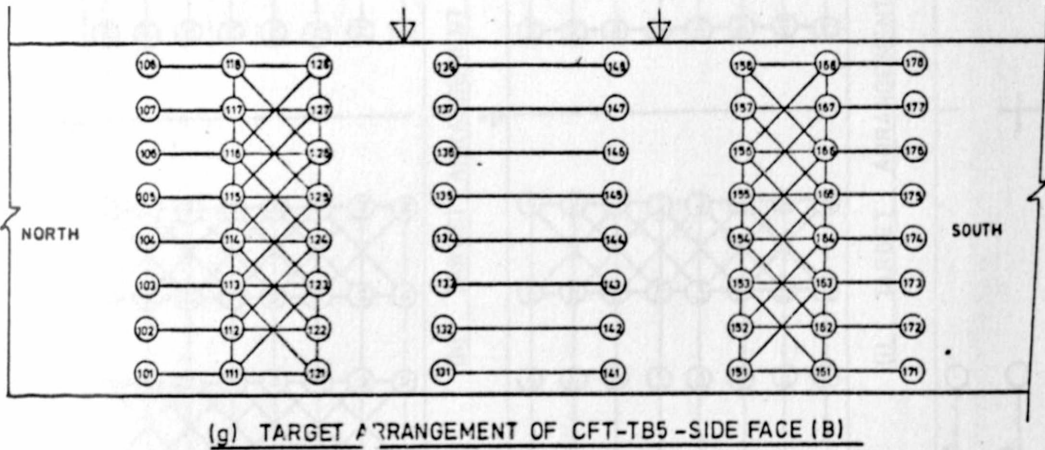
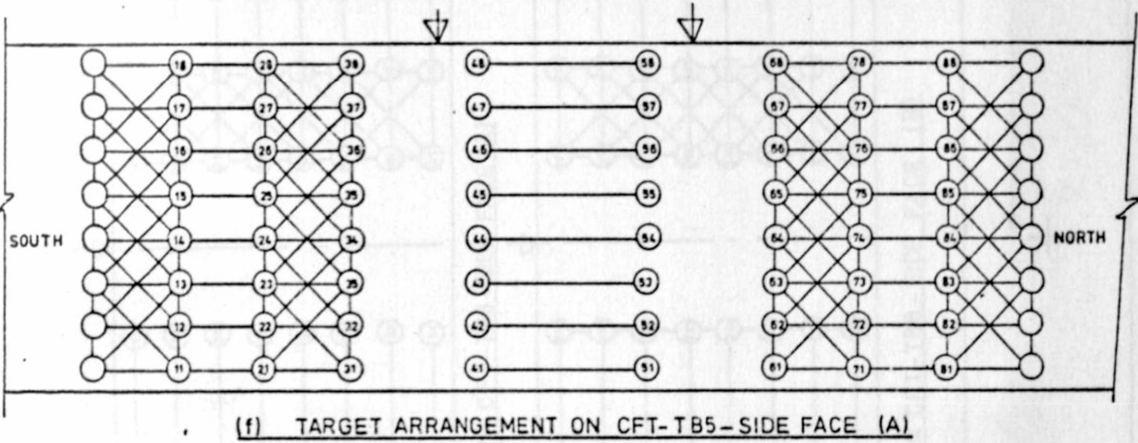
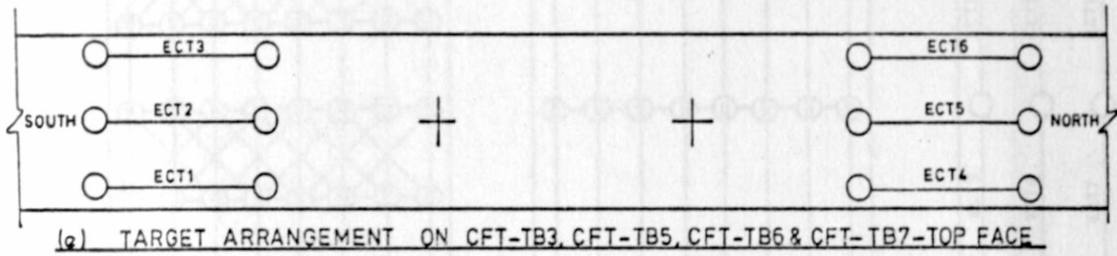
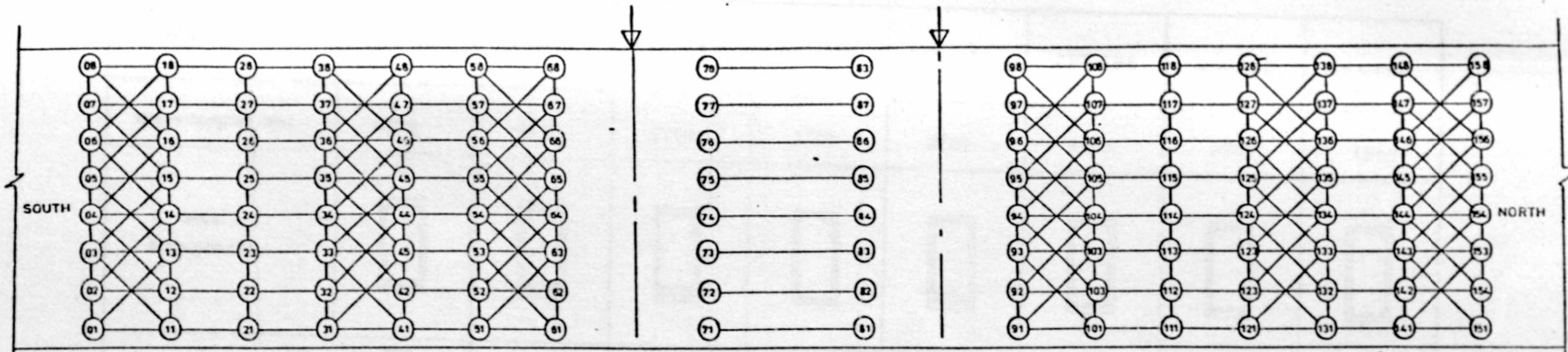
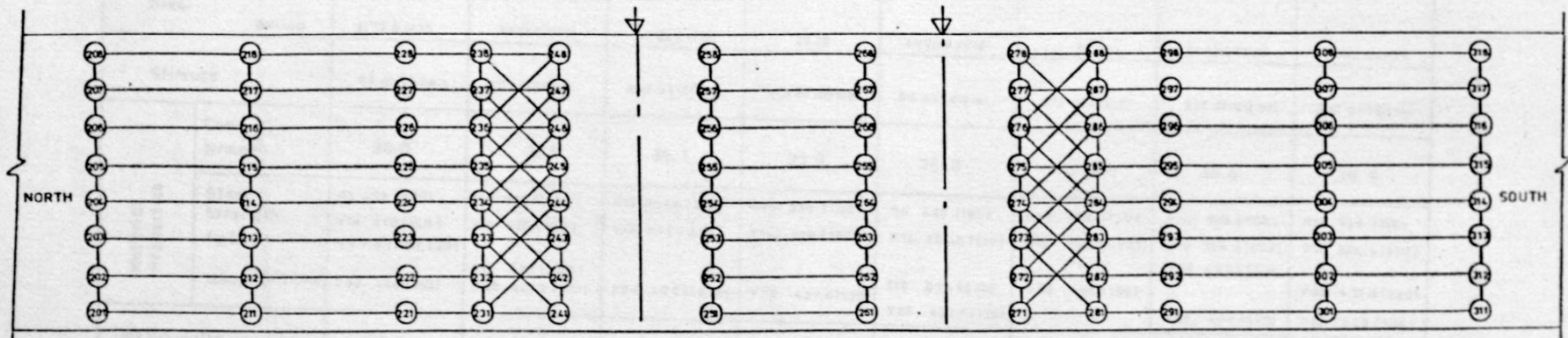


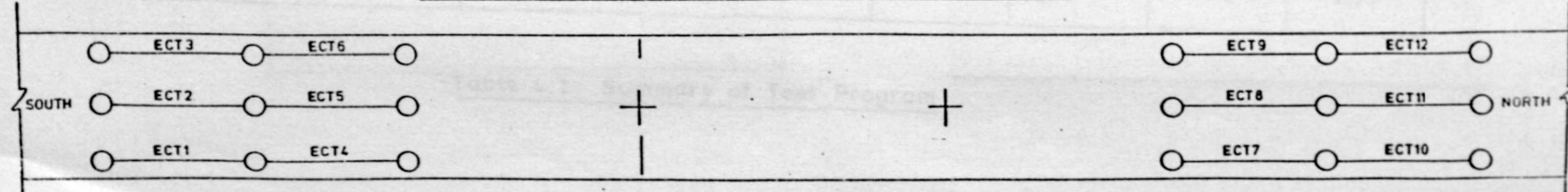
Fig 4.7 : Target Patterns



(h) TARGET ARRANGEMENT ON CFT-TB8-SIDE FACE (A)



(i) TARGET ARRANGEMENT ON CFT-TB8-SIDE FACE (B)



(j) TARGET ARRANGEMENT ON CFT-TB8-TOP FACE


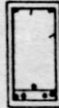




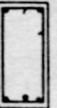
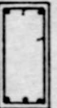
BEAM NAME		CFT-TB1	CFT-TB2	CFT-TB3	CFT-TB4	CFT-TB5	CFT-TB6	CFT-TB7	CFT-TB8
Beam length (mm)		2600	2700	2700	2700	2700	2700	2700	4000
Steel Arrangement									
Longitudinal Steel	Top	2Y10	2Y10	2R12	2Y10	2R12	2R12	2R12	2R12
	Bottom	2Y32 & 1Y25	4Y25 & 1Y12	4Y25 & 1Y12	2Y25	4Y25 & 1Y12	3Y32	2Y32 & 1Y25	2Y32 & 1Y25
Stirrups		R8 at 100 mm	R10 at 100 mm	R12 at 100 mm	R10 at 100 mm	R6 at 50 mm	R10 at 100 mm	R10 at 100 mm	R10 at 100 mm
Material Properties	Conc. f_c N/mm ²	30.0	26.6	39.1	22.9	38.8	19.8	36.6	28.9
	Steel Strength f_y (E)	R8 495 (200) Y10 410 (160) Y25 427.5 (220)	R10 330 (190) Y10 410 (160)	R12 304.8 (220) Y12 522 (230)	R10 330 (190) Y10 410 (160)	R6 445 (185) R12 304.8 (220)	R10 330 (190) R12 304.8 (220)	R10 330 (190) R12 304.8 (220) Y25 427.5 (220)	R10 330 (190) R12 304.8 (220)
	N/mm ² (kN/mm ²)	Y32 340 (145)	Y12 522 (230) Y25 427.5 (220)	Y25 427.5 (220)	Y25 427.5 (220)	Y12 522 (230) Y25 427.5 (220)	Y32 405 (190)	Y32 405 (190)	Y25 427.5 (220) Y32 405 (190)
M/Vd ratio		2.5	2.5	2.5	2.5	2.5	2.5	2.5	4.125

Table 4.1: Summary of Test Program

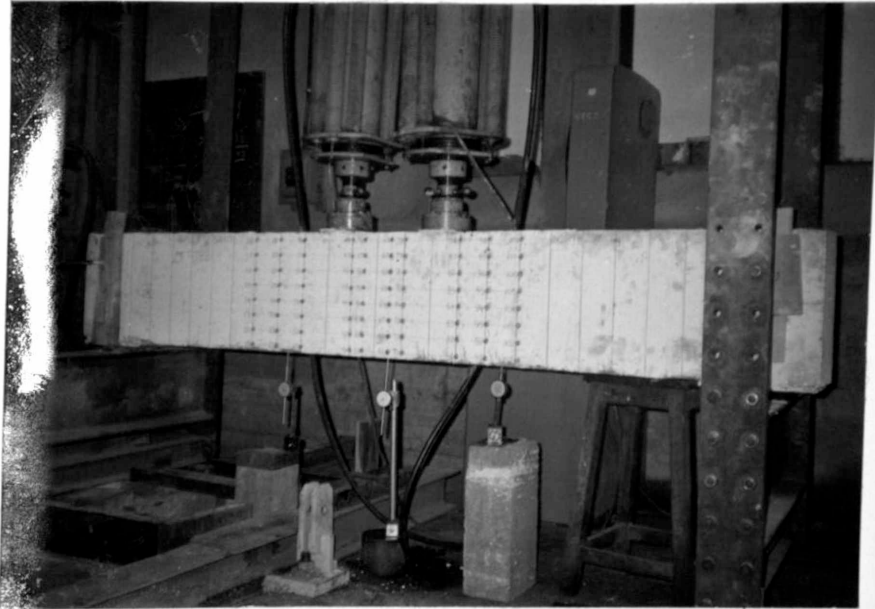


Plate 4.1: Initial Set up of Test Rig
 (Notice the packing against
 left hand side support)

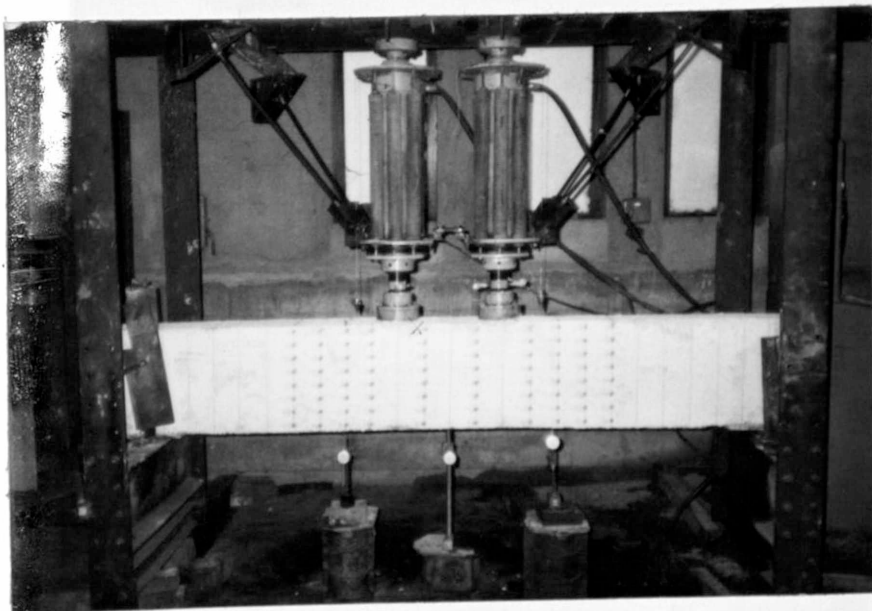


Plate 4.2: Revised Set up of Test Rig
 (Notice introduced anchorage on jacks and
 see revised propping of left hand side support
 in plate 4.3)
 (Notice also the plumb bobs)

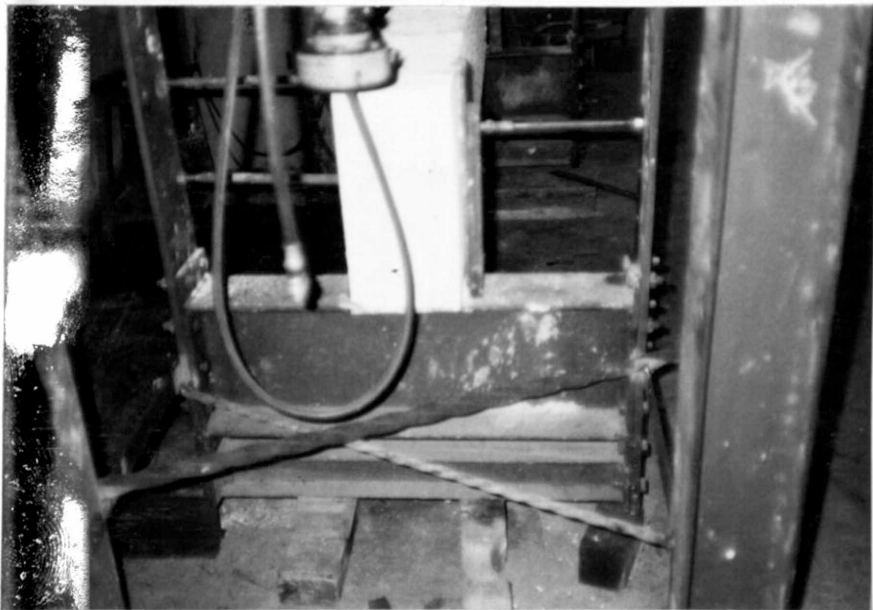


Plate 4.3: Anchorage of Support

(Notice the trussed square twisted bar)

CHAPTER 5
ANALYSIS AND DISCUSSION

A comparative study of the predictions of the theoretical model developed in Chapter 3 and the results of the experimental program reported in Chapter 4 is presented in this chapter. It is recalled that the parameters of the test program were the longitudinal steel content, the transverse steel content, the concrete strength and the $\frac{M}{Vd}$ ratio. These were chosen so as to test the validity of the trends indicated in Figures 3.7 to 3.9. In addition to these trends, other profiles involving the measured strains are studied. Where transverse and principal compression strains are plotted, the theory is plotted only in the region below the neutral axis since the model assumes that it is this region which is cracked.

To enable easy comparison of behavioral trends, the experimental results and the theoretical predictions are plotted side by side on suitable graphs. Before these comparisons are made, the observed behaviour of test specimens and the limitations of the test specimens and testing equipment are presented.

5.1 Behaviour of Test Specimens

All the test specimens, except beams CFT-TB1 and

CFT-TB6 failed by crushing of concrete in flexure in the region between the loads. The tests for all these beams failing in flexure were completed within a day except for beams CFT-TB5 which was unloaded at a load stage of 249.7kN after the rods used in anchoring the test rig bent. The testing for this beam was resumed seven days later after the test rig was upgraded to the state described in chapter 4. Plates 5.1 to 5.6 show the typical trend for beams which failed in flexure.

Beam CFT-TB1 had a typical shear failure. On the first day of the test, testing was stopped after spalling occurred at one of the supports premature to the beam failure. The spalled end was reclaimed by means of concrete mortar and in addition, 300mm x 300mm x 12mm seating plates were used at each of the supports. The beam was tested to failure seven days later. Some of the stages of loading are shown in plates 5.7 to 5.11.

As shown in plate 5.12, beam CFT-TB6 had bond failure.

The mode of cracking was observed to be generally the same for all the test specimens. Flexural cracks, which are practically vertical, formed first. As the load was increased, these developed into inclined cracks. The spacing of the cracks in the longitudinal direction varied from about 100mm in the regions near the load to more than 200mm towards the supports.

Vertical stirrups rarely had more than three inclined cracks crossing them and most of the cracks did not extend beyond the surface 150mm from the top face. These crack patterns can be observed in plates 5.1 to 5.3

5.2 Limitations of Test Specimens and Testing Equipment

It is assumed, in the development of theory that the model is uniformly cracked and that the cracks are closely spaced in the region below the neutral axis. The description of the test specimens in the last section shows that uniform cracking assumed in the theoretical model did not take place for the specimens tested. With only very few cracks some of the gauge lengths for measurement of strains did not cross any cracks. However, for analysis, average strains evaluated in a manner shown in Appendix C were used. The averaging of strains was assumed to minimise the local effects due to the sparse cracking.

The stress picture of the prediction model is assumed to be free from any localised stress concentration effects which occur at and around loading and reaction points. According to Saint Venant's Principle the complex stress condition resulting at such load transfer points can be considered to be confined to the region within a radius equal to the effective depth of the beam as illustrated in Figure 5.1. Due to the

size of the test specimens, which was limited by the available testing facilities, some of the gauge lengths extended into such regions. However, these localised effects are more severe at the load transfer point and less severe towards the boundaries of these described regions and it is assumed that in the chosen gauge lengths (see Figure 4.7) extreme effects of stress concentrations are avoided. Moreover, it was of interest to find out how well the response of a specimen with stress concentrations is predicted by the compression field theory.

The strains were obtained by means of mechanical demec meters. These were calibrated in inches per division with one division equivalent to 0.0001 inches. Readings were taken to the nearest one division. The possible error in readings due to these meters was computed based on repeated readings over a given gauge length using the meters. These readings showed that an error of ± 2 divisions could occur when the meter is held steadily on the target points. This means an error in the measured strains of upto $\pm 0.05 \times 10^{-3}$ for the 4 inch gauge lengths $\pm 0.025 \times 10^{-3}$ for the 8 inch gauge lengths and $\pm 0.044 \times 10^{-3}$ for the 4.56 inch gauge lengths is possible. For a beam with bottom longitudinal steel yield strain value of 2.3×10^{-3} the respective errors that can occur at yield expressed as percentages are $\pm 2.2\%$, $\pm 1.1\%$ and $\pm 1.9\%$. These percentages are larger at lower strains.

Orange (1978) and included in Appendix C. Average values of the measured strains are used and plots similar to those for average transverse strain profiles are given in Figure 5.3.

The loading jacks were calibrated as explained in Chapter 4. The loads were read to the nearest 5psi (0.45KN) in units of pressure and the equivalent load in metric units obtained from the calibration curve. The final load used is subject to errors that arise from determining the calibration curve and reading the loads. Using the graph of Figure 4.5, an average error of about $\pm 3.75\%$ is estimated.

5.3 Transverse Strains Profiles and Principal Compression Strains Profiles.

The experimental average transverse strains at six levels in the section were obtained from the measured strains as illustrated in Appendix C. The six levels were 50mm apart, the first and the sixth being 75mm clear of the edges. As already noted, theoretical predictions for transverse and principal diagonal strains were restricted to the region below the neutral axis. Typical transverse strains profiles are plotted in Figure 5.2.

The experimental average principal compression strains are computed based on Mohr's circle of compatibility of strains by a method developed by Onsongo (1978) and included in Appendix C. Average values of the measured strains are used and plots similar to those for average transverse strains profiles are given in Figure 5.3.

As expected, it is observed from Figures 5.2 and 5.3 that for both theoretical and experimental trends, the strains increased with load. For transverse strains, the increase was greatly accelerated after the yield of transverse steel. However, although theory predicts that for a given load the strains are consistently largest at the bottom of the section decreasing towards the neutral axis, the experimental plots do not exhibit a similar pattern. In the later case, higher strains at rows other than the bottom level are observed.

Observation of the test specimens revealed that the variation of strains was related to the crack patterns. Rows with high strains were those in gauge lengths crossed by cracks. As shown in Figure 5.2, the transverse strain values in the uncracked region above the neutral axis are low. Although a complete picture requires observation of both faces of the beam, due to the process of averaging, this effect of the crack distribution can also be studied by observation of Plates 5.1 to 5.12 and also Plates C.1 to C.5

The trend of low transverse strains in uncracked concrete is expected. It is likely that the experimental strain profiles were affected by the distribution of cracks and that these differed from the theoretical predictions because specimens were not uniformly cracked.

However, looking at Figures 5.2 and 5.3, for any given load, it is observed that the maximum strains in the section predicted by theory is comparable to the maximum average strain from experiment with the predictions being generally higher than the measured values.

5.4 Longitudinal Strains Profiles

Using the assumed linear variation, prediction of longitudinal strains is possible over the entire section given the extreme compression fibre strain and the depth to the neutral surface. The experimental and theoretical plots are presented in Figures 5.4 and 5.5, average longitudinal strains having been obtained from measured strains as shown in Appendix C.

In Figure 5.4, the profiles from experiment from a region of combined flexure and shear are compared to those from a region in pure flexure. A linear regression analysis of the experimental data plotted in Figures 5.4 and 5.5 yields correlation coefficients close to 1 which are denoted r in the figures. The comparable nature of plots in Figure 5.4(a) and (b) and computed correlation coefficients show that the assumption plane sections remain plane provides a good approximation of the strain profiles.

In most of the plots in Figures 5.4 and 5.5, the experimental strains tended to be higher than the

predicted strains. However, the difference hardly exceeds 5% of the predicted values. Considering the limitations of the test specimens and the testing equipment already discussed, in particular local effects and errors due to testing equipment, the strains obtained from experiment and theory are quite comparable. It is also noted that near failure, where errors due to equipment tend to be minimised and the cracking is more, the theory predicts larger strains than measured over most of the sections.

5.5 Shear Force - Shear Strain Relationships

Typical shear force - shear strain relationships are plotted in Figure 5.6. The maximum shear strains were obtained by use of equation (3.18). The experimental response corresponds to average strains at row 2 of Target Patterns given in Figure 4.7 while the theoretical prediction is done at the bottom longitudinal steel level which gives the maximum value of maximum shear strain. Row 2 was chosen because it gives maximum values of the maximum shear strain in most cases; (see Figure 5.7). Although row 4 gives the maximum values in some cases, they do not differ very much from those given by row 2 (see typical plots of shear strain variation in Appendix C).

Figure 5.6 shows that the predicted and the experimental trends of shear force - shear strain

are the same. For any given load, the predicted shear strains are generally greater than those obtained from experiment showing that the theory predicts shear strains conservatively.

5.6. Shear Force-Angles' of Principal Compression Relationships

The experimental angles of principal compression were deduced from measured strains using Mohr's circle (see Appendix C). Typical relationships are plotted together with the theoretical predictions in Figure 5.8

There is good agreement between the trends exhibited by predictions from theory and those deduced from experiment; angles decrease as we move from the bottom level up the section. Comparing experimental and predicted angles at the bottom level, the experimental angles are found to be greater than the predicted ones (Figure 5.8 (a)) by as large a factor as 1.5 in most cases. However, there was comparable agreement in a few cases (Figure 5.8 (b)). One possible explanation of the results of Figure 5.8 (a) may be that the angles were deduced from the longitudinal strains, transverse strains and principal compression strains using equation (3.16) which is non linear. The effect of non uniform cracking on the individual strains has been noted. Combination of these strains in the equation mentioned above is likely to have

affected the angles of principal compression strains to cause the observed difference. The plots of Figure 5.8 (b) were obtained from beam CFT-TB8 in a region that had inclined cracks and considered free from local effects as defined by Figure 5.1. The capability of the theory in predicting trends is, however, shown.

5.7 Moment-Curvature Relationships

Some of the moment-curvature relationships determined for the test specimens are compared with theoretical predictions in Figure 5.9. The trends for theory and experiment are observed to be similar.

It is noted that the moment-curvature relationships were plotted for a given section on the beam. The theory assumes that the section under prediction is loaded to ultimate capacity. This was not the condition on the test specimens as failure occurred in one region only, typically in the central region with pure flexure. However, with the exception of the plot for beam CFT-TB6 in Figure 5.9 (d), the typical plots of Figure 5.9 show that the theory predicts ultimate loads well and conservatively. As has been noted in section 5.1, beam CFT-TB6 had local bond failure before the expected capacity load was reached.

5.8 Response with Varying Material Properties and Loading Condition

Figures 3.7 to 3.9 were obtained by varying

material properties and loading conditions for a chosen beam section. Similar plots for the test specimens are presented in Figure 5.10. It is, however, noted that a strict control on concrete strength could not be achieved for the test specimens. Table 4.1 also reveals that the modulus of elasticity and the stress at yield varied from one bar size to another for both mild and square twisted steel. This is a factor not considered in the development of Figures 3.7 to 3.9 where steel contents were varied with the modulus of elasticity and the stress at yield assumed constant.

Figure 5.10(a) presents the trends for varying longitudinal steel content, other parameters being nearly constant. The general trend of curves from experiment and theory are in agreement.

Comparing the plot of beam CFT-TB2 in Figure 5.10(a) and that of beam CFT-TB8 in Figure 5.10(b), it is seen that the predicted relationship is confirmed; there is an increase in moment capacity for an increase in $\frac{M}{Vd}$ ratio, other parameters being held constant.

In Figure 5.10(c) variation of transverse steel content is considered. The general trends are observed to agree well. The displacement of beam CFT-TB5 above CFT-TB3 at ultimate is likely due to the fact that the test for beam CFT-TB5 was done on two

separate days leading to a change in concrete strength.

Figure 5.10(d) shows good agreement in predicted and experimental trends for varying concrete strength, other parameters being held constant.

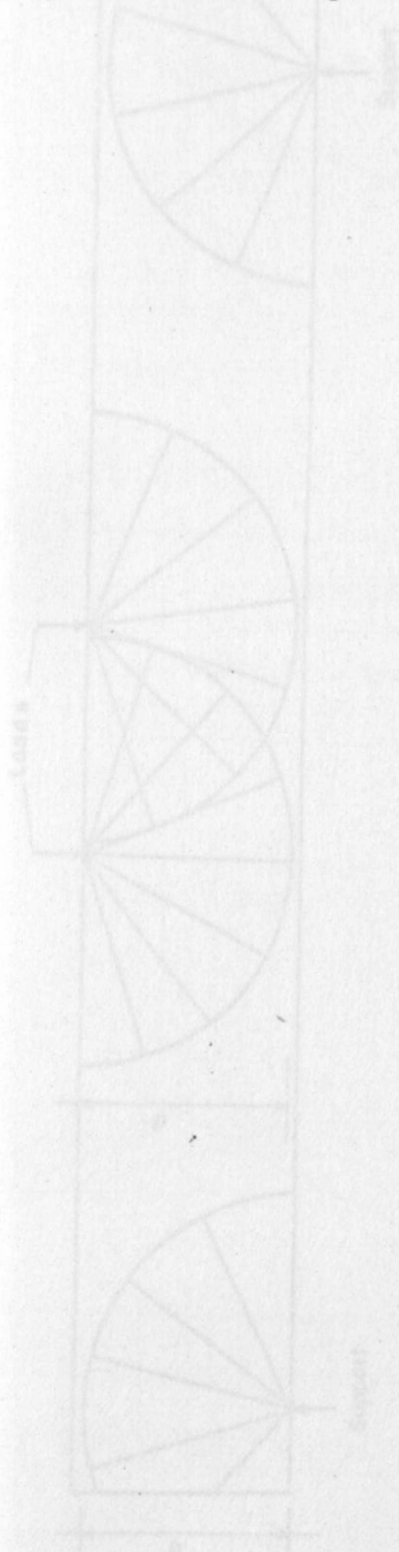


Fig 5.1: Stress concentrations
(Shaded regions indicate areas affected by load effects)

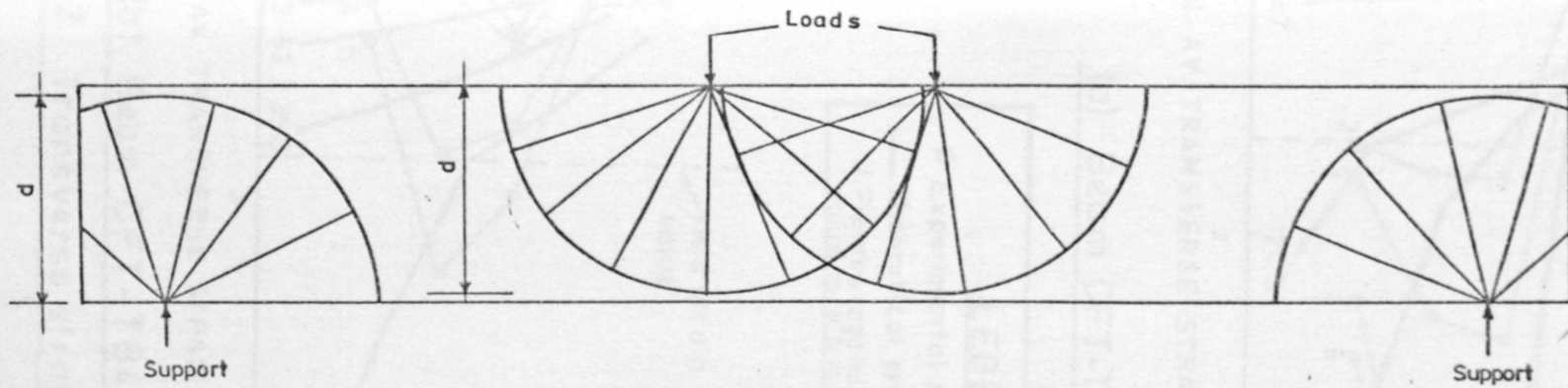
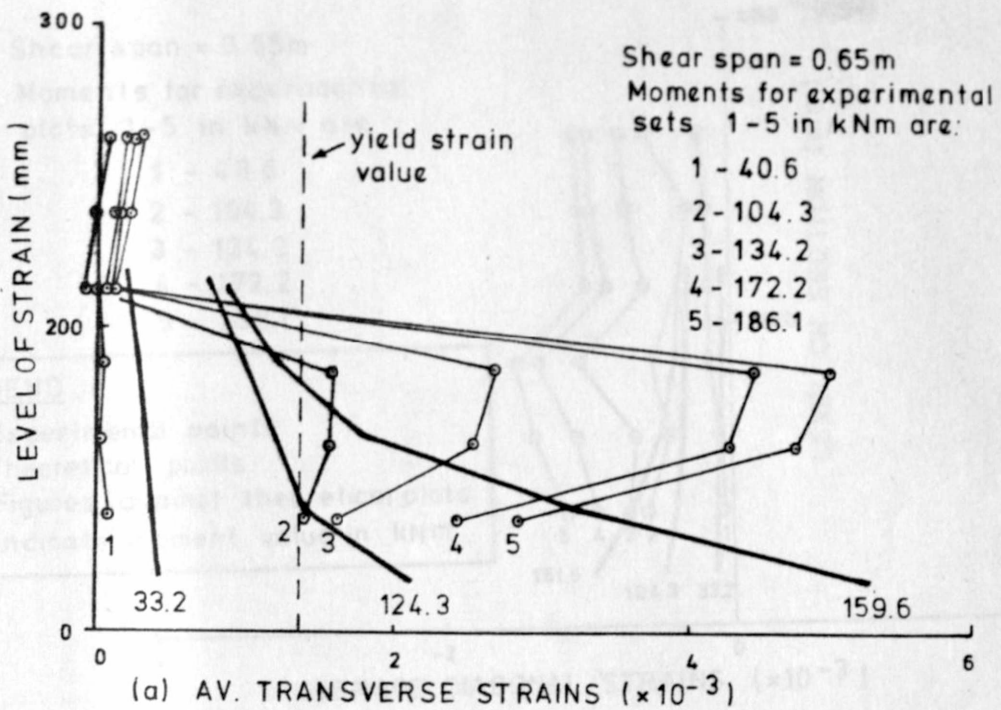
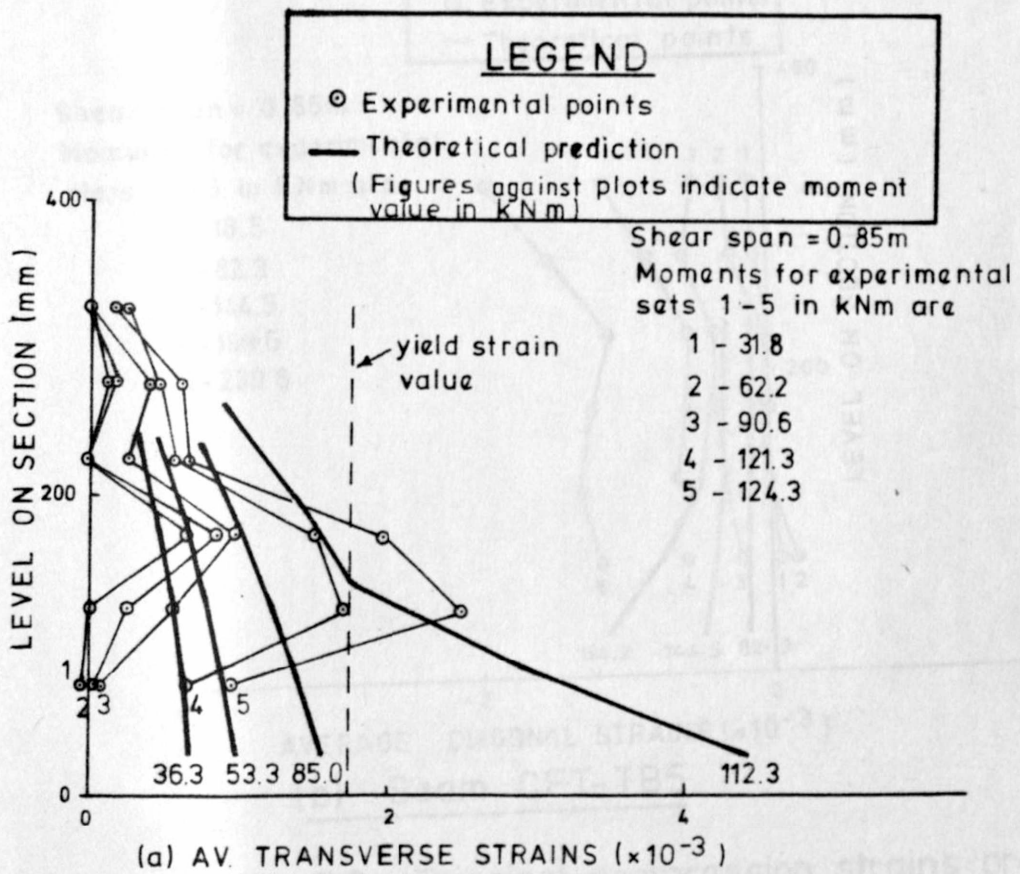


Fig. 5.1: Stress concentrations
(Shaded regions indicate areas affected by
local effects)



(a) Beam CFT-TB3



(a) Beam CFT-TB4

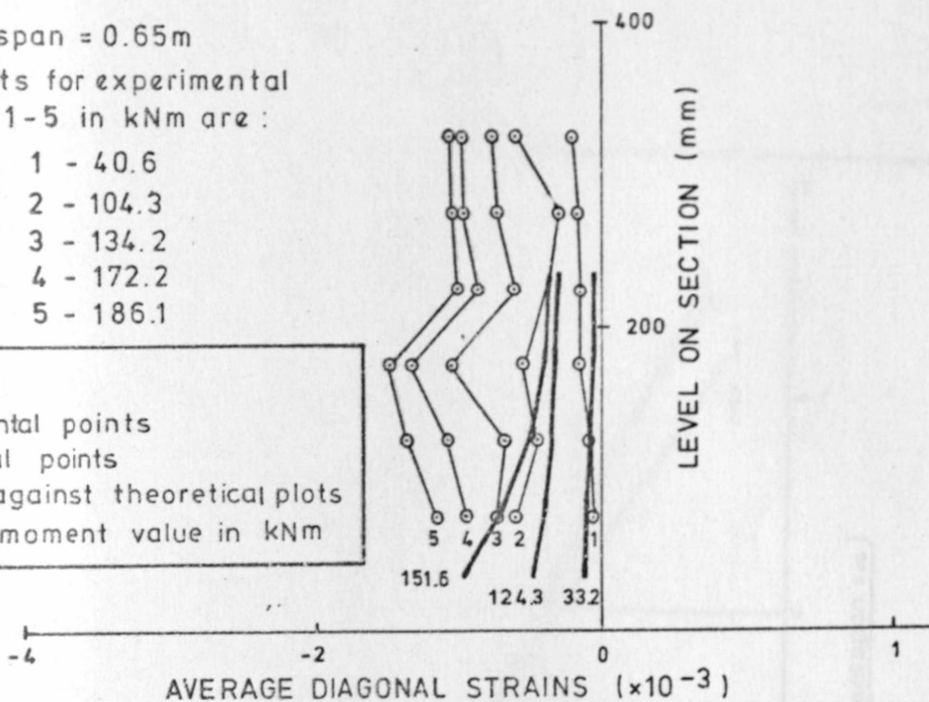
Fig. 5.2 : Transverse strains profiles

Shear span = 0.65m
 Moments for experimental plots 1-5 in kNm are :

- 1 - 40.6
- 2 - 104.3
- 3 - 134.2
- 4 - 172.2
- 5 - 186.1

LEGEND

- Experimental points
- Theoretical points
- Figures against theoretical plots indicate moment value in kNm



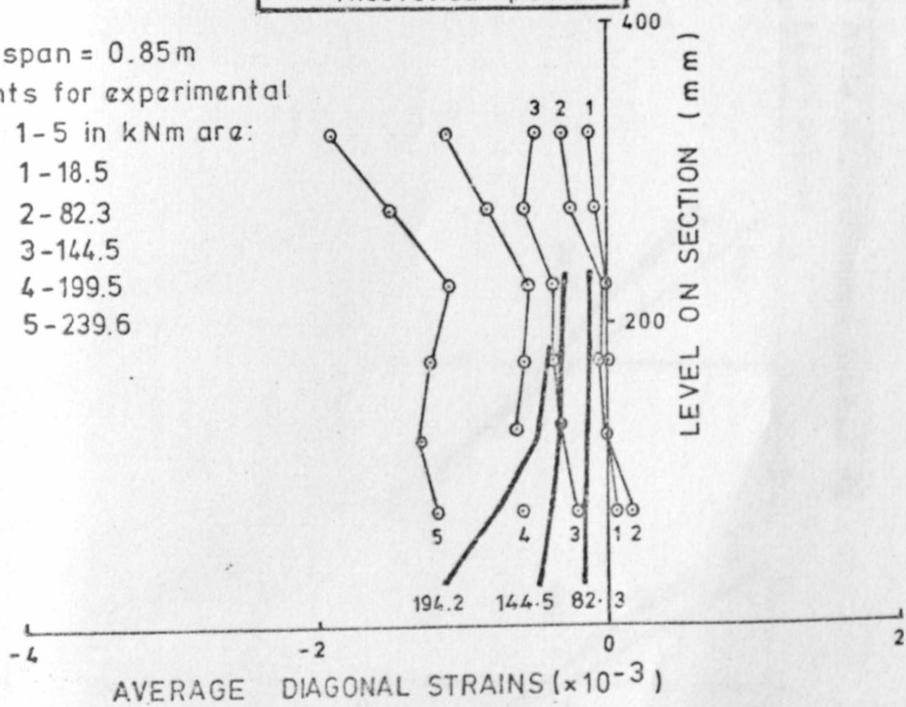
(a) Beam CFT-TB3

LEGEND

- Experimental points
- Theoretical points

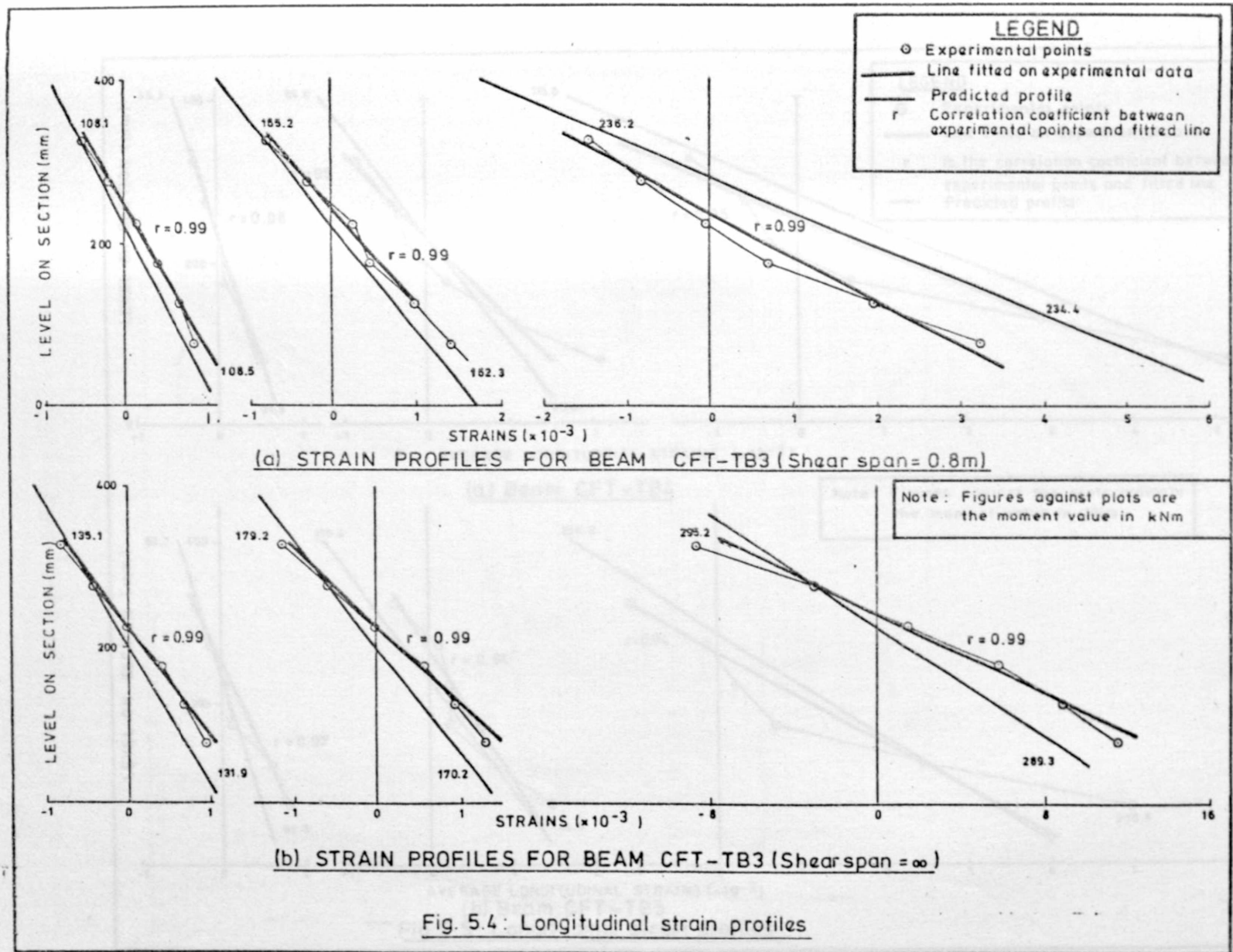
Shear span = 0.85m
 Moments for experimental plots 1-5 in kNm are :

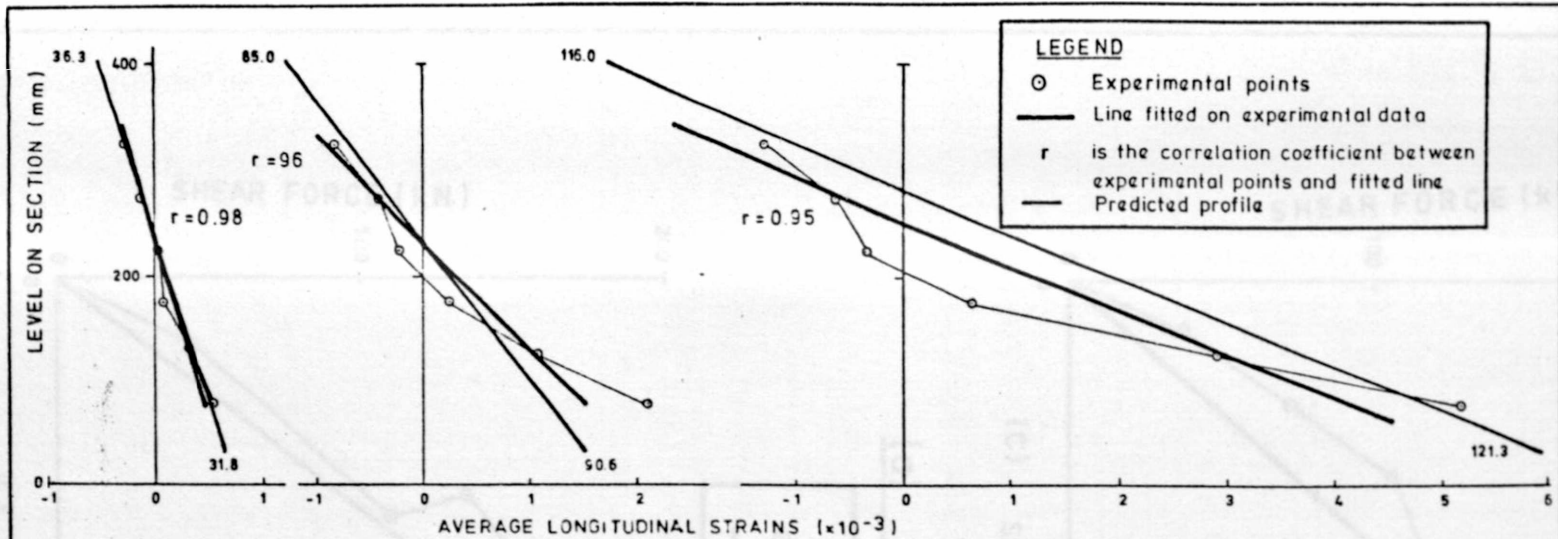
- 1 - 18.5
- 2 - 82.3
- 3 - 144.5
- 4 - 199.5
- 5 - 239.6



(b) Beam CFT-TB5

Fig. 5.3 : Principal compression strains profiles





Note: Figures against the plots indicate the moment value in kNm

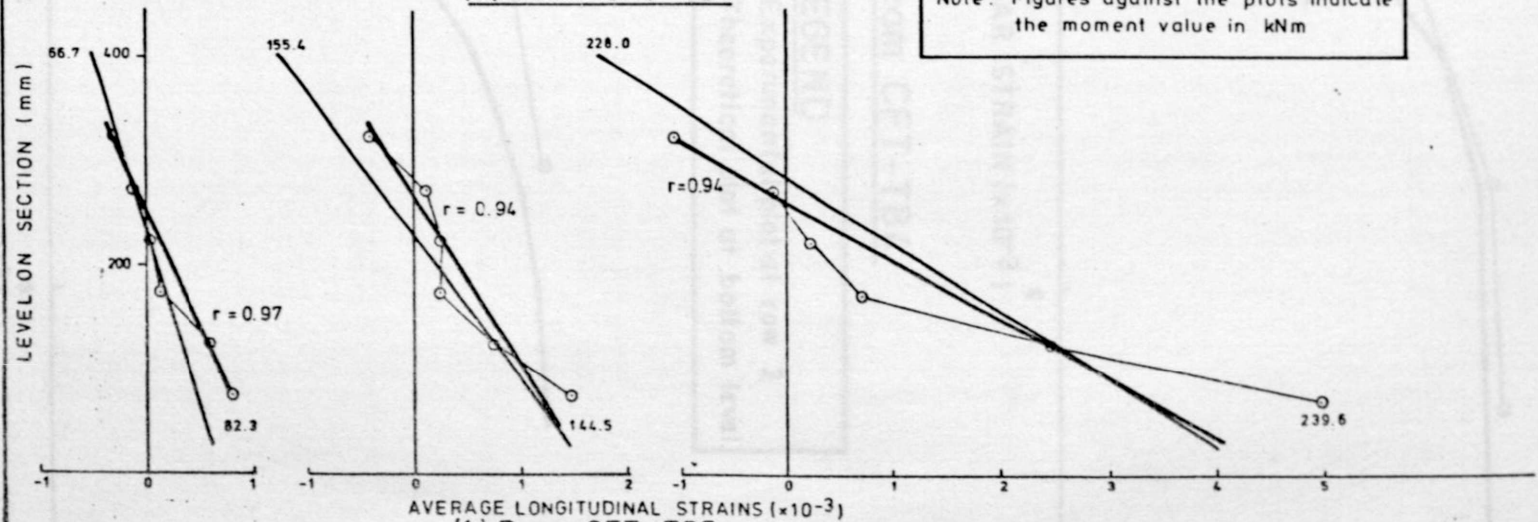
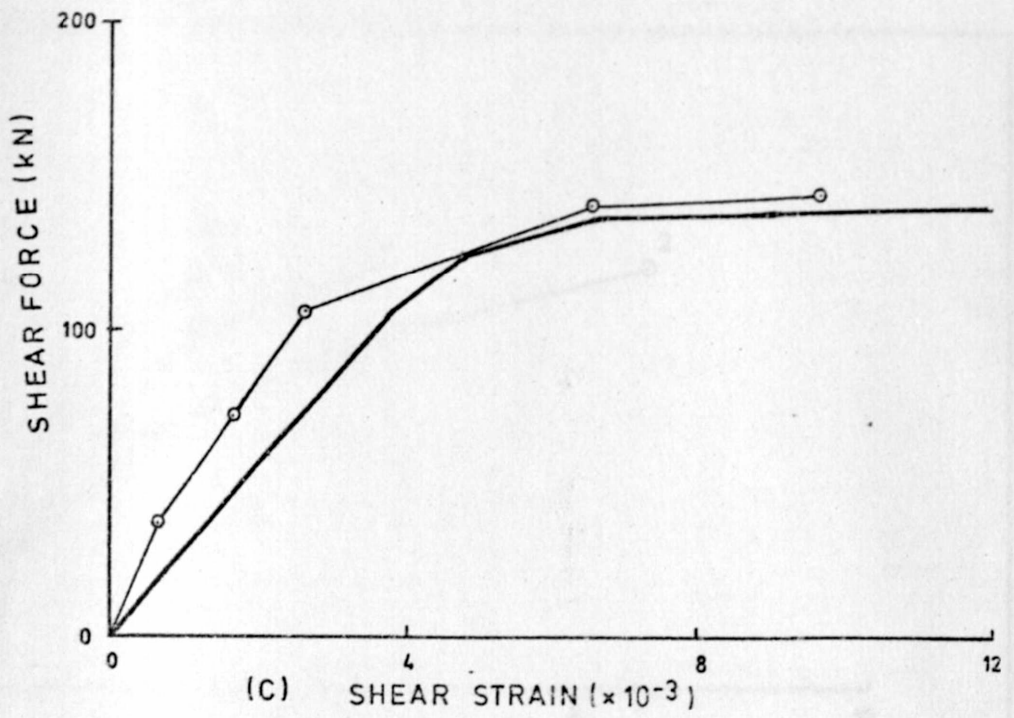


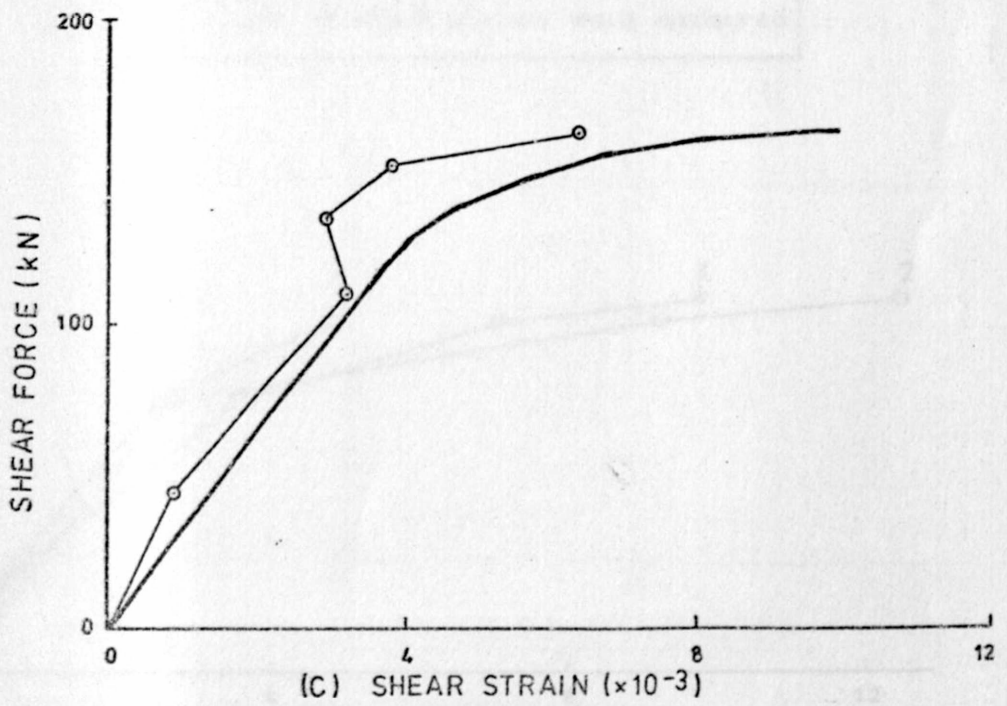
Fig. 5.5: Longitudinal strain profiles



(a) Beam CFT-TB4

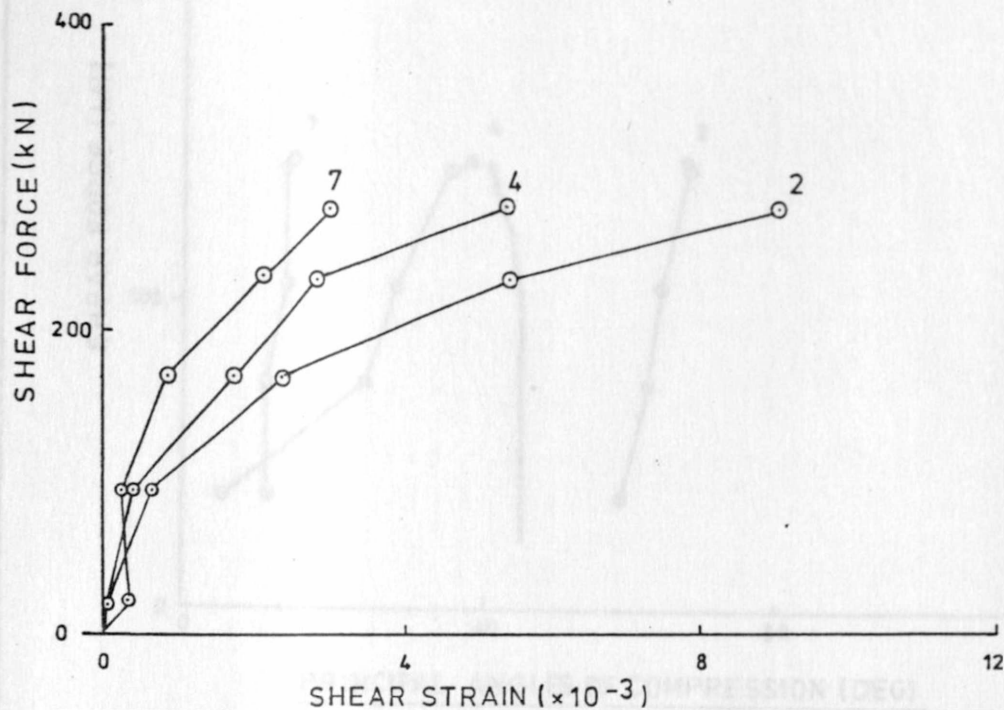
LEGEND

- Experimental plot at row 2
- Theoretical plot at bottom level



(b) Beam CFT-TB8

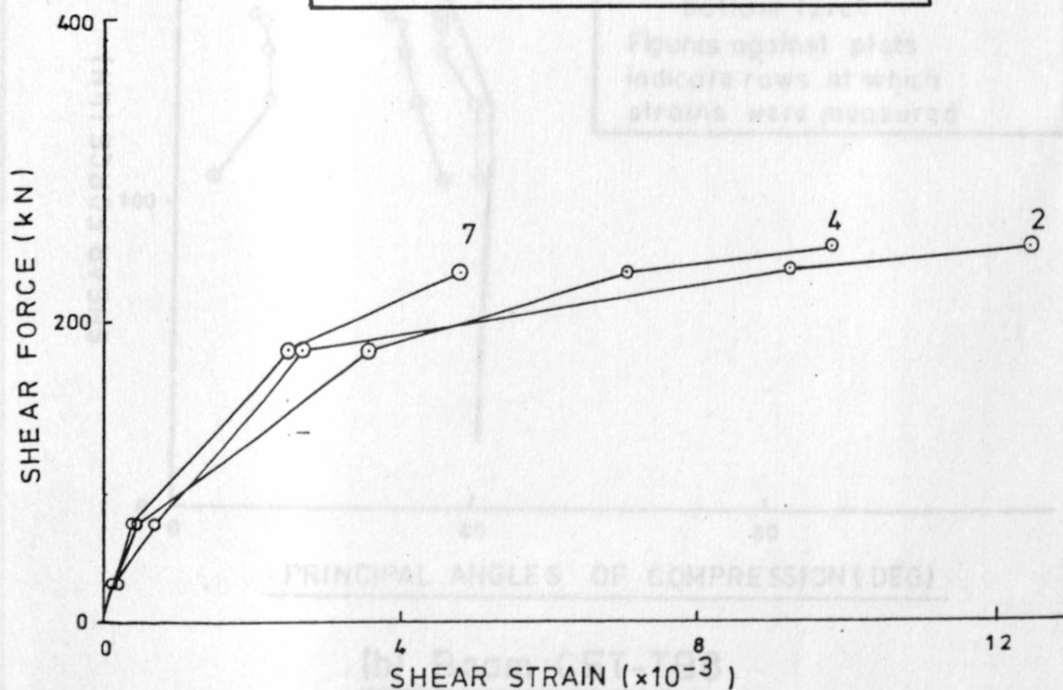
Fig. 5.6 : Shear Force - Shear Strain Relationships



(a) Beam CFT-TB5

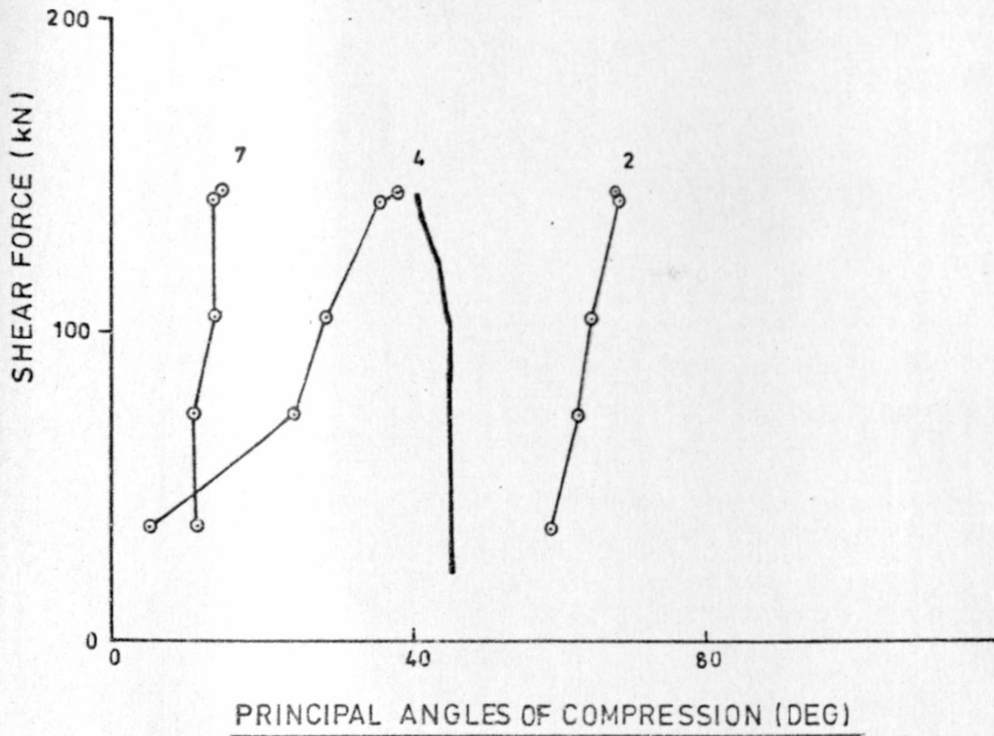
LEGEND

Figures against the plots indicate rows at which strains were measured

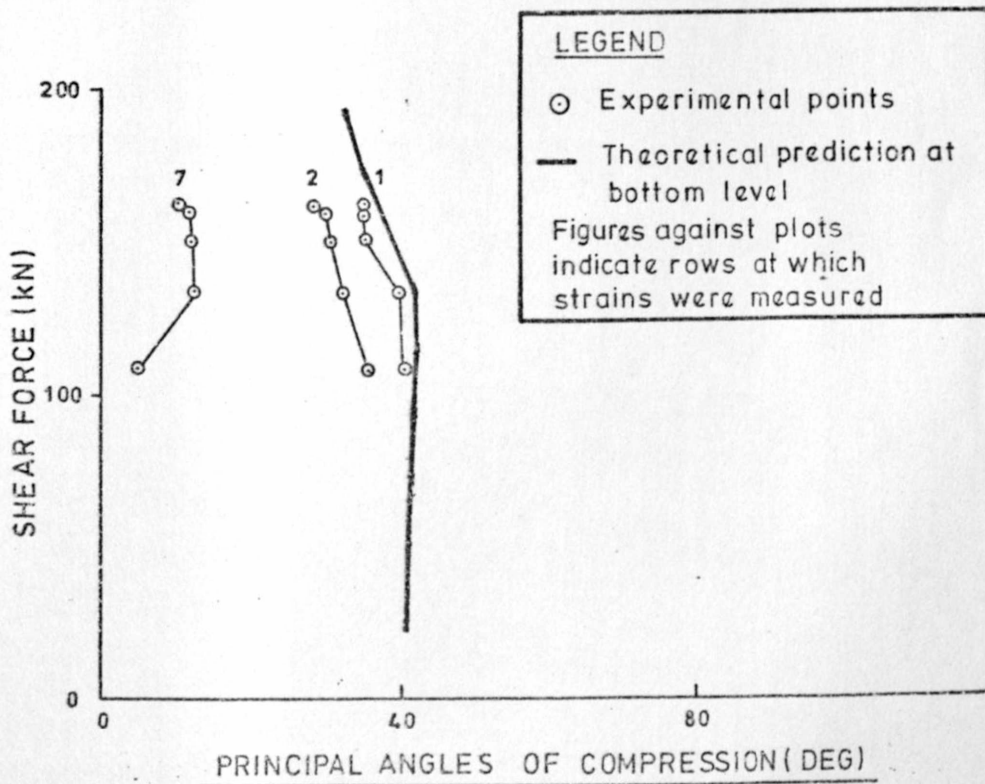


(b) Beam CFT-TB6

Fig. 5.7 : Variation shear force



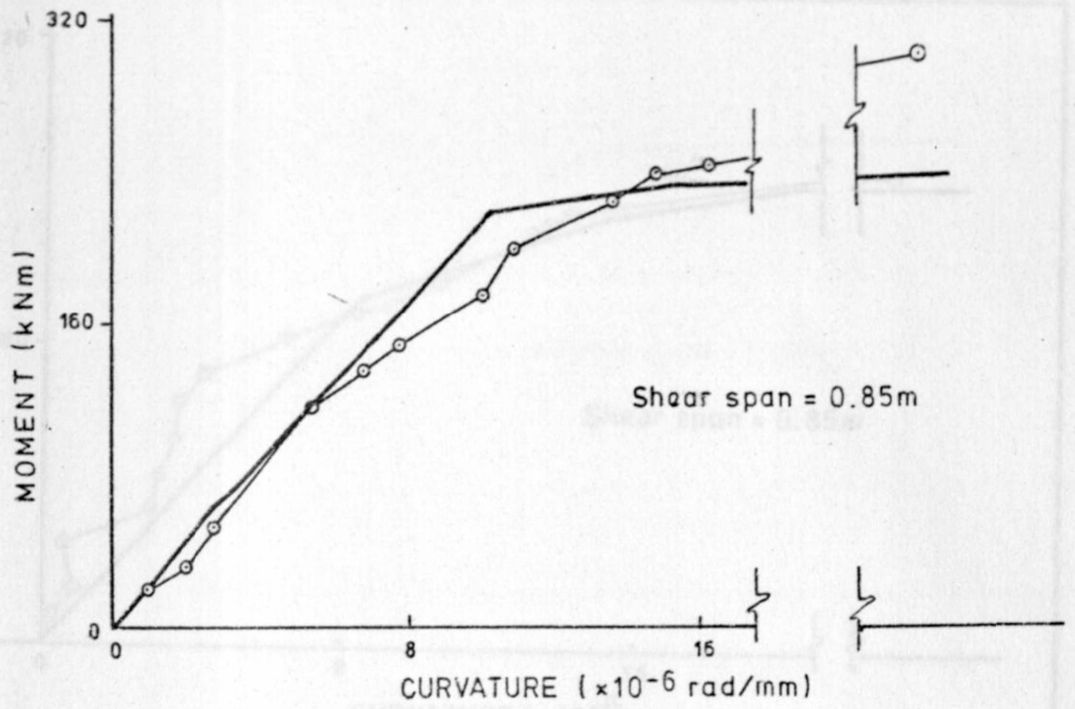
(a) Beam CFT-TB4



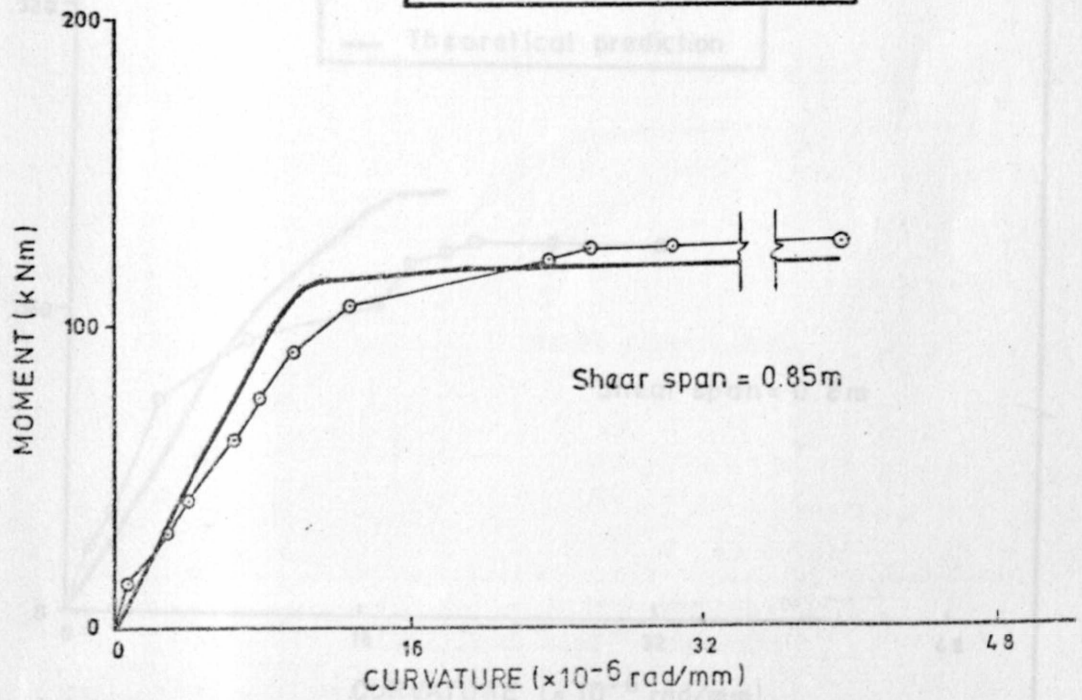
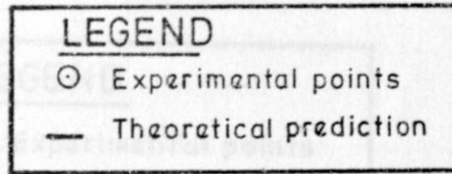
LEGEND
○ Experimental points
— Theoretical prediction at bottom level
Figures against plots indicate rows at which strains were measured

(b) Beam CFT-TB8

Fig. 5.8: Shear Force- Principal Angles of compression Relationships

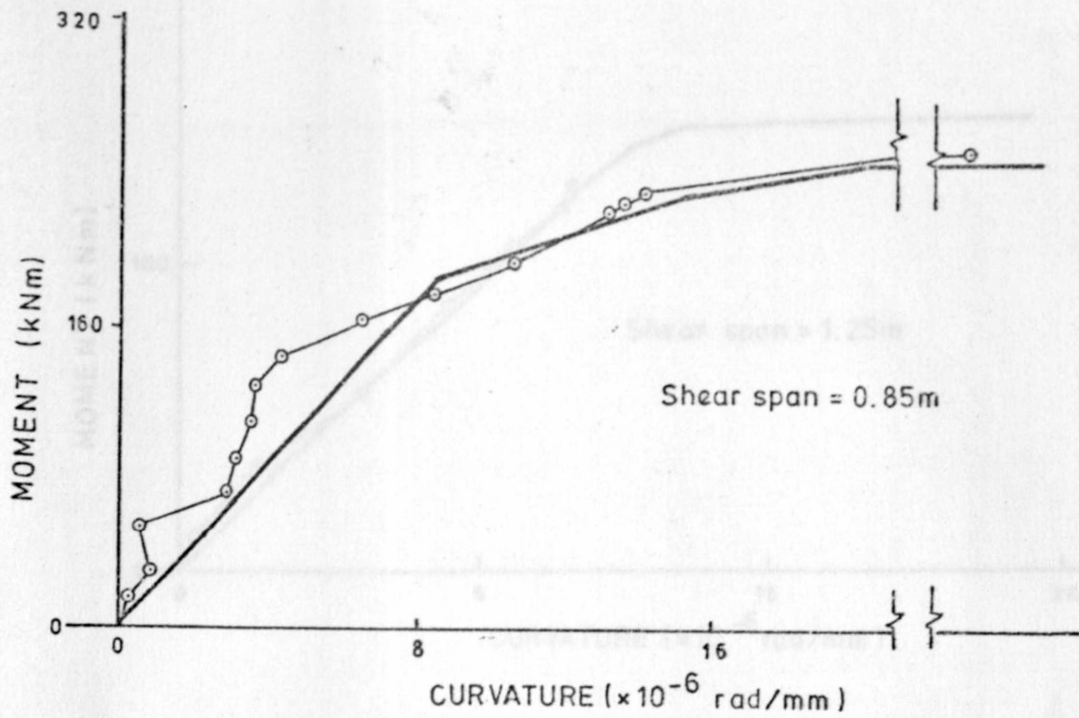


(a) Beam CFT-TB3

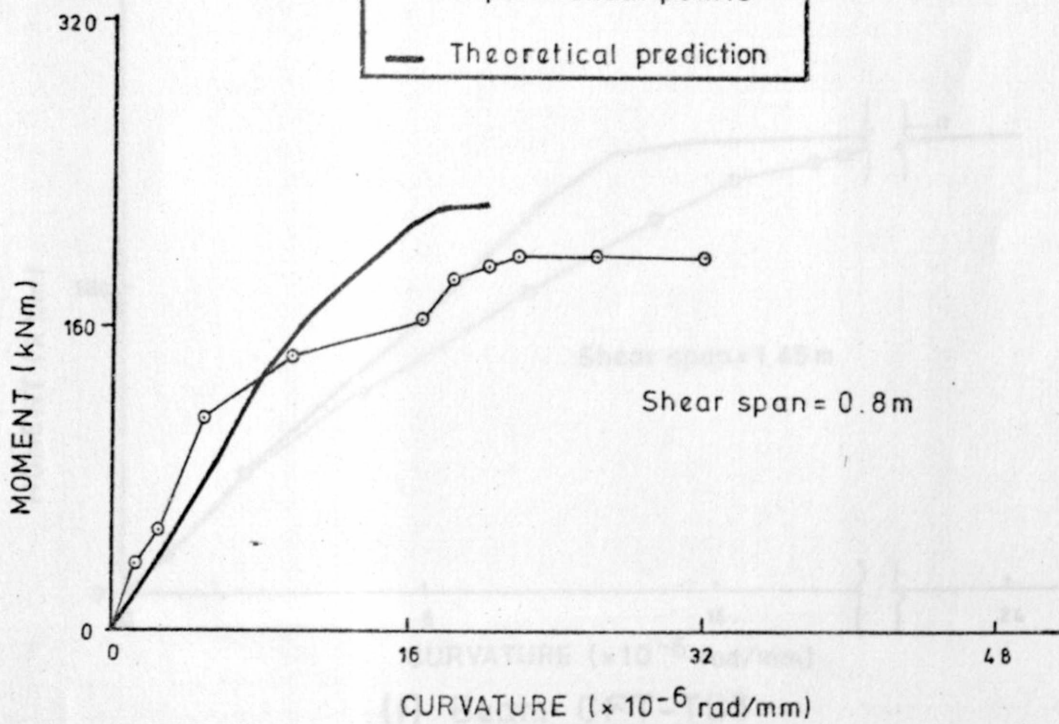
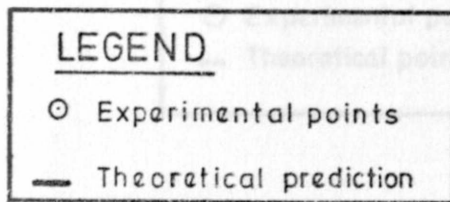


(b) Beam CFT-TB4

Fig. 5.9 : Moment-curvature Relationships

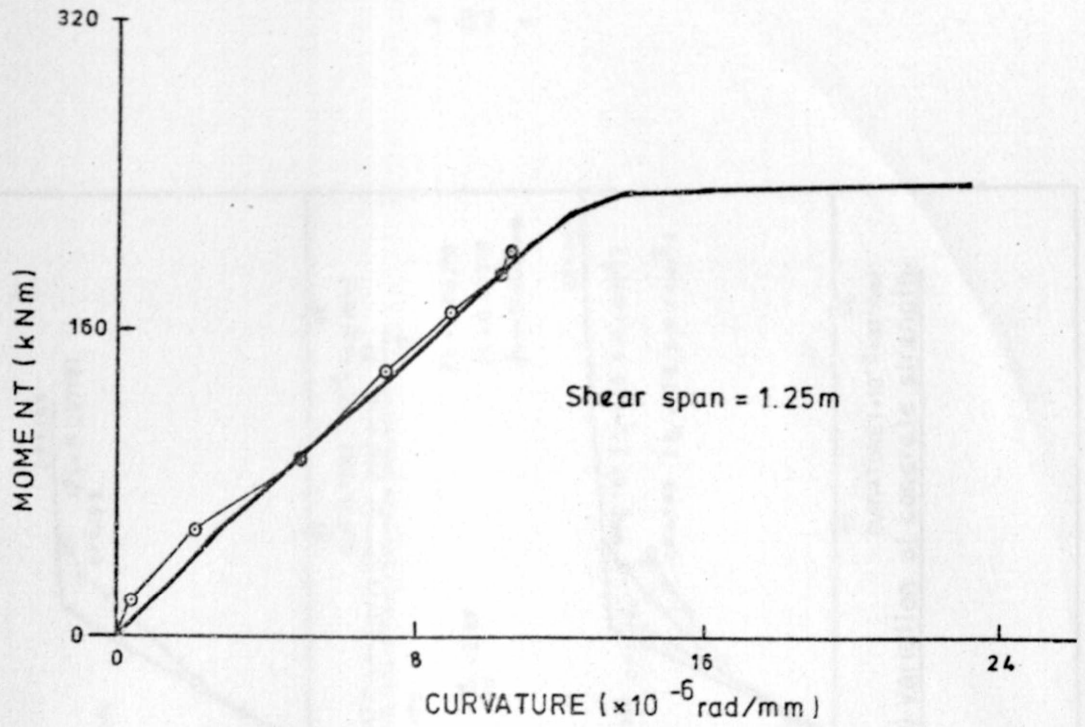


(c) Beam CFT-TB5



(d) Beam CFT-TB6

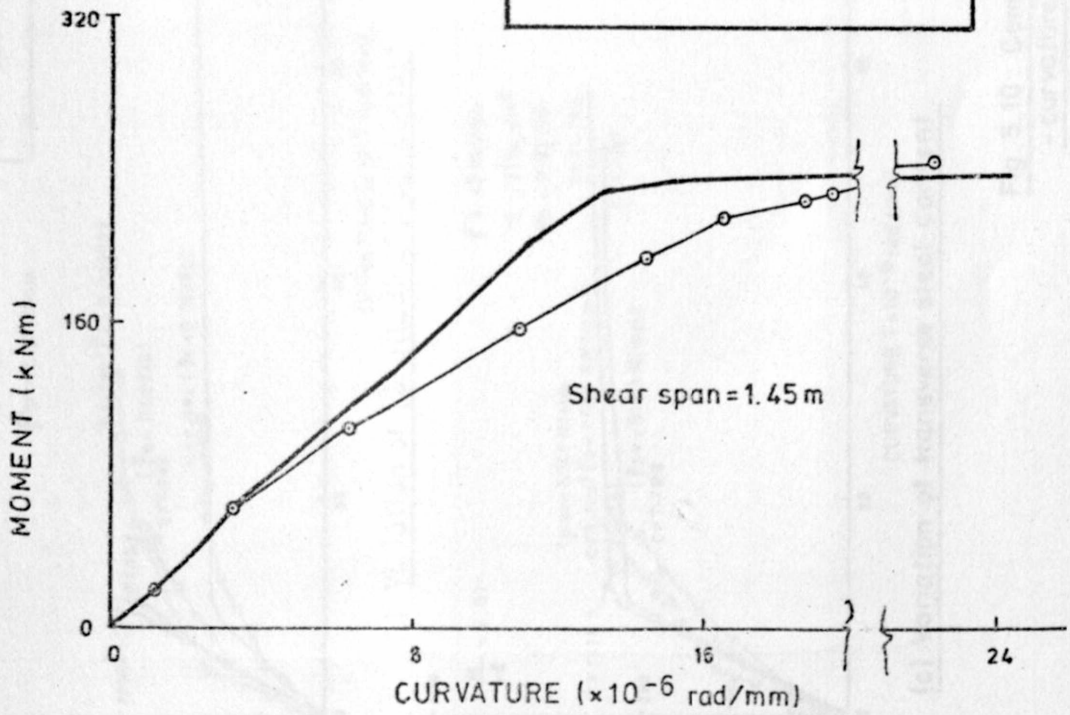
Fig. 5.9: Moment - curvature Relationships



(e) Beam CFT-TB8

LEGEND

- Experimental points
- Theoretical points



(f) Beam CFT-TB8

Fig. 5.9: Moment - curvature Relationships

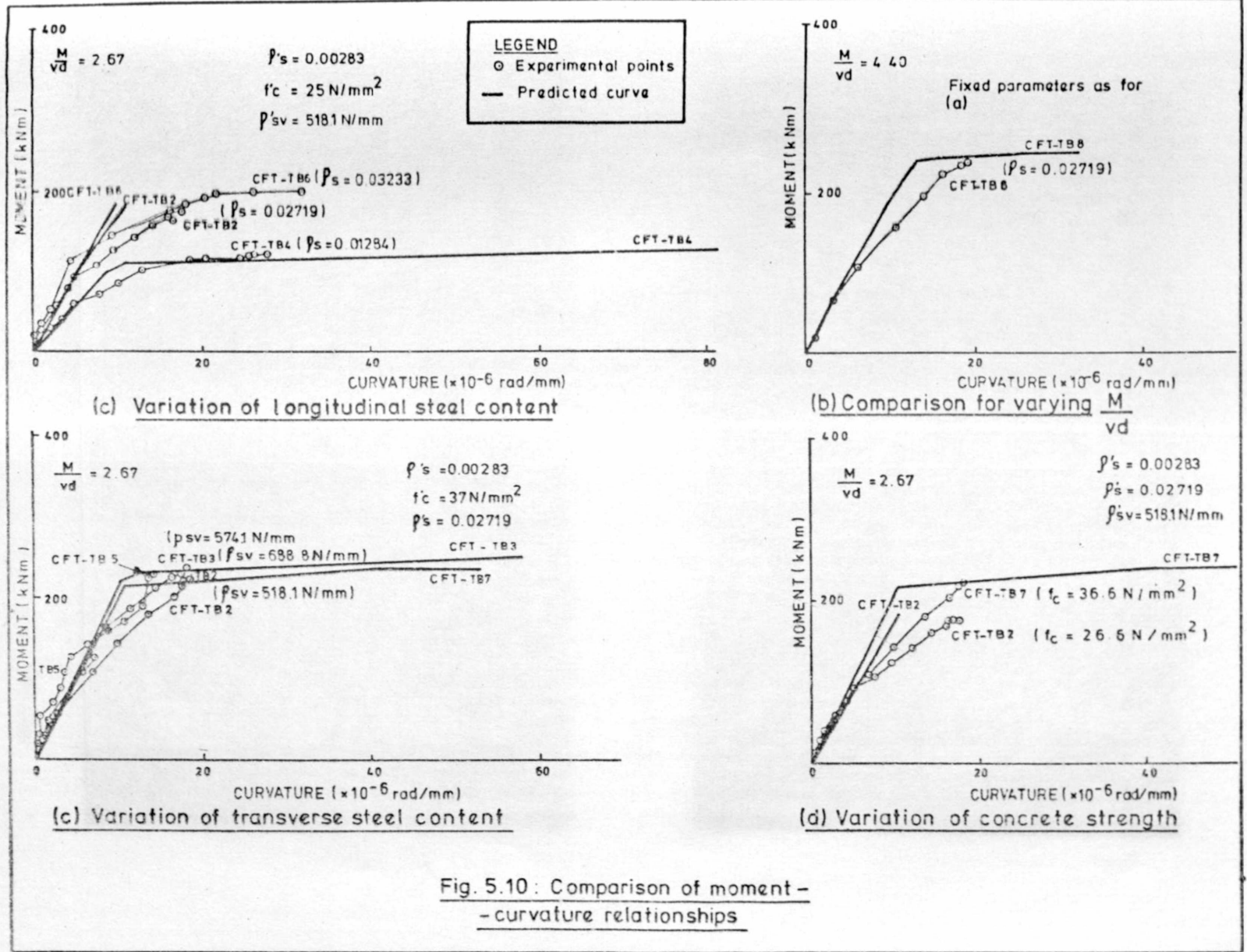


Fig. 5.10 : Comparison of moment - curvature relationships

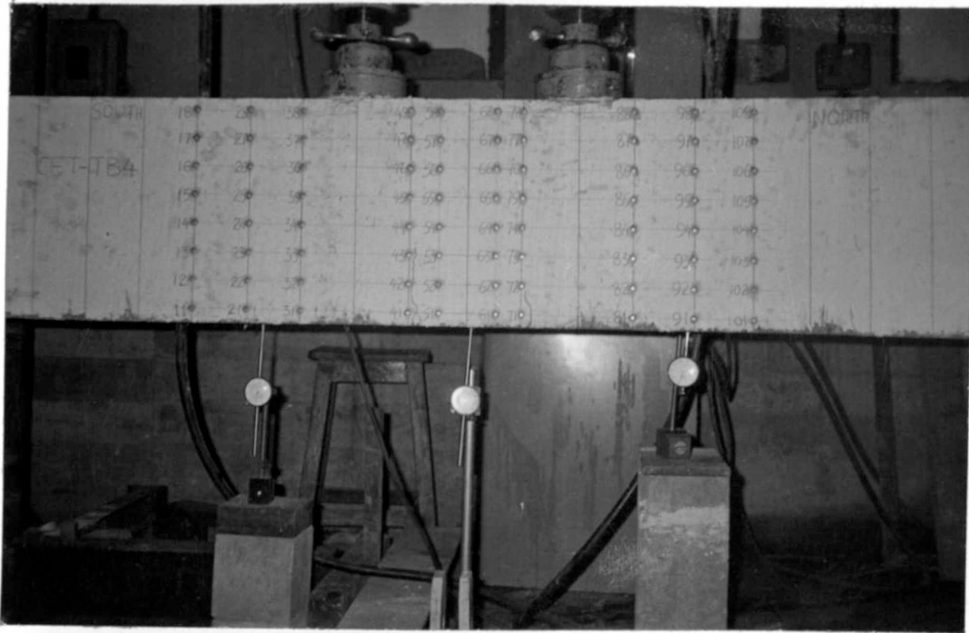


Plate 5.1: Beam CFT-TB4 at Flexural Cracking Capacity

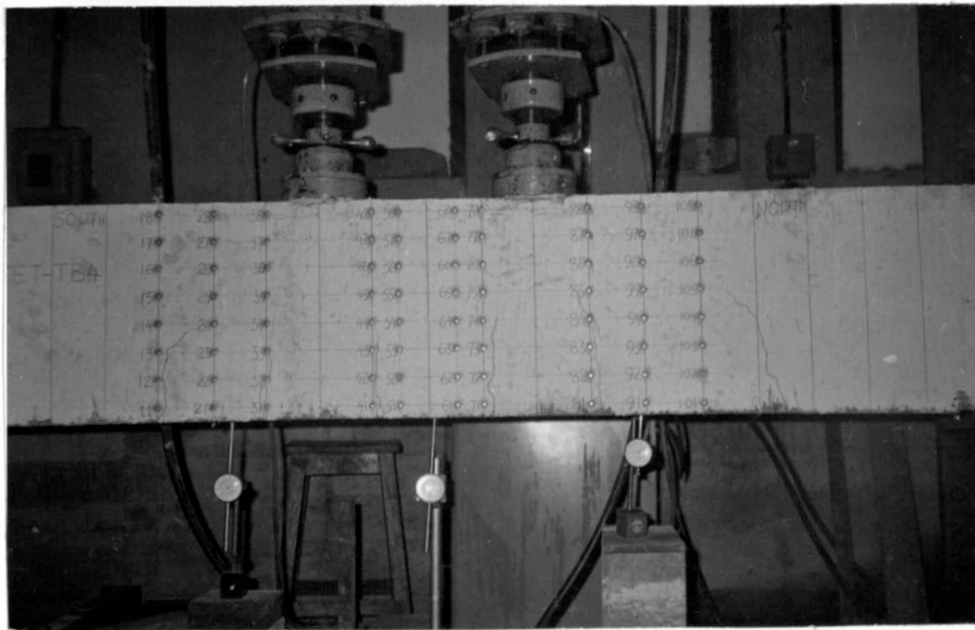


Plate 5.2: Beam CFT-TB4 at Start of Inclined Cracks

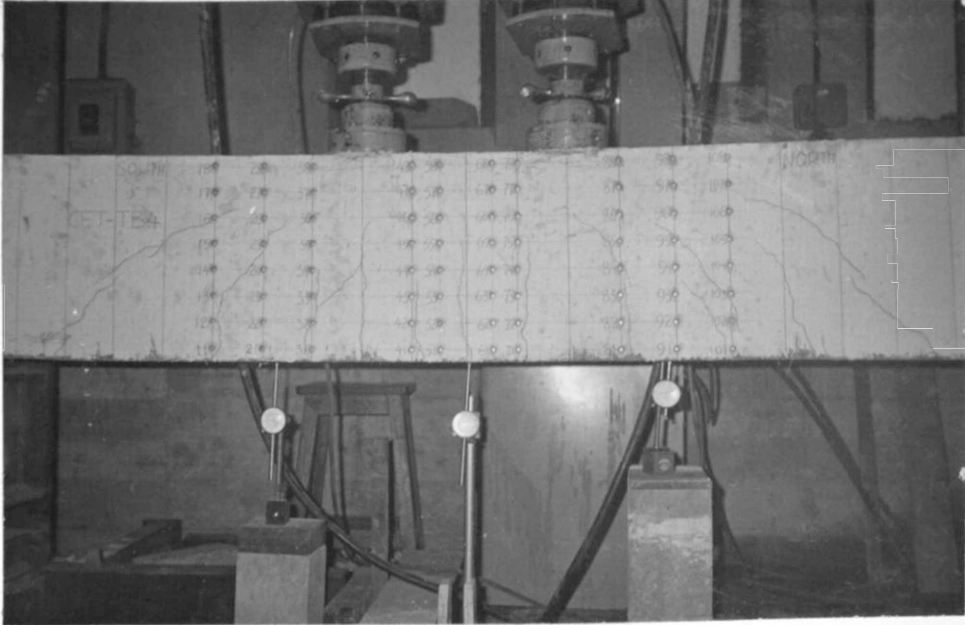


Plate 5.3: Beam CFT-TB4 at about 3/4 Capacity

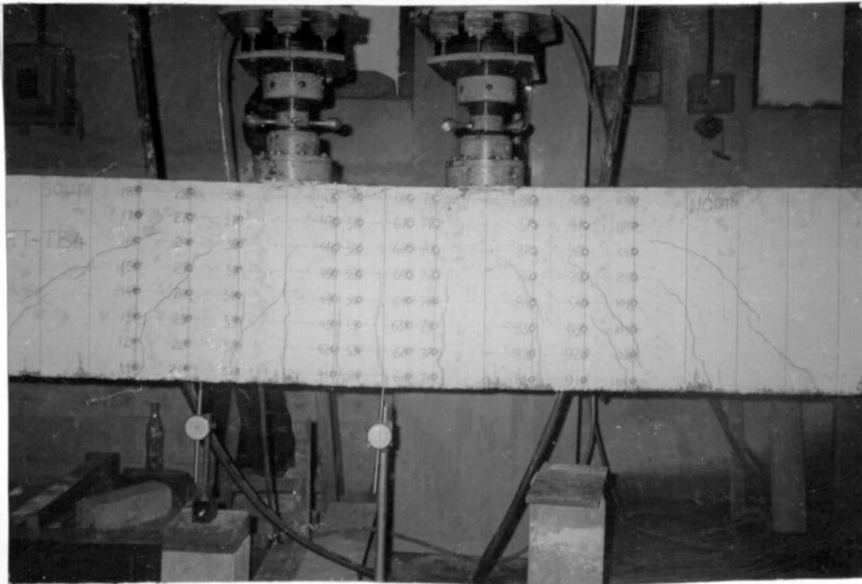


Plate 5.4: Beam CFT TB4 Near Capacity Loading
(Notice start of crushing in concrete
at the top between loads)

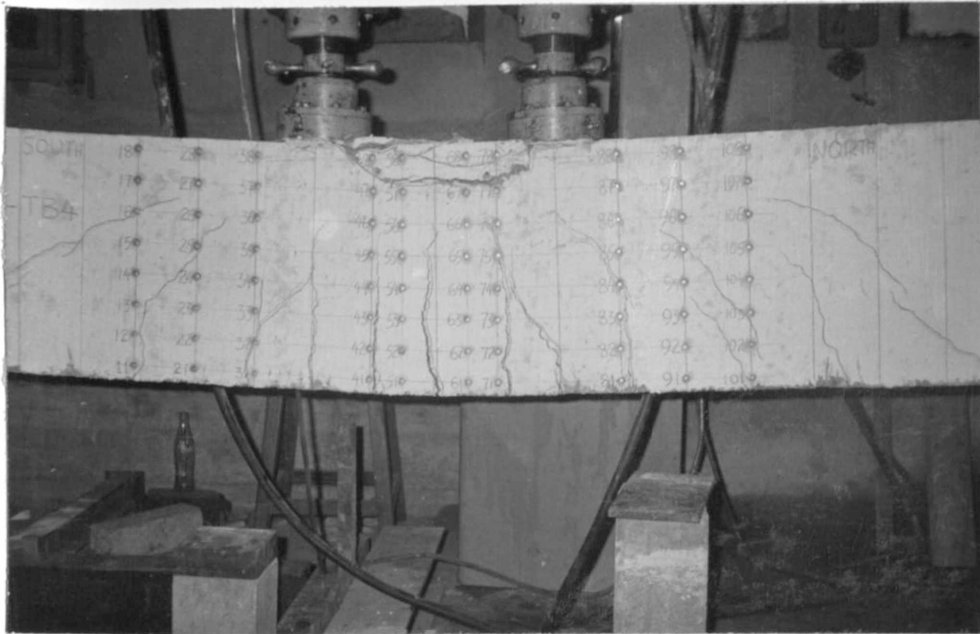


Plate 5.5: Beam CFT-TB4 at Capacity Loading

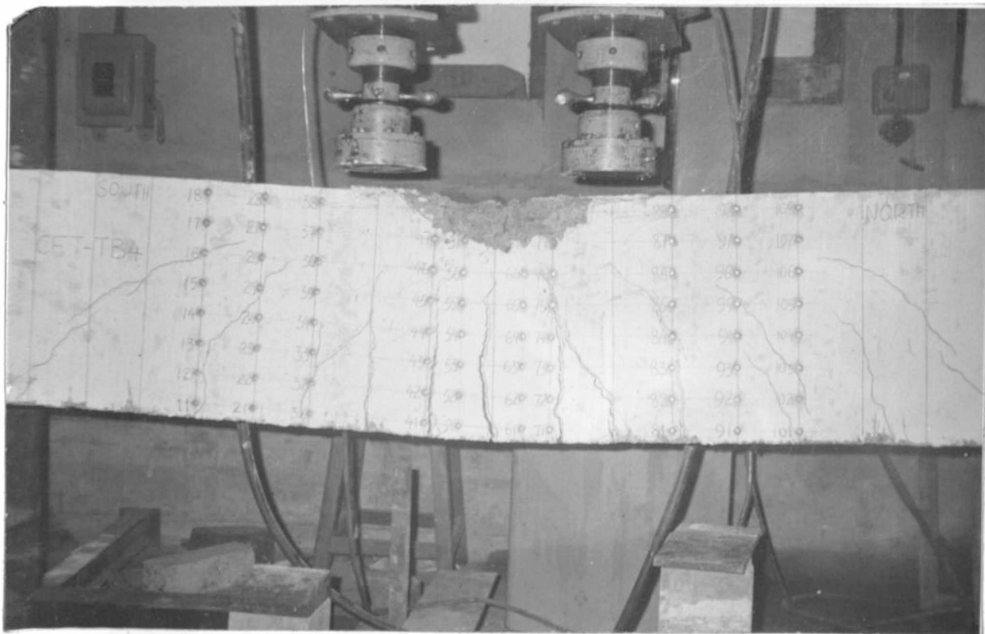


Plate 5.6: Beam CFT-TB4 at Failure (Sequence of Beam CFT-TB4 was typical of Beam CFT-TB2, CFT-TB3, CFT-TB7 and CFT-TB8)

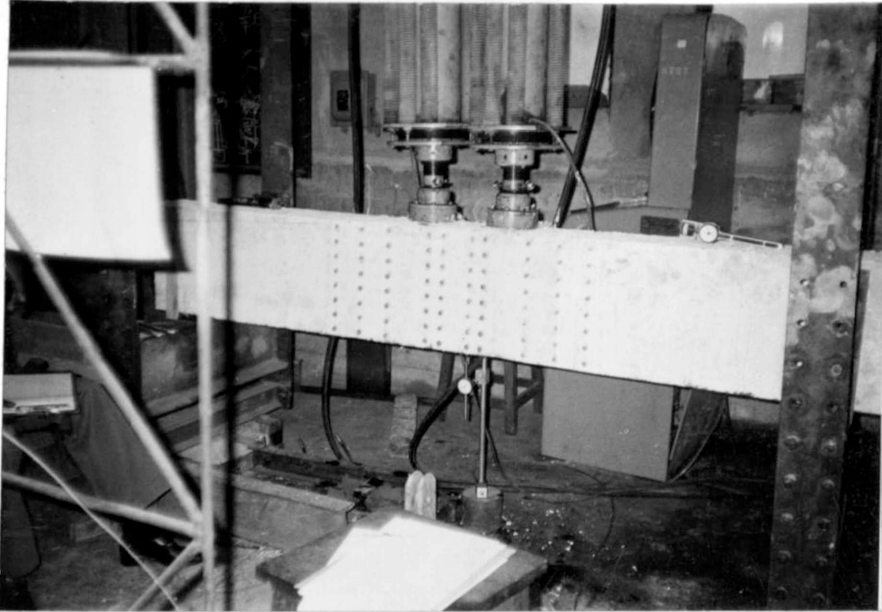


Plate 5.7: Beam CFT-TB1 in Test Rig (front side)

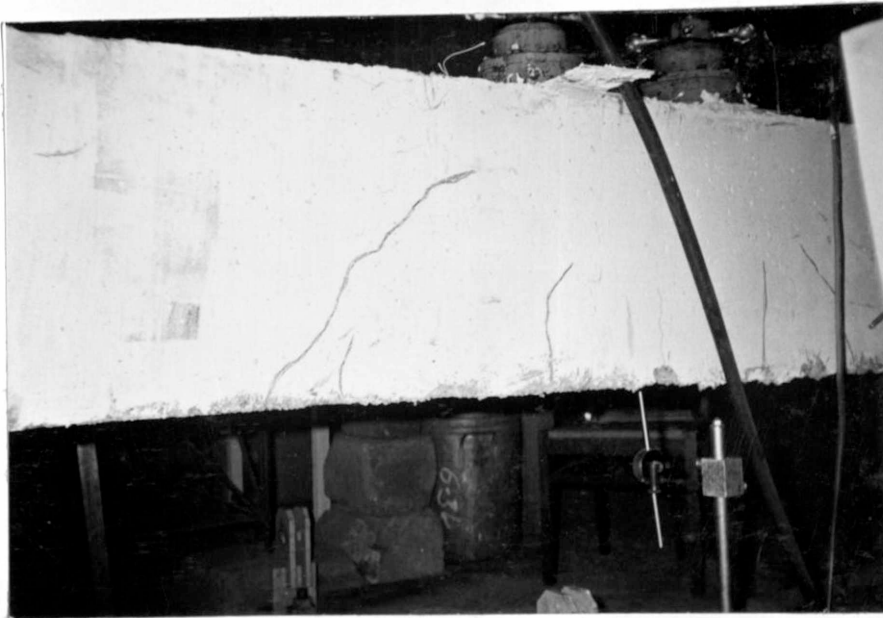


Plate 5.8: Beam CFT TB1 at about Half Capacity (rear side)

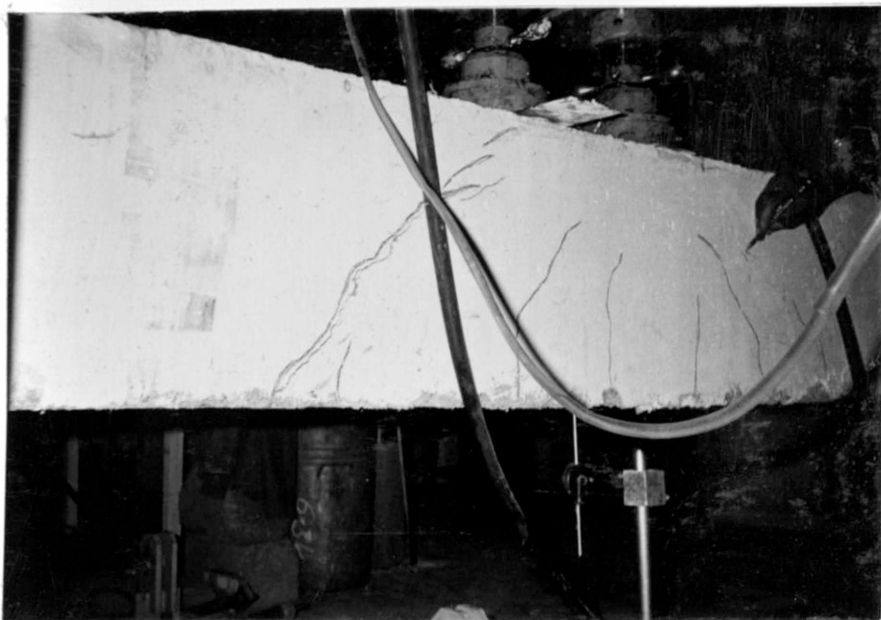


Plate 5.9 : Beam CFT-TB1 at Near Full Capacity
(rear side)

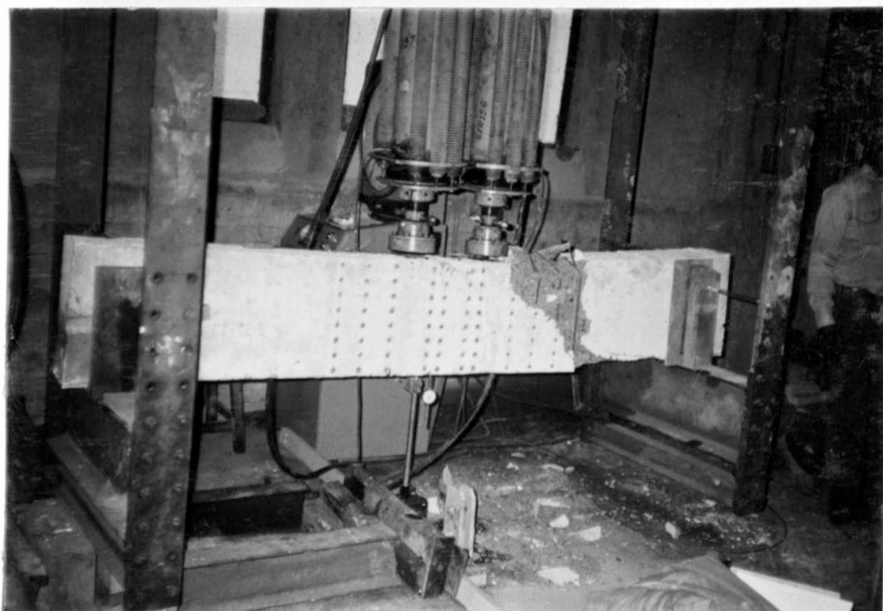


Plate 5.10 : Beam CFT-TB1 at Failure (front side)
(Notice failure is in the shear span)

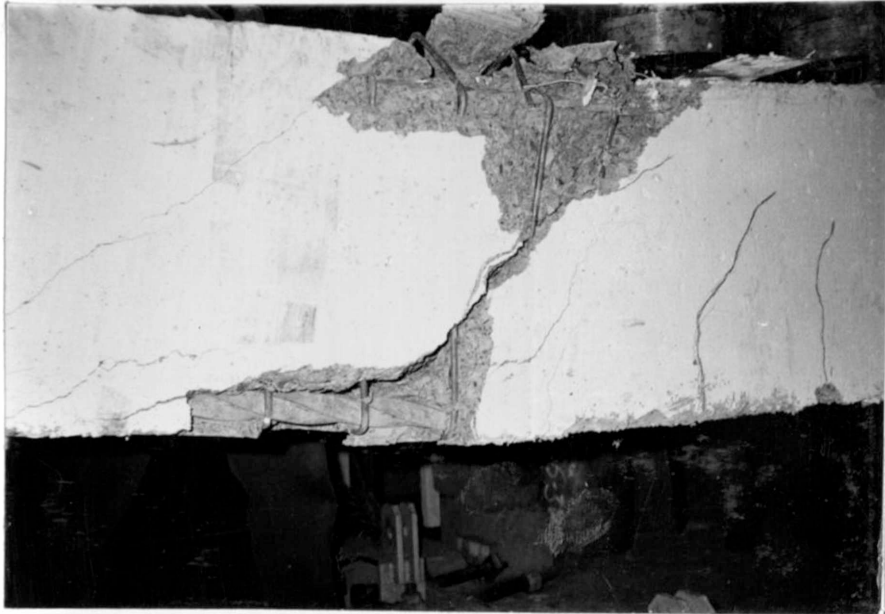


Plate 5.11: Beam CFT-TB1 at Failure (rear side)



Plat 5.12 : Beam CFT-TB6 at Failure (front side)

CHAPTER 6

CONCLUSIONS AND RECOMMENDATIONS

6.1 Conclusions

From the study of predictions using the compression field theory and the data from the experimental specimens tested, the following conclusions may be made about structural concrete beams loaded in flexure and shear:-

- (i) Due to non-uniform cracking of test specimens, the transverse strains and the principal compression strains profiles obtained from experiment differ from those obtained from theory. However, the maximum average transverse strains and the average principal compression strains obtained from experiment are generally comparable to those obtained from theoretical predictions.
- (ii) Application of the Bernoulli-Navier hypothesis which states that longitudinal strains along any line in a section vary linearly, is reasonable.

- (iii) The plots for the maximum shear strain from experimental data and from theoretical model are in good agreement.
- (iv) The moment-curvature response for the test specimens is predicted well by the compression field theory.
- (v) The compression field theory predicts the ultimate loadswell and conservatively.
- (vi) The predicted and the experimental trends as material properties and loading conditions are varied, are generally in agreement.

6.2 Recommendations

The following recommendations are made for further research on present work:

- (i) It is recognized that the experimental program was restricted to only rectangular solid beam sections. It is recommended that tests be extended to other types of beam sections as further investigation of application of theory.

REFERENCES

(ii) Tests should be carried out on many identical specimens in order to yield statistically more significant data.

(iii) As a further development of the theoretical model, the tensile strength of concrete should be taken into account.

1. Mitchell, D., and Collins, M.P. (1974). "Diagonal Compression Field Theory - A Design Method for Reinforced Concrete Beams Subjected to Combined Tension, Flexure and Axial Load", PhD Thesis, University of Toronto, Canada, 1978, 246 pp.
2. Joint ASCE-ACI Task Committee (26 (1973)). "The Shear Strength of Reinforced Concrete Members", Journal of the Structural Division, ASCE, Vol. 99, No. 576, Proc. Paper, June, 1973, pp 1871-1877.
3. Joint ASCE-ACI Task Committee (26 (1974)). "The Shear Strength of Reinforced Concrete Members - Slabs", Journal of the Structural Division, ASCE, Vol. 100, No. 578, Proc. Paper 10733, August, 1974, pp 1849 - 1891.
4. Leonhardt, F. and Walther, R. (1964). "The Outright Shear Tests, 1931", Translation No. 111, Cement and Concrete Association, London, England, 1964.
5. Leonhardt, F. (1965). "Reducing the Shear Reinforcement in Reinforced Concrete Beams and Slabs", Magazine of Concrete Research, Vol. 17, No. 33, Dec. 1965, pp 187 - 194.
6. Corwick, R.C. and Pausley, T. (1968). "Mechanisms of Shear Resistance of Concrete Beams", Journal of the Structural Division, ASCE, Vol. 94, No. 5815, Proc. Paper 1021, Oct. 1968, pp. 2325 - 2350.
7. Gergely, P. (1969). "Splitting Cracks Along the Main Reinforcement in Concrete Members", Report to Bureau of Public Roads, U.S. Department of Transportation, Cornell University, Ithaca, N.Y., Apr. 1969.

REFERENCES

1. Collins, M.P., and Mitchell, D. (1980), "Shear and Torsion Design of Prestressed and Non-Prestressed Concrete Beams", Journal of the Prestressed Concrete Institute, Vol.25, No.5 September - October 1980, pp 32-100
2. Mitchell, D., and Collins, M.P. (1974), "Diagonal Compression Field Theory - A Rational Model for Structural Concrete in Pure Torsion", American Concrete Institute Journal, Vol. 71, Aug., 1974, pp. 396 - 408
3. Onsongo, W.M. (1978), "The Diagonal Compression Field Theory for Reinforced Concrete Beams Subjected to Combined Torsion, Flexure and Axial Load", PhD Thesis, University of Toronto, Canada, 1978, 246 pp.
4. Joint ASCE-ACI Task Committee 426 (1973), "The Shear Strength of Reinforced Concrete Members", Journal of the Structural Division, ASCE, Vol 99, No. ST6, Proc. Paper, June, 1973, pp 1091-1187.
5. Joint ASCE-ACI Task Committee 426 (1974), "The Shear Strength of Reinforced Concrete Members-Slabs", Journal of the Structural Division, ASCE, Vol.100, No. ST8, Proc. Paper 10733, August, 1974, pp 1543 - 1591.
6. Leonhardt, F. and Walther, R. (1964), "The Stuttgart Shear Tests, 1961, "Translation No. 111, Cement and Concrete Association, London, England, 1964.
7. Leonhardt, F. (1965), "Reducing the Shear Reinforcement in Reinforced Concrete Beams and Slabs", Magazine of Concrete Research, Vol. 17, No. 53, Dec.1965, pp 187 - 194.
8. Fenwick, R.C. and Paulay, T. (1968), "Mechanisms of Shear Resistance of Concrete Beams", Journal of the Structural Division, ASCE, Vol.94, No. ST10, Proc. Paper 2325, Oct. 1968, pp. 2325 - 2350.
9. Gergely, P. (1969), "Splitting Cracks Along the Main Reinforcement in Concrete Members", Report to Bureau of Public Roads, U.S. Department of Transportation, Cornell University, Ithaca, N.Y., Apr. 1969

10. Hofbeck, J.A., Ibrahim, I.A. and Mattock, A.H. (1969), "Shear Transfer in Reinforced Concrete", Journal of the American Concrete Institute, Vol. 66, No. 2, Feb., 1969, pp 119 - 128.
11. Jimenez, R., White, R.N., and Gergely, P. (1982), "Cyclic Shear and Dowel Action Models in Reinforced Concrete", Journal of the Structural Division, Proc. ASCE Vol. 108 No. ST5, May 1982, pp 1106 - 1123.
12. Bresler, B. and MacGregor, J.G. (1967), "Review of Concrete Beams Failing in Shear", Journal of the Structural Division, ASCE, Vol 93, No. ST1, Proc. Paper 5106, Feb. 1967, pp 343 - 372.
13. Collins, M.P. (1978), "Towards a Rational Theory for RC Members in Shear", Journal of the Structural Division, ASCE, Vol. 104 No. ST4, Proc. Paper 13697, April, 1978, pp 649 - 666.
14. Vecchio, F. and Collins M.P. (1982) "The Response of Reinforced Concrete to In-Plane Shear and Normal Stresses", University of Toronto, Dept. of Civil Engineering, Publication No. 82 - 03, March 1982, 332 pp.
15. Collins, M.P. (1983), "Prestressed Concrete Structures", A Post-Graduate Course at the University of Stellenbosch, March 1983.
16. Neville, A.M. (1973), "Properties of Concrete".
17. Road Note No.4 (1969), TRRL Publication.

APPENDIX A

EQUATIONS FOR USE IN SOLUTION TECHNIQUE
AND EXAMPLE CALCULATIONS

A.1 Further Details on Solution Technique to Reinforced Concrete Beams

Steps of the solution procedure were outlined in Section 3.6. The pure flexure and the combined flexure-shear cases are examined here with further detail.

Referring to Figure 3.1, for a known top face strain ϵ_{ct} , the following relationships can be deduced from the pure flexure theory.

$$\alpha\beta = \Omega_{ct} - \frac{1}{3} \Omega_{ct}^2 \dots\dots\dots (A.1)$$

$$\beta = \frac{4 - \Omega_{ct}}{6 - 2\Omega_{ct}} \dots\dots\dots (A.2)$$

If y is the depth to the neutral axis,

$$\phi = \frac{\epsilon_{ct}}{y} \dots\dots\dots (A.3)$$

$y = y_p$ for pure flexure case and

$y = y_n$ for combined flexure and shear case.

From the geometry of the diagram for strains (Figure 3.1 (c)) the following relationships are deduced:-

$$\epsilon'_\ell = -\frac{y - d'}{y} \epsilon_{ct} \dots\dots\dots (A.4)$$

$$\epsilon_\ell = \frac{d - y}{y} \epsilon_{ct} \dots\dots\dots (A.5)$$

A.1.1 Pure Flexure Case

Given the extreme compression fibre strain, ϵ_{ct} , for a rectangular section the pure flexure case is solved if the correct neutral surface depth y_p is known so as to define the correct strain profile. Using the well known equivalent rectangular compression stress block theory, the following cases are possible for y_p .

- (i) For both top and bottom steel yielding, equilibrium of forces requires that

$$\alpha\beta f'_c b y_p + A'_l f'_{ly} = A_l f_{ly}$$

hence
$$y_p = \frac{A_l f_{ly} - A'_l f'_{ly}}{\alpha\beta f'_c b} \dots\dots\dots (A.6)$$

- (ii) For only bottom steel yielding, equilibrium of forces requires that

$$\alpha\beta f'_c b y_p + A'_l f'_l = A_l f_{ly}$$

and by using equation (A.4) the neutral surface depth can be shown to be:

$$y_p = -\left(\frac{\epsilon_{ct} E A'_l - A_l f_{ly}}{2\alpha\beta f'_c b} \right) + \sqrt{\left(\frac{\epsilon_{ct} E A'_l - A_l f_{ly}}{2\alpha\beta f'_c b} \right)^2 + \frac{A'_l d' \epsilon_{ct} E}{2\alpha\beta f'_c b}}$$

..... (A.7)

(iii) For all steel in elastic range, equilibrium of forces gives

$$\alpha\beta f'_c b y_p + A'_l \epsilon_{ct} E \left(\frac{y_p - d'}{y_p} \right) - A_l \epsilon_{ct} E \left(\frac{d - y_p}{y_p} \right) = 0$$

If the modulus of elasticity for bottom and top longitudinal steel are assumed equal then the neutral surface depth for this case is given by:-

$$y_p = - \frac{\epsilon_{ct} E (A'_l + A_l)}{2\alpha\beta f'_c b} + \sqrt{\left(\frac{\epsilon_{ct} E (A'_l + A_l)}{2\alpha\beta f'_c b} \right)^2 + \frac{\epsilon_{ct} E (A'_l d' + A_l d)}{\alpha\beta f'_c b}} \dots \dots \dots (A.8)$$

(iv) For only top steel yielding equilibrium of forces yields

$$\alpha\beta f'_c b y_p + A'_l f'_l y = A_l f_l y$$

and y_p is given by:-

$$y_p = - \frac{A'_l f'_l y + \epsilon_{ct} E A_l}{2\alpha\beta f'_c b} + \sqrt{\left(\frac{A'_l f'_l y + \epsilon_{ct} E A_l}{2\alpha\beta f'_c b} \right)^2 + \frac{\epsilon_{ct} E A_l d}{\alpha\beta f'_c b}} \dots \dots \dots (A.9)$$

Having determined y_p , the flexural moment, M_p , can be evaluated as:-

$$M_p = A'_l f'_l h_l + \alpha\beta f'_c b y_p \left(d - \frac{\beta y_p}{2} \right) \dots \dots (A.10)$$

A.1.2 Combined Loading Case

The shear force in the section is given by

$$V = \frac{M}{a} \dots\dots\dots(A.11)$$

and the lever arm, jd, by

$$jd = \frac{M}{\bar{A}_l f_l} \dots\dots\dots(A.12)$$

As a start of the iteration process the depth to the neutral axis is estimated to some value less than the known pure flexure value. A strain profile is thus established from which internal forces are calculated such that the section is in equilibrium. From the internal forces, the moment, M, and the lever arm, jd, are computed. The value of jd is used to determine q_b (see equation (3.6)) which in turn is used to determine q_n (see equation (3.7)). These define the shear flow distribution.

A.1.2.1 Evaluation of Angles and Strains

With the known shear flow distribution, the angles and strains at any level in the cracked concrete can be evaluated through an iterative process similar to that developed by Onsongo (1978) for the case of combined moment and torsion.

Equation (3.20) can be rewritten as:

$$q = \frac{bf_{cp} \tan \theta}{1 + \tan^2 \theta} \dots\dots\dots(A.13)$$

For any given level, j , in the cracked concrete the strains and the principal angle of compression can be evaluated from the following relationships.

(i) Case of Transverse Steel Yielding

If q_j is the shear flow and θ_j the principal angle at the level j , equation (3.9) takes the form:-

$$\tan \theta_j = \frac{A_v f_{vy}}{q_j s_v}$$

Define $t_v = \frac{A_v}{s_v} \dots \dots \dots (A.14)$

and let $c = \frac{t_v f_{vy}}{q_j} \dots \dots \dots (A.15)$

then $f_{cp} = \frac{q_j (1+c^2)}{bc} \dots \dots \dots (A.16)$

(see equation A.13)

The value of f_{cp} is then used to calculate the principal compression strain, ϵ_{cp} , from equation (3.21). By a systematic evaluation of response from low values of ϵ_{ct} , it is possible to choose which of the two roots of equation (3.21) is applicable. By calculating the longitudinal strain, ϵ_s , from the strain profile, the transverse strain is deduced from equation (3.16)

as:-
$$\epsilon_v = \frac{\epsilon_{cp} (1 - c^2) + \epsilon_s}{c^2} \geq \epsilon_{vy}$$

(ii) Case of Transverse Steel in Elastic Range

Let $\epsilon_v = \eta \epsilon_{vy}$

Then, using equation (3.16) the following expression is deduced:-

$$\Omega_{cp} = \frac{\eta^3 c^2 \Omega_{vy} - \Omega_l}{1 - \eta^2 c^2} \dots \dots \dots (A.17)$$

For $\Omega_{cp} \geq 0$ the following boundaries for Ω are recognised.

$$\left[\frac{\Omega_l}{\Omega_{vy}} \cdot \frac{1}{c^2} \right]^{\frac{1}{3}} \leq \eta \leq \frac{1}{c}$$

or $\frac{1}{c} < \eta < \left[\frac{\Omega_l}{\Omega_{vy}} \cdot \frac{1}{c^2} \right]^{\frac{1}{3}}$

Equation (A.13) can be rewritten in terms of η as:

$$q_i = \frac{b\lambda (2\Omega_{cp} - \Omega_{cp}^2) \eta c}{1 + \eta^2 c^2}$$

leading to the function

$$f(\eta) = \frac{\eta c}{1 + \eta^2 c^2} (2\Omega_{cp} - \Omega_{cp}^2) - \frac{q_i}{b\lambda} \dots \dots (A.18)$$

This function is conveniently differentiated to allow use of the recursion formula for obtaining a solution for η . The first differential takes the form:-

$$f'(\eta) = \frac{\eta^3 c^3 \Omega_{vy} - c \Omega_\ell}{(1 + \eta^2 c^2)^2} (2 - \Omega_{cp}) + \frac{2(\eta^3 c^3 \Omega_{vy} ((3 - \eta^2 c^2) - 2\eta^2) - 2\eta^2 c^3 \Omega_\ell)(1 - \Omega_{cp})}{(1 + \eta^2 c^2)(1 - \eta^2 c^2)^2} \dots \dots \dots (A.19)$$

A value of η is first guessed within suitable limits established. Subsequent iteration steps are then obtained using the recursion formula.

$$\eta_{i+1} = \eta_i - \frac{f(\eta_i)}{f'(\eta_i)} \dots \dots \dots (A.20)$$

This gives quadratic convergence close to the root of $f(\eta) = 0$. Once a solution is found, the transverse strain and the angle of principal strain are calculated. The principal tensile strain in concrete, ϵ_t , is then computed as:-

$$\epsilon_t = \epsilon_{cp} + \epsilon_v + \epsilon_\ell$$

This enables determination of the effective peak concrete stress, λ . The effective peak concrete stress is calculated in an iterative scheme.

Initially, λ is assumed equal to f'_c . Subsequent values for λ are calculated from:-

$$\lambda_{i+1} = \frac{\lambda_i}{0.8 + 0.34 \Omega_t}$$

For every new value of λ , if there is no satisfactory convergence (between λ_i and λ_{i+1}), a new set of strains is computed using the latest value of λ as the effective peak concrete stress until convergence is obtained.

The evaluation of angles and strains is done at all chosen levels in the section to enable use of Simpson's integration formulae. This in turn enables the evaluation of new values for the moment and shear. These are compared with the previous values. If the difference is significant, the whole process is repeated until acceptable convergence is obtained. A sample calculation to show how the iterative process works is presented in the following section.

A.2 Sample Calculation

Consider the beam section shown in Figure 3.1 Given:

A_ℓ	=	1905mm^2	ϵ_{CO}	=	0.002
A'_ℓ	=	226mm^2	f'_c	=	36.8N/mm^2
b	=	200mm	f_y	=	462N/mm^2
h_ℓ	=	345.8mm	f'_y	=	282N/mm^2
d	=	368.8mm	E	=	200kN/mm^2
d'	=	23mm	ϵ'_ℓ	=	1.41×10^{-3}
h	=	400mm	ϵ_ℓ	=	2.31×10^{-3}
Ω_{vy}	=	0.705			

Consider a case loading with top face strain $\epsilon_{ct} = 0.001$.

Then Ω_{ct}	=	0.5
β	=	0.7
$\alpha\beta$	=	0.417

Step 1

Assume both top and bottom longitudinal steel are yielding for pure flexure loading.

equation (A.6) , $y_p = 271.91\text{mm}$

equation (A.4) $\epsilon'_l = 0.915 \times 10^{-3} < \epsilon'_{ly}$ Not O.K.

equation (A.5) $\epsilon_l = 0.356 \times 10^{-3} < \epsilon_{ly}$ Not O.K.

Hence try both steels in elastic range.

equation (A.8) gives $y_p = 157.46\text{mm}$

Check values of ϵ'_l and ϵ_l

equation (A.4) $\epsilon'_l = 0.854 \times 10^{-3} < \epsilon'_{ly}$ O.K.

equation (A.5) $\epsilon_l = 1.342 \times 10^{-3} < \epsilon_{ly}$ O.K.

Hence $C_S = A'_l E \epsilon'_l = 38.60\text{kN}$

$T = A_l E \epsilon_l = 511.30\text{kN}$

$C_1 = \alpha \beta f'_c b y_p = 472.76\text{kN}$

Using equation (A.10), find the pure moment value, M_p

as: $M_p = 160.96\text{kNm}$

Step 2

For the combined flexure - shear case, we start by guessing a value for y_n .

Guess A: $y_n = 120\text{mm}$

Equation (A.4) $\epsilon_c = 0.808 \times 10^{-3}$ hence $C_s = 36.54 \text{ kN}$

Equation (A.5) $\epsilon_s = 2.073 \times 10^{-3}$ hence $T = 789.94 \text{ kN}$

$C_1 = \alpha \beta f'_c b y_n$ hence $C_1 = 360.29 \text{ kN}$

Take $C_2 = T - C_s - C_1$ $C_2 = 398.11 \text{ kN}$

Take $\bar{x}_2 = \frac{d - y_n}{2}$ $\bar{x}_2 = 129.17 \text{ mm}$

Step 3

Taking moments about bottom longitudinal steel, new moment, M , is deduced as:

$M = 181.16 \text{ kNm}$

and $jd = 229.33 \text{ mm}$

hence for $a = 1 \text{ m}$, $V = 181.16 \text{ kN}$

Equation (3.6) $q_b = 0.7899 \text{ kN/mm}$

Equation (3.7) $q_n = 0.4495 \text{ kN/mm}$

hence $q_m = 0.6197 \text{ kN/mm}$

Step 4

Evaluate θ_n

Equation (A.15) $c = 0.94523$; $0 < \eta < \frac{1}{c}$

$$\frac{1}{c} = 1.079$$

$$c^2 = 0.89346$$

Try $\eta_1 = 0.50$

$$\text{Equation (A.17)} \quad \Omega_{cp} = 0.10138$$

$$\text{Equation (A.18)} \quad f(\eta) = 0.01193$$

$$\text{Equation (A.19)} \quad f'(\eta) = 0.59776$$

Hence using the recursion formula (equation A.20)

$$\eta_2 = 0.48004$$

Repeat step 4 until convergence in η is obtained and then deduce θ_n from

$$\tan \theta_n = \eta c$$

From the strains, work out λ , the effective peak concrete stress. If the difference from the previous value of λ is significant, repeat step 4 with the new value of λ until satisfactory convergence is obtained. Further progress of the iteration process is shown in Table A.1.

Consider the evaluation of θ_b

$$c = 0.53789 \quad 0 < \eta < \frac{1}{c}$$

$$\frac{1}{c} = 1.8591$$

$$c^2 = 0.28933$$

Assume transverse steel yielding

$$\text{Equation (A.16)} f_{cp} = 9.467$$

$$\text{Equation (3.21)} n_{cp} = 0.14151$$

$$\text{Hence } \epsilon_{cp} = 0.283 \times 10^{-3}$$

$$\text{and } \epsilon_v = 7.860 \times 10^{-3} > \epsilon_{vy}$$

Transverse steel yielding and hence

$$\tan \theta_b = c = 0.53789$$

The above procedures are repeated at all the chosen levels depending on whether or not the transverse steel is yielding. On obtaining the full set, a new value for C_2 , the compression in cracked concrete below the neutral axis is determined together with its point of action.

Step 5

With the new value of C_2 check the equilibrium of the section. If equilibrium does not exist, repeat steps 2, 3 and 4 with new values for y_n until equilibrium is established. See Table A.1.

Note that in Table A.1, the effective peak concrete stress was not revised and so the results

represent only one step of iteration with respect to the peak concrete stress, λ .

The image shows a large, faint grid or table structure, likely a data table or iteration log, which is mostly illegible due to fading. It appears to have multiple columns and rows, possibly representing iterative calculations or data points.

Y _n (mm)	Level	q N/mm	c	Links elastic YES/NO	Links elastic Iterations for η					Principal angle of compression	Initial value of C ₂	Final value of C ₂	REMARKS
					1	2	3	4	5				
120	1	449.5	0.945		0.500	0.480	0.478			24.35			
	2	613.7	0.686	YES	-	-	-			34.44	393.11	252.19	Guess another Y _n
	3	789.9	0.538	YES	-	-	-			28.28			
80	1	284.4	1.494	NO	0.400	0.335	0.285	0.307	0.302	24.26			
	2	582.3	0.730	YES	-	-	-	-	-	36.12	607.92	389.74	Guess another Y _n
	3	800.1	0.483	YES	-	-	-	-	-	25.77			
148.9	1	555.1	0.765	NO	0.500	0.622	0.595	0.592		24.40			
	2	558.9	0.770	NO	0.980	0.399	0.998			37.19	77.39	259.59	Guess another Y _n
	3	562.7	0.755	YES	-	-	-	-	-	37.24			
132.6	1	526.5	0.807	NO	0.550	0.502				24.39			
	2	602.6	0.705	YES	-	-	-	-	-	35.19	243.19	223.30	Guess another Y _n
	3	676.7	0.626	YES	-	-	-	-	-	32.06			
134.2	1	513.5	0.827	NO	0.547	0.548	-	-	-	24.38			
	2	589.8	0.720	YES	-	-	-	-	-	35.77	225.64	213.48	Guess another Y _n
	3	606.0	0.650	YES	-	-	-	-	-	32.54			
136.7	1	514.2	0.826	NO	0.548	0.549	-	-	-	24.38			
	2	580.6	0.732	YES	-	-	-	-	-	36.20	198.83	205.07	Guess another Y _n
	3	646.9	0.657	YES	-	-	-	-	-	33.30			
135.9	1	507.2	0.838	NO	0.541	0.541	-	-	-	24.38			
	2	580.1	0.732	YES	-	-	-	-	-	36.22	207.36	205.94	Satisfactory Convergence
	3	652.9	0.651	YES	-	-	-	-	-	33.05			

Table A1 : Iteration Process

APPENDIX B

COMPUTER PROGRAM

B.1 Program Capabilities

The program is capable of solving the response of solid rectangular reinforced concrete section whose material and geometrical properties and the ratio of moment to shear are known. It will also handle prestressed concrete sections for certain values of prestressing force.

B.2 Input of data

The following symbols are used in the program for input of data. Their respective descriptions are included here.

NLCB	Number of different sections to be analysed
NSPECIMEN	Beam number (for example 1 for CFT-TB1)
SMSR	Ratio of moment to shear in section
ACS	Area of top longitudinal steel
YSH	Yield strain of transverse steel
YST	Yield strain of bottom longitudinal steel
YHS	Yield stress of transverse steel
MES	Modulus of elasticity of bottom longitudinal steel
YTS	Yield stress of bottom longitudinal steel
BRS	Width of section
EPZERO	Concrete strain at peak concrete stress

YSC	Yield strain of top longitudinal steel
DP	Depth to centre of mass of prestress steel
AHS	Area of transverse steel
ATS	Area of bottom longitudinal steel
PCS	Peak concrete stress
SPACING	Spacing of transverse steel
D1	Depth to centre of mass of bottom longitudinal steel
D2	Depth to centre of mass of top longitudinal steel
MESC	Modulus of elasticity of top longitudinal steel
MESH	Modulus of elasticity of transverse steel
APS	Area of prestressing steel
YPS	Yield stress of prestressing steel
YSP	Yield strain of prestressing steel

The input data is accessed by READ statements in the program. In Appendix B.6, the input data for the eight test beams is presented. The data is in six separate subfiles as shown separated by the horizontal lines. At the beginning of each subfile, the number of different sections to be analysed is entered. On the next line the beam number and ratio of moment to shear in the section under consideration are entered. Material and section properties are then entered on the next two lines. Hereafter, other sections can be

considered upto the maximum number specified, by repeating operation of lines 2 to 4. Note that the data is entered in the order in which the symbols have been described above.

B. 3 Steps of the Program

The program carries out an iterative scheme as discussed in the theory presented in Chapter 3. The working of the program is summarised by the flow charts presented in figures B.1 (a) - (j). In this program, Simpson's Integration rule has been applied for five ordinates instead of the three considered in the theory. Equations (3.11) and 3.12) are therefore revised to:-

$$C_2 = \frac{d-y_n}{12} (q_n \cot\theta_n + 4q_u \cot\theta_u + 2q_m \cot\theta_m + 4q_l \cot\theta_l + q_b \cot\theta_b)$$

and

$$\bar{x}_2 = d-y_n \left(\frac{q_n \cot\theta_n + 3q_u \cot\theta_u + q_m \cot\theta_m + q_l \cot\theta_l}{q_n \cot\theta_n + 4q_u \cot\theta_u + 2q_m \cot\theta_m + 4q_l \cot\theta_l + q_b \cot\theta_b} \right)$$

Where u and l are new positions at the mid-points of the top half and bottom half, respectively of the region below the neutral axis (see Figure 3.1). The other symbols are as defined before. Further information about the steps of the program is available from the program listing given in Appendix B.5 by means of comment statements.

B.4 Output of Results

The notation used in the input of data is also used in the printout of the input data except where specified. The required convergence parameters for a chosen top face strain value are output in a suitable tabular form as shown in Table B.1. The new symbols used are as defined below:-

SHS	Spacing of transverse steel
PMOMENT	Pure moment value from consideration of pure flexure theory
PCUR	Curvature due to the pure moment
MOMENT	Moment for the combined moment and shear loading consideration
CUR	Curvature due to the above moment
SHEAR	Shear force in section
ANGLES	The angles of principal compression at each of the five levels considered
SHEAR FLOW	Corresponding shear flow values
LSTR	Corresponding longitudinal strains
TRST	Corresponding transverse strains
DIAGST	Corresponding principal compression strains
FCP	Corresponding principal compressive stresses
FCD	Corresponding effective peak concrete stresses
COUNTERS	Number of iterations to convergence: the first five corresponding respectively to convergence in strains at each of the chosen levels and the last representing the overall number for convergence of the forces on section

B.5 Program Listing

FORTRAN COMPILATION BY XAFAT MK GA DATE 21/11/84 TIME 11/00/07

```

0005      SEND TO (20,SEMICOMPILED)
0006      LIST
0007      ADD UNP (20,PROGRAM HTXX)
0008      LIBRARY(SUBGROUPSRF7)
0009      LIBRARY(SUBGROUPSRGP)
0010      LIBRARY(SUBGROUPSFCE)
0011      LIBRARY(SUBGROUPS-RS)
0012      PROGRAM (MIMI)
0013      COMPRESS INTEGER AND LOGICAL
0014      EXTENDED DATA
0015      TRACE 2
0016      INPUT 100 =CRJ
0017      OUTPUT 200 =LPO
0018      END

0019      MASTER CLASS
0020      WRITE(2,103)
0021      WRITE(2,101)
0022      WRITE(2,102)
0023      COMMON /BLK1/ D1,D2,T3,T1,PRODUCT,XBAR,YST,YTS,CE
0024      COMMON /BLK2/ YN,PUREMOMENT,IND3
0025      COMMON /BLK4/ PCS,BRS,EPZERO,PCUR,ETA,I,IF,MA1,MA2,MA3,MA4,MA5
0026      COMMON /BLK5/ MES,YSC,ATS,B2,YCS,ACS,SMSR
0027      COMMON /BLK6/ Q3,QN,QM,QU,QL,VM,V,YSH,YHS,AHG,SPACING,L
0028      COMMON /BLK7/ RATIO2,RATIO3,K,KX
0029      COMMON /BLK9/ ANGLES(S),A(S),B(S),CE(S)
0030      COMMON /BLK11/ RLOS(S),TRST(S),DIAG(S)
0031      COMMON /BLK12/ VA(S),CST(S),FRACTION(1000),DD(100)
0032      COMMON /BLK14/ M1,M2,M3,M4,M5,KC1,KC2,KC3,KC4,KC5,KC6
0033      COMMON /BLK15/ APS,YPS,YSP,MESP,DEP,DP,KA,KE,KI,RNVC,RNGC,RCH
0034      DIMENSION IC(50,5)
0035      READ(1,5000) NLCB
0036      5000  FORMAT(L0)
0037      IPAGE=1
0038      DO 600 N=1,NLCB
0039      IF=0
0040      ILLNL=J
0041      IPAGE=IPAGE+1
0042      READ(1,5005) NSPECIMEN,SMSR
0043      5005  FORMAT(10,F0.0)
0044      WRITE(2,500) NSPECIMEN
0045      200  FORMAT('1',//////////,10X,'PREDICTIONS FOR BEAM CFT-TB',
0046      11X,10X,'SOURCES SHITOTE UNIVERSITY OF NAIROBI(1985)')
0047      WRITE(2,500)
0048      300  FORMAT(7,50X,'TABLE OF INPUT MATERIAL AND SECTION PROPERTIES')
0049      WRITE(2,400)
0050      400  FORMAT(10X,'BRS',9X,'DTS',9X,'DCS',9X,'ATS',9X,'ACS',9X,'AHG',
0051      19X,'SHJ')
0052      READ(1,500) ACS,YSH,YST,YHS,MES,YTS,BRS,EPZERO,YSC,YCS,DP
0053      500  FORMAT(4F0.0,10,6F0.0)
0054      READ(1,700) AHG,ATS,PCS,SPACING,D1,D2,NLSC,MESP,APS,YPS,YSP,
0055      100P
0056      700  FORMAT(6F0.0,210,4F0.0)
0057      WRITE(2,500) BRS,D1,D2,ATS,ACS,AHG,SPACING
0058      600  FORMAT(10X,7(2X,E10.4))
0059      WRITE(2,900)
0060      900  FORMAT(7,10X,'YTS',9X,'YCS',9X,'YHS',9X,'PCS',9X,'YST',9X,'YSC',
0061      19X,'YSH')
0062      WRITE(2,1000) YTS,YCS,YHS,PCS,YST,YSC,YSH
0063      1000  FORMAT(10X,7(2X,E10.4))
0064      WRITE(2,105) EPZERO
0065      WRITE(2,5010) SMSR
0066      5010  FORMAT(//,40X,'MOMENT-SHEAR RATIO=',F0.1)
0067      WRITE(2,5015) IPAGE
0068      5015  FORMAT('1',//////////,110X,'PAGE',14)
0069      C    VARY WRITE STATEMENTS ACCORDINGLY IF RC OR PC IS BEING
0070      C    ANALYSED
0071      C    BRS-BREADTH OF SECTION

```

```

0072 C DIS-DEPTH TO TENSION STEEL
0073 C DC-DEPTH TO COMPRESSION STEEL
0074 C AT5-AREA OF TENSION STEEL
0075 C AC3-AREA OF COMPRESSION STEEL
0076 C AH5-AREA OF HOOP STEEL
0077 C SH5-SPACING OF HOOP STEEL
0078 C TY-YIELD STRESS OF TENSION STEEL
0079 C YCS-YIELD STRESS OF COMPRESSION STEEL
0080 C YHS-YIELD STRESS OF HOOP STEEL
0081 C PC3-PLAK CONCRETE STRESS
0082 C YST-YIELD STRAIN OF TENSION STEEL
0083 C YSC-YIELD STRAIN OF COMPRESSION STEEL
0084 C YSH-YIELD STRAIN OF HOOP STEEL
0085 C MS-MODULUS OF ELASTICITY OF STEEL
0086 C U1-STRESS BLOCK FACTOR FOR ULTIMATE STRENGTH
0087 C U2-STRESS BLOCK FACTOR FOR DEPTH TO NEUTRAL AXIS
0088 C ABS-AREA OF PRESTRESS STEEL
0089 C YSP-YIELD STRAIN OF PRESTRESS STEEL
0090 C YPS-YIELD STRESS OF PRESTRESS STEEL
0091 C DDP-STRAIN DIFFERENCE DUE TO PRESTRESSING OPERATION
0092 C UP-DEPTH TO PRESTRESS STEEL
0093 C MSP-MODULUS OF ELASTICITY OF PRESTRESS STEEL
0094 C MS3-MODULUS OF ELASTICITY OF COMPRESSION STEEL
0095 C T1-TOP FACE STRAIN
0096 C K=0
0097 C U1=100 *STRAINLUMP=1/21
0098 C K1=K2=K3=K4=K5=K6=0
0099 C T1=T2=U0002
0100 C M1=M2=U003/100 *M3=M4=M5=J
0101 C U2=U4-(U1/LE*LR0)/(6-(U*TI/EP*LR0))
0102 C PRODUCE=(TI/PL*LR0)-((T1+*2)/(3*(EPL*KO**2)))
0103 C CALL POK
0104 C X=Y
0105 C Y=U0/2*M
0106 C CALL TRAPL
0107 C KAR=(O1-YND)/2
0108 C CALL UPDATE
0109 C IFC(=,=,1) GO TO 1101
0110 C IFC(=,=,1) YN=SP
0111 C IFC(=,=,1) GO TO 7000
0112 C IFC(=,=,1) GO TO 7000
0113 C IFC(=,=,1) YN=SP
0114 C IFC(=,=,1) GO TO 7000
0115 C IFC(=,=,1) GO TO 7000
0116 C K=0
0117 C CALL SOLUTION
0118 C IFC(=,=,1) GO TO 1030
0119 C IFC(=,=,1) GO TO 1030
0120 C YN=U0/2*M
0121 C CALL TRAPL
0122 C CALL UPDATE
0123 C IFC(=,=,1) GO TO 1100
0124 C IFC(=,=,1) YN=SP
0125 C IFC(=,=,1) GO TO 7000
0126 C CALL SOLUTION
0127 C IFC(=,=,1) GO TO 1040
0128 C IFC(=,=,1) GO TO 1030
0129 C CALL LINKAKFIT
0130 C CALL TRAPL
0131 C CALL UPDATE
0132 C IFC(=,=,1) GO TO 101
0133 C IFC(=,=,1) YN=SP
0134 C IFC(=,=,1) GO TO 7000
0135 C CALL SOLUTION
0136 C IFC(=,=,1) GO TO 1030
0137 C IFC(=,=,1) GO TO 1030
0138 C IFC(=,=,1) WRITE(2,103) T1
0139 C F=MIN(T1,K*TOP FACE STRAIN=1/7.5//10X**NO CONVERGENCE AFTER 15
0140 C I=MAX(U003//15X**ITERATIONS ABANDONED*)
0141 C IFC(=,=,1) GO TO 1100
0142 C GO TO 1040
0143 C POK=11/A
0144 C IFC(A(4)-LT-CST(5)) M5=5
0145 C IFC(A(4)-LT-CST(6)) AND M5=U0.5) M4=4
0146 C IFC(A(5)-LT-CST(3)) AND M5=U0.5) M3=3
0147 C IFC(A(7)-LT-CST(2)) AND M5=U0.5) M2=2
0148 C IFC(A(1)-LT-CST(1)) AND M5=U0.5) M1=1
0149 C JN=MIN(LUMP+K

```

7000

1020

1040

1050

1030

```

POK=11/A
IFC(A(4)-LT-CST(5)) M5=5
IFC(A(4)-LT-CST(6)) AND M5=U0.5) M4=4
IFC(A(5)-LT-CST(3)) AND M5=U0.5) M3=3
IFC(A(7)-LT-CST(2)) AND M5=U0.5) M2=2
IFC(A(1)-LT-CST(1)) AND M5=U0.5) M1=1
JN=MIN(LUMP+K

```

AFTER 15


```

0327 SUBROUTINE UPDAT
0328 SEGMENT UPDAT, MAJOR VARIABLES DURING ITERATIONS
0329 MMY AND THE MOMENT AND SHEAR RESPECTIVELY
0330 MMYN IS THE LEVER ARM
0331 SHEARARM/LEVER ARE THE SHEAR FLOW'S
0332 SEGMENT ENDURES SHEAR EQUILIBRIUM ON SECTION
0333 COMMON /OLK1/ D1/D2/T1/T1/PRODUCT/XBAR,YST,YTS,C2
0334 COMMON /OLK2/ YN/PURCHMOMENT/IND3
0335 COMMON /OLK3/ T2/CHFORCE
0336 COMMON /OLK4/ PCSI/PBSP/EPI/PCUR/ETA1/IF/MAT/MA2/MA3/MA4/MA5
0337 COMMON /OLK5/ MES/YSCGATS/BZ/YCS/ACS/MSR
0338 COMMON /OLK6/ QU/VA/QU/QL/RM/V/YSH/YHS/AHS/SPACING/L
0339 COMMON /OLK9/ ANGLE(S)/A(S)/B(S)/C(S)
0340 COMMON /LKI0/ FORCE(C2)/DIST(C2)
0341 COMMON /LKI1/ RLUS(C3)/TRJ(C5)/DIAG(C5)
0342 COMMON /OLK13/ FCD/FCP/ECP/EV/RLS/C
0343 COMMON /OLK14/ M1/M2/M3/M4/M5/KC1/KC2/KC3/KC4/KC5/KC6
0344 COMMON /OLK15/ APS/YPS/YSP/RES/DEF/UP/KA/KL/KI/RNVC/RNSC/RCH
0345 KAI=0
0346 IND3=0
0347 KAPAL=0
0348 CS=ACS*ALC+CFL2
0349 IFTL=GT*YSC.DR.T.L.L2.YSC) CS=ACS*YCS
0350 T=AT*ALC*F)
0351 IFTD=GT*YST.DR.T3.C2.YST) T=ATS*YTS
0352 T=AP*ALC*P*F4
0353 IFT4=GT*YSP.DR.T4.E4.YSP) TP=APS*YPS
0354 C2=I+TP-C2-CONFORCE
0355 RLVLEN=((C2*(D1-D2))+CONFORCE*(D1-(D2*YND/2)))+(C2*XDAN)
0356 1-(TP*(D1-D2))/T
0357 FORCE(1)=C2
0358 D1GT(1)=XDANR
0359 R4=I*ALVLEN
0360 Y=R4/ALVLEN
0361 Q3=Y/RLVLEN
0362 Q4=(C2*V/D1)*(1-(D1-YN)/(C2*LEVER))
0363 Q5=(Q4+Q3)/2

```

15
14

```

0309 1-(G*P2*Y*P*(O1-QP))
0300 RETURN
0301 PUNCHMOMENT=(ACC*YCS*(O1-O2))+C*V*FORCC*(O1-((O2*YN)/2))
0302 1-(G*P2*Y*P*(O1-QP))
0303 RETURN
0304 PUNCHMOMENT=(ACC*ME*G*T2*(O1-O2))+CONFORCC*(O1-((O2*YN)/2))
0305 1-(G*P2*Y*P*(O1-QP))
0306 RETURN
0307 PUNCHMOMENT=(ACC*YCS*(O1-O2))+CONFORCC*(O1-((O2*YN)/2))
0308 1-(G*P2*ME*P*T4*(O1-QP))
0309 RETURN
0310 END

```

END OF SEGMENT, LENGTH 1129, NAME PURE

```

0311 DO ROUTINE TRIPLE
0312 SEGMENT COMPUTES STRAIN PROFILE FOR GIVEN TOP FACE STRAIN
0313 AND DEPTH TO N.A
0314 CONFORCC IS THE TOP CONCRETE FORCE ABOVE THE N.A
0315 COMMON /DLK1/ D1/D2/T1/T2/PRODUCT/XBAR/YST/YTS/C2
0316 COMMON /DLK2/ YN/PURFOMENT/IDU-
0317 COMMON /DLK3/ T2/CONFORCE
0318 COMMON /DLK4/ PCS/DURS/EDZERO/PCUR/LTA/LEF/MAT/MAS/MAS4/MAS
0319 COMMON /DLK5/ APS/YPS/YSP/RESP/DEP/DPR/KX/KY/RNYC/RNSC/RCH
0320 T2=((Y*V*O2)*T1)/YN
0321 T3=((O1-Y*H)*T1)/YN
0322 CONFORCC=PRODUCT*PCS*3R3*YN
0323 F5=C*V*O2*(O1-QP)
0324 F4=C*V*O2*P
0325 RETURN
0326 END

```

END OF SEGMENT, LENGTH 1129, NAME TRIPLE

```

0304 QU=1+((40-20)/4)
0305 QL=AN+(Q*(45-40)/4)
0306 IF(AN.LT.0.0) RETURN
0307 RMCV=QU
0308 RMCJ=AN
0309 DO 10 ML=1,5
0370 L=ML-1
0371 IND10=IND11,IND12,IND13=0
0372 FC0=C2(L+1)
0373 CALL ACCHOLD3
0374 IF(XF.CM.1) RETURN
0375 ONEACP=CP/EPZERO
0376 ECT=V*U*P*RLS
0377 FCE=PCS/(.6+(.34*ECT/EPZERO))
0378 RUI=(FC0-FCE)/FC0
0379 FGD=FLL
0380 IF(AJ(CRCH).LT..001) GO TO 10
0381 INDJ=1
0382 IF(M1-SOF(200,AVL-.E2,0)) GO TO 10
0383 IF(M2-SOF(200,AND.L.E2,1)) GO TO 10
0384 IF(M3-SOF(200,AND.L.E2,2)) GO TO 10
0385 IF(M4-SOF(200,AND.L.E2,3)) GO TO 10
0386 IF(M5-SOF(200,AND.L.E2,4)) GO TO 10
0387 INDJ=0
0388 GO TO 5
0389 CONFIND
0390 MAT=MR,MA3,MA4,MAJ=J
0391 KA=KAI+1
0392 RNV=C*(RNV-20)/20
0393 RNS=C*(RNS-QN)/QN
0394 IF(AJ(KR1/C).LT..001,AND,ABS(RNSC).LT..001) GO TO 20
0395 IF(AJ(RNVC).LT..001,AND,ABS(RNSC).GT..001) GO TO 25
0396 IF(M1-SOF(15)) GO TO 2)
0397 MLEV=L*V/QU
0398 GO TO 1)
0399 IF(M1-SOF(15)) GO TO 20
0400 V=1*01*REVER/(2*REVER)-01-YN)
0401 R=V*3*H*H
0402 Q3=V*REVER*
0403 GO TO 14
0404 CALL EVALUATION
0405 IF(KAI-SOF(15)) KA=1
0406 IF(INDJ.CM.1) KL=1
0407 RETURN
0408 END

```

END OF SEGMENT, LENGTH 999, MAKE UPDATE

```

0409 SUBROUTINE LINKYIELDING
0410 SEGMENT COMPUTES STRAINS FOR A CASE OF TRANSVERSE STEEL
0411 YIELDING
0412 K1,K2,K3,K4,K5,K6,K7,K8 ARE LOOP COUNTERS FOR ITERATIONS AT
0413 RESPECTIVE LEVELS
0414 CUP-PRINCIPAL DIAGONAL CONCRETE STRAIN
0415 LV-TRANSVERSE STEEL STRAIN
0416 CONDM /CONK4/ PCS,IRS,PCP,ZERO,PCUR,CTA,LEIF,MA1,MA2,MA3,MA4,MA5
0417 CONDM /CONK5/ QJ,QR,QM,QU,RL,RV,YSH,YHS,AHS,SPACING,L
0418 CONDM /CONK13/ FCD,FCP,CEP,VE,RLS,C
0419 CONDM /CONK14/ Y1,YS,Y3,MS,KC1,KC2,KC3,KC4,KC5,KC6
0420 IF(L1-SOF(1)) KC1=KC1+1
0421 IF(L2-SOF(1)) KC2=KC2+1
0422 IF(L3-SOF(1)) KC3=KC3+1
0423 IF(L4-SOF(1)) KC4=KC4+1
0424 IF(L5-SOF(1)) KC5=KC5+1
0425 IF(L6-SOF(1)) MA1=MA1+1
0426 IF(L7-SOF(1)) MA2=MA2+1
0427 IF(L8-SOF(1)) MA3=MA3+1
0428 IF(L9-SOF(1)) MA4=MA4+1
0429 IF(L10-SOF(1)) MA5=MA5+1
0430 IF(L11-SOF(1)) MAJ=MAJ+1
0431 IF(L12-SOF(1)) MA1=MA1,MA2=MA2,MA3=MA3,MA4=MA4,MA5=MA5
0432 IF(L13-SOF(1)) MA2=MA2,MA3=MA3,MA4=MA4,MA5=MA5
0433 IF(L14-SOF(1)) MA3=MA3,MA4=MA4,MA5=MA5
0434 IF(L15-SOF(1)) MA4=MA4,MA5=MA5
0435 IF(L16-SOF(1)) MA5=MA5
0436 GO TO 2
0437 GO TO 2
0438 GO TO 2
0439 GO TO 2
0440 GO TO 2
0441 GO TO 2
0442 GO TO 2
0443 GO TO 2
0444 GO TO 2
0445 GO TO 2
0446 GO TO 2
0447 GO TO 2
0448 GO TO 2
0449 GO TO 2
0450 GO TO 2
0451 GO TO 2
0452 GO TO 2
0453 GO TO 2
0454 GO TO 2
0455 GO TO 2
0456 GO TO 2
0457 GO TO 2
0458 GO TO 2
0459 GO TO 2
0460 GO TO 2
0461 GO TO 2
0462 GO TO 2
0463 GO TO 2
0464 GO TO 2
0465 GO TO 2
0466 GO TO 2
0467 GO TO 2
0468 GO TO 2
0469 GO TO 2
0470 GO TO 2
0471 GO TO 2
0472 GO TO 2
0473 GO TO 2
0474 GO TO 2
0475 GO TO 2
0476 GO TO 2
0477 GO TO 2
0478 GO TO 2
0479 GO TO 2
0480 GO TO 2
0481 GO TO 2
0482 GO TO 2
0483 GO TO 2
0484 GO TO 2
0485 GO TO 2
0486 GO TO 2
0487 GO TO 2
0488 GO TO 2
0489 GO TO 2
0490 GO TO 2
0491 GO TO 2
0492 GO TO 2
0493 GO TO 2
0494 GO TO 2
0495 GO TO 2
0496 GO TO 2
0497 GO TO 2
0498 GO TO 2
0499 GO TO 2
0500 GO TO 2
0501 GO TO 2
0502 GO TO 2
0503 GO TO 2
0504 GO TO 2
0505 GO TO 2
0506 GO TO 2
0507 GO TO 2
0508 GO TO 2
0509 GO TO 2
0510 GO TO 2
0511 GO TO 2
0512 GO TO 2
0513 GO TO 2
0514 GO TO 2
0515 GO TO 2
0516 GO TO 2
0517 GO TO 2
0518 GO TO 2
0519 GO TO 2
0520 GO TO 2
0521 GO TO 2
0522 GO TO 2
0523 GO TO 2
0524 GO TO 2
0525 GO TO 2
0526 GO TO 2
0527 GO TO 2
0528 GO TO 2
0529 GO TO 2
0530 GO TO 2
0531 GO TO 2
0532 GO TO 2
0533 GO TO 2
0534 GO TO 2
0535 GO TO 2
0536 GO TO 2
0537 GO TO 2
0538 GO TO 2
0539 GO TO 2
0540 GO TO 2
0541 GO TO 2
0542 GO TO 2
0543 GO TO 2
0544 GO TO 2
0545 GO TO 2
0546 GO TO 2
0547 GO TO 2
0548 GO TO 2
0549 GO TO 2
0550 GO TO 2
0551 GO TO 2
0552 GO TO 2
0553 GO TO 2
0554 GO TO 2
0555 GO TO 2
0556 GO TO 2
0557 GO TO 2
0558 GO TO 2
0559 GO TO 2
0560 GO TO 2
0561 GO TO 2
0562 GO TO 2
0563 GO TO 2
0564 GO TO 2
0565 GO TO 2
0566 GO TO 2
0567 GO TO 2
0568 GO TO 2
0569 GO TO 2
0570 GO TO 2
0571 GO TO 2
0572 GO TO 2
0573 GO TO 2
0574 GO TO 2
0575 GO TO 2
0576 GO TO 2
0577 GO TO 2
0578 GO TO 2
0579 GO TO 2
0580 GO TO 2
0581 GO TO 2
0582 GO TO 2
0583 GO TO 2
0584 GO TO 2
0585 GO TO 2
0586 GO TO 2
0587 GO TO 2
0588 GO TO 2
0589 GO TO 2
0590 GO TO 2
0591 GO TO 2
0592 GO TO 2
0593 GO TO 2
0594 GO TO 2
0595 GO TO 2
0596 GO TO 2
0597 GO TO 2
0598 GO TO 2
0599 GO TO 2
0600 GO TO 2
0601 GO TO 2
0602 GO TO 2
0603 GO TO 2
0604 GO TO 2
0605 GO TO 2
0606 GO TO 2
0607 GO TO 2
0608 GO TO 2
0609 GO TO 2
0610 GO TO 2
0611 GO TO 2
0612 GO TO 2
0613 GO TO 2
0614 GO TO 2
0615 GO TO 2
0616 GO TO 2
0617 GO TO 2
0618 GO TO 2
0619 GO TO 2
0620 GO TO 2
0621 GO TO 2
0622 GO TO 2
0623 GO TO 2
0624 GO TO 2
0625 GO TO 2
0626 GO TO 2
0627 GO TO 2
0628 GO TO 2
0629 GO TO 2
0630 GO TO 2
0631 GO TO 2
0632 GO TO 2
0633 GO TO 2
0634 GO TO 2
0635 GO TO 2
0636 GO TO 2
0637 GO TO 2
0638 GO TO 2
0639 GO TO 2
0640 GO TO 2
0641 GO TO 2
0642 GO TO 2
0643 GO TO 2
0644 GO TO 2
0645 GO TO 2
0646 GO TO 2
0647 GO TO 2
0648 GO TO 2
0649 GO TO 2
0650 GO TO 2
0651 GO TO 2
0652 GO TO 2
0653 GO TO 2
0654 GO TO 2
0655 GO TO 2
0656 GO TO 2
0657 GO TO 2
0658 GO TO 2
0659 GO TO 2
0660 GO TO 2
0661 GO TO 2
0662 GO TO 2
0663 GO TO 2
0664 GO TO 2
0665 GO TO 2
0666 GO TO 2
0667 GO TO 2
0668 GO TO 2
0669 GO TO 2
0670 GO TO 2
0671 GO TO 2
0672 GO TO 2
0673 GO TO 2
0674 GO TO 2
0675 GO TO 2
0676 GO TO 2
0677 GO TO 2
0678 GO TO 2
0679 GO TO 2
0680 GO TO 2
0681 GO TO 2
0682 GO TO 2
0683 GO TO 2
0684 GO TO 2
0685 GO TO 2
0686 GO TO 2
0687 GO TO 2
0688 GO TO 2
0689 GO TO 2
0690 GO TO 2
0691 GO TO 2
0692 GO TO 2
0693 GO TO 2
0694 GO TO 2
0695 GO TO 2
0696 GO TO 2
0697 GO TO 2
0698 GO TO 2
0699 GO TO 2
0700 GO TO 2

```

```

0435      OR(LWACP=1-JAKT(1)-(FCP/FCO))
0436      GO TO 1
0437      OR-LACP=1+JART(1)-(FCP/FCO)
0438      ECP=OR(LWACP)*EPELR0
0439      EV=(LCP*(1-(C**2)))+(RLD)/(C**2)
0440      ETA=LW/YSH
0441      RETURN
0442      END
    
```

END OF SEGMENT, LENGTH 340, NAME LINKSYIELDING

```

0443      SUBROUTINE ALLANGLES
0444      SEGMEN COMPUTES ANGLES AT ALL LEVELS
0445      AND SINKING FOR A CASE OF TRANSVERSE STEEL IN ELASTIC RANGE
0446      ETA IS ASSUMED TRANSVERSE STRAIN FACTOR
0447      FIVE FAVORABLE FUNDAMENTAL ARE TERMS FOR USE IN THE RECURSION
0448      FORMULA
0449      COMMON /LKN1/ 01,02,15,T1,PRODUCT,XVAR,YST,YTS,C2
0450      COMMON /LKN4/ PCS,JR3,EPELR0,PCOR,LTATA,IF,MT1,M2,M3,MA4,MA5
0451      COMMON /LKN6/ 35,29,24,QU,DL,RM,V,YSH,VHS,ALS,SPACING,L
0452      COMMON /LKN9/ ANGLESCS),ACD),D(3),E(3)
0453      COMMON /LKN11/ RLOS(CS),TRST(CS),DIAG(CS)
0454      COMMON /LKN12/ VACJ),CST(CS),FRACTION(1000),DD(100)
0455      COMMON /LKN13/ FCO,FCP,ECP,REV,RLS,C
0456      COMMON /LKN14/ M1,M2,M3,M4,M5,KC1,KC2,KC3,KC4,KC5,KC6
0457      DIMENSION UJ5(100)
0458      ME=J
0459      N1=J
0460      IF(L-LWCO) Q=2N
0461      IF(L-LWCO+1) Q=2U
0462      IF(L-LWCO) Q=2M
0463      IF(L-LWCO+1) Q=2L
0464      IF(L-LWCO+2) Q=2J
0465      OR(LAS=1)/L,PLERU
0466      O1,SAVI=FORN/EPELR0
0467      C=(MHS*YH0)/(CSPACING**2)
0468      RL=10**L/4
0469      FCP=(Q*(1+(C**2)))/(CURS*C)
0470      IF(L-PL-L-11,OR,FCO,LT-U,0,OR,FCP,LT-U,0) IF=1
0471      CALL LINKSYIELDING
0472      GO TO UJ5
0473      Q=J*Q+1
0474      ME=ME+1
0475      C=(MHS*YH0)/(CSPACING**2)
0476      FCP=(Q*(1+(C**2)))/(CURS*C)
0477      IF(L-PL-L-11,OR,FCO,LT-U,0,OR,FCP,LT-U,0) IF=1
0478      IF(L-PL-L-1) WRITE(2,1000) T1
0479      D=1-(FV/FCO)
0480      AFRA=OF-100) WRITE(2,1000) T1
0481      F=VAL(100,*,TOP FACE STRAIN=*,F,*,4,*,10X,*,FOR GREATR DEFORMATION
0482      15 CALCVANTO CONCRETE STRESSES CONSISTENTLY EXCEED CALCULATED PEAK
0483      2,*/10X,*,CONCRETE STRESSES-FURTHER ITERATIONS ADVANCED*)
0484      IF(L-PL-L-10,OR,IF,CA,1) RETURN
0485      AFRA=OF-100,OR,IF,CA,1) RETURN
0486      ME=J
0487      CALL LINKSYIELDING
0488      IF(L-PL-L-10,OR,LV,LA,YSH) GO TO U
0489      UJ5=1/L
0490      UJ5=UJ5*(OMEGA3*L/(4*01EGAWV*(C**2)))+(1-075)
0491      INO=U
0492      IF(UJ5=01-LT-UJ5ND2) INO=1
0493      IF(UJ5=01-OT-UJ5ND2) INO=2
0494      IF(UJ5=01-LT-UJ5) UJ5ND2=0,0
0495      STA=(COU*UJ5+UJ5ND2)/Z,0
0496      N1=J
0497      FRA=100*(1)=ETA
0498      I=1
0499      X1=CTA*L
0500      X1=L-LWCO) KC1=KC1+1
0501      X1=L-LWCO+1) KC2=KC2+1
0502      X1=L-LWCO+2) KC3=KC3+1
0503      X1=L-LWCO+3) KC4=KC4+1
0504      X1=L-LWCO+4) KC5=KC5+1
0505      X1=L-LWCO+5) MA1=MA1+1
    
```

```

0500 IFC(L=EQ.1) MA2=MA2+1
0507 IFC(L=EQ.2) MA3=MA3+1
0508 IFC(L=EQ.3) MA4=MA4+1
0509 IFC(L=EQ.4) MA5=MA5+1
0510 X2=AL**2
0511 A2=A2*CTA
0512 K2=K2*CT
0513 A2=A1*A2
0514 K2=(1+K2)**2
0515 A2=A2**L
0516 K2=K2**L
0517 A2=A2*CTA
0518 A2=A2**2
0519 A2=A2**2
0520 OMEGA=SQ((K2*OMEGA**2)/(GMS*CTA*C)
0521 IFC(L=EQ.OMEGA.M1-EG.1) GO TO 50
0522 IFC(L=EQ.OMEGA.M1-EG.1) GO TO 50
0523 IFC(L=EQ.1.OMEGA.M2-EG.2) GO TO 50
0524 IFC(L=EQ.1.OMEGA.M2-EG.2) GO TO 50
0525 IFC(L=EQ.OMEGA.M3-EG.3) GO TO 50
0526 IFC(L=EQ.OMEGA.M3-EG.3) GO TO 50
0527 IFC(L=EQ.OMEGA.M5-EG.5) GO TO 50
0528 IFC(L=EQ.OMEGA.M5-EG.5) GO TO 50
0529 GO TO 92
0530 I=I+1
0531 N=1
0532 IFC(L=GT.7) GO TO 7
0533 OUNO1=LIA
0534 GO TO 92
0535 IFC(OMEGA.P.GT.1.0) GO TO 92
0536 I=I+1
0537 K1=1
0538 IFC(L=GT.7) GO TO 7
0539 BOUND2=CTA
0540 GO TO 92
0541 I=I+1
0542 X10=(COS(OMEGA*P)-(OMEGA*CP**2)
0543 X11=2-COS(OMEGA*P
0544 X12=1-COS(OMEGA*P
0545 Y1=2/(COS(OMEGA*P)+COS(
0546 FN=(K1*X10)/(1+X2)-Y1
0547 FNDASH1=((((X2*OMEGA*V)-((C*OMEGA*L/4.)))*X11)/X2
0548 FNDASH2=((((2.0+X12)/(1+X2)*X2))*((X2*OMEGA*V)*X2)-((X4*
0549 1*OMEGA*L/2.0))
0550 FNDASH3=FNDASH1+FNDASH2
0551 CTA=CTA*(F1/FNDASH3)
0552 IFC(L=EQ.1) GO TO 645
0553 IFC(L=LT.OUNO1-AMD-CTA.GT.OUNO2) GO TO 646
0554 IFC(L=GT.OUNO1) INO1=1
0555 IFC(L=GT.OUNO1) ETA=(OUNO1+FRACTION(I-1))/2.0
0556 IFC(L=LT.OUNO2) INO1=1
0557 IFC(L=LT.OUNO2) ETA=(OUNO2+FRACTION(I-1))/2.0
0558 GO TO 645
0559 IFC(L=LT.OUNO1) INO12=1
0560 IFC(L=LT.OUNO1) ETA=(OUNO1+FRACTION(I-1))/2.0
0561 IFC(L=GT.OUNO2) INO13=1
0562 IFC(L=GT.OUNO2) ETA=(OUNO2+FRACTION(I-1))/2.0
0563 FRACTION(I)=CTA
0564 RATIO=(FRACTION(I)-FRACTION(I-1))/FRACTION(I)
0565 IFC(L=LT.0.5) ETA=0.5
0566 IFC(ABS(RATIO).LT.0.01) GO TO 7
0567 GO TO 20
0568 ABOLE=(L+1)=ATAN(ETA*C)
0569 EV=CTA*YOH
0570 X1=CTA*CT
0571 X2=AL**L
0572 X3=AL*CTA
0573 X7=1-AL
0574 OMEGA=SQ((K3*OMEGA*V)-((OMEGA*L/4.)))/A7
0575 CP=OMEGA*CP*PLERO
0576 RLO=(L+1)=KL3
0577 TRS(L+1)=CV
0578 DIAJ(L+1)=CGP
0579 VAC*(1)=W
0580 IFC(L=EQ.0) QN=Q
0581 IFC(L=EQ.1) QU=Q
0582 IFC(L=EQ.2) Q1=2
0583 IFC(L=EQ.3) Q2=2
0584 IFC(L=EQ.4) Q3=2
0585 IFC(L=EQ.5) Q4=2

```

91
50
92
100
645
040
7

```

0004 A(L+1)=FUP
0535 U(L+1)=FUD
0536 RETURN
0537 FUP=(U*(1+(C**2)))/(CUR3+C)
0538 ANGLE5(L+1)=ATAN(C)
0539 RUD=(L+1)=RLJ
0540 RLU(L+1)=LV
0541 DIMU(L+1)=LCP
0542 VAL(L+1)=4
0543 IFF(L,L+U) QN=Q
0544 IFF(L,L+1) QU=Q
0545 IFF(L,L+2) QR=Q
0546 IFF(L,L+3) QS=Q
0547 IFF(L,L+4) QT=Q
0548 AL(L+1)=FUP
0549 U(L+1)=FUD
0600 RETURN
END

```

END OF SEGMENT, LENGTH 1031, NAME ALLANGLES

```

0002 SUBROUTINE EVALUATION
0003 SUBROUTINE EVALUATES NEW VALUES OF C2 AND X2AR
0004 COMMON /JLN1/ D1,D2,F3,T1,PRODUCT,X2AR,Y3T,YT5,C2
0005 COMMON /JLN2/ YN,PURCHMENT,IND3
0006 COMMON /JLN3/ Q3,Q4,Q5,Q6,Q7,Q8,Q9,Q10,Q11,Q12,Q13,Q14,Q15,Q16,Q17,Q18,Q19,Q20,Q21,Q22,Q23,Q24,Q25,Q26,Q27,Q28,Q29,Q30,Q31,Q32,Q33,Q34,Q35,Q36,Q37,Q38,Q39,Q40,Q41,Q42,Q43,Q44,Q45,Q46,Q47,Q48,Q49,Q50,Q51,Q52,Q53,Q54,Q55,Q56,Q57,Q58,Q59,Q60,Q61,Q62,Q63,Q64,Q65,Q66,Q67,Q68,Q69,Q70,Q71,Q72,Q73,Q74,Q75,Q76,Q77,Q78,Q79,Q80,Q81,Q82,Q83,Q84,Q85,Q86,Q87,Q88,Q89,Q90,Q91,Q92,Q93,Q94,Q95,Q96,Q97,Q98,Q99,Q100
0007 COMMON /JLN4/ ANGLE5(5),A(5),B(5),C2(5)
0008 COMMON /JLN10/ FORCE(2),DIST(2)
0009 COTN=1/TAN(ANGLE5(1))
0010 COTJ=1/TAN(ANGLE5(2))
0011 COTN=1/TAN(ANGLE5(3))
0012 COTL=1/TAN(ANGLE5(4))
0013 COT=1/TAN(ANGLE5(5))
0014 C2=(COT1-FH)/I2)*(C4N+COTN)+(4*QU+COTJ)+(2*Q5+COTN)+
0015 1*(4*QL+COTL)+(Q3+COTB)
0016 X2AR=((COT1-YN)*(C2N+COTN)+(3*QU+COTJ)+(Q8+COTM)+(Q1L+COTL))
0017 1/((Q4+COTN)+(4*Q2+COTJ)+(2*Q6+COTM)+(4*Q1+COTL)+(Q3+COTB))
0018 FORCE(C2)=C2
0019 DIST(2)=X2AR
0020 RETURN
0021 END

```

END OF SEGMENT, LENGTH 201, NAME EVALUATION

```

0022 SUBROUTINE SOLUTION
0023 SEGMENT FINDS RATIOS FOR TESTING CONVERGENCE
0024 C
0025 K,KL,AK, LOOP COUNTERS
0026 COMMON /JLN1/ YN,PURCHMENT,IND3
0027 COMMON /JLN2/ RATIO5,K,X
0028 COMMON /JLN3/ DELTA(100),DEPTH(100)
0029 COMMON /JLN4/ FORCE(2),DIST(2)
0030 COMMON /JLN14/ Y1,M2,M3,M4,M5,KC1,KC2,KC3,KC4,KC5,KC6
0031 RATIO5=(DIST(2)-DIST(1))/DIST(2)
0032 K=+1
0033 KC6=KC5+1
0034 DELTA(K)=FORCE(1)-FORCE(2)
0035 DEPTH(K)=Y1
0036 RETURN
0037 END

```

END OF SEGMENT, LENGTH 25, NAME SOLUTION

```

0038 SUBROUTINE LINEARFIT
0039 SEGMENT APPROXIMATES NEXT DEPTH USING A LINEARFIT
0040 COMMON /JLN1/ D1,D2,F3,T1,PRODUCT,X2AR,Y3T,YT5,C2
0041 COMMON /JLN2/ YN,PURCHMENT,IND3

```

```

0642 COMMON /JLNK7/ RATIO,RAIIO,JK,K
0643 COMMON /JLNK3/ DELTA(I),DEPTH(I),D
0644 DIFF1=DELPTH(K)-DEPTH(K-1)
0645 DIFF2=DELTA(K)-DELTA(K-1)
0646 IF(DIFF1.LT.4.0).OR.(DIFF2.GT.4.0) GO TO 701
0647 JUP=DIFF1/DIFF2
0648 Y=DELPH(K)-(SLUPE*DELTA(K))
0649 IF(Y.LT.0.0) Y=DELPTH(K)/2.0
0650 RETURN
0651 Y=0.7*Y4
0652 LIND=J
0653 RETURN
0654 END

```

END OF SEGMENT, LNK7N 1000 NAME LINEAKFIT

```

0655 SUBROUTINE FIRSTCRACKS
0656 SEGMENT COMPUTED MOMENT AT FIRST CRACKING
0657 T=TOTAL FACI STRAIN
0658 CC=COMPRESSION FORCE IN CONCRETE ABOVE N.A
0659 CC=COMPRESSION FORCE IN TOP STEEL
0660 TC=TOTAL FORCE IN CONCRETE BELOW N.A
0661 T=TOTAL TENSILE FORCE FROM STEEL BELOW N.A
0662 COMMON /JLNK1/ D1,D2,T3,T1,PRODUCT,XDAR,YJT,YT5,C2
0663 COMMON /JLNK2/ YH,PURMOMENT,IND5
0664 COMMON /JLNK3/ T2,CONFORCE
0665 COMMON /JLNK4/ PC5,DURS,EPZERO,PCUR,DELTA,I,IF,MA1,MA2,MA3,MA4,MA5
0666 COMMON /JLNK5/ NEG,Y5C,AT5,B2,YC5,ACS,SMR
0667 COMMON /JLNK7/ RATIO,RAIIO,JK,K,X
0668 COMMON /JLNK8/ DELTA(I),DEPTH(I),D
0669 COMMON /JLNK9/ APS,YP3,YSP,MSGP,DEP,PKA,KE,KI,RAVC,RNSC,RCH
0670 DIMENSION CRACK(1000)
0671 T3=0.0001
0672 YH=X
0673 I=1
0674 CRA:K(I)=YH
0675 T1=(YH*T1)/(4J0.0-YN)
0676 J2=(4-(T1/EPZERO))/(6-(C2*T1/EPZERO))
0677 PRDUCI=(T1/EPZERO)-((T1*2)/(3*(EPZERO**2)))
0678 T2=(YH-0.2)*T1/YN
0679 CC=PRDUCI*PCS*GRS*YN
0680 CS=AC5*ML5C*T2
0681 IFF(T2.GT.Y5C) CS=AC3*YCS
0682 TC=(CGR5*(4J0.0-YN)-AT5)*34500.0*T3/2.0
0683 T3=(M15*ML5*(01-YN)*T3/(4J0.0-YN))+APS*ML5P*((CP-YN)
0684 *T3)/(4J00.-YN)+0.0P)
0685 CF=C*CLC
0686 TF=FC+T3
0687 DELFA(I)=CF-TF
0688 YH=0.75*X
0689 I=I+1
0690 CRA:K(I)=YH
0691 T1=(YH*T1)/(4J0.0-YN)
0692 J2=(4-(T1/EPZERO))/(6-(C2*T1/EPZERO))
0693 PRDUCI=(T1/EPZERO)-((T1*2)/(3*(EPZERO**2)))
0694 T2=(YH-0.2)*T1/YN
0695 CC=PRDUCI*PCS*GRS*YN
0696 CS=AC5*ML5C*T2
0697 IFF(T2.GT.Y5C) CS=AC3*YCS
0698 TC=(CGR5*(4J0.0-YN)-AT5)*34500.0*T3/2.0
0699 T3=(M15*ML5*(01-YN)*T3/(4J0.0-YN))+APS*ML5P*((CP-YN)
0700 *T3)/(4J00.-YN)+0.0P)
0701 CF=C*CLC
0702 TF=FC+T3
0703 DELFA(I)=CF-TF
0704 RATIO=DELFA(I)/TF
0705 RATIO=DELTA(I)/TF
0706 IFF(ABS(RATIO)>.LT.0.21) GO TO 375
0707 SLP2=(CRA:K(I)-CRACK(I-1))/(DELTA(I)-DELTA(I-1))
0708 YH=CRA:K(I)-(SLOPE2*DELTA(I))
0709 IFF(YH.GT.400.0) YH=(CRACK(I)+400.0)/2.0
0710 GO TO 370
0711 PURMOMENT=(T3*01)+(TC*(YH+(4J0.0-YN)*2.0/3))-
0712 I(CC*CLC*(I/2.0)-(CC*02)
0713 AFTN.LT.0.LAND.YN.GT.0.) PURMOMENT=(CC*02)*(T3*01)+

```

701

350

875


```

0714      1 (TC*(YH+(01-YH)*2.0/3))-(CC*JC*YH/2.0)
0715      IF(YN.GT.0.0) PCUR=T1/YH
0716      WRITE(0,88)
0717      885  FORMAT(1,44X,'AT FIRST CRACKING:')
0718      WRITE(0,89J) PUREMENT,PCUR
0719      890  FORMAT(3JX,'MOMENT=',E10.4,3X,'CURVATURE=',E10.4)
0720      RETURN
0721      END

```

END OF SEGMENT, LENGTH 039, NAME FIRSTCRACKS

0722 FINISH

END OF COMPILATION - NO ERRORS

S/C SJBFILE: 158 BUCKETS USED

**** END OF STREAM HT00 795

B.6 Input Data

2

1 800.

196. .00248 .0022 495. 166060 364.6 200. .0035 .00256 410. 0.

90.7 1828.2 30. 100. 368.4 23.2 160000 0 0. 0. 0. 0.

2 800.

196. .00174 .00196 330. 220560 432.8 200. .0035 .00256 410. 0.

143. 2175.4 26.6 100. 365.9 25.1 160000 0 0. 0. 0. 0.

2

3 800.

210.6 .00139 .00196 304.8 220560 432.8 200. .0035 .00139 304.8 0.

210.6 2175.4 39.1 100. 363.9 27.4 220000 0 0. 0. 0. 0.

3 850.

210.6 .00139 .00196 304.8 220560 432.8 200. .0035 .00139 304.8 0.

210.6 2175.4 39.1 100. 363.9 27.4 220000 0 0. 0. 0. 0.

4

4 800.

196. .00174 .00194 330. 220000 427.5 200. .0035 .00256 410. 0.

143. 1827. 22.9 100. 367.7 25.1 160000 0 0. 0. 0. 0.

4 850.

196. .00174 .00194 330. 220000 427.5 200. .0035 .00256 410. 0.

143. 1827. 22.9 100. 367.7 25.1 160000 0 0. 0. 0. 0.

2

5 800.

210.6 .00241 .00196 445. 220560 432.8 200. .0035 .00139 304.8 0.

48.2 2175.4 38.8 50. 369.9 21.3 220000 0 0. 0. 0. 0.

5 850.

210.6 .00241 .00196 445. 220560 432.8 200. .0035 .00139 304.8 0.

48.2 2175.4 38.8 50. 369.9 21.3 220000 0 0. 0. 0. 0.

3

6 800.

210.6 .00174 .00213 330. 190000 405. 200. .0035 .00139 304.8 0.

143. 2587.8 25.8 100. 363.9 25.3 220000 0 0. 0. 0. 0.

6 850.

210.6 .00174 .00213 330. 190000 405. 200. .0035 .00139 304.8 0.

143. 2587.8 25.8 100. 363.9 25.3 220000 0 0. 0. 0. 0.

6 650.

210.6 .00174 .00213 330. 190000 405. 200. .0035 .00139 304.8 0.

143. 2587.8 25.8 100. 363.9 25.3 220000 0 0. 0. 0. 0.

3

7 800.

210.6 .00174 .00208 330. 196880 410.2 200. .0035 .00139 304.8 0.

143. 2238.7 36.6 100. 364.8 25.3 220000 0 0. 0. 0. 0.

7 850.

210.6 .00174 .00208 330. 196880 410.2 200. .0035 .00139 304.8 0.

143. 2238.7 36.6 100. 364.8 25.3 220000 0 0. 0. 0. 0.

7 650.

210.6 .00174 .00208 330. 196880 410.2 200. .0035 .00139 304.8 0.

143. 2238.7 36.6 100. 364.8 25.3 220000 0 0. 0. 0. 0.

9

8 1000.

210.6 .00174 .00208 330. 196880 410.2 200. .0035 .00139 304.8 0.

143. 2238.7 28.9 100. 364.8 25.3 220000 0 0. 0. 0. 0.

8 1050.

210.6 .00174 .00208 330. 196880 410.2 200. .0035 .00139 304.8 0.

143. 2238.7 28.9 100. 364.8 25.3 220000 0 0. 0. 0. 0.

8 1100.

210.6 .00174 .00208 330. 196880 410.2 200. .0035 .00139 304.8 0.

143. 2238.7 28.9 100. 364.8 25.3 220000 0 0. 0. 0. 0.

8 1200.

210.6 .00174 .00208 330. 196880 410.2 200. .0035 .00139 304.8 0.

143. 2238.7 28.9 100. 364.8 25.3 220000 0 0. 0. 0. 0.

8 1250.

210.6 .00174 .00208 330. 196880 410.2 200. .0035 .00139 304.8 0.

143. 2238.7 28.9 100. 364.8 25.3 220000 0 0. 0. 0. 0.

8 1300.

210.6 .00174 .00208 330. 196880 410.2 200. .0035 .00139 304.8 0.

143. 2238.7 28.9 100. 364.8 25.3 220000 0 0. 0. 0. 0.

8 1400.

210.6 .00174 .00208 330. 196880 410.2 200. .0035 .00139 304.8 0.

143. 2238.7 28.9 100. 364.8 25.3 220000 0 0. 0. 0. 0.

8 1450.

210.6 .00174 .00208 330. 196880 410.2 200. .0035 .00139 304.8 0.

143. 2238.7 28.9 100. 364.8 25.3 220000 0 0. 0. 0. 0.

8 1500.

210.6 .00174 .00208 330. 196880 410.2 200. .0035 .00139 304.8 0.

143. 2238.7 28.9 100. 364.8 25.3 220000 0 0. 0. 0. 0.

B.7 Printout of Input Data and Start of Output Printout

BEHAVIORAL RESPONSE PREDICTION FOR STRUCTURAL CONCRETE BEAM IN COMBINED MOMENT AND SHEAR LOADING USING COMPRESSION FIELD THEORY ANALYSIS

PREDICTIONS FOR BEAM CFT-F38

SOURCE: S SHITOTE UNIVERSITY OF NAIROBI (1983)

TABLE OF INPUT MATERIAL AND SECTION PROPERTIES

URS	UTS	DCS	ATS	ACS	AHS	SHS
0.2000E 03	0.3040E 03	0.2530E 02	0.2239E 04	0.2106E 03	0.1430E 03	0.1000E 03
YTS	YCS	YHS	PCS	YST	YSC	YSH
0.4102E 03	0.3040E 03	0.3300E 03	0.2690E 02	0.2080E 02	0.1390E 02	0.1740E 02

CONCRETE STRAIN AT PEAK STRESS=0.3500E-02

MOMENT-SHEAR RATIO=1050.0

TOP FACE STRAIN=0.00025

	MOMENT	PCUR	MOMENT	CUR	SHEAR
	0.2468E 06	0.1205E 05	0.2529E 08	0.1304E 05	0.2409E 05
	ANGLES/SHEAR FLOWS/LSTR/TRST/DIAGST AT LEVELS SHOWN				
	1	2	3	4	5
	20.07	32.60	36.45	39.21	41.31
	87.09	89.00	90.92	92.84	94.75
	0.0000E 00	0.564E-04	0.113E-03	0.169E-03	0.226E-03
	0.161E-03	0.210E-03	0.248E-03	0.279E-03	0.307E-03
	0.544E-04	0.497E-04	0.487E-04	0.496E-04	0.504E-04
FCP	0.109E 01	0.980E 00	0.951E 00	0.946E 00	0.955E 00
FCU	0.352E 02	0.348E 02	0.344E 02	0.341E 02	0.337E 02
COUNTERS	40	63	30	72	6

TOP FACE STRAIN=0.00050

	MOMENT	PCUR	MOMENT	CUR	SHEAR
	0.4630E 06	0.2393E 05	0.4954E 08	0.2585E 05	0.4718E 05
	ANGLES/SHEAR FLOWS/LSTR/TRST/DIAGST AT LEVELS SHOWN				
	1	2	3	4	5
	26.34	32.69	36.51	39.25	41.34
	171.31	174.96	173.62	182.27	185.93
	0.0000E 00	0.111E-03	0.221E-03	0.332E-03	0.443E-03
	0.520E-03	0.414E-03	0.488E-03	0.549E-03	0.603E-03
	0.110E-03	0.102E-03	0.101E-03	0.103E-03	0.105E-03
FCP	0.213E 01	0.192E 01	0.186E 01	0.186E 01	0.187E 01
FCU	0.343E 02	0.336E 02	0.329E 02	0.323E 02	0.317E 02
COUNTERS	28	58	56	56	6

TOP FACE STRAIN=0.00075

	MOMENT	PCUR	MOMENT	CUR	SHEAR
	0.7102E 06	0.3562E 05	0.7273E 08	0.3642E 05	0.6926E 05
	ANGLES/SHEAR FLOWS/LSTR/TRST/DIAGST AT LEVELS SHOWN				
	1	2	3	4	5
	27.06	32.79	36.57	39.29	41.37
	252.60	257.82	263.04	268.26	273.48
	0.0000E 00	0.163E-03	0.326E-03	0.489E-03	0.652E-03
	0.475E-03	0.612E-03	0.720E-03	0.809E-03	0.888E-03
	0.167E-03	0.156E-03	0.156E-03	0.160E-03	0.165E-03
FCP	0.312E 01	0.283E 01	0.274E 01	0.273E 01	0.276E 01
FCU	0.335E 02	0.325E 02	0.316E 02	0.307E 02	0.299E 02
COUNTERS	35	56	60	61	6

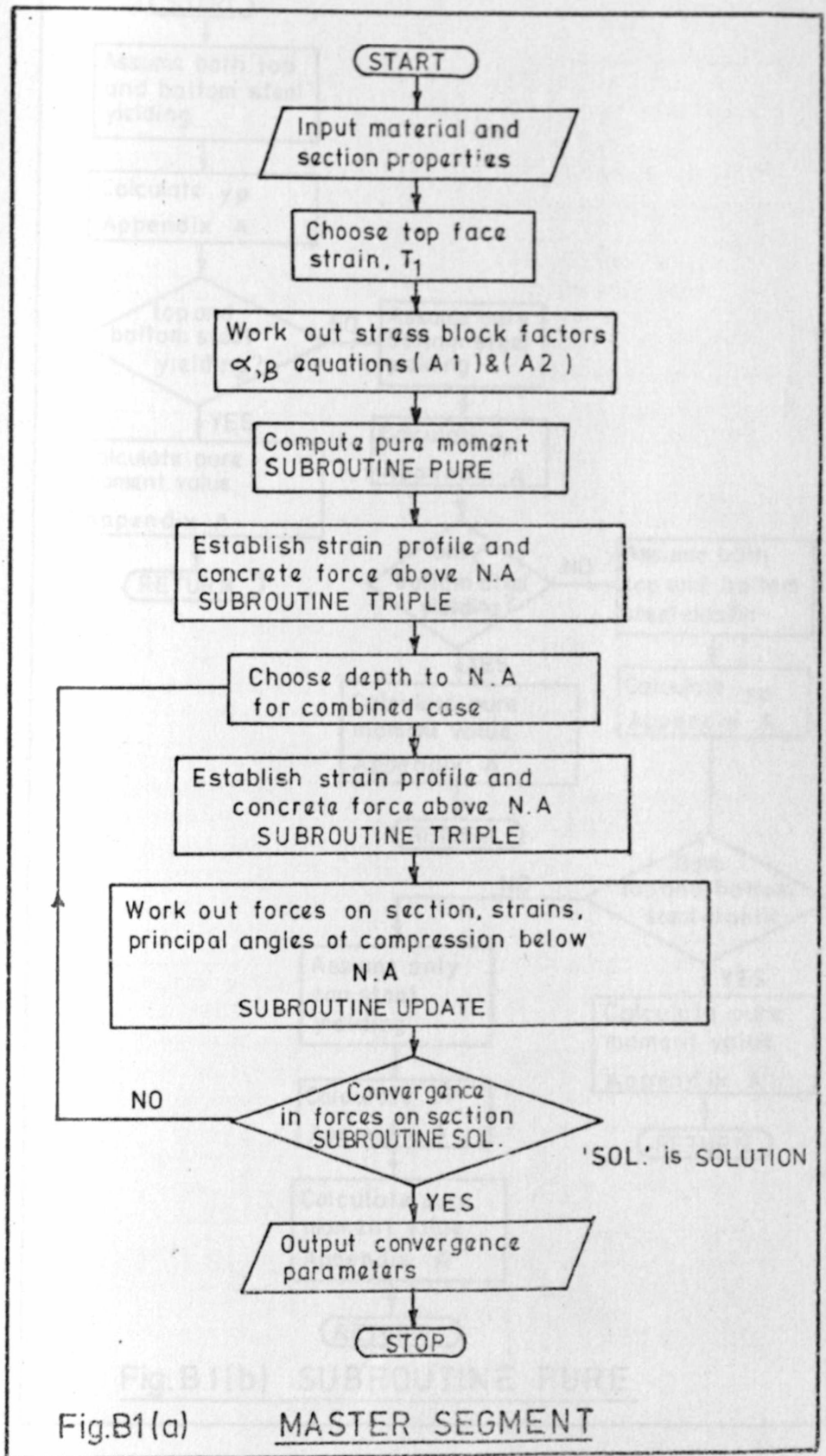


Fig.B1(a)

MASTER SEGMENT

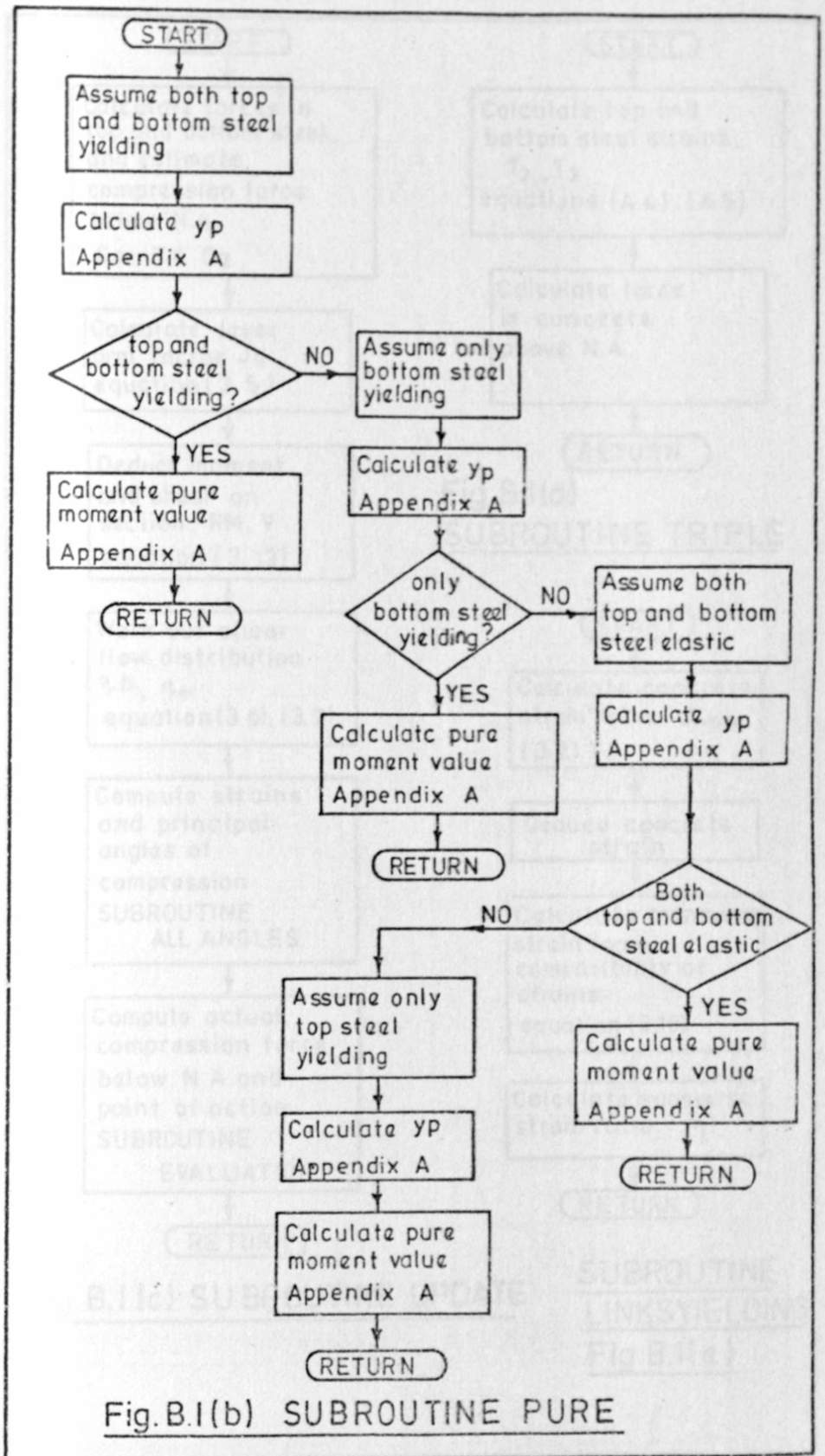
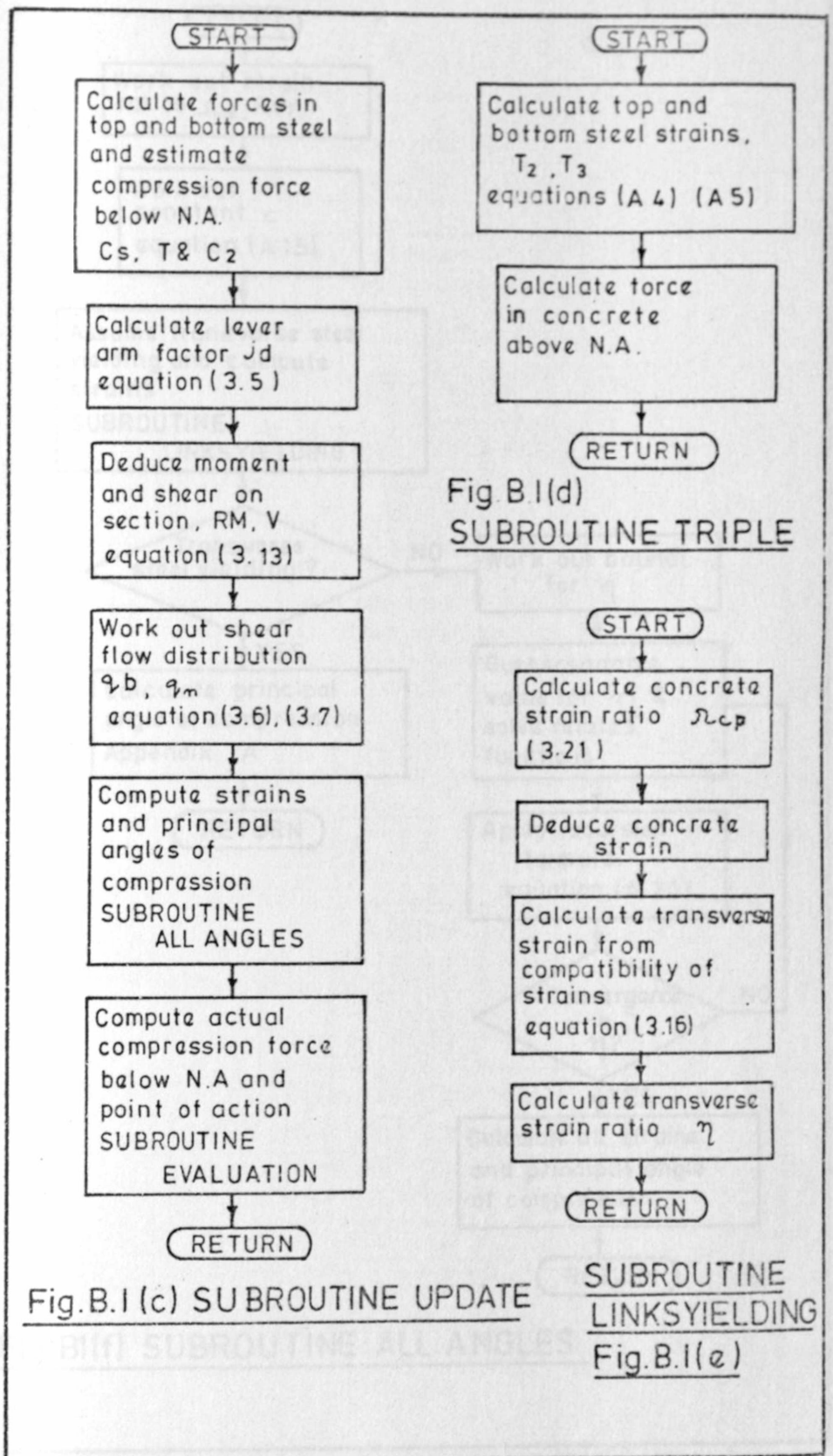


Fig.B.1(b) SUBROUTINE PURE



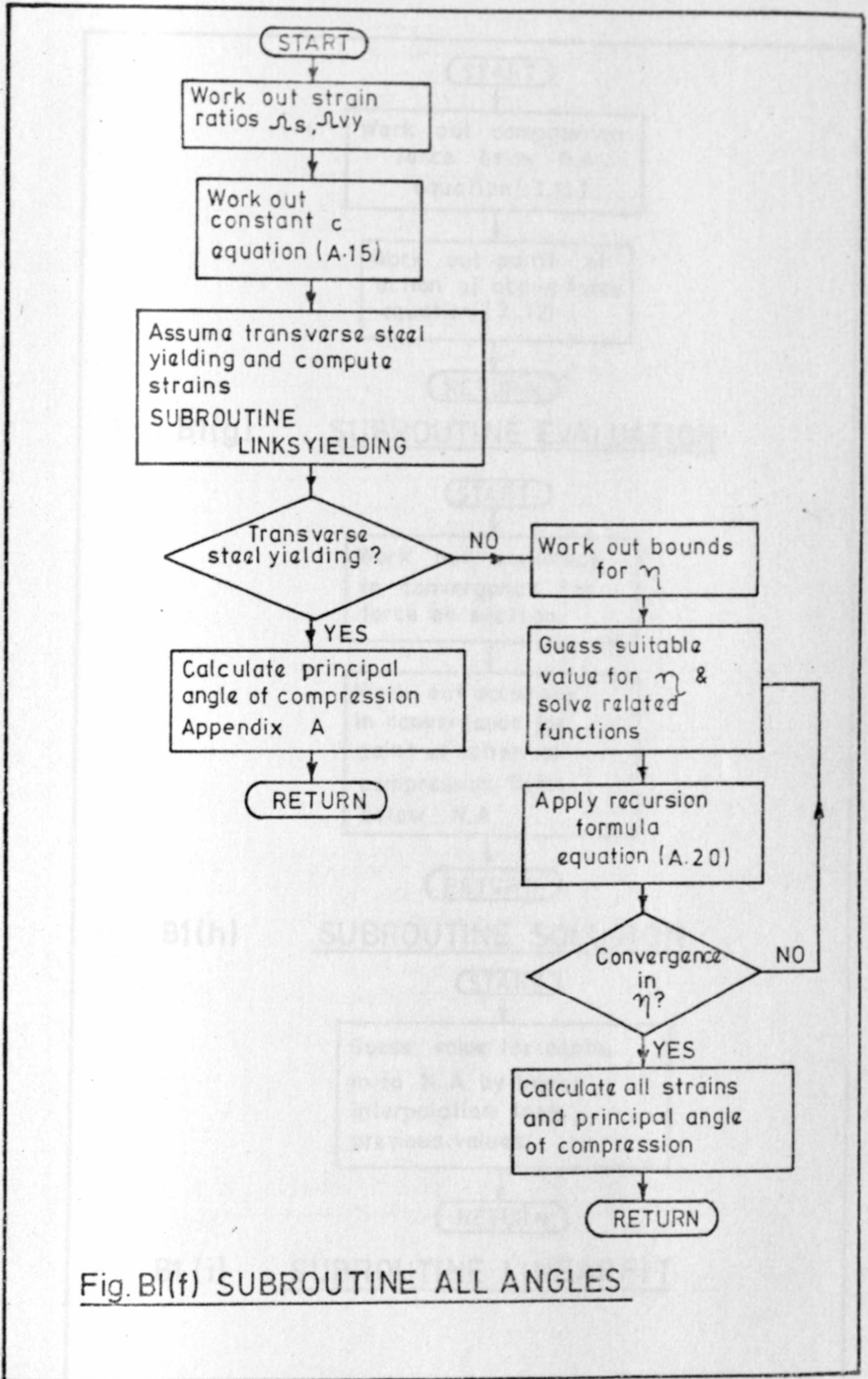


Fig. B1(f) SUBROUTINE ALL ANGLES

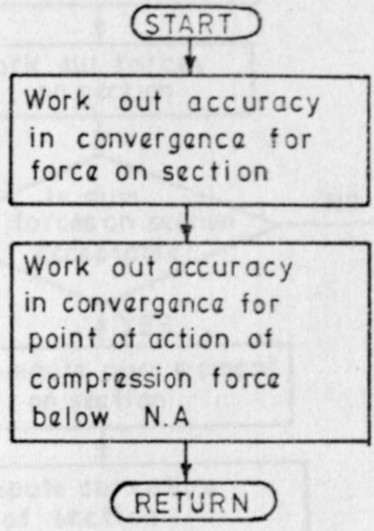
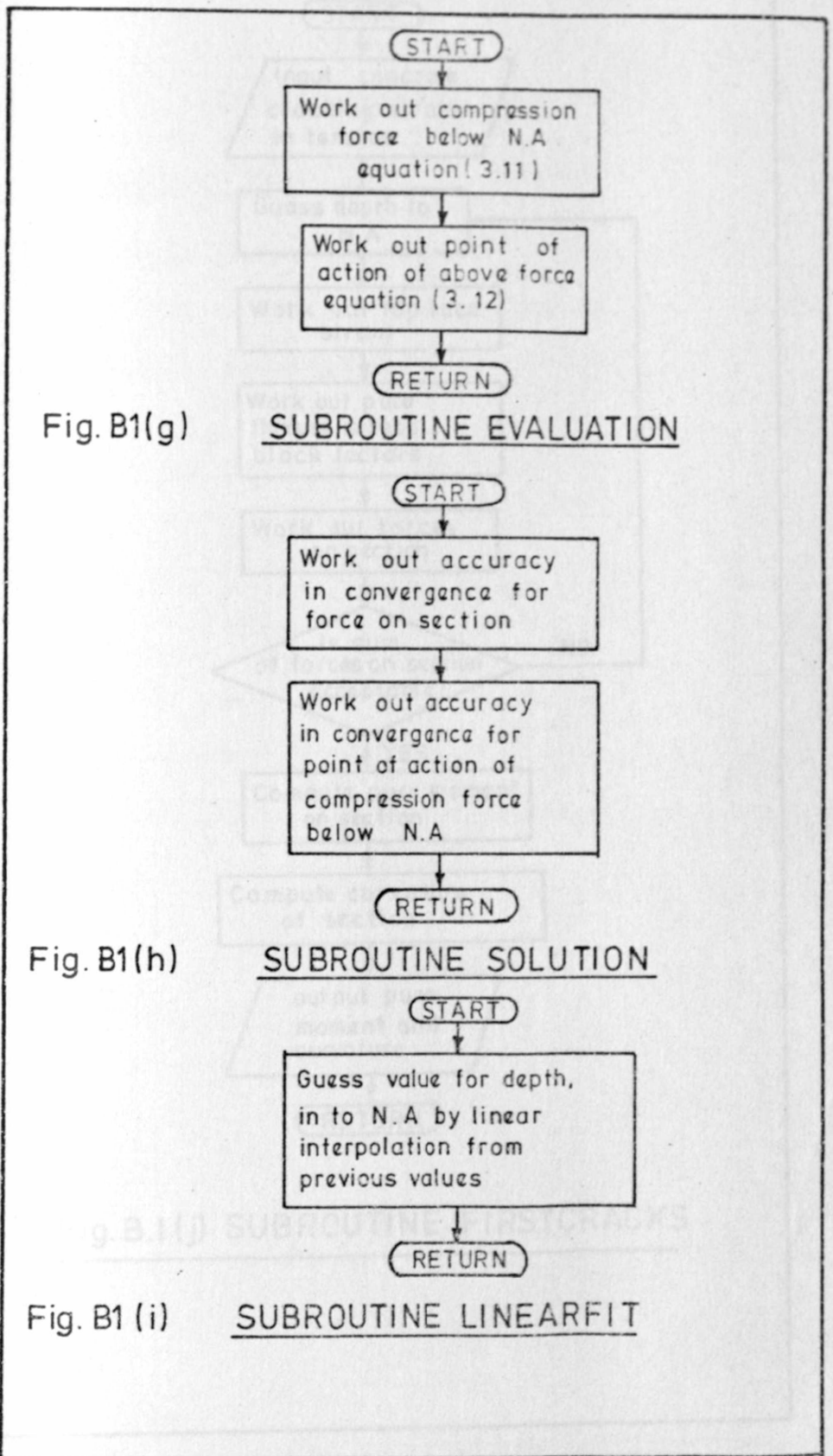


Fig. B1(h) SUBROUTINE SOLUTION

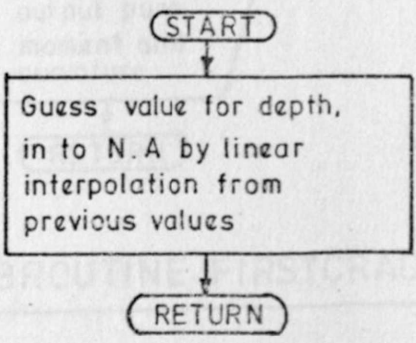


Fig. B1 (i) SUBROUTINE LINEARFIT

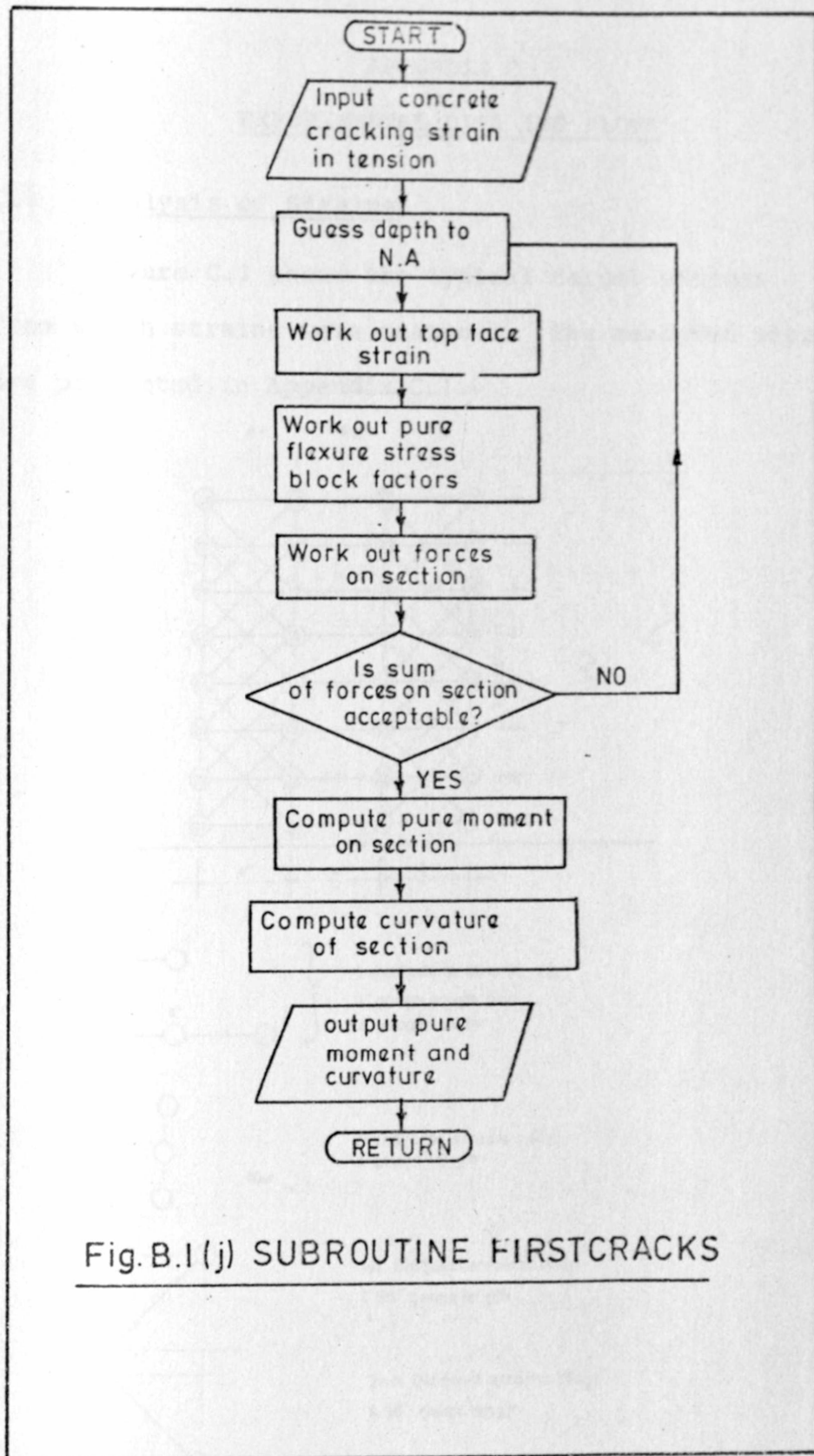


Fig.B.1(j) SUBROUTINE FIRSTCRACKS

APPENDIX C

EXPERIMENTAL DATA AND PLOTS

C.1 Analysis of Strains

Figure C.1 shows the typical target pattern from which strains were measured. The measured strains are presented in Appendix C.1.4

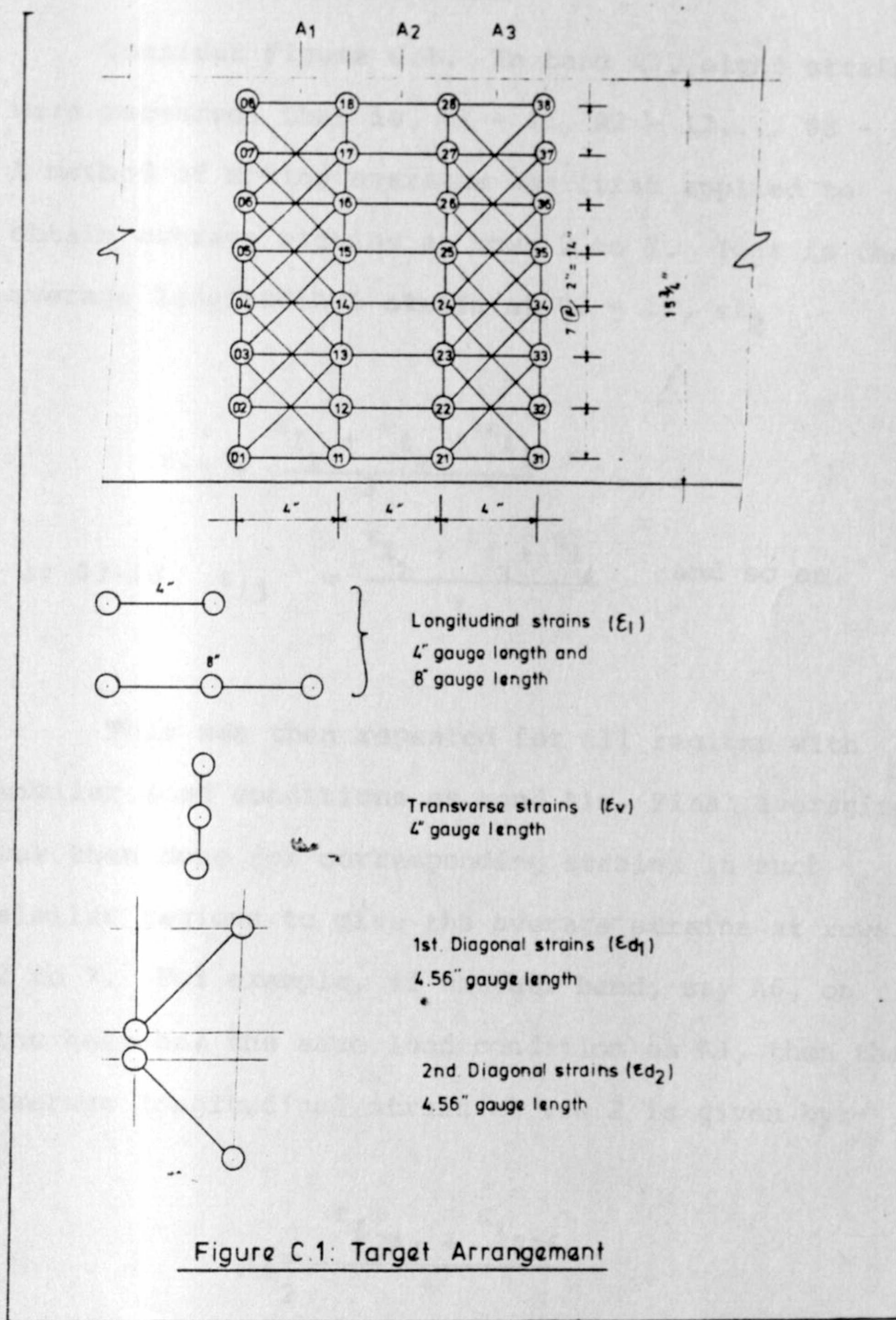


Figure C.1: Target Arrangement

Measurements for the various types of strains were taken over the gauge lengths indicated. For reasons already given in Chapter 5, average strains were considered in the analysis of the test specimens. The average strains were computed as outlined below:-

C.1.1 Longitudinal Strains

Consider Figure C.1. In band A1, eight strains were measured, that is, 01 - 11, 02 - 12.... 08 - 18. A method of moving averages was first applied to obtain average strains at rows 2 to 7. That is the average longitudinal strain at 02 - 12, ϵ_{l2}

$$\epsilon_{l2} = \frac{\epsilon_{l1} + \epsilon_{l2} + \epsilon_{l3}}{3}$$

at 03-13. $\epsilon_{l3} = \frac{\epsilon_{l2} + \epsilon_{l3} + \epsilon_{l4}}{3}$ and so on.

This was then repeated for all regions with similar load conditions as band A1. Final averaging was then done for corresponding strains in such similar regions to give the average strains at rows 2 to 7. For example, if another band, say A6, on the beam has the same load condition as A1, then the average longitudinal strain at row 2 is given by:-

$$\epsilon_{l2} = \frac{\epsilon_{l2A1} + \epsilon_{l2A6}}{2}$$

C.1.2 Transverse Strains

Still considering band A1, averaging of transverse strains from adjacent columns was first done and assumed representing the strain at the middle of the band. That is measurement on 01-03 was averaged with that on 11-13, that on 02-04 with that on 12-14 and so on. The final average transverse strain was then obtained in the same way as for longitudinal strains by considering corresponding regions.

C.1.3 Diagonal Strains

For these, there was no averaging in the individual band. Averaging of corresponding diagonal strains was done directly to obtain two sets of diagonal strains; one set being predominantly compressive (ϵ_{d1}) and the other predominantly tensile (ϵ_{d2}). ϵ_{d1} and ϵ_{d2} are chosen with respect to the load and care must be exercised to avoid obtaining wrong averages. Note that ϵ_{d1} and ϵ_{d2} are mutually perpendicular.

With the average longitudinal strains, average transverse strains and the average diagonal strains, it has been shown by Onsongo (1978) that the principal compression strains can be deduced using Mohr's circle of strains. Consider Figure C.2

From the circle, it can be seen that $\Delta A'A''B''$ is similar to $\Delta C''D''D'$ and $C''D''=A'A''=\gamma_{lt}$. If tension strains are taken to be positive then ϵ_{cp} will be negative; and assuming ϵ_{d1} is compressive deduce

$$\epsilon_{d1} + \epsilon_{d2} = \epsilon_l + \epsilon_v \dots\dots\dots (C.1)$$

and the shear strain γ_{lt} is evaluated at

$$\gamma_{lt} = \epsilon_{d2} - \epsilon_{d1} \dots\dots\dots (C.2)$$

Using equations (3.9) and (3.10) and considering that ϵ_{cp} is negative, it follows that

$$\left(\frac{\gamma_{lt}}{2}\right)^2 = (\epsilon_l - \epsilon_{cp}) (\epsilon_v - \epsilon_{cp})$$

$$\text{Hence } \epsilon_{cp}^2 = (\epsilon_v + \epsilon_l) \epsilon_{cp} + \epsilon_v \epsilon_l - \left(\frac{\gamma_{lt}}{2}\right)^2 = 0$$

$$\begin{aligned} \epsilon_{cp} &= \frac{1}{2} (\epsilon_v + \epsilon_l) - \sqrt{(\epsilon_v + \epsilon_l)^2 - 4 \left(\epsilon_v \epsilon_l - \frac{\gamma_{lt}^2}{4}\right)} \\ &= \frac{1}{2} ((\epsilon_v + \epsilon_l) - \sqrt{(\epsilon_v - \epsilon_l)^2 + \gamma_{lt}^2}) \dots\dots\dots (C.3) \end{aligned}$$

Multiplying equations (3.14) and (3.5) leads to equation (3.16) from which the angle of principal compression is evaluated as

$$\tan^2 \theta_p = \frac{\gamma_{lt}}{\epsilon_v - \epsilon_l} = \frac{\epsilon_{d2} - \epsilon_{d1}}{\epsilon_v - \epsilon_l} \dots\dots\dots (C.4)$$

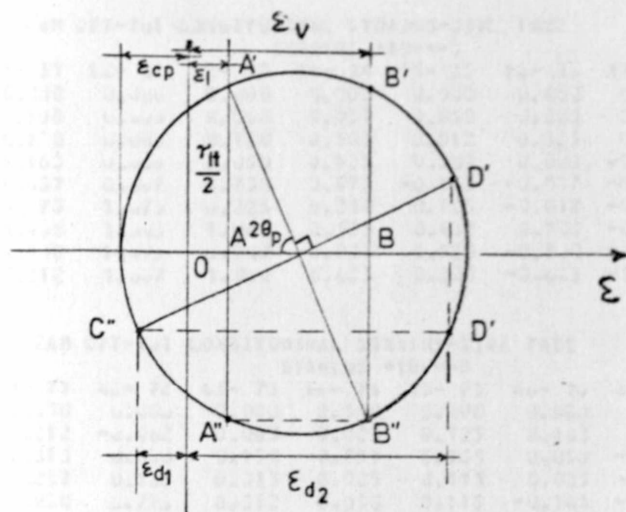


Fig.C.2 : Mohr's Circle For Measured Strains

C.1.4 Measured Strains

The demec readings taken during the experiment were used to compute strains. The computed strains are presented in this appendix consistent with the target patterns drawn in Figure 4.7. For each set of strains, the dynamic and static moments observed during the test have been recorded. In the rare cases that target points fell off during the test, demec readings were abandoned at those particular locations. Such locations are represented by blank spaces in the tables.

MOMENT			STRAINS *10**-3		
0	0.0	0.000	0.000	0.000	0.000
5	15.2	0.350	0.025	0.012	0.000
10	30.5	0.425	0.057	0.037	0.007
15	41.7	0.400	0.150	0.057	0.003
20	47.7	0.425	0.427	0.027	0.007
25	75.5	0.663	0.663	0.227	0.000
30	94.8	1.337	1.167	0.775	0.400
35	113.7	1.907	1.907	0.900	0.600
40	130.8	2.467	1.900	0.125	0.200
45	151.0	2.802	2.103	0.157	0.287
			STRAINS *10**-3		
0	0.0	0.000	0.000	0.000	0.000
5	17.5	0.000	0.063	-0.025	0.125
10	35.7	0.215	0.150	-0.037	0.035
15	49.0	0.257	0.313	0.025	0.113
20	69.2	0.270	0.512	0.035	0.113
25	89.2	0.250	0.715	0.163	0.163
30	111.5	1.012	0.700	0.185	0.125
35	133.8	1.963	0.963	0.912	0.185
40	153.8	1.663	1.062	0.158	0.157
45	180.5	1.612	1.062	0.000	0.500
			STRAINS *10**-3		
0	0.0	0.000	0.000	0.000	0.000
5	14.5	0.100	0.033	0.050	0.150
10	28.5	0.170	0.150	0.125	0.100
15	39.2	0.163	0.050	0.000	0.000
20	59.2	0.657	0.738	0.475	0.163
25	71.5	0.657	0.907	0.000	0.000
30	99.2	1.403	1.062	0.525	0.467
35	107.0	1.403	1.062	0.525	0.467
40	123.1	1.910	1.475	0.725	0.200
45	144.5	2.212	1.607	0.625	0.325
			STRAINS *10**-3		
0	0.0	0.000	0.000	0.000	0.000
5	19.0	0.000	0.037	0.050	0.150
10	38.0	0.000	0.150	0.125	0.100
15	57.0	0.000	0.475	0.000	0.000
20	76.0	0.657	0.738	0.475	0.163
25	95.0	0.657	0.907	0.000	0.000
30	124.0	1.403	1.062	0.525	0.467
35	143.0	1.403	1.062	0.525	0.467
40	162.0	1.910	1.475	0.725	0.200
45	181.0	2.212	1.607	0.625	0.325

BEAM CFT-T82 LONGITUDINAL STRAINS-SIDE FACE
STRAINS *10**⁻³

MOMENT		11- 31	12- 32	13- 33	14- 34	15- 35	16- 36	17- 37	18- 38
0	0	0.000	0.000	0.000	0.000	0.000	0.000	0.000	0.000
15.0	14.5	0.050	0.037	0.012	-0.037	-0.025	-0.067	-0.100	-0.112
29.3	28.5	0.212	0.100	0.037	-0.012	-0.062	-0.112	-0.200	-0.200
57.1	57.1	0.662	0.315	0.125	0.063	-0.150	-0.237	-0.438	-0.537
76.7	76.7	0.925	0.525	0.612	0.300	-0.050	-0.350	-0.637	-0.812
92.7	91.0	1.150	0.700	0.750	0.412	-0.025	-0.450	0.412	-1.025
107.4	106.7	1.550	0.967	0.937	0.500	0.012	-0.512	-1.012	-1.312
125.2	124.9	1.937	1.312	1.212	0.600	-0.062	-0.683	-1.325	-1.650
143.0	142.7	2.275	1.600	1.537	0.738	-0.125	-0.925	-1.662	-2.013
159.6	158.0	2.475	1.837	1.825	0.850	-0.175	-1.125	-1.950	-2.325
168.4	168.4	2.562	1.950	2.000	0.900	-0.262	-1.300	-2.250	-2.650
175.9	169.8	2.337	1.725	2.038	0.750	-0.637	-1.075	-2.650	-2.807
175.9	154.1	2.163	1.600	1.900	0.600	-0.713	-1.712	-2.650	-2.875
175.9	165.9	2.225	1.637	1.950	0.625	-0.762	-1.762	-2.737	-3.012
176.6	176.2	2.275	1.650	2.025	0.637	-0.757	-1.863	-2.900	-3.125

BEAM CFT-T82 LONGITUDINAL STRAINS-SIDE FACE
STRAINS *10**⁻³

MOMENT		41- 71	42- 72	43- 73	44- 74	45- 75	46- 76	47- 77	48- 78
0	0.0	0.000	0.000	0.000	0.000	0.000	0.000	0.000	0.000
18.7	17.8	0.050	0.025	0.000	-0.037	-0.062	-0.100	-0.163	-0.175
36.6	35.7	0.212	0.113	0.063	-0.012	-0.112	-0.183	-0.262	-0.313
71.3	71.3	0.575	0.400	0.212	0.033	-0.125	-0.313	-0.550	-0.675
95.9	95.9	0.825	0.600	0.375	0.038	-0.225	-0.512	-0.887	-1.067
115.9	113.7	1.012	0.750	0.450	0.113	-0.275	-0.650	-1.137	-1.337
134.2	132.9	1.255	0.925	0.575	0.150	-0.325	-0.825	-1.437	-1.737
156.5	156.1	1.537	1.067	0.662	0.100	-0.475	-1.125	-1.925	-2.388
175.2	177.5	1.850	1.300	0.750	0.125	-0.612	-1.488	-2.575	-3.225
199.3	197.1	2.175	1.512	0.900	0.125	-0.750	-1.825	-3.187	-3.962
211.3	211.3	2.575	1.637	0.975	-0.150	-1.575	-3.475	-5.650	-7.000
219.3	192.0	2.712	1.712	0.725	-0.225	-1.637	-3.483	-5.812	-7.175
219.3	206.9	2.562	1.600	0.825	-0.250	-1.712	-3.637	-6.075	-7.512
220.7	219.6	2.325	1.100	0.975	-0.237	-1.875	-4.075	-6.787	-8.458

BEAM CFT-T82 LONGITUDINAL STRAINS-SIDE FACE
STRAINS *10**⁻³

MOMENT		81-101	82-102	83-103	84-104	85-105	86-106	87-107	88-108
0	0.0	0.000	0.000	0.000	0.000	0.000	0.000	0.000	0.000
15.0	15.0	0.125	0.137	0.100	0.037	0.063	0.037	0.000	0.025
29.3	28.5	0.200	0.136	0.100	-0.025	0.000	-0.062	-0.112	-0.062
57.1	57.1	0.437	0.425	0.513	0.100	0.000	-0.150	-0.300	-0.400
76.7	76.3	0.713	0.612	0.462	0.188	0.225	0.012	-0.462	-0.638
92.7	92.7	0.900	0.775	0.575	0.163	0.267	-0.300	-0.563	-0.875
107.4	107.4	1.238	1.012	0.738	0.175	0.250	-0.433	-0.837	-1.162
125.2	124.5	1.512	1.200	0.850	0.175	0.225	-0.625	-1.075	-1.475
143.0	143.0	1.767	1.425	0.975	0.175	0.038	-0.875	-1.413	-1.937
159.3	155.9	2.038	1.575	1.062	0.175	-0.112	-1.125	-1.725	-2.238
168.4	147.0	2.038	1.500	0.812	-0.275	-0.963	-1.787	-2.238	-2.775
175.9	154.1	1.950	1.268	0.713	-0.300	-1.075	-1.900	-2.575	-2.950
175.9	165.2	1.912	1.512	0.725	-0.313	-1.137	-1.987	-2.437	-3.062
176.6	175.5	1.975	1.575	0.750	-0.325	-1.225	-2.100	-2.612	-3.237

MOMENT		BEAM CFT-TUB LONGITUDINAL STRAINS-SIDE FACE STRAINS *10**3							
θ	S	11-31	12-32	13-33	14-34	15-35	16-36	17-37	18-38
0.0	0.0	0.000	0.000	0.000	0.000	0.000	0.000	0.000	0.000
19.0	17.0	0.175	0.012	0.012	0.000	0.012	-0.037	-0.025	-0.037
30.0	30.0	4.175	0.012	-0.050	-0.075	-0.100	-0.150	-0.150	-0.200
49.7	47.4	6.57	0.000	-0.025	-0.012	-0.050	-0.137	-0.225	-0.313
100.1	107.7	1.137	0.000	-0.137	0.750	0.400	0.025	-0.350	-0.612
143.4	142.3	1.350	1.350	-0.262	0.362	0.512	-0.025	-0.550	-0.912
165.2	165.2	2.400	1.625	-0.275	0.375	0.550	-0.012	-0.617	-1.050
167.3	187.3	2.937	2.300	-0.275	0.933	0.557	-0.037	-0.700	-1.200
211.7	211.9	2.913	3.025	-0.325	1.000	0.668	-0.125	-0.912	-1.500
227.7	220.3	4.825	3.725	-0.367	0.847	0.563	-0.262	-1.025	-1.612
229.0	224.7	5.300	4.150	-0.438	0.775	0.425	-0.425	-1.125	-1.700
232.2	216.9	5.252	4.312	-0.450	0.713	0.337	-0.475	-1.127	-1.675
230.2	228.3	5.255	4.475	-0.475	0.637	0.275	-0.550	-1.200	-1.725

MOMENT		BEAM CFT-TUB LONGITUDINAL STRAINS-SIDE FACE STRAINS *10**3							
θ	S	1-11	2-12	3-13	4-14	5-15	6-16	7-17	8-18
0.0	0.0	0.000	0.000	0.000	0.000	0.000	0.000	0.000	0.000
49.0	36.5	0.500	0.000	0.200	0.025	-0.050	-0.075	-0.175	-0.250
67.0	87.2	0.430	2.000	2.175	-0.125	-0.175	-0.225	-0.250	-0.425
104.3	103.2	0.325	3.175	2.500	0.070	-0.200	-0.225	-0.375	-0.475
110.5	115.0	0.275	3.175	2.550	0.175	-0.175	-0.225	-0.400	-0.550
142.2	133.9	0.275	3.275	2.250	0.375	-0.125	-0.350	-0.475	-0.625
152.2	150.7	0.250	3.275	2.625	0.875	-0.100	-0.350	-0.525	-0.725
171.2	170.4	0.150	3.525	2.300	1.075	-0.150	-0.400	-0.625	-0.825
182.0	177.7	-0.350	3.525	2.375	0.900	-0.325	-0.550	-0.800	-0.975
180.1	162.0	-0.075	3.150	2.500	0.900	-0.325	-0.550	-0.750	-0.950

MOMENT		BEAM CFT-TUB LONGITUDINAL STRAINS-SIDE FACE STRAINS *10**3							
θ	S	21-31	22-32	23-33	24-34	25-35	26-36	27-37	28-38
0.0	0.0	0.000	0.000	0.000	0.000	0.000	0.000	0.000	0.000
20.3	19.0	0.050	0.000	0.050	-0.025	-0.025	-0.100	-0.300	-0.125
32.0	31.0	0.725	0.125	0.075	0.000	0.000	-0.100	-0.375	-0.225
53.3	50.4	0.975	0.375	0.100	0.000	0.000	-0.175	-0.400	-0.325
114.3	114.1	2.425	1.350	-0.100	-0.225	-0.375	0.150	-0.625	-0.725
130.4	134.9	2.950	2.000	-0.125	-0.250	-0.400	0.225	-0.675	-0.850
132.4	151.2	3.675	2.975	-0.175	-0.275	-0.450	0.225	-0.700	-0.975
173.3	174.9	4.375	4.000	-0.175	-0.300	-0.500	0.250	-0.725	-1.200
199.3	190.7	6.000	3.275	-0.225	-0.350	-0.600	0.175	-1.025	-1.425
229.2	222.9	6.175	0.900	-0.375	-0.375	-0.600	0.175	-1.250	-1.725
233.3	230.0	10.225	0.300	-0.425	-0.525	-0.775	-0.100	-1.300	-1.950
243.4	236.0	11.350	0.100	-0.425	-0.575	-0.825	-0.250	-1.425	-2.025

MOMENT		BEAM CFT-TUB TRANSVERSE STRAINS-SIDE FACE STRAINS *10**3											
θ	S	1-3	2-4	3-5	4-6	5-7	6-8	11-13	12-14	13-15	14-16	15-17	16-18
0.0	0.0	0.000	0.000	0.000	0.000	0.000	0.000	0.000	0.000	0.000	0.000	0.000	0.000
40.0	36.5	0.025	-0.000	0.025	-0.025	-0.075	0.000	-0.075	0.075	0.000	0.000	-0.025	0.100
67.0	87.2	2.225	-0.200	-0.050	0.125	0.000	0.100	-0.975	2.075	2.150	-0.100	-0.150	0.050
104.3	102.0	2.900	0.325	0.475	0.025	0.075	0.150	-0.100	2.850	2.700	-0.150	-0.100	0.325
110.5	115.0	3.150	0.750	0.600	-0.075	-0.025	0.100	-0.150	3.150	3.150	-0.050	0.000	0.925
134.2	133.3	3.225	1.450	1.600	0.000	0.070	0.225	-0.250	3.625	3.750	0.075	0.225	0.100
152.2	151.0	4.125	2.100	2.375	-0.075	0.075	0.175	-0.225	4.375	4.425	0.025	0.325	0.200
171.2	170.4	5.175	2.750	2.975	0.050	0.050	0.325	-0.325	5.775	5.725	0.250	0.350	0.200
182.0	176.0	5.900	3.000	3.075	-0.075	-0.050	0.200	-0.450	6.450	6.525	0.225	0.300	0.100
180.1	162.0	6.050	2.825	3.250	-0.050	-0.025	0.250	-0.375	6.625	6.700	0.250	0.325	0.200

MOMENT		BEAM CFT-TUB TRANSVERSE STRAINS-SIDE FACE STRAINS *10**3											
θ	S	21-23	22-24	23-25	24-26	25-27	26-28	31-33	32-34	33-35	34-36	35-37	36-38
0.0	0.0	0.000	0.000	0.000	0.000	0.000	0.000	0.000	0.000	0.000	0.000	0.000	0.000
20.3	18.2	0.025	0.000	-0.075	-0.075	-0.025	-0.125	-0.025	-0.100	-0.050	-0.100	-0.075	-0.100
32.0	31.0	-0.025	0.000	-0.125	-0.075	0.025	-0.100	-0.025	-0.050	-0.100	-0.050	-0.100	-0.075
53.3	50.4	0.000	0.000	-0.150	-0.175	-0.150	-0.100	-0.025	0.050	-0.125	-0.150	-0.100	-0.075
114.3	114.1	0.000	0.000	-0.525	0.700	1.500	-0.100	0.025	0.025	-0.125	-0.100	0.175	-0.475
130.4	134.2	-0.050	0.025	-0.425	1.175	1.550	-0.175	1.225	1.025	-0.050	-0.125	0.175	-0.275
132.4	149.7	-0.325	-0.075	-0.600	1.500	1.525	-0.250	1.475	1.600	-0.200	-0.200	0.100	0.350
173.3	174.3	-0.375	0.000	-0.550	1.775	2.675	-0.075	2.275	2.175	-0.075	-0.175	0.175	0.475
199.3	190.2	-0.750	0.075	-0.625	1.500	2.825	-0.500	1.100	3.100	-0.200	-0.200	0.275	-1.925
229.2	222.9	-0.350	0.150	-0.725	2.300	3.025	0.175	4.650	4.675	-0.750	-0.325	0.250	0.825
233.3	235.7	-0.275	-0.075	-0.625	3.000	4.100	0.050	5.575	5.250	-0.425	-0.400	0.225	0.700
243.4	236.0	-0.400	0.025	-0.625	3.150	4.325	0.125	7.250	7.025	-0.100	-0.350	0.250	0.725

BEAM CFT-TD3 DIAGONAL STRAINS-SIDE FACE
STRAINS *10**-3

MOMENT	D	S	1- 13	2- 14	3- 14	4- 15	5- 17	6- 18	11- 3	12- 4	13- 5	14- 6	15- 7	16- 8
0.0	0.0	0.0	0.000	0.000	0.000	0.000	0.000	0.000	0.000	0.000	0.000	0.000	0.000	0.000
40.6	36.5	-0.219	-0.194	-0.219	-0.219	-0.219	-0.329	0.235	0.197	0.197	0.066	0.022	-0.366	-0.366
87.2	37.5	-0.214	-0.293	-0.371	-0.373	-0.439	-0.570	1.421	3.070	2.673	0.197	0.132	0.366	0.366
104.3	104.2	-0.214	-0.417	-0.373	-0.417	-0.526	-0.660	2.947	2.949	2.982	0.086	-0.265	0.154	0.154
110.5	115.9	-0.206	-0.417	-0.373	-0.432	-0.482	-0.724	4.145	4.759	4.252	0.329	0.241	0.197	0.197
134.2	134.2	-0.702	-0.417	-0.432	-0.543	-0.660	-0.811	4.368	5.570	5.044	0.724	0.482	0.213	0.213
152.2	152.0	-0.759	-0.431	-0.504	-0.653	-0.811	-0.877	4.757	6.711	6.031	1.053	0.592	0.307	0.307
172.2	170.4	-0.833	-0.504	-0.439	-0.746	-0.877	-0.967	5.570	8.160	7.259	1.272	0.724	0.321	0.321
182.3	176.7	-0.899	-0.520	-0.154	-0.702	-0.855	-0.555	5.945	8.728	7.568	1.272	0.555	0.202	0.202
180.1	183.3	-0.877	-0.504	-0.351	-0.739	-0.855	-0.835	6.021	8.772	7.719	1.294	0.702	0.411	0.411

BEAM CFT-TD3 DIAGONAL STRAINS-SIDE FACE
STRAINS *10**-3

MOMENT	D	S	21- 33	22- 34	23- 35	24- 36	25- 37	26- 38	31- 23	32- 24	33- 25	34- 26	35- 27	36- 28
0.0	0.0	0.000	0.000	0.000	0.000	0.000	0.000	0.000	0.000	0.000	0.000	0.000	0.000	0.000
20.3	16.1	0.265	0.197	0.000	0.175	0.000	0.066	0.000	0.351	0.044	0.110	0.811	0.175	0.175
32.0	32.0	0.000	-0.000	-0.366	-0.033	-0.154	-0.154	0.154	0.622	0.622	-0.152	0.088	-0.211	-0.211
53.0	50.4	0.044	-0.175	-0.110	-0.066	-0.175	-0.219	0.204	0.461	-0.088	-0.351	-0.132	-0.431	-0.431
114.3	114.3	-0.154	-0.197	-0.241	-0.526	-0.241	-0.592	1.627	1.301	-0.175	1.096	1.294	0.571	0.571
130.4	130.9	-0.307	-0.373	-0.432	-0.614	-0.373	-0.758	2.325	2.171	-0.241	1.382	1.601	0.651	0.651
152.4	151.4	-0.351	-0.351	-0.439	-0.702	-0.373	-0.855	3.044	3.004	-0.329	1.404	1.162	0.571	0.571
175.5	175.5	-0.432	-0.373	-0.504	-0.811	-0.439	-1.007	4.101	3.969	-0.325	1.645	1.316	0.741	0.741
193.0	197.0	-0.570	-0.320	-0.614	-0.937	-0.526	-1.225	5.417	5.529	-0.373	1.930	1.535	0.921	0.921
209.2	222.9	-0.570	-0.439	-0.660	-1.075	-0.661	-1.316	7.325	7.171	-0.395	2.456	1.776	1.104	1.104
230.3	232.0	-0.724	-0.340	-0.611	-1.143	-0.395	-1.300	9.649	8.991	-0.432	2.478	2.105	1.140	1.140
240.4	239.5	-0.680	-0.340	-0.658	-0.943	-0.241	-1.330	11.007	10.175	-0.439	2.522	1.754	1.140	1.140

BEAM CFT-TD3 LONGITUDINAL STRAINS-SIDE FACE
STRAINS *10**-3

MOMENT	D	S	41- 51	42- 52	43- 53	44- 54	45- 55	46- 56	47- 57	48- 58
0.0	0.0	0.000	0.000	0.000	0.000	0.000	0.000	0.000	0.000	0.000
24.5	16.0	0.100	0.000	0.050	-0.012	-0.053	-0.112	-0.100	-0.125	-0.125
30.5	37.5	0.212	0.137	0.125	-0.012	-0.037	-0.212	-0.212	-0.275	-0.275
40.4	59.3	0.350	0.207	0.330	0.033	-0.037	-0.275	-0.275	-0.450	-0.450
130.1	134.7	1.200	0.900	1.225	0.287	0.012	-0.402	-0.351	-1.137	-1.137
160.0	160.0	1.507	1.100	1.512	0.313	0.066	-0.550	-1.077	-1.387	-1.387
170.5	170.4	1.505	1.057	1.725	0.375	0.025	-0.675	-1.251	-1.662	-1.662
200.5	200.5	2.167	1.637	2.112	0.525	0.075	-0.775	-1.562	-2.062	-2.062
234.1	234.1	2.700	2.015	2.537	0.675	0.725	-0.912	-1.913	-2.600	-2.600
260.9	262.2	3.237	2.707	3.450	1.037	0.275	-1.202	-2.337	-3.250	-3.250
280.9	279.1	4.000	4.400	4.900	2.112	0.002	-1.950	-4.402	-8.112	-8.112
300.3	282.3	4.250	4.175	5.025	3.375	1.100	-2.300	-5.312	-11.600	-11.600
301.3	271.1	11.500	10.700	7.167	3.025	1.702	-2.900	-6.250	-15.400	-15.400
290.2	279.0	14.537	10.700	3.637	3.562	2.212	-3.900	-6.213	-15.967	-15.967

BEAM CFT-TD3 LONGITUDINAL STRAINS-SIDE FACE
STRAINS *10**-3

MOMENT	D	S	61- 81	62- 82	63- 83	64- 84	65- 85	66- 86	67- 87	68- 88
0.0	0.0	0.000	0.000	0.000	0.000	0.000	0.000	0.000	0.000	0.000
19.6	14.0	0.003	0.025	-0.012	0.037	-0.025	-0.075	-0.037	-0.025	-0.025
30.0	30.3	0.157	0.033	0.050	0.050	-0.050	-0.150	-0.157	-0.150	-0.150
49.7	47.4	0.350	0.212	0.100	0.037	-0.100	-0.225	-0.225	-0.267	-0.267
100.1	107.7	1.275	0.975	0.775	0.423	0.000	-0.325	-0.537	-0.925	-0.925
120.4	120.4	1.657	1.212	0.925	0.563	0.100	-0.350	-0.600	-0.963	-0.963
143.4	142.7	1.957	1.437	1.082	0.651	0.125	-0.412	-0.713	-1.125	-1.125
160.2	160.2	2.257	1.702	1.300	0.762	0.175	-0.462	-0.853	-1.300	-1.300
187.3	186.0	2.557	2.000	1.488	0.825	0.137	-0.503	-1.012	-1.575	-1.575
211.9	209.6	3.275	2.600	1.700	0.900	0.075	-0.650	-1.225	-1.912	-1.912
240.7	220.1	3.530	2.900	1.702	0.937	-0.062	-0.805	-1.527	-2.067	-2.067
269.0	225.3	3.767	2.600	1.812	0.962	-0.100	-0.862	-1.650	-2.133	-2.133
290.3	210.9	3.975	2.300	1.750	0.737	-0.103	-0.903	-1.650	-2.150	-2.150
280.2	223.7	4.230	2.900	1.725	0.733	-0.250	-0.963	-1.475	-2.200	-2.200

BEAM CFT-TD3 LONGITUDINAL STRAINS-SIDE FACE
STRAINS *10**-3

MOMENT	D	S	69- 71	62- 72	63- 73	64- 74	65- 75	66- 76	67- 77	68- 78
0.0	0.0	0.000	0.000	0.000	0.000	0.000	0.000	0.000	0.000	0.000
20.0	15.0	0.100	0.000	0.075	0.000	-0.025	-0.051	-0.051	-0.050	-0.050
30.0	31.0	0.150	0.000	0.125	0.025	-0.025	-0.150	-0.151	-0.150	-0.150
50.0	50.4	0.300	0.000	0.330	0.100	-0.075	-0.175	-0.250	-0.250	-0.250
110.3	114.3	1.200	0.700	0.900	0.475	0.225	-0.300	-0.575	-0.950	-0.950
130.4	130.4	1.500	0.700	0.925	0.575	0.325	-0.300	-0.675	-1.325	-1.325
152.4	149.7	1.750	0.600	0.475	0.600	0.575	-0.430	-0.800	-1.550	-1.550
170.0	174.3	1.750	0.900	0.475	1.025	0.450	-0.500	-0.950	-2.000	-2.000
190.0	198.0	2.250	0.900	0.175	1.000	0.500	-0.575	-1.075	-2.000	-2.000
209.2	202.9	2.600	0.800	0.250	1.225	0.500	-0.725	-1.350	-2.325	-2.325
230.3	232.7	2.975	-0.100	0.100	1.275	0.300	-0.851	-1.500	-2.325	-2.325
240.4	239.0	2.600	0.100	0.075	1.200	0.175	-0.950	-1.375	-2.450	-2.450

BEAM CFT-T03 LONGITUDINAL STRAINS-SIDE FACE

MOMENT		STRAINS *10***3							
U	S	81- 91	82- 92	83- 93	84- 94	85- 95	86- 96	87- 97	88- 98
0.0	0.0	0.000	0.000	0.000	0.000	0.000	0.000	0.000	0.000
40.0	38.0	0.100	-0.125	0.075	0.000	-0.100	-0.100	-0.125	-0.250

BEAM CFT-T03 TRANSVERSE STRAINS-SIDE FACE

MOMENT		STRAINS *10***3											
U	S	61- 63	62- 64	63- 65	64- 66	65- 67	66- 68	71- 73	72- 74	73- 75	74- 76	75- 77	76- 78
0.0	0.0	0.000	0.000	0.000	0.000	0.000	0.000	0.000	0.000	0.000	0.000	0.000	0.000
20.0	13.0	0.025	0.000	-0.175	0.025	0.000	-0.025	0.025	0.400	-0.025	0.075	-0.150	0.025
30.0	31.0	0.050	0.000	0.100	0.000	-0.025	-0.025	0.025	0.375	-0.025	0.000	0.075	0.125
50.0	50.4	-0.025	0.050	0.075	-0.050	-0.175	-0.025	0.000	0.400	-0.050	-0.025	0.050	-0.050
110.0	114.0	-0.025	-0.075	0.050	-0.025	-0.125	0.050	0.000	0.150	0.175	0.275	-0.025	0.025
130.0	136.1	0.050	-0.050	0.100	0.125	0.075	0.125	0.000	0.525	0.750	0.550	0.050	0.000
150.0	149.3	0.100	-0.100	-0.025	0.150	0.075	0.150	0.000	0.650	0.950	0.675	0.000	0.000
170.0	172.0	0.225	-0.225	-0.075	0.500	0.425	0.350	0.000	0.925	1.475	0.800	0.025	0.125
190.0	198.0	-0.725	1.100	-0.700	1.500	-0.325	0.675	-1.350	1.000	2.225	-0.450	0.000	0.175
210.0	197.1	-0.075	1.000	-0.725	1.725	-0.525	0.600	-1.500	1.000	2.200	-0.450	0.000	0.125
230.0	222.9	1.025	-0.425	-0.125	0.175	0.175	0.400	-0.175	1.550	2.275	0.925	-0.050	0.150
240.0	232.5	2.525	-0.000	-0.350	0.050	0.175	0.375	-0.275	1.950	2.625	0.750	-0.175	0.275
247.0	239.2	0.000	-0.275	-0.400	0.000	0.150	0.250	-0.375	2.175	2.875	0.750	-0.200	0.175

BEAM CFT-T03 TRANSVERSE STRAINS-SIDE FACE

MOMENT		STRAINS *10***3											
U	S	81- 83	82- 84	83- 85	84- 86	85- 87	86- 88	91- 93	92- 94	93- 95	94- 96	95- 97	96- 98
0.0	0.0	0.000	0.000	0.000	0.000	0.000	0.000	0.000	0.000	0.000	0.000	0.000	0.000
40.0	36.0	-0.025	-0.100	-0.100	-0.075	0.000	0.100	0.000	0.000	-0.175	-0.025	-0.050	-0.025

BEAM CFT-T03 DIAGONAL STRAINS-SIDE FACE

MOMENT		STRAINS *10***3											
U	S	61- 73	62- 74	63- 75	64- 76	65- 77	66- 78	71- 83	72- 84	73- 85	74- 86	75- 87	76- 88
0.0	0.0	0.000	0.000	0.000	0.000	0.000	0.000	0.000	0.000	0.000	0.000	0.000	0.000
20.0	10.0	0.175	0.000	0.022	0.044	0.044	-0.175	0.000	0.132	0.110	0.110	0.044	0.132
30.0	31.0	0.350	0.110	0.044	0.022	0.000	-0.197	0.132	0.000	0.044	-0.000	-0.044	-0.100
50.0	50.4	0.175	0.177	0.018	0.022	0.000	-0.022	0.241	0.154	0.022	-0.132	-0.110	-0.307
110.0	114.1	0.056	0.072	0.055	0.431	0.154	-0.217	0.275	0.044	-0.175	-0.110	-0.351	-0.357
130.0	134.9	0.058	0.030	1.053	0.543	0.000	-0.614	0.307	0.154	-0.022	-0.088	-0.329	-0.351
150.0	150.6	0.072	0.000	1.404	0.943	0.205	-0.432	0.307	0.000	-0.263	-0.154	-0.504	-0.246
170.0	175.3	1.022	1.140	1.711	1.113	0.373	-0.429	0.217	-0.000	-0.307	-0.241	-0.630	-0.614
190.0	199.0	2.001	1.200	1.908	1.184	0.401	-0.520	0.132	-0.175	-0.351	-0.205	-0.724	-0.704
210.0	222.9	2.525	1.001	2.303	1.425	0.461	-0.439	-0.110	-0.329	-0.482	-0.351	-0.987	-1.031
230.0	234.0	0.044	1.000	0.150	1.404	0.401	-0.197	-0.401	-0.114	-0.351	-1.031	-0.740	-0.740
243.0	239.0	0.228	2.000	2.632	1.601	0.482	-0.504	-0.225	-0.326	-0.014	-0.636	-1.140	-1.025

BEAM CFT-T03 DIAGONAL STRAINS-SIDE FACE

MOMENT		STRAINS *10***3											
U	S	81- 93	82- 94	83- 95	84- 96	85- 97	86- 98	91- 93	92- 94	93- 95	94- 96	95- 97	96- 98
0.0	0.0	0.000	0.000	0.000	0.000	0.000	0.000	0.000	0.000	0.000	0.000	0.000	0.000
40.0	35.5	0.044	0.000	0.022	0.044	-0.066	-0.088	0.022	-0.044	0.000	-0.022	-0.066	0.000
87.0	87.1	0.044	0.044	0.066	0.132	-0.132	-0.217	-0.154	-0.110	-0.197	-0.175	-0.044	-0.110

BEAM CFT-T03 LONGITUDINAL STRAINS-SIDE FACE

MOMENT		STRAINS *10***3							
U	S	111-131	112-132	113-133	114-134	115-135	116-136	117-137	118-138
0.0	0.0	0.000	0.000	0.000	0.000	0.000	0.000	0.000	0.000
30.0	30.0	0.000	0.075	0.012	-0.075	-0.125	-0.200	-0.200	-0.250
49.0	47.4	0.287	0.000	0.113	-0.025	-0.125	-0.200	-0.250	-0.325
100.0	107.7	0.950	1.000	0.925	0.550	0.150	-0.200	-0.450	-0.725
120.0	120.1	1.075	1.000	1.125	0.700	0.200	-0.212	-0.512	-0.675
140.0	142.7	1.102	1.707	1.337	0.325	0.237	-0.275	-0.537	-1.000
160.0	165.2	1.312	2.107	1.637	0.975	0.300	-0.307	-0.725	-1.225
180.0	187.3	1.303	2.500	1.603	1.037	0.267	-0.315	-0.825	-1.415
210.0	209.0	1.475	2.900	2.038	1.112	0.175	-0.512	-1.037	-1.707
240.0	213.3	1.525	3.000	2.125	1.075	0.050	-0.600	-1.275	-1.912
270.0	225.4	1.575	3.107	2.175	1.075	0.000	-0.650	-1.250	-1.907
280.0	216.9	1.537	3.100	2.163	1.025	-0.025	-0.700	-1.250	-1.907
230.0	223.7	1.537	3.107	2.100	0.987	-0.075	-0.700	-1.312	-2.013

MOMENT		BEAM CFT-T03 LONGITUDINAL STRAINS-SIDE FACE							
D	S	STRAINS *10**+3							
0.0	0.0	101-111	102-112	103-113	104-114	105-115	106-116	107-117	108-118
43.0	38.5	0.000	0.000	0.000	0.000	0.000	0.000	0.000	0.000
		-0.075	-0.000	0.050	0.000	-0.050	-0.100	-0.150	-0.250

MOMENT		BEAM CFT-T03 LONGITUDINAL STRAINS-SIDE FACE							
D	S	STRAINS *10**+3							
0.0	0.0	121-131	122-132	123-133	124-134	125-135	126-136	127-137	128-138
53.0	50.4	0.000	0.000	0.000	0.000	0.000	0.000	0.000	0.000
152.4	149.0	0.125	0.000	0.075	0.000	-0.050	-0.075	-0.075	-0.425
225.2	222.9	-0.250	1.325	0.825	1.775	0.825	-0.275	-0.675	-1.225
		-0.050	1.450	0.775	2.525	0.875	-0.600	-1.225	-2.325

MOMENT		BEAM CFT-T03 TRANSVERSE STRAINS-SIDE FACE											
D	S	STRAINS *10**+3											
0.0	0.0	101-103	102-104	103-105	104-106	105-107	106-108	111-113	112-114	113-115	114-116	115-117	116-118
43.0	0.0	0.000	0.000	0.000	0.000	0.000	0.000	0.000	0.000	0.000	0.000	0.000	

MOMENT		BEAM CFT-T03 TRANSVERSE STRAINS-SIDE FACE											
D	S	STRAINS *10**+3											
0.0	0.0	121-123	122-124	123-125	124-126	125-127	126-128	131-133	132-134	133-135	134-136	135-137	136-138
53.0	50.4	0.000	0.000	0.000	0.000	0.000	0.000	0.000	0.000	0.000	0.000	0.000	
152.4	149.0	0.075	0.000	-0.050	-0.075	0.000	0.025	0.150	-0.125	0.050	-0.050	-0.025	0.000
225.2	222.9	0.075	1.450	1.375	-0.225	0.050	0.150	0.000	-0.025	0.025	0.775	0.900	0.175
		1.350	2.700	2.700	-0.325	-0.025	0.450	0.550	-0.150	-0.075	1.100	1.125	0.325

MOMENT		BEAM CFT-T03 DIAGONAL STRAINS-SIDE FACE											
D	S	STRAINS *10**+3											
0.0	0.0	101-113	102-114	103-115	104-116	105-117	106-118	111-103	112-104	113-105	114-106	115-107	116-108
43.0	38.5	0.000	0.000	0.000	0.000	0.000	0.000	0.000	0.000	0.000	0.000	0.000	
		-0.022	-0.044	-0.022	-0.044	-0.110	-0.022	-0.022	0.072	-0.066	0.044	-0.022	0.000

MOMENT		BEAM CFT-T03 DIAGONAL STRAINS-SIDE FACE											
D	S	STRAINS *10**+3											
0.0	0.0	121-133	122-134	123-135	124-136	125-137	126-138	131-123	132-124	133-125	134-126	135-127	136-128
53.0	50.4	0.000	0.000	0.000	0.000	0.000	0.000	0.000	0.000	0.000	0.000	0.000	
152.4	149.1	-0.022	-0.044	-0.073	-0.073	-0.070	-0.600	1.272	2.329	2.368	-0.461	1.294	-0.044
225.2	224.4	-0.037	-0.110	-0.763	-0.520	-0.705	-0.811	2.053	4.304	3.509	2.500	1.535	-0.219

MOMENT		BEAM CFT-T03 LONGITUDINAL STRAINS-SIDE FACE							
D	S	STRAINS *10**+3							
0.0	0.0	141-151	142-152	143-153	144-154	145-155	146-156	147-157	148-158
30.0	37.0	0.000	0.000	0.000	0.000	0.000	0.000	0.000	0.000
62.4	59.3	0.000	0.000	0.100	-0.025	-0.100	-0.175	-0.225	-0.300
133.1	134.7	0.500	0.000	0.212	0.075	-0.100	-0.200	-0.300	-0.450
160.0	160.1	1.125	0.000	0.402	0.475	0.012	-0.307	-0.735	-1.137
179.5	170.4	1.200	0.000	0.537	0.575	0.037	-0.475	-0.935	-1.400
200.0	200.0	1.437	0.000	0.533	0.650	0.037	-0.512	-1.067	-1.687
234.1	234.1	1.007	1.000	0.608	0.800	0.037	-0.600	-1.207	-2.125
264.0	262.2	2.012	1.000	0.312	0.950	0.037	-0.850	-1.750	-2.662
280.0	272.9	2.012	0.000	1.100	1.325	0.000	-1.262	-2.662	-4.125
280.0	272.9	2.012	0.000	2.233	2.350	0.150	-2.204	-4.912	-8.325
280.0	261.0	2.012	0.000	3.675	3.362	0.350	-2.025	-5.137	-12.775
291.0	271.0	11.375	0.000	0.312	5.112	0.933	-3.750	-6.325	-15.775
293.2	280.5	14.775	11.400	0.275	0.937	1.262	-4.000	-7.400	

MOMENT		BEAM CFT-T03 LONGITUDINAL STRAINS-SIDE FACE							
D	S	STRAINS *10**+3							
0.0	0.0	161-161	162-162	163-163	164-164	165-165	166-166	167-167	168-168
30.0	30.0	0.000	0.000	0.000	0.000	0.000	0.000	0.000	0.000
49.0	47.4	0.125	0.100	-0.012	-0.050	-0.125	-0.175	-0.183	-0.225
103.1	107.7	0.075	0.775	0.000	0.437	0.438	-0.025	-0.325	-0.600
123.4	128.1	1.075	1.012	0.037	0.512	0.037	-0.362	-0.735	-1.067
143.4	142.7	1.050	1.000	0.757	0.558	0.037	-0.412	-0.862	-1.253
163.2	165.2	2.075	1.000	1.050	0.775	0.063	-0.402	-1.000	-1.450
180.0	180.0	2.000	2.100	1.337	0.807	0.037	-0.550	-1.187	-1.712
211.0	209.0	3.050	0.000	1.650	1.007	-0.002	-0.775	-1.525	-2.100
246.7	217.0	4.362	0.000	2.163	1.150	-0.250	-0.963	-1.607	-2.200
267.0	225.4	4.000	0.000	2.363	1.187	-0.313	-1.037	-1.762	-2.225
233.5	217.0	4.750	0.000	2.413	1.175	-0.275	-1.075	-1.757	-2.230
230.2	224.4	5.100	0.000	2.437	1.137	-0.425	-1.112	-1.837	-2.263

BEAM CFT-T03 LONGITUDINAL STRAINS-SIDE FACE
STRAINS *10**3

MOMENT	161-171	162-172	163-173	164-174	165-175	166-176	167-177	168-178
0	0.000	0.000	0.000	0.000	0.000	0.000	0.000	0.000
53.0	0.575	0.400	0.250	0.075	-0.075	-0.125	-0.275	-0.525
152.4	3.350	2.550	1.750	1.200	-0.075	-0.250	-0.550	-1.250
225.2	6.075	6.200	4.075	2.525	-0.275	-0.650	-1.625	-2.225

BEAM CFT-T03 LONGITUDINAL STRAINS-SIDE FACE
STRAINS *10**3

MOMENT	161-171	162-172	163-173	164-174	165-175	166-176	167-177	168-178
0	0.000	0.000	0.000	0.000	0.000	0.000	0.000	0.000
53.0	0.250	0.225	0.150	-0.050	-0.100	-0.125	-0.175	-0.225
152.4	0.500	0.425	1.650	1.075	-0.100	-0.325	-0.500	-0.650
172.2	0.350	2.075	1.625	1.950	-0.175	-0.575	-0.800	-1.000

BEAM CFT-T03 TRANSVERSE STRAINS-SIDE FACE
STRAINS *10**3

MOMENT	161-163	162-164	163-165	164-166	165-167	166-168	171-173	172-174	173-175	174-176	175-177	176-178
0	0.000	0.000	0.000	0.000	0.000	0.000	0.000	0.000	0.000	0.000	0.000	
53.0	-0.025	-0.125	0.025	0.000	0.050	-0.025	-0.025	-0.150	-0.100	-0.025	-0.025	
152.4	-0.075	-0.075	0.350	0.700	-0.175	-0.025	-0.025	-0.050	0.050	0.100	0.250	
225.2	-0.100	0.075	2.800	2.400	-0.350	0.250	1.125	-0.275	-0.175	0.475	0.650	

BEAM CFT-T03 TRANSVERSE STRAINS-SIDE FACE
STRAINS *10**3

MOMENT	161-163	162-164	163-165	164-166	165-167	166-168	191-193	192-194	193-195	194-196	195-197	196-198
0	0.000	0.000	0.000	0.000	0.000	0.000	0.000	0.000	0.000	0.000	0.000	
53.0	-0.050	-0.025	0.000	0.025	0.050	0.000	-0.075	0.025	-0.025	0.175	0.000	
152.4	0.025	0.400	1.250	1.225	0.050	0.775	1.850	0.200	0.125	0.150	0.100	
172.2	-0.225	0.400	2.575	2.400	-0.100	0.400	4.025	1.375	1.125	-0.100	-0.025	

BEAM CFT-T03 DIAGONAL STRAINS-SIDE FACE
STRAINS *10**3

MOMENT	161-173	162-174	163-175	164-166	165-177	166-178	171-163	172-164	173-165	174-166	175-167	176-168
0	0.000	0.000	0.000	0.000	0.000	0.000	0.000	0.000	0.000	0.000	0.000	
53.0	0.375	0.200	0.110	-0.022	-0.083	-0.154	0.197	0.366	0.022	0.044	-0.033	
152.4	2.675	2.257	1.778	1.310	-0.307	-0.437	0.417	0.022	-0.241	-0.265	-0.461	
225.2	6.535	5.030	4.539	3.443	-0.329	-0.329	0.110	-0.548	-0.526	-0.626	-0.811	

BEAM CFT-T03 DIAGONAL STRAINS-SIDE FACE
STRAINS *10**3

MOMENT	161-193	162-194	163-195	164-196	165-197	166-198	191-183	192-184	193-185	194-186	195-187	196-188
0	0.000	0.000	0.000	0.000	0.000	0.000	0.000	0.000	0.000	0.000	0.000	
53.0	0.154	0.000	-0.044	-0.110	-0.066	-0.154	0.152	-0.066	-0.022	0.066	-0.044	
152.4	2.753	2.959	2.127	1.363	-0.038	-0.307	-0.175	-0.461	-0.197	0.000	-0.241	
172.2	3.794	5.173	3.860	2.917	-0.110	-0.417	-0.395	-1.294	-0.592	-0.461	-0.504	

BEAM CFT-T03 LONGITUDINAL STRAINS-TOP FACE
STRAINS *10**3

MOMENT	ECT1	ECT2	ECT3	ECT4	ECT5	ECT6
0	0.000	0.000	0.000	0.000	0.000	0.000
19.6	-0.067	-0.109	-0.037	-0.112	-0.075	-0.062
50.6	-0.250	-0.237	-0.250	-0.262	-0.237	-0.237
49.9	-0.287	-0.333	-0.325	-0.317	-0.325	-0.313
103.1	-0.575	-0.612	-0.700	-0.800	-0.633	-0.650
143.4	-0.862	-0.900	-1.000	-0.975	-0.850	-0.787
105.2	-0.963	-1.037	-1.162	-1.037	-0.933	-0.925
177.3	-1.037	-1.175	-1.350	-1.275	-1.100	-1.050
211.9	-1.200	-1.375	-1.562	-1.475	-1.262	-1.225
247.7	-1.300	-1.415	-1.637	-1.707	-1.537	-1.525
249.0	-1.363	-1.475	-1.650	-1.512	-1.600	-1.525
233.3	-1.300	-1.400	-1.525	-1.812	-1.532	-1.512
236.2	-1.337	-1.437	-1.650	-1.863	-1.650	-1.512

MOMENT		BEAM CFT-T04 LONGITUDINAL STRAINS-SIDE FACE							
0	S	STRAINS *10**3							
		41- 71	42- 72	43- 73	44- 74	45- 75	46- 76	47- 77	48- 78
0.0	0.0	0.000	0.000	0.000	0.000	0.000	0.000	0.000	0.000
19.2	19.2	0.150	0.150	0.033	0.025	-0.012	-0.100	-0.100	-0.125
37.5	37.5	0.550	0.402	0.325	0.175	0.000	-0.150	-0.262	-0.350
49.0	49.0	0.753	0.600	0.400	0.225	0.075	-0.175	-0.362	-0.457
73.1	73.1	1.100	0.857	0.583	0.252	0.012	-0.300	-0.612	-0.812
89.2	89.2	1.567	1.075	0.725	0.362	0.037	-0.333	-0.725	-1.012
106.0	106.1	1.762	1.375	0.900	0.475	0.050	-0.475	-1.050	-1.375
125.7	125.3	2.537	2.000	1.363	0.738	0.157	-0.550	-1.387	-1.863
142.7	141.8	5.525	4.583	3.163	1.950	1.050	-0.575	-0.923	-3.300
146.3	145.8	6.925	5.467	3.987	2.525	1.433	-0.575	-2.553	-3.875
146.3	144.9	10.650	8.457	6.200	4.112	2.675	-0.450	-7.537	-4.662
149.4	145.4	14.012	11.057	8.175	5.412	4.037	-0.437	-4.737	-4.650
149.3	146.3	16.713	13.575	10.137	6.850	5.400	-0.350	-5.362	-4.412
150.3	147.6		16.937	11.787	8.062	6.830	-0.137	-6.712	-4.150
151.0	147.1		17.036	14.737	9.925	8.850	0.250	-7.962	-3.700

MOMENT		BEAM CFT-T04 LONGITUDINAL STRAINS-SIDE FACE							
0	S	STRAINS *10**3							
		51- 61	52- 62	53- 63	54- 64	55- 65	56- 66	57- 67	58- 68
0.0	0.0	0.000	0.000	0.000	0.000	0.000	0.000	0.000	0.000
19.2	18.7	0.225	0.125	0.075	0.025	0.025	-0.075	-0.050	-0.100
37.4	37.1	0.425	0.200	0.175	0.150	0.125	-0.075	-0.175	-0.250
49.1	49.1	0.325	0.100	0.000	0.025	0.000	-0.125	-0.250	-0.425
73.2	73.2	0.725	0.375	0.125	0.025	-0.025	-0.225	-0.475	-0.675
89.2	89.2	1.100	0.650	0.325	0.125	-0.075	-0.325	-0.625	-0.875
106.6	106.6	1.725	1.100	0.675	0.350	-0.025	-0.325	-0.800	-1.075
125.3	125.6	2.675	1.675	1.400	0.775	0.075	-0.500	-1.050	-1.500
142.7	141.8	6.325	5.200	6.075	2.300	0.750	-0.400	-1.300	-2.600
146.2	145.6	8.550	6.850	4.725	2.900	1.225	-0.425	-2.100	-3.000
146.2	144.9	12.875	7.750	7.750	5.025	2.350	-0.275	-3.000	-3.575

MOMENT		BEAM CFT-T04 LONGITUDINAL STRAINS-SIDE FACE							
0	S	STRAINS *10**3							
		81-101	82-102	83-103	84-104	85-105	86-106	87-107	88-108
0.0	0.0	0.000	0.000	0.000	0.000	0.000	0.000	0.000	0.000
15.3	15.3	0.000	0.000	0.053	-0.012	-0.037	-0.050	-0.112	-0.062
30.0	29.6	0.588	0.325	0.362	0.063	-0.050	-0.100	-0.133	-0.250
39.2	39.2	0.975	0.650	0.637	0.125	-0.025	-0.112	-0.250	-0.325
53.5	58.5	1.650	-0.200	1.012	0.012	-0.037	-0.150	-0.250	-0.563
71.3	71.3	2.175	1.512	1.450	0.225	0.025	-0.163	-0.433	-0.713
85.3	84.2	2.987	2.112	1.952	0.362	0.125	-0.200	-0.563	-0.975
100.6	100.2	4.013	2.962	2.637	0.487	0.188	-0.225	-0.668	-1.288
114.2	114.2	6.267	4.675	4.062	0.637	0.262	-0.262	-0.775	-1.567
117.0	116.3	6.862	5.325	4.425	0.637	0.262	-0.237	-0.837	-1.625
117.0	115.2	8.200	6.362	5.225	0.762	0.350	-0.275	-0.837	-1.700
119.5	115.9	8.750	6.657	5.437	0.750	0.313	-0.300	-0.938	-1.762
120.0	117.0	9.550	7.237	5.800	0.738	0.313	-0.313	-0.975	-1.737
120.0	118.1	9.657	7.462	5.925	0.750	0.313	-0.325	-0.957	-1.800
121.3	117.7	10.113	7.650	6.175	0.750	0.300	-0.325	-0.987	-1.812

MOMENT		BEAM CFT-T04 LONGITUDINAL STRAINS-SIDE FACE							
0	S	STRAINS *10**3							
		81- 91	82- 92	83- 93	84- 94	85- 95	86- 96	87- 97	88- 98
0.0	0.0	0.000	0.000	0.000	0.000	0.000	0.000	0.000	0.000
13.3	15.9	0.275	0.000	-0.025	0.000	-0.025	-0.050	-0.150	-0.100
31.8	31.8	0.750	0.000	0.600	0.200	-0.050	-0.025	-0.200	-0.300
41.7	41.7	1.150	0.925	0.850	0.125	-0.100	-0.150	-0.350	-0.500
62.2	62.2	2.275	2.000	1.725	-0.100	-0.150	-0.200	-0.475	-0.625
73.3	75.8	2.650	2.525	2.200	0.000	-0.150	-0.100	-0.600	-1.000
90.6	90.2	3.850	3.625	2.675	-0.250	-0.300	-0.150	-0.800	-1.425
105.7	106.5	4.650	3.900	3.250	-0.300	-0.425	-0.075	-0.875	-1.725
121.3	120.5	5.900	7.000	5.675	-0.350	-0.425	-0.175	-1.175	-2.225
124.3	123.9	9.300	7.775	6.275	-0.400	-0.400	-0.150	-1.250	-2.300
124.3	123.2	11.225	9.350	7.475	-0.425	-0.450	-0.150	-1.300	-2.450

MOMENT		BEAM CFT-T04 TRANSVERSE STRAINS-SIDE FACE											
D	S	STRAINS *10**--3											
		81- 83	82- 84	83- 85	84- 86	85- 87	86- 88	91- 93	92- 94	93- 95	94- 96	95- 97	96- 98
0-0	0.0	0.000	0.000	0.000	0.000	0.000	0.000	0.000	0.000	0.000	0.000	0.000	0.000
10-3	15.9	-0.025	-0.025	0.075	0.100	0.125	0.025	0.000	-0.025	2.475	0.100	0.100	0.000
31-3	31.4	0.050	-0.050	0.125	0.050	0.325	0.025	0.075	0.100	2.525	0.075	0.175	0.025
41-7	41.7	-0.025	0.075	0.325	0.000	0.100	0.025	0.000	0.025	2.525	0.100	0.100	0.050
62-2	62.2	-0.125	0.650	0.675	-0.225	0.025	0.025	0.075	0.100	2.700	0.200	0.300	0.100
75-3	75.8	0.050	1.250	0.975	-0.175	0.025	0.100	0.150	0.100	2.575	0.400	0.425	0.050
90-6	90.2	-0.100	1.550	1.425	-0.475	0.150	0.275	0.150	0.175	2.475	0.250	0.775	-0.050
100-9	106.5	-0.075	2.150	1.800	-1.525	0.025	0.400	-0.100	0.050	2.500	1.325	1.275	-0.100
121-3	121.3	0.000	3.000	3.475	-0.750	-0.175	0.950	-0.075	0.100	2.675	1.925	1.775	0.075
124-3	123.6	0.175	4.450	3.950	-0.775	-0.225	1.000	-0.050	0.125	2.700	2.150	1.900	-0.075
124-3	122.8	0.000	5.000	5.175	-0.800	-0.250	1.150	-0.100	0.225	2.775	2.375	2.150	-0.050

MOMENT		BEAM CFT-T04 DIAGONAL STRAINS-SIDE FACE											
D	S	STRAINS *10**--3											
		81- 93	82- 94	83- 95	84- 96	85- 97	86- 98	91- 93	92- 94	93- 95	94- 96	95- 97	96- 98
0-0	0.0	0.000	0.000	0.000	0.000	0.000	0.000	0.000	0.000	0.000	0.000	0.000	0.000
10-3	16.3	0.053	0.053	0.000	-0.035	0.035	0.053	0.000	0.018	-0.071	-0.124	-0.124	-0.053
31-3	31.5	0.424	0.536	0.265	0.033	-0.018	-0.008	0.124	-0.053	-0.106	-0.124	-0.212	-0.230
41-7	41.7	0.760	0.707	0.583	-0.053	-0.035	-0.035	0.265	0.018	-0.124	-0.177	-0.265	-0.265
62-2	62.2	1.519	1.300	1.307	-0.124	-0.018	-0.071	0.405	0.124	-0.194	-0.212	-0.317	-0.406
75-3	75.8	1.704	1.714	1.572	-0.053	-0.035	-0.035	0.457	0.000	-0.194	-0.247	-0.336	-0.495
90-6	89.8	2.367	2.120	1.890	0.159	-0.035	-0.035	0.495	0.018	-0.247	-0.310	-0.457	-0.654
100-9	106.1	3.216	2.643	2.509	0.718	0.313	-0.013	0.530	0.071	-0.247	-0.406	-0.406	-0.513
121-3	120.9	5.505	4.905	4.399	0.548	0.583	0.124	0.742	-0.071	-0.300	-0.442	-0.583	-0.330
124-3	123.6	6.290	5.050	4.982	0.654	0.656	0.141	0.833	-0.035	-0.233	-0.442	-0.656	-0.330
124-3	122.0	7.800	7.120	6.290	0.760	0.742	0.177	0.843	-0.141	-0.300	-0.459	-0.671	-0.866

MOMENT		BEAM CFT-TDS LONGITUDINAL STRAINS-SIDE FACE							
0	S	STRAINS *10**3							
		11- 31	12- 32	13- 33	14- 34	15- 35	16- 36	17- 37	18- 38
0.0	0.0	0.000	0.000	0.000	0.000	0.000	0.000	0.000	0.000
10.4	16.1	0.025	0.000	0.000	0.000	-0.012	-0.062	-0.050	-0.075
31.4	26.7	0.163	0.000	0.008	0.063	0.000	-0.062	-0.075	-0.125
53.3	54.9	0.400	0.000	0.175	0.080	0.037	-0.075	-0.150	-0.225
75.1	72.9	0.700	0.010	0.462	0.250	0.150	-0.062	-0.262	-0.412
97.5	89.5	0.975	0.010	1.000	0.612	0.362	-0.012	-0.257	-0.500
108.1	106.1	1.075	0.000	0.912	0.750	0.500	0.037	-0.387	-0.650
128.4	128.4	1.325	-0.000	0.975	0.787	0.688	0.050	-0.525	-0.787
143.0	143.0	1.667	-0.000	1.012	0.800	0.800	0.063	-0.588	-0.938
162.3	162.1	2.050	0.000	1.025	0.750	0.800	-0.012	-0.700	-1.012
177.3	177.3	2.625	0.000	0.967	0.575	0.837	-0.087	-0.950	-1.250
193.0	192.5	3.250	1.010	1.025	0.975	0.925	-0.175	-0.965	-1.425
202.3	201.2	3.650	1.410	0.957	0.550	0.837	-0.262	-1.050	-1.562
213.0	209.6	3.967	1.000	1.000	-0.725	0.825	-0.311	-1.162	-1.750
220.5	218.0	4.250	1.000	0.959	0.462	0.812	-0.375	-1.250	-1.900
224.4	222.0	4.700	0.000	0.725	0.400	0.713	-0.450	-1.262	-1.837
229.4	227.2	5.300	0.000	0.802	0.562	0.637	-0.550	-1.325	-1.837

MOMENT		BEAM CFT-TDS LONGITUDINAL STRAINS-SIDE FACE							
0	S	STRAINS *10**3							
		21- 31	22- 32	23- 33	24- 34	25- 35	26- 36	27- 37	28- 38
0.0	0.0	0.000	0.000	0.000	0.000	0.000	0.000	0.000	0.000
13.5	18.5	0.130	0.100	0.000	0.025	-0.025	-0.050	-0.050	-0.100
33.3	32.5	0.250	0.000	0.075	0.050	-0.025	-0.075	-0.100	-0.175
62.2	62.2	0.525	-0.000	0.000	-0.550	-0.050	-0.125	-0.150	-0.550
82.3	82.3	1.325	-0.000	-0.100	-0.175	0.100	-0.150	-0.400	-0.550
100.7	100.5	1.625	-0.000	-0.125	-0.175	0.575	0.050	-0.325	-0.675
121.0	120.8	2.075	-0.000	-0.125	-0.175	0.950	0.200	-0.400	-0.650
144.5	143.9	2.675	-0.000	-0.100	-0.250	1.225	0.225	-0.450	-1.025
160.7	159.3	3.300	-0.000	-0.150	-0.250	1.400	0.275	-0.600	-1.250
162.0	161.0	4.250	0.750	-0.175	-0.500	1.575	0.225	-0.850	-1.375
199.5	198.0	5.200	1.075	-0.125	-0.275	1.575	0.175	-0.725	-1.525
217.1	217.1	6.075	2.000	-0.125	-0.250	1.775	0.100	-1.000	-1.750
227.0	225.5	7.075	2.600	-0.275	-0.375	1.900	0.050	-1.375	-1.950
239.0	236.0	8.500	3.100	-0.325	-0.425	1.950	0.000	-1.425	-2.100

MOMENT		BEAM CFT-TDS TRANSVERSE STRAINS-SIDE FACE											
0	S	STRAINS *10**3											
		21- 23	22- 24	23- 25	24- 26	25- 27	26- 28	31- 33	32- 34	33- 35	34- 36	35- 37	36- 38
0.0	0.0	0.000	0.000	0.000	0.000	0.000	0.000	0.000	0.000	0.000	0.000	0.000	0.000
10.4	18.5	0.000	0.000	-0.025	0.075	0.025	0.050	-0.025	-0.100	-0.050	0.000	0.000	0.025
33.3	32.5	0.030	0.075	0.030	0.050	0.000	0.075	0.025	-0.025	0.025	0.050	0.025	-0.025
62.2	62.2	0.100	0.100	0.100	0.075	-0.050	0.075	0.025	-0.100	-0.175	0.000	0.025	0.000
82.3	82.3	0.250	0.050	0.425	0.250	-0.275	0.025	0.225	-0.325	-0.125	-0.075	-0.025	0.000
100.7	100.5	0.675	0.050	1.275	1.025	-0.475	-0.375	0.225	-0.100	0.000	-0.025	-0.100	-0.400
121.0	120.8	0.925	0.000	2.025	1.675	-0.325	0.000	0.400	-0.150	0.025	-0.050	0.250	0.350
144.5	144.0	-0.075	-0.000	2.625	2.525	-0.225	-0.075	0.600	-0.200	-0.100	-0.100	0.500	0.600
160.7	160.3	-0.175	-0.200	3.475	2.375	-0.525	-0.125	0.900	-0.400	0.000	-0.050	0.750	0.775
162.0	161.0	-0.225	-0.050	3.900	3.275	-0.750	-0.125	1.950	0.475	-0.175	-0.150	0.775	0.825
199.5	182.0	-0.150	0.000	4.750	3.325	-0.500	0.100	2.550	1.025	-0.075	-0.100	0.925	1.025
217.1	217.1	-0.325	0.000	5.425	4.225	-0.550	-0.075	3.125	1.575	-0.175	-0.125	0.975	1.175
227.0	227.0	-0.425	-0.100	6.000	5.625	-0.700	-0.050	4.375	2.650	-0.175	-0.225	1.300	1.450
239.0	236.4	-0.475	-0.000	7.000	5.950	-1.050	-1.325	4.900	2.625	-0.375	-0.350	1.250	1.500

MOMENT		BEAM CFT-TDS DIAGONAL STRAINS-SIDE FACE											
0	S	STRAINS *10**3											
		21- 33	22- 34	23- 35	24- 36	25- 37	26- 38	31- 33	32- 34	33- 35	34- 36	35- 37	36- 38
0.0	0.0	0.000	0.000	0.000	0.000	0.000	0.000	0.000	0.000	0.000	0.000	0.000	0.000
10.4	18.5	0.044	-0.022	-0.022	-0.022	-0.022	-0.022	0.081	0.044	0.066	0.022	0.329	-0.044
33.3	32.5	0.110	0.044	0.000	-0.022	-0.044	-0.044	0.175	0.022	0.088	0.088	0.329	0.000
62.2	62.2	0.110	0.000	-0.044	-0.088	-0.132	-0.132	0.571	-0.066	0.022	0.022	0.285	-0.022
82.3	82.3	0.110	-0.044	-0.088	-0.154	-0.219	-0.245	0.397	-0.066	0.195	0.197	0.439	-0.044
100.7	100.5	0.177	0.022	-0.110	-0.175	-0.239	-0.239	1.113	-0.088	1.250	0.789	0.789	0.219
121.0	121.0	0.175	-0.022	-0.154	-0.241	-0.432	-0.526	1.491	-0.154	2.018	1.338	1.225	0.504
144.5	144.0	0.152	-0.022	-0.175	-0.239	-0.650	-0.702	2.015	-0.154	2.807	1.864	1.754	0.154
160.7	160.7	0.000	-0.000	-0.219	-0.285	-0.811	-0.811	2.675	-0.154	3.443	2.215	2.018	0.905
162.0	161.0	-0.044	-0.132	-0.285	-0.359	-0.999	-0.999	4.013	0.877	3.772	2.500	2.171	1.009
199.5	199.3	-0.177	-0.241	-0.307	-0.373	-1.140	-1.090	4.390	1.601	4.013	2.675	2.281	1.096
217.1	216.5	-0.175	-0.000	-0.373	-0.417	-1.272	-1.184	5.162	2.474	4.093	3.026	2.583	1.000
227.0	227.1	-0.014	-0.000	-0.653	-0.630	-1.792	-1.908	7.237	3.377	5.331	3.487	3.092	1.316
239.0	236.4	-0.719	-0.000	-0.746	-0.653	-2.171	-2.061	8.092	3.902	5.570	3.684	3.240	1.300

MOMENT		BEAM CFT-T05 LONGITUDINAL STRAINS-SIDE FACE							
D	S	STRAINS *10**-3							
0-0	0-0	11- 12	13- 14	15- 16	17- 18	19- 20	21- 22	23- 24	25- 26
0-0	0-0	0.000	0.000	0.000	0.000	0.000	0.000	0.000	0.000
164.5	162.9	2.275	1.500	3.125	1.150	-0.275	-0.450	-0.300	-0.150
173.0	170.1	2.700	1.575	3.125	1.800	-0.425	-0.550	-0.750	-0.775

MOMENT		BEAM CFT-T05 TRANSVERSE STRAINS-SIDE FACE											
D	S	STRAINS *10**-3											
0-0	0-0	11- 13	12- 14	13- 15	14- 16	15- 17	16- 18	17- 19	18- 20	19- 21	20- 22	21- 23	22- 24
0-0	0-0	0.000	0.000	0.000	0.000	0.000	0.000	0.000	0.000	0.000	0.000	0.000	0.000
164.5	164.0	4.775	4.225	-0.150	-0.075	0.025	0.050	1.050	2.050	2.375	2.750	-0.075	0.025
173.0	170.7	5.075	4.925	-0.150	-0.275	0.500	0.950	3.875	3.375	2.725	3.250	-0.075	0.025

MOMENT		BEAM CFT-T05 DIAGONAL STRAINS-SIDE FACE							
D	S	STRAINS *10**-3							
0-0	0-0	11- 14	13- 16	17- 18	11- 12	13- 14	15- 16	17- 18	19- 20
0-0	0-0	0.000	0.000	0.000	0.000	0.000	0.000	0.000	0.000
164.5	163.6	1.340	1.250	1.515	1.333	1.220	1.382	10.855	2.757
173.0	170.4	-0.417	-0.905	-0.702	-0.877	-0.937	-0.658	9.033	7.961

MOMENT		BEAM CFT-T05 LONGITUDINAL STRAINS-SIDE FACE										
D	S	STRAINS *10**-3										
0-0	0-0	41- 51	42- 52	43- 53	44- 54	45- 55	46- 56	47- 57	48- 58	49- 59	50- 60	51- 61
0-0	0-0	0.000	0.000	0.000	0.000	0.000	0.000	0.000	0.000	0.000	0.000	0.000
27.5	20.5	0.075	0.025	-0.012	-0.037	-0.037	-0.050	-0.100	-0.137	-0.175	-0.212	-0.250
37.2	36.1	0.237	0.150	0.190	0.012	-1.712	-0.037	-0.125	-0.175	-0.212	-0.250	-0.287
67.1	68.9	0.225	0.000	0.462	0.225	0.025	-0.037	-0.750	-0.400	-0.462	-0.500	-0.537
91.4	91.4	0.750	0.900	0.638	0.350	0.037	-0.175	-0.400	-0.625	-0.662	-0.700	-0.737
111.7	111.9	0.938	1.102	0.925	0.475	0.100	-0.200	-0.512	-0.600	-0.687	-0.775	-0.862
135.1	134.7	1.112	1.405	1.150	0.612	0.113	-0.262	-0.650	-0.787	-0.875	-0.962	-1.050
160.5	160.5	1.300	1.000	1.413	0.757	0.137	-0.313	-0.825	-1.262	-1.300	-1.337	-1.375
173.0	178.6	1.478	2.050	1.612	0.925	0.168	-0.375	-1.300	-1.525	-1.562	-1.590	-1.625
202.9	202.2	1.647	2.400	1.875	1.037	0.225	-0.450	-1.233	-1.857	-1.895	-1.932	-1.969
221.0	221.6	1.900	2.757	2.112	1.252	0.250	-0.583	-1.500	-2.288	-2.325	-2.362	-2.399
241.2	240.6	2.375	3.575	2.750	1.675	0.433	-0.633	-1.900	-2.950	-3.000	-3.050	-3.100
252.8	251.5	2.538	4.175	3.175	2.100	0.625	-0.675	-2.200	-3.475	-3.525	-3.575	-3.625
262.2	262.2	3.062	5.025	3.875	2.625	0.733	-0.700	-2.600	-4.150	-4.200	-4.250	-4.300
272.2	272.2	3.275	6.013	6.537	4.512	1.950	-0.775	-3.937	-5.500	-5.550	-5.600	-5.650
280.5	278.0	7.450	11.737	9.037	6.200	2.937	-0.653	-4.533	-10.300	-10.350	-10.400	-10.450
280.7	284.5	11.212	16.250	13.562	9.400	5.025	-0.250	-6.187	-14.213	-14.263	-14.313	-14.363

MOMENT		BEAM CFT-T05 LONGITUDINAL STRAINS-SIDE FACE							
D	S	STRAINS *10**-3							
0-0	0-0	61- 61	62- 62	63- 63	64- 64	65- 65	66- 66	67- 67	68- 68
0-0	0-0	0.000	0.000	0.000	0.000	0.000	0.000	0.000	0.000
16.4	16.4	0.075	-0.075	0.012	-0.037	0.083	-0.025	-0.100	-0.100
31.4	28.9	0.138	0.075	0.113	0.012	0.037	-0.037	-0.112	-0.150
52.5	55.5	0.412	0.225	0.290	-1.157	0.050	-0.075	-0.212	-0.250
73.1	73.1	0.525	0.302	0.250	-1.200	0.313	-0.062	-0.333	-0.450
82.5	89.2	0.512	0.433	0.262	-1.162	0.462	-0.053	-0.325	-0.550
100.1	107.6	0.237	0.050	0.225	-1.325	0.500	-0.037	-0.400	-0.662
126.4	123.2	1.262	0.975	0.150	-0.125	0.563	-0.050	-0.575	-0.837
143.0	142.3	1.000	1.275	0.150	-0.137	0.787	0.050	-0.583	-0.987
162.5	161.6	2.002	1.000	0.212	-0.175	0.350	0.025	-0.725	-1.125
177.5	170.3	2.050	2.050	0.500	-0.150	0.900	0.050	-0.787	-1.325
193.1	192.6	2.338	2.767	1.900	-0.125	0.975	0.037	-0.900	-1.450
202.5	201.5	3.050	3.125	1.375	-0.100	0.925	-1.325	-1.150	-1.662
213.0	209.8	4.225	3.413	1.562	-0.075	0.925	-0.057	-1.225	-1.775
220.5	218.0	4.737	3.000	1.325	-0.012	0.912	-0.150	-1.500	-1.850
224.4	222.2	5.038	3.937	1.912	-0.012	0.337	-0.175	-1.350	-1.887
229.4	227.9	5.525	4.150	2.038	-0.025	0.637	-0.250	-1.363	-1.950

MOMENT		BEAM CFT-T05 LONGITUDINAL STRAINS-SIDE FACE							
D	S	STRAINS *10**-3							
0-0	0-0	61- 71	62- 72	63- 73	64- 74	65- 75	66- 76	67- 77	68- 78
0-0	0-0	0.000	0.000	0.000	0.000	0.000	0.000	0.000	0.000
17.4	17.2	0.110	0.100	0.025	0.050	0.000	-0.050	-0.025	0.025
33.4	30.7	0.075	0.000	0.125	0.053	0.050	0.000	-0.075	-0.075
53.3	58.7	0.075	0.475	0.350	0.175	0.025	-0.075	-0.225	-0.275
77.7	77.7	0.175	0.025	0.525	0.353	0.100	-0.075	-0.275	-0.400
95.1	94.8	0.150	0.025	0.350	0.275	0.075	-0.025	-0.375	-0.600
114.3	114.6	0.050	0.075	0.525	0.175	0.000	0.075	-0.475	-0.650
130.5	130.4	1.525	4.250	0.425	0.153	-0.050	0.150	-0.500	-0.875
152.3	151.6	2.100	4.775	0.450	0.075	-0.125	0.350	-0.650	-1.050
172.3	171.9	3.000	5.525	0.375	0.050	-0.175	0.350	-0.750	-1.250
183.4	180.0	3.725	6.275	1.200	0.193	-0.100	0.450	-0.900	-1.325
202.1	204.5	4.650	7.750	2.325	0.050	-0.175	0.400	-1.000	-1.550
214.7	213.0	5.525	8.425	3.225	-0.125	-0.250	0.400	-1.150	-1.775
220.5	222.9	6.075	8.950	3.625	-0.225	-0.350	0.350	-1.275	-1.950

BEAM CFT-T03 TRANSVERSE STRAINS-SIDE FACE
STRAINS *10**3

MOMENT		61- 63	62- 64	63- 65	64- 66	65- 67	66- 68	71- 73	72- 74	73- 75	74- 76	75- 77	76- 78
0	0	0.000	0.000	0.000	0.000	0.000	0.000	0.000	0.000	0.000	0.000	0.000	0.000
0.0	0.0	0.000	0.000	0.000	0.000	0.000	0.000	0.000	0.000	0.000	0.000	0.000	0.000
17.4	16.9	0.125	0.100	0.075	0.175	0.275	0.125	0.200	-0.025	0.025	0.020	0.025	0.150
33.4	30.7	0.100	0.000	-0.250	0.150	0.250	0.100	0.225	0.000	0.025	0.075	0.025	0.200
53.3	53.0	0.100	0.000	-0.325	0.175	0.300	0.150	0.250	0.150	0.025	0.100	0.075	0.200
77.7	77.7	0.200	0.175	0.100	0.175	0.400	0.250	0.425	15.275	-0.575	0.225	0.150	0.275
93.1	95.1	0.100	0.075	0.100	0.275	0.475	0.200	0.425	15.250	0.025	0.575	0.525	0.175
114.3	114.7	0.525	0.300	0.350	0.250	0.400	0.250	0.450	15.300	0.075	1.050	0.925	0.275
130.5	130.4	0.800	0.625	0.100	0.200	0.450	0.325	0.350	15.275	0.025	1.400	1.400	0.200
152.0	152.0	1.000	1.125	0.025	0.125	0.600	0.475	0.450	15.275	-0.050	1.925	-0.600	0.100
172.5	172.5	1.475	1.375	0.175	0.125	0.300	0.575	0.275	15.250	-0.050	2.300	2.300	0.150
183.4	188.2	1.575	2.000	0.400	0.050	0.775	0.625	0.575	15.200	-0.100	2.625	2.675	0.125
203.1	204.5	1.800	3.025	1.300	0.000	0.925	0.700	1.100	15.275	-0.050	3.075	3.050	0.175
214.9	213.8	1.275	3.500	2.050	-0.300	0.875	0.750	1.375	15.200	-0.250	3.700	3.725	-0.100
220.3	222.9	1.225	3.600	2.275	-1.025	0.850	0.750	1.425	15.200	-0.275	3.875	3.900	-0.075

BEAM CFT-T03 DIAGONAL STRAINS-SIDE FACE
STRAINS *10**3

MOMENT		61- 73	62- 74	63- 75	64- 76	65- 77	66- 78	71- 83	72- 84	73- 85	74- 86	75- 87	76- 88
0	0	0.000	0.000	0.000	0.000	0.000	0.000	0.000	0.000	0.000	0.000	0.000	0.000
0.0	0.0	0.000	0.000	0.000	0.000	0.000	0.000	0.000	0.000	0.000	0.000	0.000	0.000
17.4	17.4	0.088	0.000	0.038	0.066	0.066	0.066	0.083	0.044	0.083	0.088	-0.044	0.083
33.4	30.7	0.056	0.000	0.044	0.022	0.044	-0.044	0.066	0.066	0.066	0.154	-0.088	0.044
53.3	58.7	0.373	0.197	0.110	0.022	0.000	-0.285	0.066	0.811	0.132	0.000	-0.175	-0.175
77.7	77.5	0.592	0.417	0.307	0.197	0.066	-0.132	-0.022	11.031	0.132	0.022	-0.197	-0.175
93.1	94.6	0.656	0.373	0.263	0.543	0.307	-0.110	-0.031	10.965	0.088	-0.066	-0.197	-0.263
114.3	114.1	1.134	0.677	0.235	0.353	0.504	0.000	-0.154	10.767	0.000	-0.110	-0.241	-0.373
130.5	135.9	1.930	1.379	0.219	1.114	0.744	0.044	-0.223	11.053	-0.044	-0.241	-0.263	-0.526
152.0	150.7	2.500	2.147	0.217	1.711	1.075	0.307	-0.329	10.965	-0.110	-0.329	-0.241	-0.614
172.5	171.5	3.399	2.703	0.417	2.057	1.223	0.417	-0.461	10.997	-0.329	-0.351	-0.263	-0.660
183.4	180.4	4.320	3.610	0.335	2.051	1.360	0.461	-0.543	10.877	-0.197	-0.548	-0.263	-0.766
203.1	205.0	5.010	5.002	1.930	2.654	1.657	0.573	-0.543	10.811	-0.241	-0.626	-0.307	-0.965
214.9	214.9	6.711	5.053	2.917	2.673	1.798	0.439	-0.702	10.439	-0.543	-0.877	-0.526	-1.404
220.3	223.2	7.412	6.533	3.333	2.307	1.842	0.461	-0.702	10.461	-0.570	-0.943	-0.504	-1.325

BEAM CFT-T03 LONGITUDINAL STRAINS-SIDE FACE
STRAINS *10**3

MOMENT		81- 82	83- 84	85- 86	87- 88
0	0	0.000	0.000	0.000	0.000
0.0	0.0	0.000	0.000	0.000	0.000
164.3	163.2	1.800	1.075	0.450	1.500
173.0	170.4	1.900	1.200	0.525	1.475

BEAM CFT-T03 TRANSVERSE STRAINS-SIDE FACE
STRAINS *10**3

MOMENT		81- 83	82- 84	83- 85	84- 86	85- 87	86- 88
0	0	0.000	0.000	0.000	0.000	0.000	0.000
0.0	0.0	0.000	0.000	0.000	0.000	0.000	0.000
164.3	163.2	0.000	0.000	4.275	5.625	0.300	-0.025
173.0	170.4	-0.050	1.050	4.725	5.500	0.100	-0.075

BEAM CFT-T03 DIAGONAL STRAINS-SIDE FACE
STRAINS *10**3

MOMENT		81- 82	83- 84	85- 86	87- 88
0	0	0.000	0.000	0.000	0.000
0.0	0.0	0.000	0.000	0.000	0.000
164.3	164.3	1.900	3.110	4.649	3.923
173.0	171.3	2.237	3.300	5.023	4.123

BEAM CFT-T03 LONGITUDINAL STRAINS-SIDE FACE
STRAINS *10**3

MOMENT		101-121	102-122	103-123	104-124	105-125	106-126	107-127	108-128
0	0	0.000	0.000	0.000	0.000	0.000	0.000	0.000	0.000
0.0	0.0	0.000	0.000	0.000	0.000	0.000	0.000	0.000	0.000
53.3	55.3	0.418	0.425	0.412	0.000	0.012	0.025	-0.167	-0.250
103.1	107.0	0.956	0.600	-0.125	0.375	0.558	-0.087	-0.487	-0.762
177.3	176.4	2.500	1.710	0.333	0.500	0.500	-0.100	-1.275	-1.500
202.3	200.5	3.356	1.400	1.022	0.113	0.512	-0.375	-1.325	-1.863
213.0	209.0	3.750	2.937	-0.050	0.353	0.450	-0.333	-1.425	-2.075
220.3	217.6	4.537	3.400	1.337	0.100	0.333	-0.437	-2.112	-2.175
224.4	222.2	4.775	3.413	1.413	0.333	0.300	-0.525	-1.553	-2.258
229.4	228.3	5.075	3.037	1.500	0.075	0.262	-0.583	-1.612	-2.300

STRAIN	MOMENT	0	5	10	15	20	25	30	35	40	45	50	55	60	65	70	75	80	85	90	95	100
111-121	111-121	111-121	111-121	111-121	111-121	111-121	111-121	111-121	111-121	111-121	111-121	111-121	111-121	111-121	111-121	111-121	111-121	111-121	111-121	111-121	111-121	111-121
111-121	111-121	111-121	111-121	111-121	111-121	111-121	111-121	111-121	111-121	111-121	111-121	111-121	111-121	111-121	111-121	111-121	111-121	111-121	111-121	111-121	111-121	111-121

MOMENT		BEAM CFT-TJ5 DIAGONAL STRAINS-SIDE FACE												
S	S	STRAINS *10**3												
0.0	0.0	0.000	0.000	0.000	0.000	0.000	0.000	0.000	0.000	0.000	0.000	0.000	0.000	0.000
53.3	50.7	0.263	0.197	0.132	0.071	0.044	0.000	0.154	-0.175	0.000	-0.241	-0.175	-0.241	-0.241
114.3	113.5	0.699	0.724	1.360	0.743	0.526	-0.132	0.175	-0.235	-0.008	-0.265	-0.439	-0.392	-0.392
188.4	186.3	3.640	3.640	3.004	2.193	1.404	-0.044	-0.329	-0.491	-0.395	-0.395	-1.162	-1.206	-1.206

MOMENT		BEAM CFT-TJ5 LONGITUDINAL STRAINS-TOP FACE					
S	S	STRAINS *10**3					
		ECT1	ECT2	ECT3	ECT4	ECT5	ECT6
0.0	0.0	0.000		0.000	0.000		0.000
10.4	10.1	-0.075		-0.100	0.012		-0.087
31.4	28.7	-0.163		-0.137	0.009		-0.159
53.3	54.9	-0.325		-0.333	-0.325		-0.325
72.1	72.9	-0.500		-0.525	-0.537		-0.537
89.5	89.5	-0.637		-0.675	-0.659		-0.700
103.1	100.1	-0.737		-0.775	-0.837		-0.712
115.4	120.4	-0.975		-1.062	-1.037		-1.125
143.0	140.0	-1.087		-1.212	-1.225		-1.325
162.3	160.1	-1.350		-1.350	-1.425		-1.600
177.3	177.5	-1.425		-1.537	-1.612		-1.665
193.0	192.5	-1.612		-1.737	-1.812		-2.150
202.3	201.2	-1.750		-1.937	-2.109		-2.512
213.0	209.8	-1.837		-2.175	-2.230		-2.775
220.5	218.0	-2.000		-2.212	-2.337		-2.612
224.4	222.0	-2.015		-2.250	-2.345		-2.567
227.4	227.2	-2.062		-2.275	-2.437		-2.937

MOMENT		BEAM CFT-100 LONGITUDINAL STRAINS-SIDE FACE		STRAINS *10**-3		BEAM CFT-100 LONGITUDINAL STRAINS-SIDE FACE		STRAINS *10**-3	
0.0	0.0	0.000	0.000	11-31	12-32	0.000	0.000	11-31	12-32
21.9	197.5	0.500	0.000	12-32	13-33	0.000	0.000	12-32	13-33
204.7	196.1	0.500	0.000	13-33	14-34	0.000	0.000	13-33	14-34
199.8	187.0	0.500	0.000	14-34	15-35	0.000	0.000	14-34	15-35
177.0	170.1	0.500	0.000	15-35	16-36	0.000	0.000	15-35	16-36
153.9	153.5	0.500	0.000	16-36	17-37	0.000	0.000	16-36	17-37
120.2	117.9	0.500	0.000	17-37	18-38	0.000	0.000	17-37	18-38
50.1	50.0	0.500	0.000	18-38	19-39	0.000	0.000	18-38	19-39
37.1	30.4	0.500	0.000	19-39	20-40	0.000	0.000	19-39	20-40
22.4	20.1	0.500	0.000	20-40	21-41	0.000	0.000	20-40	21-41
0.0	0.0	0.500	0.000	21-41	22-42	0.000	0.000	21-41	22-42
0.0	0.0	0.500	0.000	22-42	23-43	0.000	0.000	22-42	23-43
0.0	0.0	0.500	0.000	23-43	24-44	0.000	0.000	23-43	24-44
0.0	0.0	0.500	0.000	24-44	25-45	0.000	0.000	24-44	25-45
0.0	0.0	0.500	0.000	25-45	26-46	0.000	0.000	25-45	26-46
0.0	0.0	0.500	0.000	26-46	27-47	0.000	0.000	26-46	27-47
0.0	0.0	0.500	0.000	27-47	28-48	0.000	0.000	27-47	28-48
0.0	0.0	0.500	0.000	28-48	29-49	0.000	0.000	28-48	29-49
0.0	0.0	0.500	0.000	29-49	30-50	0.000	0.000	29-49	30-50
0.0	0.0	0.500	0.000	30-50	31-51	0.000	0.000	30-50	31-51
0.0	0.0	0.500	0.000	31-51	32-52	0.000	0.000	31-51	32-52
0.0	0.0	0.500	0.000	32-52	33-53	0.000	0.000	32-52	33-53
0.0	0.0	0.500	0.000	33-53	34-54	0.000	0.000	33-53	34-54
0.0	0.0	0.500	0.000	34-54	35-55	0.000	0.000	34-54	35-55
0.0	0.0	0.500	0.000	35-55	36-56	0.000	0.000	35-55	36-56
0.0	0.0	0.500	0.000	36-56	37-57	0.000	0.000	36-56	37-57
0.0	0.0	0.500	0.000	37-57	38-58	0.000	0.000	37-57	38-58
0.0	0.0	0.500	0.000	38-58	39-59	0.000	0.000	38-58	39-59
0.0	0.0	0.500	0.000	39-59	40-60	0.000	0.000	39-59	40-60
0.0	0.0	0.500	0.000	40-60	41-61	0.000	0.000	40-60	41-61
0.0	0.0	0.500	0.000	41-61	42-62	0.000	0.000	41-61	42-62
0.0	0.0	0.500	0.000	42-62	43-63	0.000	0.000	42-62	43-63
0.0	0.0	0.500	0.000	43-63	44-64	0.000	0.000	43-63	44-64
0.0	0.0	0.500	0.000	44-64	45-65	0.000	0.000	44-64	45-65
0.0	0.0	0.500	0.000	45-65	46-66	0.000	0.000	45-65	46-66
0.0	0.0	0.500	0.000	46-66	47-67	0.000	0.000	46-66	47-67
0.0	0.0	0.500	0.000	47-67	48-68	0.000	0.000	47-67	48-68
0.0	0.0	0.500	0.000	48-68	49-69	0.000	0.000	48-68	49-69
0.0	0.0	0.500	0.000	49-69	50-70	0.000	0.000	49-69	50-70
0.0	0.0	0.500	0.000	50-70	51-71	0.000	0.000	50-70	51-71
0.0	0.0	0.500	0.000	51-71	52-72	0.000	0.000	51-71	52-72
0.0	0.0	0.500	0.000	52-72	53-73	0.000	0.000	52-72	53-73
0.0	0.0	0.500	0.000	53-73	54-74	0.000	0.000	53-73	54-74
0.0	0.0	0.500	0.000	54-74	55-75	0.000	0.000	54-74	55-75
0.0	0.0	0.500	0.000	55-75	56-76	0.000	0.000	55-75	56-76
0.0	0.0	0.500	0.000	56-76	57-77	0.000	0.000	56-76	57-77
0.0	0.0	0.500	0.000	57-77	58-78	0.000	0.000	57-77	58-78
0.0	0.0	0.500	0.000	58-78	59-79	0.000	0.000	58-78	59-79
0.0	0.0	0.500	0.000	59-79	60-80	0.000	0.000	59-79	60-80
0.0	0.0	0.500	0.000	60-80	61-81	0.000	0.000	60-80	61-81
0.0	0.0	0.500	0.000	61-81	62-82	0.000	0.000	61-81	62-82
0.0	0.0	0.500	0.000	62-82	63-83	0.000	0.000	62-82	63-83
0.0	0.0	0.500	0.000	63-83	64-84	0.000	0.000	63-83	64-84
0.0	0.0	0.500	0.000	64-84	65-85	0.000	0.000	64-84	65-85
0.0	0.0	0.500	0.000	65-85	66-86	0.000	0.000	65-85	66-86
0.0	0.0	0.500	0.000	66-86	67-87	0.000	0.000	66-86	67-87
0.0	0.0	0.500	0.000	67-87	68-88	0.000	0.000	67-87	68-88
0.0	0.0	0.500	0.000	68-88	69-89	0.000	0.000	68-88	69-89
0.0	0.0	0.500	0.000	69-89	70-90	0.000	0.000	69-89	70-90
0.0	0.0	0.500	0.000	70-90	71-91	0.000	0.000	70-90	71-91
0.0	0.0	0.500	0.000	71-91	72-92	0.000	0.000	71-91	72-92
0.0	0.0	0.500	0.000	72-92	73-93	0.000	0.000	72-92	73-93
0.0	0.0	0.500	0.000	73-93	74-94	0.000	0.000	73-93	74-94
0.0	0.0	0.500	0.000	74-94	75-95	0.000	0.000	74-94	75-95
0.0	0.0	0.500	0.000	75-95	76-96	0.000	0.000	75-95	76-96
0.0	0.0	0.500	0.000	76-96	77-97	0.000	0.000	76-96	77-97
0.0	0.0	0.500	0.000	77-97	78-98	0.000	0.000	77-97	78-98
0.0	0.0	0.500	0.000	78-98	79-99	0.000	0.000	78-98	79-99
0.0	0.0	0.500	0.000	79-99	80-100	0.000	0.000	79-99	80-100

MOMENT		BEAM CFT-T06 LONGITUDINAL STRAINS-SIDE FACE							
D	S	STRAINS *10 ⁻³							
0.0	0.0	41- 51	42- 52	43- 53	44- 54	45- 55	46- 56	47- 57	48- 58
26.3	24.3	0.000	0.000	0.000	0.000	0.000	0.000	0.000	0.000
43.7	43.3	0.237	0.163	0.050	-0.025	-0.112	-0.137	-0.137	-0.175
66.0	59.5	0.337	0.267	0.163	0.012	-0.087	-0.166	-0.300	-0.275
141.4	138.7	0.487	0.362	0.225	0.075	-0.075	-0.300	-0.425	-0.400
181.0	180.0	1.150	0.637	0.512	0.237	-0.150	-0.688	-1.037	-1.275
208.2	207.3	1.650	1.100	0.700	0.362	-0.225	-1.000	-1.650	-2.000
235.0	221.2	2.013	1.363	0.837	0.300	-0.420	-1.625	-2.283	-2.950
240.8	230.5	2.337	1.663	1.037	0.252	-0.512	-2.038	-3.288	-3.625
249.3	232.3	3.002	2.037	1.137	0.313	-0.625	-2.952	-3.562	-4.013
251.0	227.9	3.712	2.462	1.375	0.412	-0.938	-3.762	-4.162	
		3.962	2.662	1.463	0.433	-0.975	-4.075	-4.725	

MOMENT		BEAM CFT-T06 LONGITUDINAL STRAINS-SIDE FACE							
D	S	STRAINS *10 ⁻³							
0.0	0.0	61- 61	62- 62	63- 63	64- 64	65- 65	66- 66	67- 67	68- 68
21.0	19.6	0.000	0.000	0.000	0.000	0.000	0.000	0.000	0.000
35.0	34.2	0.475	0.375	0.150	0.120	-0.150	-0.150	0.100	-0.150
52.8	47.8	0.600	0.600	0.325	0.100	-0.150	-0.150	0.025	-0.325
113.1	110.9	1.125	0.600	0.475	0.375	-0.075	-0.250	-0.350	-0.475
114.8	143.9	2.050	1.150	0.350	0.325	1.650	0.375	-0.300	-1.725
166.0	165.9	3.725	2.425	1.175	1.300	1.900	-0.050	-1.675	-2.825
188.0	176.0	5.350	4.075	2.350	3.150	2.075	-0.500	-2.200	-4.450
192.6	184.8	7.300	5.375	3.350		2.175	-0.625	-3.300	-5.825
199.4	185.9	9.300	6.225	4.250		2.100	-0.975	-3.850	-6.800
200.8	182.3	10.375	7.000			3.075	-0.750	-5.350	
200.8	172.7	14.225	9.650			5.325	0.450	-7.550	
		15.700	10.575			6.800	3.475	-9.425	

MOMENT		BEAM CFT-T06 LONGITUDINAL STRAINS-SIDE FACE							
D	S	STRAINS *10 ⁻³							
0.0	0.0	61- 71	62- 72	63- 73	64- 74	65- 75	66- 76	67- 77	68- 78
22.4	21.0	0.000	0.000	0.000	0.000	0.000	0.000	0.000	0.000
37.1	36.4	0.250	0.275	0.150	0.353	-0.050	-0.025	0.075	-0.100
56.1	50.4	0.600	0.475	0.325	0.100	-0.075	-0.050	-0.050	-0.175
120.2	117.9	0.825	0.675	0.500	0.175	-0.025	-0.075	-0.100	-0.300
153.7	153.5	1.275	0.650	0.500	0.325	-0.800	0.650	-0.475	-1.050
177.0	175.9	2.000	0.725	1.775	0.950	-1.100	0.575	-0.825	-1.650
199.8	187.0	2.475	2.450	3.500	1.075	-1.325	0.150	-1.650	-2.750
204.7	190.0	4.075	4.100	4.300	2.375	-1.375	-0.100	-2.150	-3.675
211.9	197.5	5.300	5.400	5.750	2.725	-1.375	-0.425	-2.650	-4.475
		6.000	7.100	8.975	3.300	-1.225	-0.550	-3.450	

MOMENT		BEAM CFT-T06 LONGITUDINAL STRAINS-SIDE FACE							
D	S	STRAINS *10 ⁻³							
0.0	0.0	81- 91	82- 92	83- 93	84- 94	85- 95	86- 96	87- 97	88- 98
91.9	90.1	0.000	0.000	0.000	0.000	0.000	0.000	0.000	0.000
117.7	117.4	0.300	0.600	2.525	3.275	-0.125	-0.325	-0.350	-0.475
135.3	134.8	0.275	0.600	7.525	4.075	-0.200	-0.425	-0.425	-0.600
152.8	143.5	0.250	1.800	6.650	4.600	0.350	-0.525	-0.725	-0.875
150.5	149.8	0.200	10.200	9.800		0.775	-0.675	-0.750	-1.050
162.0	151.0	0.200	10.375	10.200		1.225	-0.825	-1.000	-1.125
		0.500	32.175	32.175		1.850	-0.950	-1.075	-1.175

MOMENT		BEAM CFT-T06 TRANSVERSE STRAINS-SIDE FACE												
D	S	STRAINS *10 ⁻³												
0.0	0.0	61- 63	64- 64	63- 65	64- 66	65- 67	66- 68	71- 73	72- 74	73- 75	74- 76	75- 77	76- 78	
22.4	22.4	0.000	0.000	0.000	0.000	0.000	0.000	0.000	0.000	0.000	0.000	0.000	0.000	
37.1	36.4	0.000	0.075	0.050	0.125	0.350	0.150	0.100	0.075	0.225	0.125	0.075	0.200	
56.1	50.4	-0.300	-0.050	0.150	0.250	0.500	0.150	-0.075	0.075	0.250	0.150	0.075	0.200	
120.2	117.9	0.000	0.000	0.150	0.500	1.975	1.775	0.200	0.250	0.000	4.875	4.600	0.150	
153.7	153.5	0.000	-0.000	1.750	2.475	2.325	2.575	1.500	1.675	0.000	6.525	6.550	0.225	
177.0	175.9	-0.100	-0.000	3.575	4.150	2.025	4.225	3.450	1.900	0.175	8.275	8.150	0.475	
199.8	187.0	0.225	-0.000	4.350	5.275	1.750	4.475	5.500	1.350	0.000	9.525	9.025	1.000	
204.7	190.0	0.075	-0.000	6.275	6.575	1.600	4.975	7.625	1.900	1.000	12.975	9.575	2.225	
211.9	197.1	0.200	-0.400	7.800	8.050	1.325		10.700	2.050	1.675	11.825	10.050	6.200	

MOMENT		BEAM CFT-T06 TRANSVERSE STRAINS-SIDE FACE												
D	S	STRAINS *10 ⁻³												
0.0	0.0	81- 83	84- 84	83- 85	84- 86	85- 87	86- 88	91- 93	92- 94	93- 95	94- 96	95- 97	96- 98	
91.9	90.1	-0.050	0.000	0.000	0.000	0.000	0.000	0.000	0.000	0.000	0.000	0.000	0.000	
117.7	117.1	-0.125	0.275	1.775	13.425	0.025	0.125	15.050	-0.200	0.025	0.075	-0.050	0.075	
135.3	128.5	-0.125	0.000	15.875		0.525	0.175	14.670	-0.225	2.325	2.325	-0.150	0.125	
152.8	143.5	-0.200		16.525		0.925	0.250	20.350	-0.400	3.900	3.700	-0.350	0.050	
150.5	149.8	-0.225		16.575		2.075	0.275	24.050	-0.650	5.475	5.475	-0.275	0.075	
162.0	150.4			32.350		3.200	1.075	31.900	-0.425	7.600	7.300	-0.225	0.050	

MOMENT		BEAM CFT-TJ6 DIAGONAL STRAINS-SIDE FACE													
D	S	STRAINS *10**-3													
0.0	0.0	61- 73	62- 74	63- 75	64- 76	65- 77	66- 78	71- 83	72- 84	73- 85	74- 86	75- 87	76- 88		
22.4	20.1	0.000	0.000	0.000	0.000	0.000	0.000	0.000	0.000	0.000	0.000	0.000	0.000	0.000	0.000
37.1	36.4	0.110	0.132	0.088	0.022	0.000	-0.022	-0.044	-0.219	-0.197	-0.154	-0.083	-0.066		
56.1	51.2	0.439	0.417	0.235	0.113	0.022	-0.044	-0.132	-0.132	-0.351	-0.219	-0.197	-0.197		
120.2	117.9	0.746	0.658	0.570	0.307	0.110	-0.022	-0.132	-0.197	-0.329	-0.263	-0.307	-0.461		
153.9	153.1	1.447	1.031	0.329	4.101	2.632	1.776	-0.154	-0.417	-0.592	-0.526	0.241	-0.833		
177.0	177.0	6.535	2.504	4.364	9.825	3.555	2.346	-0.526	-1.360	-0.355	-0.702	0.373	-1.116		
199.0	188.4	10.789	7.346	6.113	11.667	4.037	2.456	-0.273	-2.105	-1.075	-0.877	0.219	-0.877		
199.3	196.3	10.614	11.228	7.917	12.961	3.632	2.697	-0.154	-2.500	-1.272	-1.031	0.066	-1.336		
204.7	197.3	15.504	13.399	10.132	14.890	4.035	3.684	-0.132	-4.057	-1.557	-1.228	-0.263	-1.140		

MOMENT		BEAM CFT-TJ6 DIAGONAL STRAINS-SIDE FACE													
D	S	STRAINS *10**-3													
0.0	0.0	81- 93	82- 94	83- 95	84- 96	85- 97	86- 98	91- 83	92- 84	93- 85	94- 86	95- 87	96- 88		
91.7	90.1	0.000	0.000	0.000	0.000	0.000	0.000	0.000	0.000	0.000	0.000	0.000	0.000	0.000	0.000
117.7	117.4	6.579	8.130	7.325	6.134	0.044	0.000	-0.570	-2.325	-0.417	-0.307	-0.175	-0.504		
135.3	135.1	13.130	12.301	10.377	3.747	0.038	0.022	-0.877	-3.050	-0.614	-0.417	-0.263	-0.656		
152.3	143.9	16.513	15.219	16.009	15.180	0.630	0.154	-1.162	-5.263	-0.724	-0.175	-0.417	-0.333		
150.3	150.1	21.645	17.902	19.946		1.342	0.241	-1.294		-0.768	0.088	-0.504	-0.743		
162.0	151.1	22.544	22.765	23.246		2.346	0.395	-1.362		-0.859	0.373	-0.570	-0.767		
		26.377	26.688	30.307		3.509	0.175			-0.877	0.636	-0.658	-0.768		

MOMENT		BEAM CFT-TJ6 LONGITUDINAL STRAINS-SIDE FACE													
D	S	STRAINS *10**-3													
0.0	0.0	111-131	112-132	113-133	114-134	115-135	116-136	117-137	118-138						
21.0	19.4	0.000	0.000	0.000	0.000	0.000	0.000	0.000	0.000	0.000	0.000	0.000	0.000	0.000	0.000
35.0	34.8	-1.050	0.000	-0.100	0.012	-0.050	0.000	-0.100	-0.067	-0.100	-0.175	-0.067	-0.067	-0.067	-0.067
52.3	48.9	0.525	0.250	-0.100	0.357	0.000	-0.050	-0.112	-0.163	-0.250	-0.163	-0.250	-0.163	-0.250	-0.163
113.1	110.9	0.475	0.375	-0.075	0.050	-0.037	-0.037	-0.163	-0.250	-0.163	-0.250	-0.163	-0.250	-0.163	-0.250
144.3	144.5	1.075	0.775	-0.200	1.312	0.425	-0.212	-0.662	-0.963	-0.662	-0.963	-0.662	-0.963	-0.662	-0.963
160.6	160.6	1.920	1.400	0.225	1.357	0.012	-0.333	-0.887	-1.375	-0.887	-1.375	-0.887	-1.375	-0.887	-1.375
183.0	177.3	3.012	2.502	1.175	2.413	0.975	-0.350	-1.275	-2.057	-1.275	-2.057	-1.275	-2.057	-1.275	-2.057
192.3	184.8	3.500	3.423	1.737	2.637	1.112	-0.525	-1.725	-2.425	-1.725	-2.425	-1.725	-2.425	-1.725	-2.425
199.4	186.2	3.475	3.667	2.087	2.900	0.925	-0.762	-2.263	-2.675	-2.263	-2.675	-2.263	-2.675	-2.263	-2.675
200.3	182.5	3.375	4.000	2.425	3.579	1.337	-0.750	-2.950	-2.950	-2.950	-2.950	-2.950	-2.950	-2.950	-2.950
200.3	172.7	3.530	5.002	2.925	6.000	2.238	-0.525	-4.762	-4.062	-4.762	-4.062	-4.762	-4.062	-4.762	-4.062
		3.587	6.077	3.050	7.500	2.950	0.787	-6.150	-4.600	-6.150	-4.600	-6.150	-4.600	-6.150	-4.600

MOMENT		BEAM CFT-TJ6 LONGITUDINAL STRAINS-SIDE FACE													
D	S	STRAINS *10**-3													
0.0	0.0	101-111	102-112	103-113	104-114	105-115	106-116	107-117	108-118						
91.7	90.1	0.000	0.000	0.000	0.000	0.000	0.000	0.000	0.000	0.000	0.000	0.000	0.000	0.000	0.000
117.7	117.1	1.750	0.000	3.675	-0.450	-0.250	-0.275	-0.375	-0.450	-0.375	-0.450	-0.375	-0.450	-0.375	-0.450
135.3	135.4	1.750	0.000	5.775	-0.550	-0.325	-0.400	-0.525	-0.600	-0.525	-0.600	-0.525	-0.600	-0.525	-0.600
152.3	144.0	2.475	0.125	7.675	-0.750	0.000	-0.425	-0.650	-0.875	-0.650	-0.875	-0.650	-0.875	-0.650	-0.875
150.3	150.1	3.600	0.075	9.250	-0.350	0.500	-0.475	-0.700	-0.925	-0.700	-0.925	-0.700	-0.925	-0.700	-0.925
162.0	151.0	5.150	-0.050	10.650	-1.225	1.025	-0.575	-0.750	-1.000	-0.750	-1.000	-0.750	-1.000	-0.750	-1.000
		7.775	0.000	12.300	-1.100	1.700	-0.650	-0.825	-1.000	-0.825	-1.000	-0.825	-1.000	-0.825	-1.000

MOMENT		BEAM CFT-TJ6 LONGITUDINAL STRAINS-SIDE FACE													
D	S	STRAINS *10**-3													
0.0	0.0	121-131	122-132	123-133	124-134	125-135	126-136	127-137	128-138						
120.2	117.9	0.000	0.000	0.000	0.000	0.000	0.000	0.000	0.000	0.000	0.000	0.000	0.000	0.000	0.000
153.9	153.1	1.225	1.000	-0.050	-0.150	-0.250	-0.125	-0.075	-1.250	-1.250	-1.250	-1.250	-1.250	-1.250	-1.250
177.0	176.0	1.000	3.000	0.875	-0.300	-0.350	-0.325	-1.350	-1.925	-1.350	-1.925	-1.350	-1.925	-1.350	-1.925
199.0	188.4	1.700	4.975	2.675	-0.375	-0.175	-0.275	-1.825	-2.675	-1.825	-2.675	-1.825	-2.675	-1.825	-2.675
199.3	196.3	1.775	6.325	3.500	-3.425	-0.400	-0.450	-2.425	-2.375	-2.425	-2.375	-2.425	-2.375	-2.425	-2.375
204.7	196.3	1.650	6.275	4.600	-0.500	-0.500	-0.800	-3.125	-2.875	-3.125	-2.875	-3.125	-2.875	-3.125	-2.875
211.9	197.3	1.525	6.975	3.775	-0.625	-0.575	-0.875	-4.025	-2.450	-4.025	-2.450	-4.025	-2.450	-4.025	-2.450

MOMENT		BEAM CFT-TJ6 TRANSVERSE STRAINS-SIDE FACE													
D	S	STRAINS *10**-3													
0.0	0.0	101-103	102-104	103-105	104-106	105-107	106-108	111-113	112-114	113-115	114-116	115-117	116-118		
91.7	90.1	0.000	0.000	0.000	0.000	0.000	0.000	0.000	0.000	0.000	0.000	0.000	0.000	0.000	0.000
135.3	135.3	3.375	5.400	-0.375	0.000	-0.025	0.060	0.050	4.775	5.050	-0.400	0.025	0.125		
152.8	143.5	14.400	13.700	1.550	1.300	-0.125	-0.075	0.525	12.350	11.950	-0.425	0.125	0.075		
156.5	149.6	16.150	16.925	3.450	3.725	-0.050	-0.025	2.025	14.350	14.550	0.275	1.075	0.175		
162.0	150.4	21.775	20.450	5.375	5.650	-0.175	-0.050	3.925	16.375	16.400	1.075	2.075	0.250		
		25.175	27.000	7.550	7.975	-0.175	-0.050	8.500	19.850	20.125	2.825	3.675	0.750		

BEAM CFT-TDS TRANSVERSE STRAINS-SIDE FACE
STRAINS *10**3

MOMENT	D	S	121-123	122-124	123-125	124-126	125-127	126-128	127-129	128-130	129-131	130-132	131-133	132-134	133-135	134-136	135-137	136-138
0.0	0.0	0.0	0.000	0.000	0.000	0.000	0.000	0.000	0.000	0.000	0.000	0.000	0.000	0.000	0.000	0.000	0.000	0.000
120.2	117.9	0.050	-0.075	-0.275	2.475	2.700	0.025	0.450	0.500	-0.200	-0.125	0.175	0.700					
199.5	187.6	0.200	0.075	-0.350	7.375	7.375	0.375	1.351	5.050	7.300	-0.725	0.025	5.350					
211.7	196.7	0.400	0.700	-0.300	8.250	8.725	0.925	1.425	6.675	4.700	-0.475	-0.150	6.750					
		11.250	1.400	-0.425	9.575	9.300	2.550	1.500	7.950	5.975	-0.675	-0.450	8.550					

BEAM CFT-TDS DIAGONAL STRAINS-SIDE FACE
STRAINS *10**3

MOMENT	D	S	101-113	102-114	103-115	104-116	105-117	106-118	111-123	112-124	113-125	114-126	115-127	116-128
0.0	0.0	0.0	0.000	0.000	0.000	0.000	0.000	0.000	0.000	0.000	0.000	0.000	0.000	0.000
91.7	90.1	-0.219	0.000	-0.235	-0.255	-0.219	-0.551	0.264	5.653	5.197	-0.576	-0.110	-0.197	
139.3	134.9	-0.307	0.000	-0.748	-0.044	-0.548	-0.548	15.897	13.970	15.531	0.329	1.206		
152.3	143.5	-0.235	3.407	-0.600	1.177	-0.636	-0.636	20.292	15.526	17.570	1.279	1.706	-0.110	
156.3	148.5	-0.235	3.010	-0.811	1.177	-0.636	-0.636	20.833	21.102	2.275	2.205	-0.048		
162.0	150.9	0.124	3.044	-0.877	0.921	-0.655	-0.351	30.067	21.711	-1.908	3.726	-0.000		

BEAM CFT-TDS DIAGONAL STRAINS-SIDE FACE
STRAINS *10**3

MOMENT	D	S	121-123	122-124	123-125	124-126	125-127	126-128	131-123	132-124	133-125	134-126	135-127	136-128
0.0	0.0	0.0	0.000	0.000	0.000	0.000	0.000	0.000	0.000	0.000	0.000	0.000	0.000	0.000
120.2	117.9	-0.263	-0.125	-0.235	-0.375	0.132	-0.614	1.242	1.118	-0.373	1.447	0.853	0.022	
199.5	187.6	-0.395	-1.050	-0.775	-0.724	0.614	0.899	5.299	7.610	4.649	4.101	2.127	0.241	
204.7	195.6	-0.482	-1.009	-0.765	-0.759	0.724	1.903	10.375	9.513	6.096	4.366	1.976	0.154	
211.7	197.1	-0.504	-1.974	-0.905	-0.745	0.700	3.969	13.158	11.667	7.785	5.132	2.105	0.526	

BEAM CFT-TDS LONGITUDINAL STRAINS-SIDE FACE
STRAINS *10**3

MOMENT	D	S	141-151	142-152	143-153	144-154	145-155	146-156	147-157	148-158
0.0	0.0	0.0	0.000	0.000	0.000	0.000	0.000	0.000	0.000	0.000
26.3	23.0	0.257	0.175	0.125	0.065	-0.050	-0.109	-0.137	-0.150	
43.7	43.0	0.177	0.000	0.150	0.100	-0.025	-0.112	-0.163	-0.212	
60.0	60.6	0.037	0.075	0.212	-0.433	-0.100	-0.212	-0.313	-0.375	
141.4	138.7	1.132	0.357	0.400	0.387	-0.257	-0.650	-1.025	-1.250	
181.0	180.6	1.012	0.73	0.73	0.500	-0.525	-1.062	-1.700	-2.112	
203.2	208.2	1.937	1.066	-0.650	-0.775	-0.612	-1.600	-2.612	-3.163	
239.0	221.6	2.390	1.037	0.775	0.602	-0.758	-2.007	-3.425	-4.112	
240.0	229.2	2.812	1.905	0.928	0.713	-0.975	-2.875	-4.612	-6.037	
251.7	232.8	3.325	2.167	1.000	0.662	-1.300	-3.700	-6.537	-9.525	
251.7	227.9	3.302	2.325	0.937	0.538	-1.488	-4.487	-7.575	-11.325	
251.0	215.6	3.500	2.225	0.975	0.600	-1.488	-4.512	-7.612	-11.450	

BEAM CFT-TDS LONGITUDINAL STRAINS-SIDE FACE
STRAINS *10**3

MOMENT	D	S	161-181	162-182	163-183	164-184	165-185	166-186	167-187	168-188
0.0	0.0	0.0	0.000	0.000	0.000	0.000	0.000	0.000	0.000	0.000
21.0	19.4	0.175	-0.030	0.112	-1.200	0.125	0.050	-0.050	0.150	
35.0	34.9	0.350	-0.037	0.13	-0.063	0.125	0.012	-0.075	0.098	
52.3	47.8	0.475	-0.402	0.250	0.112	0.063	-0.025	-0.175	-0.062	
113.1	110.9	1.500	0.506	0.887	-0.025	-0.150	-0.125	-0.537	-0.700	
146.3	144.5	2.388	1.030	1.400	-0.050	-0.21	-0.250	-0.807	-1.137	
163.0	160.4	3.200	1.775	1.863	-0.125	-0.525	-0.525	-1.413	-1.312	
163.0	177.5	4.163	2.475	2.350	-0.100	-0.513	-0.662	-1.700	-2.136	
172.3	184.8	4.462	2.706	2.487	-0.125	-0.375	-0.857	-1.962	-2.325	
197.4	185.9	4.612	1.612	2.475	-0.225	-0.300	-1.050	-2.150	-2.412	
200.0	182.1	4.700	2.002	2.475	-0.262	-0.325	-1.112	-2.225	-2.487	

BEAM CFT-TDS LONGITUDINAL STRAINS-SIDE FACE
STRAINS *10**3

MOMENT	D	S	161-171	162-172	163-173	164-174	165-175	166-176	167-177	168-178
0.0	0.0	0.0	0.000	0.000	0.000	0.000	0.000	0.000	0.000	0.000
120.2	117.5	1.030	2.050	2.025	0.025	-0.250	-0.250	-0.650	-1.025	
153.7	133.1	1.125	4.550	3.125	-0.050	-0.375	-0.400	-1.125	-1.600	

BEAM CFT-TDS LONGITUDINAL STRAINS-SIDE FACE
STRAINS *10**3

MOMENT	D	S	181-191	182-192	183-193	184-194	185-195	186-196	187-197	188-198
0.0	0.0	0.0	0.000	0.000	0.000	0.000	0.000	0.000	0.000	0.000
91.7	90.1	0.050	-0.575	-0.575	1.400	0.625	-0.425	-0.525	-0.925	

BEAM CFT-T06 TRANSVERSE STRAINS-SIDE FACE
STRAINS *10**3

MOMENT		101-102	102-104	103-105	104-106	105-107	106-108	171-173	172-174	173-175	174-176	175-177	176-178
D	S												
0.0	0.0	0.000	0.000	0.000	0.000	0.000	0.000	0.000	0.000	0.000	0.000	0.000	0.000
120.2	117.9	-0.100	1.400	1.475	0.100	0.000	0.275	2.225	-0.300	0.050	0.175	0.525	0.675

BEAM CFT-T06 TRANSVERSE STRAINS-SIDE FACE
STRAINS *10**3

MOMENT		181-183	182-184	183-185	184-186	185-187	186-188	191-193	192-194	193-195	194-196	195-197	196-198
D	S												
0.0	0.0	0.000	0.000	0.000	0.000	0.000	0.000	0.000	0.000	0.000	0.000	0.000	0.000
91.9	90.1	-0.200	-0.075	0.025	1.975	2.375	-0.025	-0.150	4.250	4.450	-0.125	-0.200	0.025

BEAM CFT-T06 DIAGONAL STRAINS-SIDE FACE
STRAINS *10**3

MOMENT		101-173	102-174	103-175	104-165	105-177	106-173	171-163	172-164	173-165	174-166	175-167	176-168
D	S												
0.0	0.0	0.000	0.000	0.000	0.000	0.000	0.000	0.000	0.000	0.000	0.000	0.000	0.000
120.2	117.9	3.158	2.500	2.259	0.110	0.235	0.022	0.241	-0.437	-0.417	-0.526	-0.658	-0.504

BEAM CFT-T06 DIAGONAL STRAINS-SIDE FACE
STRAINS *10**3

MOMENT		181-193	182-194	183-195	184-196	185-197	186-193	191-183	192-184	193-185	194-186	195-187	196-188
D	S												
0.0	0.0	0.000	0.000	0.000	0.000	0.000	0.000	0.000	0.000	0.000	0.000	0.000	0.000
91.9	90.1	-0.132	2.741	2.939	4.342	1.491	-0.265	-0.395	-0.545	-0.656	1.711	-0.570	-0.721

BEAM CFT-T06 LONGITUDINAL STRAINS-TOP FACE
STRAINS *10**3

MOMENT		ECT1	ECT2	ECT3	ECT4	ECT5	ECT6
D	S						
0.0	0.0	0.000	0.000	0.000	0.000	0.000	0.000
21.0	19.1				-0.037	-0.062	-0.012
55.0	54.6				-0.100	-0.163	-0.087
92.0	47.4				-0.130	-0.133	-0.175
115.1	110.7	0.462	-0.725	-0.738	-0.550	-0.525	-0.537
144.3	144.0	0.125	-0.951	-1.112	-0.657	-0.530	-0.500
168.0	168.0	-0.275	-1.505	-1.562	-1.230	-1.525	-1.530
185.0	177.0	-0.462	-1.525	-1.750	-1.550	-1.437	-1.403
192.0	184.4	-0.635	-1.725	-1.962	-1.737	-1.625	-1.562
199.4	185.9	-0.837	-1.737	-1.737	-1.837	-1.737	-1.737
200.8	162.3	-0.637	-1.775	-2.025	-1.700	-1.475	-1.600
200.0	172.7	-0.500	-1.675	-1.950	-1.437	-1.312	-1.637

BEAM CFT-T07 LONGITUDINAL STRAINS-SIDE FACE
STRAINS *10**3

MOMENT	0	5	11- 31	12- 32	13- 33	14- 34	15- 35	16- 36	17- 37	18- 38
0.0	0.0	0.000	0.000	0.000	0.000	0.000	0.000	0.000	0.000	0.000
19.7	18.9	0.150	0.157	0.190	0.057	0.050	-0.012	-0.037	-0.037	-0.037
38.3	38.3	0.225	0.175	0.050	-0.025	-0.050	-0.175	-0.212	-0.237	-0.237
60.3	60.3	0.375	0.237	0.225	0.037	-0.112	-0.262	-0.400	-0.437	-0.437
109.2	109.2	0.925	0.735	0.700	0.412	0.067	-0.387	-0.775	-1.037	-1.037
144.3	144.1	1.465	1.175	0.950	0.691	0.037	-0.501	-1.112	-1.537	-1.537
176.6	176.6	2.250	1.655	1.162	0.637	-0.137	-0.500	-1.625	-2.175	-2.175
201.7	197.0	3.025	2.067	1.413	0.325	-0.325	-1.200	-2.112		
215.1	206.2	3.212	2.275	1.425	0.637	-0.500	-1.463	-2.400		
222.5	206.2	3.450	2.425	1.200	0.337	-0.650	-1.650	-2.625		
222.5	194.7	3.250	2.325	1.337	0.735	-0.332	-1.812	-2.700		
222.6	196.4	3.050	2.125	1.212	0.550	-1.000	-1.887	-2.700		

BEAM CFT-T07 LONGITUDINAL STRAINS-SIDE FACE
STRAINS *10**3

MOMENT	0	5	1- 11	2- 12	3- 13	4- 14	5- 15	6- 16	7- 17	8- 18
0.0	0.0	0.000	0.000	0.000	0.000	0.000	0.000	0.000	0.000	0.000
88.7	88.7	0.375	0.375	1.375	0.600	-0.200	-0.225	-0.475	-0.650	-0.650
147.9	143.5	0.650	0.000	2.075	0.925	-0.600	-0.550	-0.850	-1.100	-1.100
164.1	160.9	0.950	-0.150	2.425	0.375	-0.750	-0.650	-1.000	-1.250	-1.250
174.3	166.7	0.450	-0.275	2.375	0.700	-0.325	-0.750	-1.100	-1.425	-1.425
180.3	166.9	0.500	-0.400	2.150	0.400	-0.675	-0.775	-1.125	-1.400	-1.400
180.3	159.1	0.275	-0.375	1.725	0.025	-0.675	-0.825	-1.175	-1.350	-1.350

BEAM CFT-T07 LONGITUDINAL STRAINS-SIDE FACE
STRAINS *10**3

MOMENT	0	5	21- 31	22- 32	23- 33	24- 34	25- 35	26- 36	27- 37	28- 38
0.0	0.0	0.000	0.000	0.000	0.000	0.000	0.000	0.000	0.000	0.000
20.3	20.3	0.125	0.200	0.075	0.325	0.325	-0.025	-0.100	-0.100	-0.100
41.3	39.6	0.225	0.200	0.050	0.025	-0.025	-0.100	-0.175	-0.200	-0.200
64.1	64.1	0.450	0.000	0.200	0.050	-0.050	-0.225	-0.375	-0.375	-0.375
113.9	113.9	1.000	1.075	1.250	0.375	-0.200	-0.225	-0.775	-0.775	-0.775
153.9	153.9	1.800	1.300	1.750	1.400	-0.325	-0.250	-1.125	-1.525	-1.525
192.2	189.1	1.450	0.375	2.575	1.675	-0.450	-0.600	-1.800	-2.325	-2.325
214.3	210.4	1.025	4.350	3.150	1.975	-2.975	-1.025	-2.550		
223.0	219.4	1.550	4.975	3.550	2.050	-0.575	-1.225	-2.925		
223.0	219.1	1.550	3.400	3.475	2.175	-0.650	-1.550	-3.200		
230.3	207.3	1.050	5.125	3.250	1.925	-0.675	-1.775	-3.300		

BEAM CFT-T07 TRANSVERSE STRAINS-SIDE FACE
STRAINS *10**3

MOMENT	0	5	1- 3	2- 4	3- 5	4- 6	5- 7	6- 8	11- 13	12- 14	13- 15	14- 16	15- 17	16- 18
0.0	0.0	0.000	0.000	0.000	0.000	0.000	0.000	0.000	0.000	0.000	0.000	0.000	0.000	0.000
88.7	88.7	2.500	2.700	-0.175	0.050	0.400	0.425	0.550	0.550	1.475	1.400	0.125	0.175	
164.1	159.7	10.050	10.200	-0.175	1.725	3.030	1.525	0.675	0.675	7.725	7.475	-0.675	0.475	

BEAM CFT-T07 TRANSVERSE STRAINS-SIDE FACE
STRAINS *10**3

MOMENT	0	5	21- 23	24- 24	25- 25	26- 26	27- 27	28- 28	31- 33	32- 34	33- 35	34- 36	35- 37	36- 38
0.0	0.0	0.000	0.000	0.000	0.000	0.000	0.000	0.000	0.000	0.000	0.000	0.000	0.000	0.000
20.3	20.3	0.175	0.100	0.000	-0.200	0.025	-0.175	-0.075	0.200	0.175	0.275	0.050	0.075	-0.050
41.3	40.2	0.150	-0.050	0.025	-0.300	0.050	0.250	0.052	0.175	0.075	0.275	0.025	0.025	0.075
64.1	64.1	0.250	0.100	0.100	0.150	-0.325	0.200	0.150	0.250	0.075	0.975	1.050	-0.150	0.175
113.9	113.9	0.900	0.000	0.050	0.600	0.050	0.300	0.150	0.375	0.375	1.575	1.375	-0.225	0.375
153.9	153.9	1.050	-0.100	-0.025	1.775	1.675	0.275	-0.200	-0.325	-0.325	1.575	1.375	-0.225	0.150
192.2	189.1	3.225	0.000	0.050	2.725	2.750	0.325	-0.025	-0.050	2.325	2.625	2.625	-0.225	0.150
214.3	203.6	4.550	0.000	-0.025	3.450	3.550	0.525	-0.075	0.100	3.125	3.450	-0.300	-0.350	
223.0	219.4	6.200	0.000	0.050	3.975	4.050	0.625	0.075	-0.125	3.675	4.025	-0.325		
230.3	219.1	7.500	-0.025	0.000	4.450	4.450	0.650	-0.175	-0.350	4.500	4.875	-0.375		

BEAM CFT-T07 DIAGONAL STRAINS-SIDE FACE
STRAINS *10**3

MOMENT	0	5	1- 13	2- 14	3- 14	4- 16	5- 17	6- 18	11- 3	12- 4	13- 5	14- 6	15- 7	16- 8
0.0	0.0	0.000	0.000	0.000	0.000	0.000	0.000	0.000	0.000	0.000	0.000	0.000	0.000	0.000
88.7	88.7	-0.439	-0.000	-0.855	-0.614	-0.650	-0.439	3.043	3.043	2.763	1.491	1.228	-0.432	-0.370
164.1	159.8	-0.759	-1.000	-1.338	-0.599	-0.614	-0.395	8.882	7.961	6.272	6.404	0.375	-0.263	

BEAM CFT-TU7 DIAGONAL STRAINS-SIDE FACE
STRAINS *10**3

MOMENT	S	21- 33	22- 34	23- 35	24- 36	25- 37	26- 38	31- 29	32- 24	33- 25	34- 26	35- 27	36- 28
0.0	0.0	0.000	0.000	0.000	0.000	0.000	0.000	0.000	0.000	0.000	0.000	0.000	0.000
20.3	20.3	-0.219	-0.273	-0.235	-0.373	-0.351	-0.197	-0.112	-0.175	-0.197	-0.263	-0.225	-0.107
41.3	41.3	-0.263	-0.417	-0.329	-0.439	-0.351	-0.437	-0.023	-0.066	-0.066	-0.154	-0.219	-0.154
64.1	64.1	-0.197	-0.393	-0.395	-0.543	-0.526	-0.570	0.065	0.051	-0.022	0.070	-0.175	-0.307
110.4	116.2	-0.351	-0.370	-0.570	-0.702	-0.570	-0.744	1.711	1.671	1.162	1.272	-0.197	-0.461
153.7	152.2	-0.526	-0.633	-0.702	-0.897	-0.653	-1.104	3.004	2.476	1.939	2.629	0.066	-0.422
192.2	188.0	-0.620	-1.404	-0.855	-1.031	-0.658	-2.061	4.803	3.662	2.917	4.079	0.241	-0.370
214.3	208.6	-0.724	-1.790	-0.979	-1.075	-0.417	37.083	6.601	4.734	2.904	5.439	0.307	-0.576
228.3	219.1	-0.311	-2.193	-1.096	-1.250	-0.630	37.083	7.061	5.461	4.294	5.658	0.219	-0.653
236.5	219.1	-0.768	-2.719	-1.184	-1.316	-0.570	37.083	7.851	6.206	4.781	6.223	0.154	-0.377

BEAM CFT-TU7 LONGITUDINAL STRAINS-SIDE FACE
STRAINS *10**3

MOMENT	S	41- 51	42- 52	43- 53	44- 54	45- 55	46- 56	47- 57	48- 58
0.0	0.0	0.000	0.000	0.000	0.000	0.000	0.000	0.000	0.000
24.3	25.6	0.135	0.125	0.113	0.050	0.037	-0.012	-0.075	-0.033
43.3	46.6	0.237	0.173	0.125	0.012	-0.100	-0.112	-0.262	-0.375
73.4	75.4	0.525	0.300	0.200	0.033	-0.150	-0.300	-0.512	-0.575
130.4	136.4	1.057	0.602	0.425	0.113	-0.212	-0.575	-1.027	-1.262
181.3	180.1	1.433	1.012	0.575	0.163	-0.275	-0.875	-1.525	-2.030
220.1	221.2	2.125	1.437	0.387	0.262	-0.375	-1.263	-2.337	-3.075
232.4	247.0	2.175	2.300	1.403	0.537	-0.425	-1.525	-3.503	-4.437
260.7	257.7	5.212	3.000	2.475	1.162	-0.262	-1.425	-5.575	-7.775
270.2	257.7	9.537	7.133	4.838	2.737	-0.125	-4.325	-3.925	-14.037
273.2	243.5	14.375	11.323	7.275	4.025	-1.562	-8.050	-13.325	

BEAM CFT-TU7 LONGITUDINAL STRAINS-SIDE FACE
STRAINS *10**3

MOMENT	S	61- 81	62- 82	63- 83	64- 84	65- 85	66- 86	67- 87	68- 88
0.0	0.0	0.000	0.000	0.000	0.000	0.000	0.000	0.000	0.000
19.6	18.9	0.137	0.163	0.113	0.050	0.025	0.025	-0.012	-0.075
38.9	38.9	0.262	0.173	0.037	0.025	-0.050	-0.100	-0.175	-0.136
60.3	60.3	0.637	0.436	0.250	0.113	0.037	-0.163	-0.212	-0.337
109.2	109.2	1.375	1.350	0.912	0.537	0.100	-0.350	-0.675	-0.373
144.3	144.1	2.338	1.907	1.275	0.750	0.038	-0.525	-0.912	-1.325
160.9	176.9	2.975	2.273	1.675	0.912	0.025	-0.733	-1.203	-1.253
201.7	197.3	3.725	2.437	2.125	1.123	-0.050	-0.873	-1.575	-2.238
215.1	206.5	4.330	2.312	2.263	1.150	-0.100	-0.963	-1.603	-2.338
222.3	205.3	4.650	2.123	2.100	1.050	-0.262	-1.037	-1.675	-2.375
222.6	195.1	4.730	1.823	2.325	0.362	-0.375	-1.050	-1.700	-2.312
222.6	196.6	3.350	1.767	1.937	0.762	-0.450	-1.087	-1.587	-2.175

BEAM CFT-TU7 LONGITUDINAL STRAINS-SIDE FACE
STRAINS *10**3

MOMENT	S	61- 71	62- 72	63- 73	64- 74	65- 75	66- 76	67- 77	68- 73
0.0	0.0	0.000	0.000	0.000	0.000	0.000	0.000	0.000	0.000
20.3	20.3	0.230	0.175	0.230	0.130	0.075	0.050	-0.050	-0.050
41.3	41.3	0.325	0.223	0.125	0.075	-0.025	-0.075	-0.200	-0.175
64.1	64.1	0.525	0.300	0.100	0.050	0.050	-0.075	-0.275	-0.230
110.3	115.9	1.000	0.400	0.100	-0.075	0.500	-0.250	-0.700	-0.923
153.7	153.3	1.400	0.325	0.125	-0.075	0.775	-0.350	-0.925	-1.330
192.2	187.4	1.950	0.325	-0.025	-0.175	0.725	-0.600	-1.350	-2.000
214.3	208.6	2.675	0.123	-0.100	-0.225	0.675	-0.650	-1.725	-2.475
220.6	218.9	3.900	0.100	-0.150	-0.250	0.575	-0.925	-1.800	-2.600
230.3	219.1	4.325	0.050	-0.150	-2.803	0.400	-1.075	-1.050	-2.625
236.5	207.3	5.230	0.000	1.100	-0.400	0.125	-1.075	-1.850	-2.525

BEAM CFT-TU7 LONGITUDINAL STRAINS-SIDE FACE
STRAINS *10**3

MOMENT	S	81- 91	82- 92	83- 93	84- 94	85- 95	86- 96	87- 97	88- 93
0.0	0.0	0.000	0.000	0.000	0.000	0.000	0.000	0.000	0.000
83.7	88.7	-0.075	-0.063	-0.100	-0.200	-0.175	-0.125	-0.375	-0.500
147.3	145.3	1.250	0.473	-0.175	-0.353	-0.425	0.075	-0.575	-0.923
164.1	159.7	3.250	1.050	-0.225	-0.450	-0.500	-0.025	-0.700	-1.125
174.3	166.7	3.000	2.450	-0.225	-0.450	-0.525	-0.100	-0.725	-1.175
180.3	156.0	4.125	2.023	-0.175	-0.425	-0.500	-0.123	-0.675	-1.000

MOMENT

BEAM CFT-TU7 TRANSVERSE STRAINS-SIDE FACE

STRAINS *10**3

M	S	61-63	62-64	63-65	64-66	65-67	66-68	71-73	72-74	73-75	74-76	75-77	76-78
0.0	0.0	0.000	0.000	0.000	0.000	0.000	0.000	0.000	0.000	0.000	0.000	0.000	0.000
20.3	20.1	0.125	0.075	0.275	0.250	0.175	0.050	0.125	0.175	0.075	0.175	0.200	0.100
41.3	41.3	0.225	0.050	0.300	0.225	-0.025	0.025	0.075	0.125	-0.025	0.000	0.075	0.050
64.1	64.1	0.025	0.050	0.300	0.050	0.175	0.025	0.025	0.100	0.000	0.025	0.175	0.075
115.9	116.4	0.225	-0.050	0.075	0.125	0.150	-0.150	-0.050	-0.075	1.200	1.250	0.050	0.050
153.9	153.1	0.300	-0.050	0.050	0.425	0.500	0.100	0.050	-0.025	2.475	2.500	0.050	0.050
192.2	187.0	1.175	-0.050	0.025	0.450	0.575	0.150	-0.075	0.025	3.650	3.725	-0.100	0.175
214.3	207.6	2.250	-0.075	-0.025	0.775	0.700	0.200	-0.100	0.050	4.725	4.750	-0.025	0.125
223.0	219.1	3.125	-0.075	0.100	0.750	0.375	0.150	-0.250	0.000	5.300	5.300	-0.125	0.125
230.5	219.1	4.450	-0.450	0.100	1.650	1.025	0.225	-0.150	-0.025	5.850	6.000	-0.050	0.150

MOMENT

BEAM CFT-TU7 TRANSVERSE STRAINS-SIDE FACE

STRAINS *10**3

M	S	81-83	82-84	83-85	84-86	85-87	86-88	91-93	92-94	93-95	94-96	95-97	96-98
0.0	0.0	0.000	0.000	0.000	0.000	0.000	0.000	0.000	0.000	0.000	0.000	0.000	0.000
87.0	87.0	0.000	-0.075	-0.450	0.075	-0.225	0.100	-0.175	0.100	-0.050	-0.125	0.150	-0.025
164.1	160.3	6.975	0.025	0.075	0.100	0.525	0.725	-0.325	0.375	0.000	2.125	2.500	0.125

MOMENT

BEAM CFT-TU7 DIAGONAL STRAINS-SIDE FACE

STRAINS *10**3

M	S	61-73	62-74	63-75	64-76	65-77	66-78	71-83	72-84	73-85	74-86	75-87	76-88
0.0	0.0	0.000	0.000	0.000	0.000	0.000	0.000	0.000	0.000	0.000	0.000	0.000	0.000
20.3	20.0	0.058	0.000	-0.110	-0.030	-0.022	0.066	-0.066	0.000	-0.132	-0.066	-0.044	0.110
41.3	40.0	0.000	-0.197	-0.307	-0.329	-0.219	-0.132	-0.197	-0.154	-0.329	-0.548	-0.273	-0.219
64.1	64.1	0.044	-0.041	-0.241	-0.337	-0.263	-0.285	-0.110	-0.177	-0.329	-0.273	-0.375	-0.351
115.9	116.0	0.397	-0.197	0.937	0.636	0.233	-0.504	0.000	-0.175	-0.417	-0.375	-0.650	-0.600
153.9	153.7	0.397	-0.197	1.950	1.300	0.053	-0.375	-0.152	-0.307	-0.343	-0.375	-1.090	-1.050
192.2	188.4	1.409	-0.020	2.506	1.732	0.702	-0.504	-0.261	-0.432	-0.636	-0.225	-1.400	-1.447
214.3	210.4	2.719	-0.197	3.353	2.201	0.811	-0.439	-0.422	-0.614	-0.760	-0.197	-1.711	-1.722
223.0	219.3	3.991	-0.020	3.634	2.434	0.977	-0.592	-0.525	-0.746	-0.633	-0.020	-1.742	-1.356
230.5	219.1	5.439	-0.020	3.382	2.522	0.833	-0.636	1.932	-0.311	-0.333	0.066	-1.900	-1.906

MOMENT

BEAM CFT-TU7 DIAGONAL STRAINS-SIDE FACE

STRAINS *10**3

M	S	81-93	82-94	83-95	84-96	85-97	86-98	91-93	92-94	93-95	94-96	95-97	96-98
0.0	0.0	0.000	0.000	0.000	0.000	0.000	0.000	0.000	0.000	0.000	0.000	0.000	0.000
87.0	85.7	0.307	-0.197	-0.175	-0.356	-0.197	-0.307	-0.351	-0.351	-0.351	-0.355	-0.307	-0.329
164.1	160.7	0.467	1.447	1.974	1.423	0.833	0.263	-0.724	-0.636	-0.311	-0.729	-0.154	-0.722

MOMENT

BEAM CFT-TU7 LONGITUDINAL STRAINS-SIDE FACE

STRAINS *10**3

M	S	111-131	112-132	113-133	114-134	115-135	116-136	117-137	118-138
0.0	0.0	0.000	0.000	0.000	0.000	0.000	0.000	0.000	0.000
19.0	19.3	0.100	0.010	0.050	0.175	0.038	0.012	-0.075	-1.220
38.7	37.0	0.137	0.037	0.025	-0.037	-0.012	-0.125	-0.212	-1.403
60.3	60.3	0.075	0.010	0.100	0.063	0.025	-0.150	-0.275	-1.650
109.1	109.1	1.752	1.423	1.112	0.675	0.325	-0.267	-0.537	-2.973
144.3	144.0	2.350	2.000	1.612	1.037	0.462	-0.425	-0.750	-2.500
181.7	178.0	2.075	2.075	2.175	1.187	0.175	-0.650	-1.062	-2.034
201.7	198.0	3.075	2.000	2.625	1.300	0.400	-0.750	-1.112	-2.925
219.1	206.0	4.012	1.700	2.712	1.223	0.175	-0.375	-1.403	-2.762
222.0	206.2	5.175	1.900	2.725	1.212	0.025	-1.930	-1.537	-3.717
222.0	195.0	5.263	1.675	2.475	0.737	-0.175	-1.025	-1.600	-3.750

MOMENT

BEAM CFT-TU7 LONGITUDINAL STRAINS-SIDE FACE

STRAINS *10**3

M	S	101-111	102-112	103-113	104-114	105-115	106-116	107-117	108-118
0.0	0.0	0.000	0.000	0.000	0.000	0.000	0.000	0.000	0.000
85.9	85.9	0.000	-0.100	-0.125	0.025	-0.175	-0.075	-1.325	-0.500
117.7	117.1	1.230	0.475	-0.100	0.100	-0.325	0.150	-0.475	-0.650
147.0	143.8	2.750	1.900	-0.200	-0.350	-0.350	0.330	-0.575	-0.325
164.1	160.3	4.025	3.000	-0.200	-0.250	-0.425	0.275	-0.675	-0.975
174.0	167.5	4.325	3.025	-0.325	-0.350	-0.425	0.250	-0.675	-1.050
180.3	158.4	4.430	3.600	-0.250	-0.500	-0.475	0.100	-0.725	-1.025

MOMENT

DEAM CFT-TU7 LONGITUDINAL STRAINS-SIDE FACE

STRAINS *10**3

MOMENT	121-131	122-132	123-133	124-134	125-135	126-136	127-137	128-138
0.0	0.000	0.000	0.000	0.000	0.000	0.000	0.000	0.000
41.3	0.250	0.000	0.175	0.150	0.000	-0.075	-0.17	-0.250
64.1	0.400	0.000	0.000	0.250	0.075	-0.100	-0.275	-0.400
110.4	0.775	0.000	0.000	0.400	0.225	-0.275	-0.550	-1.025
192.2	1.025	1.000	0.325	0.275	1.075	-0.475	-1.125	-2.250
214.5	0.175	0.275	0.275	1.225	1.325	-0.600	-1.500	-2.950
233.5	0.275	0.275	0.175	0.150	1.175	-0.750	-1.600	-3.150

MOMENT

DEAM CFT-TD7 TRANSVERSE STRAINS-SIDE FACE

STRAINS *10**3

MOMENT	101-103	102-104	103-105	104-106	105-107	106-108	111-113	112-114	113-115	114-116	115-117	116-118
0.0	0.000	0.000	0.000	0.000	0.000	0.000	0.000	0.000	0.000	0.000	0.000	0.000
89.7	0.000	0.000	0.025	0.200	0.300	0.050	1.075	-0.275	-0.125	-0.025	-0.125	-0.050
117.7	-0.175	0.575	-0.325	1.225	1.275	0.025	3.000	-0.100	-0.025	-2.000	-0.025	0.075
147.7	-0.125	0.575	0.050	2.275	2.300	0.000	4.975	1.025	-0.075	-0.050	0.350	0.525
164.1	-0.050	0.300	-0.050	2.950	2.350	0.150	8.650	2.700	0.000	0.000	0.000	0.000
174.5	-0.150	0.575	0.100	3.325	3.225	0.075	7.925	3.775	-0.100	-0.025	0.600	1.025

MOMENT

DEAM CFT-TB7 TRANSVERSE STRAINS-SIDE FACE

STRAINS *10**3

MOMENT	121-123	122-124	123-125	124-126	125-127	126-128	131-133	132-134	133-135	134-136	135-137	136-138
0.0	0.000	0.000	0.000	0.000	0.000	0.000	0.000	0.000	0.000	0.000	0.000	0.000
110.4	0.075	0.000	1.775	1.450	-0.125	0.050	0.000	-0.050	-0.475	0.225	0.250	-0.050
214.5	0.275	0.000	2.325	2.925	-0.100	0.075	1.875	0.125	0.150	1.250	1.125	1.000

MOMENT

DEAM CFT-TU7 DIAGONAL STRAINS-SIDE FACE

STRAINS *10**3

MOMENT	101-113	102-114	103-115	104-116	105-117	106-118	111-113	112-114	113-115	114-116	115-117	116-118
0.0	0.000	0.000	0.000	0.000	0.000	0.000	0.000	0.000	0.000	0.000	0.000	0.000
89.7	-0.050	-0.050	-0.050	-0.050	-0.050	-0.050	0.750	-0.075	-2.346	-0.044	-0.219	-0.241
117.7	-0.075	-0.050	-0.050	-0.050	-0.050	-0.050	2.474	-0.110	-2.412	0.000	0.395	-0.175
147.7	-0.075	-0.050	-0.050	-0.050	-0.050	-0.050	4.715	2.918	-2.368	1.045	1.031	0.270
164.1	-0.075	-0.050	-0.050	-0.050	-0.050	-0.050	6.071	3.947	-2.346	1.900	1.250	0.760
174.5	-0.075	-0.050	-0.050	-0.050	-0.050	-0.050	7.390	4.510	-2.434	0.950	1.330	0.311

MOMENT

DEAM CFT-TU7 DIAGONAL STRAINS-SIDE FACE

STRAINS *10**3

MOMENT	121-123	122-124	123-125	124-126	125-127	126-128	131-133	132-134	133-135	134-136	135-137	136-138
0.0	0.000	0.000	0.000	0.000	0.000	0.000	0.000	0.000	0.000	0.000	0.000	0.000
110.4	0.175	-0.100	-0.029	-0.241	-0.050	-0.011	0.000	0.700	1.579	0.927	-0.329	-0.154
214.5	1.067	-0.019	-0.570	0.417	-1.754	-1.447	2.114	0.355	4.934	3.048	1.162	-0.000

MOMENT

DEAM CFT-TU7 LONGITUDINAL STRAINS-SIDE FACE

STRAINS *10**3

MOMENT	141-151	142-152	143-153	144-154	145-155	146-156	147-157	148-158
0.0	0.000	0.000	0.000	0.000	0.000	0.000	0.000	0.000
24.5	0.275	0.100	0.000	0.125	-0.025	0.000	-0.125	-0.150
43.0	0.512	0.000	0.100	0.100	-0.000	-0.075	-0.037	-0.100
73.4	0.925	0.000	0.325	0.225	-0.012	-0.100	-0.075	-0.512
103.4	1.300	1.000	0.700	0.400	0.000	-0.000	-0.775	-1.300
181.7	2.075	1.400	0.975	0.025	0.000	-0.460	-1.137	-1.737
220.1	2.700	2.000	1.350	0.500	-0.012	-0.750	-1.025	-2.725
252.4	3.037	2.312	2.112	1.337	0.144	-0.975	-2.050	-3.037
266.7	3.300	2.600	2.362	1.325	0.000	-1.000	-4.101	-4.475
278.2	3.400	2.600	2.487	1.312	0.015	-1.037	-5.467	-7.000
283.2	3.400	2.600	2.400	1.000	0.000	-1.000	-7.000	

MOMENT

DEAM CFT-TU7 LONGITUDINAL STRAINS-SIDE FACE

STRAINS *10**3

MOMENT	101-103	102-104	103-105	104-106	105-107	106-108	107-109	108-110
0.0	0.000	0.000	0.000	0.000	0.000	0.000	0.000	0.000
17.5	0.212	0.207	0.175	0.113	0.075	0.000	0.012	0.000
30.7	0.438	0.000	0.200	0.050	-0.025	-0.007	-0.101	-0.150
63.5	0.727	0.000	0.237	0.075	0.000	-0.137	-0.212	-0.313
109.1	1.082	1.000	0.300	0.313	0.425	-0.025	-0.937	-0.202
144.5	1.275	1.312	1.007	0.050	0.037	-0.112	-0.650	-1.002
160.9	1.600	2.100	1.525	0.050	0.000	-0.100	-0.812	-1.225
201.9	2.937	2.975	2.050	0.050	0.000	-0.275	-1.075	-1.712
215.1	4.400	3.000	2.238	0.012	0.775	-0.330	-1.212	-1.375
222.0	4.025	3.000	2.475	0.012	0.725	-0.307	-1.202	-1.250
222.0	4.075	3.000	2.300	-0.075	0.525	-0.575	-1.300	-1.737

BEAM CFT-TU7 LONGITUDINAL STRAINS-SIDE FACE
STRAINS *10**3

MOMENT	D	S	161-171	162-172	163-173	164-174	165-175	166-176	167-177	168-178
0.0	0.0	0.0	0.000	0.000	0.000	0.000	0.000	0.000	0.000	0.000
41.5	40.7	0.575	0.400	0.350	0.350	0.000	-0.050	-0.175	-0.100	
64.1	64.1	0.975	0.725	0.575	0.350	0.025	-0.100	-0.275	-0.275	
110.9	110.9	2.500	2.025	1.600	0.625	-0.125	0.150	-0.425	-0.650	
192.2	183.0	5.025	4.575	3.425	0.625	-0.225	0.475	-0.950	-1.325	
214.5	208.0	7.750	6.025	4.425	0.550	-0.225	0.400	-1.375	-1.750	
223.6	217.9	8.000	6.750	4.900	0.525	-0.300	0.350	-1.575	-1.925	
230.5	207.3	9.400	7.550	5.275	0.350	-0.450	0.025	-1.675	-1.850	

BEAM CFT-TU7 LONGITUDINAL STRAINS-SIDE FACE
STRAINS *10**3

MOMENT	D	S	161-191	162-192	163-193	164-194	165-195	166-196	167-197	168-198
0.0	0.0	0.0	0.000	0.000	0.000	0.000	0.000	0.000	0.000	0.000
80.7	88.7	-0.125	2.025	2.225	1.675	-0.075	-0.050	-0.075	-0.475	
117.7	110.9	-0.200	2.000	2.975	2.125	-0.375	-0.175	-0.300	-0.675	
164.1	159.7	-0.175	2.075	3.700	2.650	-0.525	-0.225	-0.400	-0.825	
174.3	160.7	-0.250	2.050	4.525	2.900	-0.675	-0.250	-0.575	-1.000	
180.3	158.2	-0.250	2.100	4.550	3.050	-0.700	-0.300	-0.500	-1.000	

BEAM CFT-TU7 TRANSVERSE STRAINS-SIDE FACE
STRAINS *10**3

MOMENT	D	S	161-163	162-164	163-165	164-166	165-167	166-168	171-173	172-174	173-175	174-176	175-177	176-178
0.0	0.0	0.0	0.000	0.000	0.000	0.000	0.000	0.000	0.000	0.000	0.000	0.000	0.000	
110.9	110.9	0.000	-0.175	0.350	1.025	0.000	0.150	0.000	0.000	0.150	0.200	0.825	0.250	
214.5	208.0	0.000	2.075	3.575	0.675	0.375	2.225	-0.250	-0.125	0.075	5.100	5.125	0.575	

BEAM CFT-TU7 TRANSVERSE STRAINS-SIDE FACE
STRAINS *10**3

MOMENT	D	S	161-183	162-184	163-185	164-186	165-187	166-188	191-193	192-194	193-195	194-196	195-197	196-198
0.0	0.0	0.0	0.000	0.000	0.000	0.000	0.000	0.000	0.000	0.000	0.000	0.000	0.000	
80.7	88.7	0.025	0.150	2.475	2.450	0.000	-0.050	2.950	0.500	-0.100	-0.150	0.325	0.025	
117.7	116.3	0.000	-0.050	5.100	5.050	-0.125	-0.125	5.800	3.350	-0.125	-0.225	1.250	1.675	
147.0	143.6	-0.100	0.125	8.025	7.775	-0.050	0.175	9.375	6.425	0.000	-0.325	2.675	2.400	
164.1	159.7	-0.125	0.200	10.325	10.375	0.075	0.000	12.675	9.425	0.000	-0.075	3.100	2.600	
174.3	167.2	-0.050	0.075	11.575	11.525	0.150	0.025	14.425	10.600	-0.125	0.025	3.375	3.150	

BEAM CFT-TU7 DIAGONAL STRAINS-SIDE FACE
STRAINS *10**3

MOMENT	D	S	161-173	162-174	163-175	164-166	165-177	166-178	171-163	172-164	173-165	174-166	175-167	176-168
0.0	0.0	0.0	0.000	0.000	0.000	0.000	0.000	0.000	0.000	0.000	0.000	0.000	0.000	
110.9	110.9	2.039	1.040	1.901	1.854	0.263	0.022	0.110	-0.768	-0.504	-0.680	-0.702	-0.333	
214.5	209.8	6.364	0.300	5.154	4.791	2.083	1.533	-0.175	-1.134	-0.789	-0.377	-0.373	-1.009	

BEAM CFT-TU7 DIAGONAL STRAINS-SIDE FACE
STRAINS *10**3

MOMENT	D	S	181-193	162-194	183-195	184-196	185-197	186-198	191-183	192-184	193-185	194-186	195-187	196-188
0.0	0.0	0.0	0.000	0.000	0.000	0.000	0.000	0.000	0.000	0.000	0.000	0.000	0.000	
80.7	89.0	3.136	1.009	2.917	4.737	-0.044	-0.063	-0.373	-1.009	-0.702	-0.877	-0.680	-0.634	
117.7	117.1	5.417	5.197	4.731	4.211	0.235	0.044	-0.439	-1.272	-0.768	-0.877	-0.592	-0.285	
147.0	143.5	8.180	7.073	7.478	6.332	0.769	0.526	-0.543	-1.513	-0.987	-0.833	-0.746	0.000	
164.1	160.1	10.014	10.219	9.518	8.130	1.053	0.592	-0.636	-1.952	-1.250	-1.031	-0.526	0.000	
174.3	167.4	11.842	11.404	10.504	9.167	1.162	0.614	-0.653	-2.061	-1.360	-1.272	-0.482	0.263	

BEAM CFT-TU7 LONGITUDINAL STRAINS-TOP FACE
STRAINS *10**3

MOMENT	D	S	ECT1	ECT2	ECT3	ECT4	ECT5	ECT6
0.0	0.0	0.0	0.000	0.000	0.000	0.000	0.000	0.000
19.6	10.9	-0.037	-0.062	0.000	-0.075	0.100	-0.025	
30.9	30.3	-0.225	-0.250	-0.163	-0.250	-0.112	-0.175	
60.3	60.3	-0.450	-0.452	-0.387	-0.412	-0.300	-0.375	
109.2	109.2	-0.963	-0.875	-0.775	-0.775	-0.625	-0.713	
144.0	144.1	-1.337	-1.225	-1.100	-1.150	-0.950	-1.100	
160.9	170.0	-1.667	-1.550	-1.400	-1.433	-1.250	-1.400	
201.9	197.0	-2.000	-1.700	-1.625	-1.750	-1.537	-1.712	
214.1	200.2	-2.100	-1.937	-1.750	-1.812	-1.550	-1.757	
223.6	200.2	-2.167	-1.950	-1.737	-1.825	-1.512	-1.725	
223.6	194.9	-2.100	-1.812	-1.625	-1.637	-1.525	-1.700	

MOMENT		BEAM CFT-T00 LONGITUDINAL STRAINS-SIDE FACE							
D	S	STRAINS *10**3							
0.0	0.0	1- 21	2- 22	3- 23	4- 24	5- 25	6- 26	7- 27	8- 28
14.5	14.5	0.000	0.000	0.000	0.000	0.000	0.000	0.000	0.000
40.4	43.5	0.163	-0.012	0.100	0.050	-0.025	-0.075	0.012	-0.012
77.3	75.8	0.338	0.100	0.190	0.025	-0.062	-0.150	-0.163	-0.200
115.5	112.8	0.612	0.325	0.290	0.125	-0.075	-0.262	-0.412	-0.525
141.9	130.6	1.350	0.430	0.193	0.038	-0.025	-0.350	-0.600	-0.763
160.1	151.7	1.437	0.736	0.063	-0.037	0.025	-0.462	-0.787	-1.062
168.1	150.3	1.837	0.930	0.063	-0.037	0.037	-0.338	-0.725	-1.262
170.4	153.0	1.712	0.675	0.000	-0.112	-0.037	-0.612	-0.950	-1.312
		1.637	0.675	-0.025	-0.125	-0.100	-0.637	-0.975	-1.400

MOMENT		BEAM CFT-T00 LONGITUDINAL STRAINS-SIDE FACE							
D	S	STRAINS *10**3							
0.0	0.0	21- 41	22- 42	23- 43	24- 44	25- 45	26- 46	27- 47	28- 48
17.3	17.3	0.000	0.000	0.000	0.000	0.000	0.000	0.000	0.000
55.2	51.3	0.125	0.150	0.037	0.063	-0.025	0.037	-0.037	-0.150
92.0	90.3	0.430	0.300	0.163	0.088	-0.050	-0.137	-0.200	-0.430
137.7	134.3	0.750	0.713	0.425	0.225	-0.075	-0.237	-0.425	-0.825
168.9	155.5	1.337	0.936	0.738	0.375	-0.150	-0.425	-0.775	-1.262
190.6	160.6	2.200	1.400	0.800	0.350	-0.212	-0.563	-1.000	-1.625
200.1	178.9	2.975	1.667	0.900	0.362	-0.300	-0.668	-1.250	-2.025
202.9	182.8	3.200	2.056	0.762	0.225	-0.400	-0.812	-1.300	-2.112
		3.237	2.075	0.700	0.183	-0.450	-0.850	-1.337	-2.138

MOMENT		BEAM CFT-T00 LONGITUDINAL STRAINS-SIDE FACE							
D	S	STRAINS *10**3							
0.0	0.0	41- 61	42- 62	43- 63	44- 64	45- 65	46- 66	47- 67	48- 68
20.0	20.0	0.000	0.000	0.000	0.000	0.000	0.000	0.000	0.000
64.0	59.5	0.433	0.250	0.375	0.150	-0.050	-0.100	-0.225	-0.250
106.7	104.7	0.950	0.563	0.725	0.300	-0.137	-0.287	-0.550	-0.700
159.7	155.2	1.537	1.230	1.125	0.500	-0.125	-0.525	-1.037	-1.375
195.9	180.4	1.562	1.350	1.762	0.837	-0.037	-0.713	-1.463	-1.912
221.1	209.5	1.637	1.523	2.225	1.025	-0.125	-1.012	-1.762	-2.400
232.1	207.5	2.062	1.150	1.912	0.750	-0.375	-1.238	-2.112	-1.263
235.3	212.1	2.175	1.012	1.825	0.612	-1.737	-1.325	-2.233	-2.612
		3.775	0.963	1.725	0.537	-0.563	-1.337	-2.275	-2.612

MOMENT		BEAM CFT-T00 LONGITUDINAL STRAINS-SIDE FACE							
D	S	STRAINS *10**3							
0.0	0.0	1- 11	2- 12	3- 13	4- 14	5- 15	6- 16	7- 17	8- 18
13.3	13.4	0.000	0.000	0.000	0.000	0.000	0.000	0.000	0.000
44.1	41.0	0.025	0.025	0.025	0.050	0.025	0.050	0.000	0.000
73.6	72.2	-0.125	0.200	0.125	0.025	4.950	-0.100	-0.200	-0.250
110.1	107.9	-0.175	0.650	0.475	0.275	-0.050	-0.225	-0.325	-0.525
135.1	124.9	-0.175	0.725	0.500	0.300	0.000	-0.350	-0.525	-0.375
152.3	144.9	-0.125	0.600	0.325	0.225	0.200	-0.450	-0.625	-1.100
163.1	144.5	-0.025	0.300	0.275	0.150	0.375	-0.500	-0.775	-1.300
162.3	146.3	0.000	0.425	0.250	0.125	0.275	-0.575	-0.325	-1.325
		0.000	0.325	0.150	0.050	0.125	-0.600	-0.850	-1.400

MOMENT		BEAM CFT-T00 LONGITUDINAL STRAINS-SIDE FACE							
D	S	STRAINS *10**3							
0.0	0.0	31- 41	32- 42	33- 43	34- 44	35- 45	36- 46	37- 47	38- 48
13.0	18.0	0.000	0.000	0.000	0.000	0.000	0.000	0.000	0.000
57.4	53.9	0.075	0.075	0.000	-0.050	-0.350	-0.650	-0.075	-0.200
94.3	93.9	0.800	0.200	0.100	0.025	-0.025	-0.175	-0.300	-0.475
143.2	139.1	1.500	0.450	0.275	0.150	-0.075	-0.250	-0.475	-0.750
175.3	161.7	2.675	0.350	0.200	0.125	-0.375	-0.450	-0.375	-1.275
193.2	185.3	4.200	1.000	0.075	0.050	-0.150	-0.650	-1.150	-1.625
203.1	166.1	5.775	2.625	0.025	0.050	-0.250	-0.850	-1.400	-2.025
		6.275	3.075	-0.075	-0.100	-0.375	-0.950	-1.550	-2.150

MOMENT		BEAM CFT-T00 LONGITUDINAL STRAINS-SIDE FACE							
D	S	STRAINS *10**3							
0.0	0.0	51- 61	52- 62	53- 63	54- 64	55- 65	56- 66	57- 67	58- 68
20.7	20.1	0.000	0.000	0.000	0.000	0.000	0.000	0.000	0.000
66.2	62.2	0.125	0.025	0.050	0.050	0.025	-0.075	-0.075	-0.125
110.4	106.4	2.675	0.050	0.600	0.325	-0.050	-0.250	-0.375	-0.475
165.2	161.9	1.025	0.300	1.300	0.650	0.025	-0.350	-0.650	-0.375
202.7	187.3	1.500	0.775	1.350	0.700	0.250	-0.600	-1.200	-1.500
223.7	217.4	2.375	1.000	2.000	0.550	0.225	-1.075	-2.275	-2.675
240.1	215.4	4.950	0.675	1.475	0.300	-0.175	-1.525	-3.550	-2.925
243.5	219.4	6.350	0.550	1.350	0.275	-0.225	-1.450	-2.675	-2.675
243.5	209.4	7.175	0.500	1.225	0.125	-0.425	-1.550	-2.775	-2.900

MOMENT		DEAM CFT-T03 TRANSVERSE STRAINS-SIDE FACE		STRAINS *10***-3	
D	S	31-33	32-34	33-35	34-36
0.0	0.0	0.000	0.000	0.000	0.000
10.0	17.4	0.075	0.000	-0.075	0.000
57.6	55.1	0.225	-0.100	0.125	-0.025
94.5	94.5	0.125	0.000	0.100	0.125

MOMENT		DEAM CFT-T03 TRANSVERSE STRAINS-SIDE FACE		STRAINS *10***-3	
D	S	51-53	52-54	53-55	54-56
0.0	0.0	0.000	0.000	0.000	0.000
60.0	63.0	0.075	0.000	-0.075	0.000
107.0	109.0	0.425	-0.175	0.025	0.025
162.0	161.0	0.275	0.075	0.150	0.000
200.0	187.5	1.050	0.000	-0.075	0.400
243.7	217.4	1.300	0.000	0.150	0.500
243.7	216.7	1.300	0.000	1.875	0.600
243.7	219.4	1.400	1.100	2.000	0.475

MOMENT		DEAM CFT-T03 DIAGONAL STRAINS-SIDE FACE		STRAINS *10***-3	
D	S	1-12	2-14	3-15	4-16
0.0	0.0	0.000	0.000	0.000	0.000
110.1	107.0	-0.132	0.000	-0.132	0.000
135.1	124.4	-0.219	-0.134	-0.154	0.832
122.5	144.4	-0.241	-0.207	-0.508	0.987
160.1	143.1	-0.285	-0.219	-0.636	1.113
162.3	146.3	-0.207	-0.204	-0.702	1.294

MOMENT		DEAM CFT-T03 DIAGONAL STRAINS-SIDE FACE		STRAINS *10***-3	
D	S	31-43	32-44	33-45	34-46
0.0	0.0	0.000	0.000	0.000	0.000
15.0	17.4	0.000	0.000	0.175	0.083
57.6	53.3	0.000	0.110	0.022	0.482
94.5	94.5	0.307	0.132	-0.110	1.007

MOMENT		DEAM CFT-T03 DIAGONAL STRAINS-SIDE FACE		STRAINS *10***-3	
D	S	51-63	52-64	53-65	54-66
0.0	0.0	0.000	0.000	0.000	0.000
60.0	61.5	0.000	0.134	-0.044	-0.175
110.0	109.0	0.285	0.307	-0.329	-0.219
162.0	161.2	0.200	0.104	-0.132	-0.335
200.0	186.6	0.197	0.104	-0.943	-1.031
224.7	214.7	0.088	0.000	-0.307	-1.425
243.7	215.4	-0.041	-0.336	-0.570	-1.001
243.7	219.4	-0.197	-0.200	-0.746	-1.711

MOMENT		BEAM CFT-T00 LONGITUDINAL STRAINS-SIDE FACE								
D	S	STRAINS *10**3								
		71- 81	72- 82	73- 83	74- 84	75- 85	76- 86	77- 87	78- 88	
0.0	0.0	0.000	0.000	0.000	0.000	0.000	0.000	0.000	0.000	0.000
22.3	22.6	0.150	0.100	0.025	0.000	-0.025	-0.050	-0.100	-0.112	
72.3	67.7	0.538	0.407	0.362	0.163	-0.075	-0.250	-0.412	-0.557	
121.4	119.2	0.902	0.912	0.650	-0.900	-0.075	-0.450	-0.762	-1.112	
181.7	176.6	0.933	1.266	0.775	0.375	-0.313	-0.900	-1.537	-2.125	
229.9	205.3	1.037	1.062	1.000	0.462	-0.450	-1.350	-2.263	-3.137	
251.3	238.4	1.500	2.475	1.337	0.775	-0.775	-2.250	-3.787	-5.150	
264.1	236.2	2.112	5.350	4.512	1.725	-1.413	-5.133	-3.075	-10.062	
267.3	240.6	4.937	0.912	6.625	2.375	-2.462	-0.000	-11.357	-15.412	
267.3	230.3	6.975	10.575	3.700	3.033	-3.275	-10.562	-14.450	-20.150	

MOMENT		BEAM CFT-T00 LONGITUDINAL STRAINS-SIDE FACE							
D	S	STRAINS *10**3							
		91-111	92-112	93-113	94-114	95-115	96-116	97-117	98-118
0.0	0.0	0.000	0.000	0.000	0.000	0.000	0.000	0.000	0.000
20.0	20.0	0.000	0.113	0.025	0.012	-0.012	-0.037	-0.137	-0.130
64.0	59.5	0.425	0.267	0.175	0.175	0.012	-0.100	-0.412	-0.462
100.7	105.4	0.625	0.550	0.313	0.313	-0.112	-0.350	-0.663	-0.958
159.7	155.2	1.012	1.162	0.700	0.438	-0.188	-0.650	-1.187	-1.652
195.7	180.4	2.170	1.575	1.000	0.475	-0.275	-0.900	-1.700	-2.550
221.1	208.2	2.962	2.167	1.375	0.552	-0.325	-1.150	-2.200	-2.925
232.1	207.5	3.175	2.512	1.312	-0.725	-0.500	-1.357	-2.750	-3.075
235.3	212.1	2.237	2.525	1.350	0.462	-0.563	-1.413	-2.425	-3.112
235.3	202.4	3.157	2.325	1.288	0.400	-0.563	-1.450	-2.462	-3.067

MOMENT		BEAM CFT-T00 LONGITUDINAL STRAINS-SIDE FACE							
D	S	STRAINS *10**3							
		111-131	112-132	113-133	114-134	115-135	116-136	117-137	118-138
0.0	0.0	0.000	0.000	0.000	0.000	0.000	0.000	0.000	0.000
17.3	17.3	0.000	-0.037	-0.212	-0.100	-0.075	-0.100	-0.137	-0.262
50.2	51.3	0.612	0.313	0.050	-0.062	-0.050	-0.133	-0.225	-0.462
92.0	90.9	1.112	0.600	1.350	-0.062	-0.163	-0.333	-0.525	-0.512
137.7	133.0	1.612	1.000	0.525	0.050	-0.188	-0.450	-0.775	-1.187
163.9	155.5	2.033	1.312	0.662	0.075	-0.262	-0.550	-0.950	-1.337
194.0	179.5	2.533	1.557	0.775	0.113	-0.137	-0.700	-1.057	-1.552
200.1	179.5	2.550	1.400	0.675	0.050	-0.425	-0.725	-1.175	-1.700
202.9	182.6	2.250	1.300	0.625	0.025	-0.425	-0.725	-1.150	-1.757

MOMENT		BEAM CFT-T00 LONGITUDINAL STRAINS-SIDE FACE							
D	S	STRAINS *10**3							
		131-151	132-152	133-153	134-154	135-155	136-156	137-157	138-158
0.0	0.0	0.000	0.000	0.000	0.000	0.000	0.000	0.000	0.000
14.5	14.5	-0.037	-0.012	-0.075	-0.050	-0.062	0.012	-0.100	-0.158
43.4	43.1	0.125	0.050	-0.012	0.000	-0.137	-0.125	-0.275	-0.462
77.5	76.3	0.425	0.267	0.100	-0.025	-0.163	-0.262	-0.475	-0.700
110.5	112.4	0.725	0.350	0.300	0.150	-0.137	-0.400	-0.713	-0.987
141.7	130.6	0.637	0.462	0.200	0.063	-0.100	-0.412	-0.827	-1.137
160.1	150.6	0.637	0.436	0.225	0.100	-0.137	-0.500	-0.933	-1.350
163.1	150.6	0.500	0.362	0.175	0.000	-0.175	-0.550	-0.950	-1.233
170.4	153.6	0.438	0.412	0.150	-0.037	-0.163	-0.537	-0.900	-1.162

MOMENT		BEAM CFT-T00 LONGITUDINAL STRAINS-SIDE FACE							
D	S	STRAINS *10**3							
		91-101	92-102	93-103	94-104	95-105	96-106	97-107	98-108
0.0	0.0	0.000	0.000	0.000	0.000	0.000	0.000	0.000	0.000
20.7	20.1	0.025	0.000	0.000	0.000	0.000	-0.050	-0.150	-0.175
66.2	61.5	0.350	0.350	0.350	0.150	2.450	-0.225	-0.400	-0.525
110.4	109.7	1.775	1.175	0.750	0.275	2.400	-0.425	-0.725	-1.025
165.2	161.2	2.775	2.300	1.575	0.725	-0.150	-0.700	-1.375	-1.875
202.7	186.6	3.550	3.065	2.050	0.925	-0.250	-1.000	-1.925	-2.625
225.7	216.7	4.350	4.575	2.325	1.200	-0.425	-1.400	-2.625	-3.400
240.1	215.4	4.025	4.600	2.925	1.075	-0.550	-1.575	-2.925	-3.600
243.5	219.4	3.925	4.650	2.925	1.025	-0.675	-1.750	-3.050	-3.725
243.5	209.4	2.725	4.775	2.350	0.975	-0.725	-1.825	-3.125	-3.750

MOMENT		BEAM CFT-T00 LONGITUDINAL STRAINS-SIDE FACE							
D	S	STRAINS *10**3							
		111-121	112-122	113-123	114-124	115-125	116-126	117-127	118-128
0.0	0.0	0.000	0.000	0.000	0.000	0.000	0.000	0.000	0.000
57.4	53.5	0.625	0.325	0.275	-0.025	-0.025	-0.250	-0.275	-0.325
95.5	95.1	1.700	1.250	0.725	-0.075	-0.125	-0.400	-0.550	-0.625
175.5	161.7	1.950	2.000	1.725	0.475	-0.300	-0.675	-1.000	-1.200
195.2	185.5	1.925	2.075	2.025	0.550	-0.375	-0.825	-1.175	-1.375
208.1	186.1	1.675	3.125	1.800	0.425	-0.450	-0.650	-1.275	-1.450

BEAM CFT-T00 LONGITUDINAL STRAINS-SIDE FACE
STRAINS *10**3

MOMENT	D	S	121-131	122-132	123-133	124-134	125-135	126-136	127-137	128-138
0-0	0.0	0.000	0.000	0.000	0.000	0.000	0.000	0.000	0.000	0.000
10-3	16.6	0.075	0.025	-0.025	0.000	0.025	-0.075	-0.050	-0.125	0.000
50-3	49.2	0.400	0.400	0.150	0.025	-0.050	-0.175	-0.250	-0.325	0.000
80-3	87.6	0.575	0.425	0.200	0.000	-0.075	-0.300	-0.450	-0.675	0.000
100-2	128.4	1.200	0.200	0.000	-0.100	-0.150	-0.425	-0.675	-1.000	0.000
160-1	149.3	2.075	0.075	-0.075	-0.200	-0.175	-0.550	-0.825	-1.275	0.000
160-3	171.2	2.900	0.075	-0.125	-0.250	-0.200	-0.625	-0.975	-1.475	0.000
192-1	171.6	2.900	-0.025	-0.125	-0.275	-0.250	-0.650	-1.025	-1.450	0.000

BEAM CFT-T00 LONGITUDINAL STRAINS-SIDE FACE
STRAINS *10**3

MOMENT	D	S	141-151	142-152	143-153	144-154	145-155	146-156	147-157	148-158
0-0	0.0	0.000	0.000	0.000	0.000	0.000	0.000	0.000	0.000	0.000
15-3	13.8	0.025	0.025	0.000	-0.025	1.225	-0.025	-0.050	-0.050	0.000
46-1	41.0	0.300	0.125	-0.025	-0.025	1.250	-0.175	-0.175	-0.250	0.000
73-6	73.1	0.625	0.225	0.075	-0.025	1.225	-0.275	-0.325	-0.525	0.000
110-1	107.0	1.275	0.925	0.725	0.400	1.300	-0.350	-0.550	-0.850	0.000
130-1	124.9	1.275	0.925	0.725	0.400	1.300	-0.350	-0.550	-0.850	0.000
152-3	144.0	1.225	0.925	0.775	0.425	1.225	-0.450	-0.675	-0.975	0.000
160-1	143.1	0.950	0.600	0.650	0.325	1.150	-0.475	-0.700	-0.975	0.000
162-3	146.3	0.900	0.325	0.625	0.325	1.125	-0.500	-0.675	-0.975	0.000

BEAM CFT-T03 TRANSVERSE STRAINS-SIDE FACE
STRAINS *10**3

MOMENT	D	S	91-93	92-94	93-95	94-96	95-97	96-98	101-103	102-104	103-105	104-106	105-107	106-108
0-0	0.0	0.000	0.000	0.000	0.000	0.000	0.000	0.000	0.000	0.000	0.000	0.000	0.000	0.000
60-2	61.5	0.100	0.000	0.125	-0.150	-0.050	0.050	0.050	0.050	0.000	0.075	0.150	0.025	0.075
110-4	108.4	0.025	0.125	0.175	-0.075	0.050	0.200	0.450	1.000	-0.125	0.025	0.125	0.050	0.175
160-2	161.2	-0.925	0.225	0.425	0.200	0.050	0.600	0.725	1.650	-0.200	-0.050	0.175	0.125	0.275
202-7	180.0	0.050	0.200	0.600	1.600	-0.025	1.225	2.650	-0.300	-0.025	0.175	0.125	0.125	0.625
220-7	210.7	-0.075	0.175	0.725	0.450	-0.025	1.225	3.650	-0.275	-0.025	0.175	0.125	0.125	0.700
240-1	215.4	-0.075	0.225	1.125	0.350	0.000	1.625	3.900	-0.400	-0.025	0.150	0.125	0.125	0.700
240-3	219.4	-0.225	0.225	1.225	0.875	-0.125	1.650	3.900	-0.400	-0.025	0.150	0.125	0.125	0.700

BEAM CFT-T03 TRANSVERSE STRAINS-SIDE FACE
STRAINS *10**3

MOMENT	D	S	111-113	112-114	113-115	114-116	115-117	116-118	121-123	122-124	123-125	124-126	125-127	126-128
0-0	0.0	0.000	0.000	0.000	0.000	0.000	0.000	0.000	0.000	0.000	0.000	0.000	0.000	0.000
13-0	18.0	0.100	0.075	-0.025	0.050	0.075	0.250	0.025	0.050	0.000	0.000	0.075	0.225	0.200
57-4	53.3	0.050	0.100	0.375	0.025	0.100	0.175	0.000	0.000	-0.025	0.025	0.025	0.250	0.250
90-0	93.9	0.125	0.300	0.225	-0.050	0.150	0.250	0.050	0.000	-0.075	0.050	0.250	0.250	0.275

BEAM CFT-T03 TRANSVERSE STRAINS-SIDE FACE
STRAINS *10**3

LOAD	D	S	131-133	132-134	133-135	134-136	135-137	136-138
0.0	0.0	0.000	0.000	0.000	0.000	0.000	0.000	0.000
15.9	12.9	-0.050	-0.025	-0.050	-0.025	-0.025	0.025	0.025
50.3	47.2	-0.050	-0.125	-0.100	-0.075	-0.075	0.025	0.025
64.0	64.1	0.000	-0.075	-0.150	-0.025	-0.025	0.050	0.050

BEAM CFT-T00 TRANSVERSE STRAINS-SIDE FACE
STRAINS *10**3

MOMENT	D	S	141-143	142-144	143-145	144-146	145-147	146-148	151-153	152-154	153-155	154-156	155-157	156-158
0-0	0.0	0.000	0.000	0.000	0.000	0.000	0.000	0.000	0.000	0.000	0.000	0.000	0.000	0.000
110-1	107.3	0.000	0.000	1.375	0.350	-0.350	0.200	0.250	0.525	0.200	1.150	1.100	0.025	0.175
130-1	124.9	0.075	0.000	2.000	3.750	-0.250	0.250	0.525	0.925	0.200	1.150	1.100	0.025	0.175
152-3	144.3	0.000	0.000	2.250	1.575	-0.225	0.275	0.925	1.225	0.300	1.225	1.250	-0.025	0.175
160-1	143.0	0.000	-0.075	2.550	1.050	-0.275	0.225	1.125	1.225	0.300	1.225	1.250	-0.025	0.175

BEAM CFT-T03 DIAGONAL STRAINS-SIDE FACE
STRAINS *10**3

MOMENT	D	S	91-93	92-94	93-95	94-96	95-97	96-98	101-93	102-94	103-95	104-96	105-97	106-98
0-0	0.0	0.000	0.000	0.000	0.000	0.000	0.000	0.000	0.000	0.000	0.000	0.000	0.000	0.000
60-2	62.4	0.240	0.329	0.000	0.044	-0.044	-0.088	0.263	0.307	0.241	0.044	0.132	0.000	0.000
110-4	108.4	1.110	0.700	0.351	0.110	-0.066	-0.266	0.526	0.219	0.154	-0.197	-0.175	-0.000	-0.000
160-2	161.9	2.000	1.044	1.118	0.570	-0.219	-0.526	0.943	0.255	0.022	-0.329	-0.295	-0.000	-0.000
202-7	186.6	2.799	2.344	1.645	0.899	-0.329	-0.614	1.253	0.219	-0.154	-0.548	-0.765	-0.255	-0.255
220-7	214.7	4.539	3.599	2.105	0.907	-0.504	-0.611	1.623	0.152	-0.195	-0.943	-1.272	-1.000	-1.000
240-1	216.7	5.000	3.947	15.034	1.118	-0.630	-0.943	1.513	-0.175	-0.195	-0.987	-1.316	-0.333	-0.333
240-3	219.4	5.255	4.010	2.336	1.206	-0.658	-0.943	1.469	-0.329	-0.548	-1.075	-1.469	-0.399	-0.399

MOMENT

BEAM CFT-TJ3 TRANSVERSE STRAINS-SIDE FACE

STRAINS *10**3

MOMENT	231-233	232-234	233-235	234-236	235-237	236-238	241-243	242-244	243-245	244-246	245-247	246-248
0	0.000	0.000	0.000	0.000	0.000	0.000	0.000	0.000	0.000	0.000	0.000	0.000
202.7	0.125	2.350	2.825	0.225	-0.300	0.350	-0.050	0.050	0.075	0.350	0.525	0.350
223.7	0.050	3.475	4.050	0.150	-0.325	0.450	-0.025	0.125	0.150	0.625	0.675	0.600

MOMENT

BEAM CFT-TJ3 DIAGONAL STRAINS-SIDE FACE

STRAINS *10**3

MOMENT	231-243	232-244	233-245	234-246	235-247	236-248	241-243	242-244	243-245	244-246	245-247	246-248
0	0.000	0.000	0.000	0.000	0.000	0.000	0.000	0.000	0.000	0.000	0.000	0.000
202.7	0.724	-0.080	-4.254	-0.526	-0.373	-0.907	-0.241	2.522	1.754	1.162	0.373	-0.614
223.7	0.030	-0.175	-0.548	-0.811	-0.653	-1.162	-0.235	3.553	2.478	1.667	0.636	-0.304

MOMENT

BEAM CFT-TJ6 LONGITUDINAL STRAINS-SIDE FACE

STRAINS *10**3

MOMENT	251-261	252-262	253-263	254-264	255-265	256-266	257-267	258-268
0	0.000	0.000	0.000	0.000	0.000	0.000	0.000	0.000
22.3	0.075	0.075	0.025	-0.012	-0.025	-0.050	0.050	-0.150
72.3	0.563	0.500	0.387	0.163	-0.012	-0.012	-0.153	-0.525
121.4	1.167	1.000	0.713	0.333	-0.037	-0.123	-0.437	-0.975
181.7	2.000	1.575	1.212	0.563	-0.050	-0.537	-1.125	-1.750
222.9	2.612	2.013	1.737	0.750	-0.137	-0.933	-1.750	-2.500
251.5	4.312	3.275	3.050	1.512	-0.012	-1.437	-2.762	-3.675
264.1	9.162	6.912	6.883	3.737	0.675	-2.875	-6.487	-8.400
267.3	13.000	10.425	10.213	5.037	1.062	-4.350	-9.775	-13.538

MOMENT

BEAM CFT-TJ6 LONGITUDINAL STRAINS-SIDE FACE

STRAINS *10**3

MOMENT	271-291	272-292	273-293	274-294	275-295	276-296	277-297	278-298
0	0.000	0.000	0.000	0.000	0.000	0.000	0.000	0.000
22.3	0.275	0.113	0.037	0.025	-0.012	-0.075	-0.037	-0.050
72.3	0.700	0.375	0.188	0.125	-0.012	-0.138	-0.313	-0.357
102.7	1.337	0.600	0.412	0.212	-0.025	-0.333	-0.575	-0.707
152.7	2.075	1.063	0.850	0.367	-0.050	-0.537	-1.050	-1.425
192.7	2.575	2.037	1.325	0.612	-0.050	-0.750	-1.463	-2.038
221.1	3.150	3.075	1.750	0.837	-0.025	-0.975	-1.700	-2.712
232.1	3.707	4.700	1.700	0.700	-0.175	-1.100	-2.025	-2.775
233.3	4.462	5.200	1.562	0.612	-0.350	-1.212	-2.150	-2.850

MOMENT

BEAM CFT-TJ6 LONGITUDINAL STRAINS-SIDE FACE

STRAINS *10**3

MOMENT	291-301	292-302	293-303	294-304	295-305	296-306	0-307	295-308
0	0.000	0.000	0.000	0.000	0.000	0.000	0.000	0.000
17.3	0.075	0.037	0.025	0.000	0.050	-0.062	-0.012	-0.037
53.2	0.400	0.062	0.113	0.063	-0.025	-0.150	-0.237	-0.375
92.0	0.825	0.075	0.387	0.212	-0.012	-0.250	-0.450	-0.723
137.7	1.475	1.150	0.713	0.337	0.050	-0.400	-0.675	-1.125
166.7	1.887	1.425	0.738	0.337	-0.037	-0.475	-0.567	-1.400
190.0	2.550	1.425	0.850	0.400	-0.112	-0.588	-1.087	-1.762
200.1	2.950	1.375	0.812	0.350	-0.150	-0.625	-1.137	-1.825
202.9	2.975	1.325	0.713	0.287	-0.212	-0.663	-1.162	-1.825

MOMENT

BEAM CFT-TJ6 LONGITUDINAL STRAINS-SIDE FACE

STRAINS *10**3

MOMENT	301-311	302-312	303-313	304-314	305-315	306-316	307-317	308-318
0	0.000	0.000	0.000	0.000	0.000	0.000	0.000	0.000
14.2	0.113	0.000	0.137	0.113	0.050	0.000	-0.037	0.012
43.4	0.275	0.025	0.212	0.113	-0.075	-0.175	-0.225	-0.225
77.2	0.600	0.063	0.375	0.163	-0.025	-0.200	-0.324	-0.512
112.0	1.150	0.025	0.275	0.083	-0.012	-0.350	-0.625	-0.787
141.7	1.375	0.250	0.200	-0.037	0.137	-0.362	-0.733	-1.037
163.1	1.575	0.200	0.163	-0.050	0.125	-0.450	-0.362	-1.167
166.1	1.502	0.100	0.100	0.000	0.100	-0.467	-0.357	-1.238
173.4	1.463	0.137	0.100	-0.025	0.012	-0.537	-0.963	-1.268

MOMENT

BEAM CFT-TJ6 LONGITUDINAL STRAINS-SIDE FACE

STRAINS *10**3

MOMENT	271-281	272-282	273-283	274-284	275-285	276-286	277-287	278-288
0	0.000	0.000	0.000	0.000	0.000	0.000	0.000	0.000
20.7	0.125	0.050	-0.025	-0.125	-0.075	-0.125	-0.150	-0.175
66.2	0.925	0.475	0.300	0.125	-0.050	-0.325	-0.450	-0.550
110.4	1.975	1.350	0.600	0.400	-0.050	-0.425	-0.725	-0.975
163.2	3.250	2.150	0.675	0.800	0.425	-0.700	-1.275	-1.750
202.7	4.025	2.550	0.600	1.350	0.025	-0.925	-1.775	-2.450
223.7	4.925	3.175	0.600	1.725	0.000	-1.200	-2.300	-3.200
240.1	6.275	3.550	0.425	1.500	-0.225	-1.350	-2.500	-3.550
243.3	6.050	0.150	0.375	1.400	-0.375	-1.450	-2.550	-3.775
243.5	6.025	0.000	0.400	1.250	-0.425	-1.450	-2.575	-3.550

MOMENT

D	S
0-0	0-0
10-6	16.1
53-0	49.0
63-3	60.7

BEAM CFT-T08 DIAGONAL STRAINS-SIDE FACE

STRAINS *10**-3

	121-133	122-134	123-135	124-136	125-137	126-138	131-123	132-124	133-125	134-126	135-127	136-128
0-0	0.000	0.000	0.000	0.000	0.000	0.000	0.000	0.000	0.000	0.000	0.000	0.000
10-6	0.197	0.197	0.197	0.197	0.154	0.044	0.175	0.263	0.197	0.154	0.154	0.154
53-0	0.307	0.219	0.154	0.022	0.044	-0.152	0.327	0.417	0.197	0.000	0.110	0.062
63-3	0.351	0.175	0.038	0.022	-0.044	-0.329	0.351	0.329	0.088	0.022	0.044	-0.066

MOMENT

D	S
0-0	0-0
110-1	107.9
135-1	124.9
152-5	144.9

BEAM CFT-T08 DIAGONAL STRAINS-SIDE FACE

STRAINS *10**-3

	141-153	142-154	143-155	144-156	145-157	146-158	151-143	152-144	153-145	154-146	155-147	156-148
0-0	0.000	0.000	0.000	0.000	0.000	0.000	0.000	0.000	0.000	0.000	0.000	0.000
110-1	1.294	1.110	1.075	0.724	-0.482	-0.083	0.375	0.219	-0.110	0.263	-0.504	-0.417
135-1	1.272	1.400	1.864	1.404	-0.395	0.222	0.207	-0.066	-0.175	0.197	-0.768	-0.724
152-5	1.667	1.007	2.261	1.754	-0.329	-0.066	0.197	-0.285	-0.175	0.110	-0.855	-0.658

MOMENT

D	S
0-0	0-0
14-5	14.0
40-4	44.3
77-3	70.3
113-6	113.0
141-9	131.1
160-1	152.0
163-1	151.7
173-4	153.0

BEAM CFT-T08 LONGITUDINAL STRAINS-SIDE FACE

STRAINS *10**-3

	201-211	202-212	203-213	204-214	205-215	206-216	207-217	208-218
0-0	0.000	0.000	0.000	0.000	0.000	0.000	0.000	0.000
14-5	-0.125	0.000	-0.112	-0.037	-0.150	-0.163	-0.150	-0.133
40-4	0.113	0.100	0.100	0.012	-0.150	-0.262	-0.313	-0.438
77-3	0.430	0.300	0.262	0.175	-0.150	-0.537	-0.453	-0.637
113-6	0.475	0.675	0.400	0.452	-0.062	-0.425	-0.683	-0.900
141-9	0.713	-0.007	0.325	0.612	-0.137	-0.563	-0.812	-1.137
160-1	1.150	-0.137	0.237	0.692	-0.125	-0.662	-0.967	-1.325
163-1	1.430	-0.100	0.227	0.537	-0.133	-0.650	-0.900	-1.325
173-4	1.312	-0.100	0.212	0.475	-0.313	-0.725	-1.025	-1.363

MOMENT

D	S
0-0	0-0
17-3	10.7
53-2	53.3
92-0	91.0
137-7	135.4
163-9	150.1
190-6	161.7
203-1	160.0
202-9	162.0

BEAM CFT-T08 LONGITUDINAL STRAINS-SIDE FACE

STRAINS *10**-3

	211-221	212-222	213-223	214-224	215-225	216-226	217-227	218-228
0-0	0.000	0.000	0.000	0.000	0.000	0.000	0.000	0.000
17-3	0.025	-0.007	-0.037	-0.062	-0.067	-0.163	-0.112	-0.200
53-2	0.400	0.175	0.100	-0.037	-0.112	-0.300	-0.325	-0.450
92-0	0.337	0.310	0.350	0.100	-0.100	-0.412	-0.437	-0.738
137-7	1.400	1.075	0.725	0.300	-0.075	-0.450	-0.713	-1.100
163-9	1.425	1.000	0.912	0.350	-0.163	-0.650	-0.925	-1.437
190-6	1.475	1.007	1.062	1.637	-0.225	-0.725	-1.137	-0.400
203-1	1.375	1.000	1.000	0.313	-0.300	-0.787	-1.137	-1.725
202-9	1.325	1.407	0.862	0.250	-0.375	-0.875	-1.233	-1.750

MOMENT

D	S
0-0	0-0
20-0	19.4
60-3	61.4
100-7	105.4
157-7	150.3
195-9	161.0
221-1	210.6
232-1	209.5
233-5	212.1

BEAM CFT-T08 LONGITUDINAL STRAINS-SIDE FACE

STRAINS *10**-3

	221-241	222-242	223-243	224-244	225-245	226-246	227-247	228-248
0-0	0.000	0.000	0.000	0.000	0.000	0.000	0.000	0.000
20-0	0.000	0.007	-0.022	-0.050	-0.037	-0.125	-0.112	-0.188
60-3	0.175	0.300	0.100	0.037	-0.075	-0.237	-0.375	-0.462
100-7	0.462	0.700	0.37	0.150	-0.075	-0.333	-0.600	-0.875
157-7	1.200	4.000	0.93	0.462	0.037	-0.462	-0.963	-1.475
195-9	1.762	2.000	1.250	0.575	0.037	-0.650	-1.325	-1.967
221-1	2.462	2.700	1.637	0.862	0.075	-0.825	-1.687	-2.500
232-1	2.037	2.075	1.775	0.787	-0.100	-0.967	-1.850	-2.662
233-5	2.550	2.000	1.712	0.675	-0.225	-1.112	-1.950	-2.750

MOMENT

D	S
0-0	0-0
20-7	20.7
60-2	62.2
110-4	108.4
163-2	160.5
202-7	166.6
223-7	214.7
240-1	214.7
243-5	217.4
243-5	207.4

BEAM CFT-T08 LONGITUDINAL STRAINS-SIDE FACE

STRAINS *10**-3

	231-241	232-242	233-243	234-244	235-245	236-246	237-247	238-248
0-0	0.000	0.000	0.000	0.000	0.000	0.000	0.000	0.000
20-7	0.125	0.125	0.000	0.000	0.150	-0.100	-0.100	-0.075
60-2	0.075	0.075	0.100	0.000	0.150	-0.225	-0.325	-0.425
110-4	0.575	0.075	0.125	-0.075	0.225	-0.325	-0.650	-0.425
163-2	0.975	0.750	0.325	0.900	0.550	-0.500	-1.100	-1.625
202-7	1.175	0.750	-0.025	1.325	0.625	-0.675	-1.400	-2.125
223-7	1.000	0.700	-0.175	1.775	0.725	-0.875	-1.800	-2.725
240-1	1.600	0.425	-0.250	1.700	0.375	-1.075	-2.025	-2.900
243-5	0.550	0.450	-0.225	1.575	0.275	-1.175	-2.075	-2.925
243-5	0.500	0.075	-0.275	1.475	0.200	-1.175	-2.050	-2.900

MOMENT

D	S
0-0	0-0
141-7	130.0
163-1	151.2

BEAM CFT-T08 TRANSVERSE STRAINS-SIDE FACE

STRAINS *10**-3

	201-203	202-204	203-205	204-206	205-207	206-208	211-211	212-214	213-215	214-216	215-217	216-218
0-0	0.000	0.000	0.000	0.000	0.000	0.000	0.000	0.000	0.000	0.000	0.000	0.000
141-7	1.700	2.075	1.025	-0.075	0.175	0.125	1.725	0.650	-0.100	0.350	0.275	0.300
163-1	2.200	2.700	1.175	-0.250	0.150	0.125	1.250	0.625	0.050	0.500	0.400	0.350

MOMENT		UCAM CFT-T08 TRANSVERSE STRAINS-SIDE FACE											
D	S	STRAINS *10**3											
U-J	U-U	271-273	272-274	273-275	274-276	275-277	276-278	281-283	282-284	283-285	284-286	285-287	286-288
163-2	160.5	0.000	0.000	0.000	0.000	0.000	0.000	0.000	0.000	0.000	0.000	0.000	0.000
202-7	186.6	0.430	0.425	-0.025	-0.025	0.000	0.150	0.000	0.500	0.175	-0.125	0.075	0.175
223-7	215.4	0.650	0.650	-0.100	-0.100	0.075	0.350	0.000	1.150	0.900	-0.250	0.000	0.125
		0.925	1.000	-0.050	0.125	0.225	0.750	0.000	1.350	1.675	-0.250	-0.050	0.525

MOMENT		BEAM CFT-T03 TRANSVERSE STRAINS-SIDE FACE											
D	S	STRAINS *10**3											
U-J	U-U	301-303	302-304	303-305	304-306	305-307	306-308	311-313	312-314	313-315	314-316	315-317	316-318
141-7	130.6	0.000	0.000	0.000	0.000	0.000	0.000	0.000	0.000	0.000	0.000	0.000	0.000
160-1	150.6	4.650	-0.150	-0.075	0.075	0.000	0.150	-0.125	0.050	2.025	2.100	0.000	0.100
		4.650	-0.200	-0.025	0.125	0.125	0.350	-0.025	0.050	2.950	3.025	0.050	0.125

MOMENT		BEAM CFT-T03 DIAGONAL STRAINS-SIDE FACE											
D	S	STRAINS *10**3											
U-J	U-U	271-283	272-284	273-285	274-286	275-287	276-288	281-293	282-294	283-295	284-296	285-297	286-298
163-2	161.2	0.000	0.000	0.000	0.000	0.000	0.000	0.000	0.000	0.000	0.000	0.000	0.000
202-7	186.6	2.610	2.237	0.638	0.217	-0.235	-0.437	0.785	-0.132	-0.307	-0.529	-0.763	-1.164
228-7	215.4	5.158	3.596	1.316	0.739	-0.197	-0.461	0.431	-0.083	-0.461	-0.548	-0.965	-1.467
		3.070	4.690	1.732	0.921	-0.263	-0.570	0.526	-0.154	-0.351	-0.482	-1.140	-1.557

MOMENT		BEAM CFT-T03 LONGITUDINAL STRAINS-TOP FACE						
D	S	STRAINS *10**3						
U	S	ECT1	ECT2	ECT3	ECT10	ECT11	ECT12	
0.0	0.0	0.000	0.000	0.000	0.000	0.000	0.000	
14.5	14.5	-0.012	-0.112	-0.075	0.000	-0.112	0.025	
46.4	43.5	-0.362	-0.237	-0.375	-0.338	-0.325	-0.150	
77.3	75.6	-0.700	-0.612	-0.638	-0.612	-0.725	-0.650	
115.6	112.6	-1.100	-0.775	-1.112	-0.963	-1.075	-1.012	
141.9	130.6	-1.350	-1.300	-1.363	-1.137	-1.325	-1.175	
160.1	151.7	-1.562	-1.450	-1.537	-1.262	-1.437	-1.337	
166.1	150.5	-1.637	-1.525	-1.587	-1.010	-1.453	-1.350	
170.4	155.6	-1.637	-1.525	-1.537	-1.000	-1.465	-1.350	

MOMENT		BEAM CFT-T03 LONGITUDINAL STRAINS-TOP FACE						
D	S	STRAINS *10**3						
U	S	ECT4	ECT5	ECT6	ECT7	ECT8	ECT9	
0.0	0.0	0.000	0.000	0.000	0.000	0.000	0.000	
17.3	17.5	-0.125	-0.173	-0.037	-0.075	-0.057	-0.157	
55.2	51.5	-0.450	-0.525	-0.497	-0.350	-0.352	-0.412	
92.0	96.5	-0.900	-0.950	-0.775	-0.738	-0.715	-0.762	
137.7	134.3	-1.450	-1.337	-1.350	-1.150	-1.212	-1.250	
163.9	155.5	-1.837	-1.637	-1.712	-1.300	-1.400	-1.463	
190.6	180.6	-2.293	-2.007	-2.125	-1.675	-1.725	-1.775	
200.1	178.9	-2.333	-2.032	-2.125	-1.375	-1.600	-1.699	
200.9	182.8	-2.425	-2.100	-2.187	-1.775	-1.625	-1.925	
202.9	174.5	-2.500	-2.125	-2.212	-1.863	-1.600	-1.875	

C.5 Further Plots from Measured Strains

Further plots similar to those in Chapter 5 are presented in Figures C.3 - C.8.

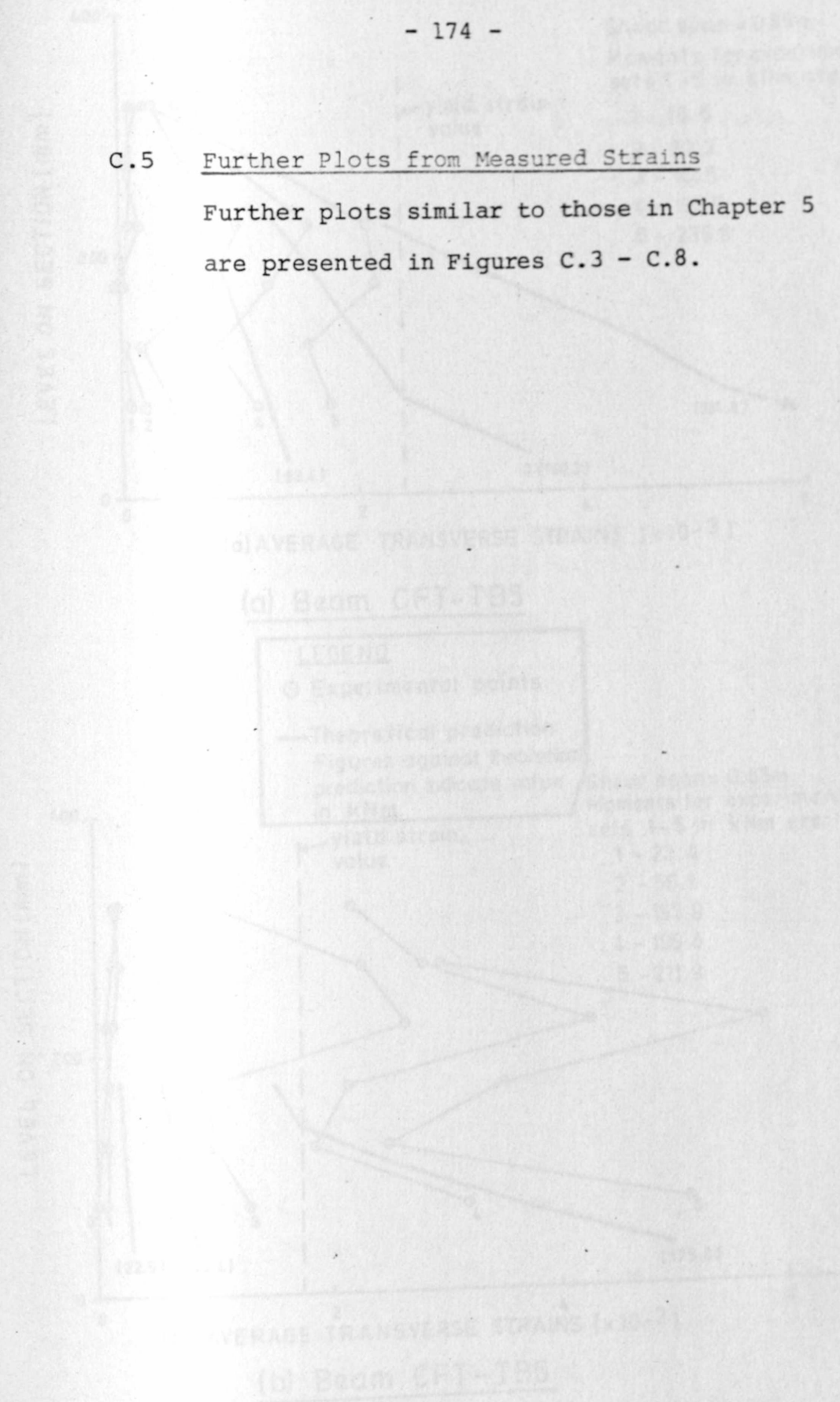
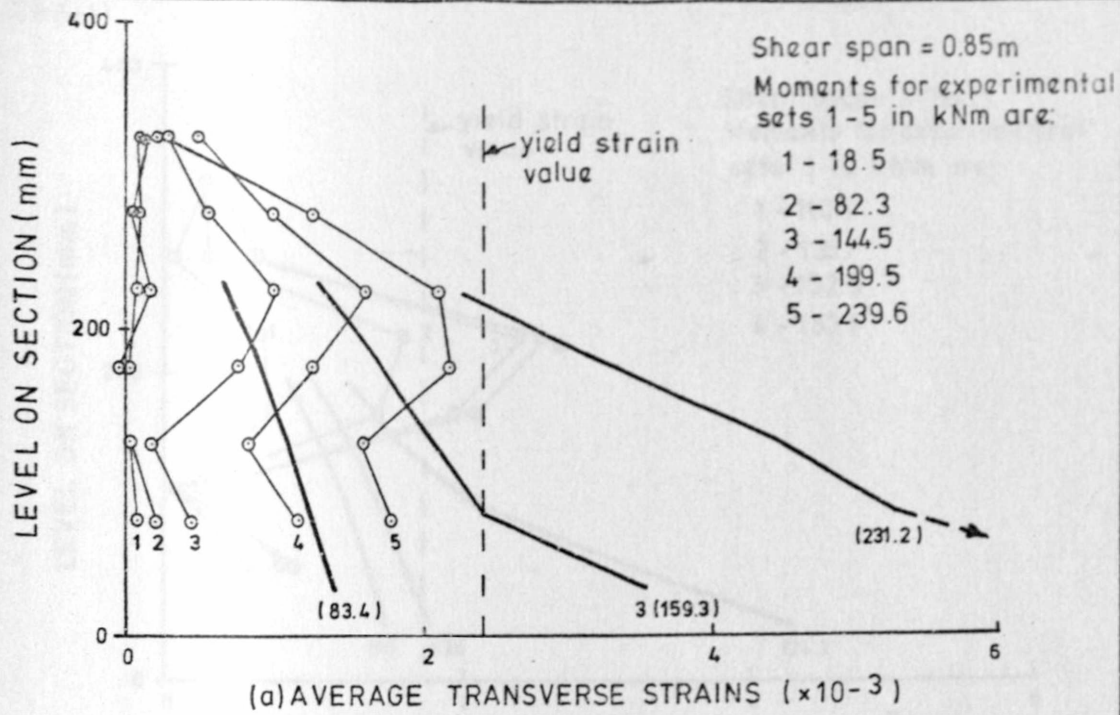
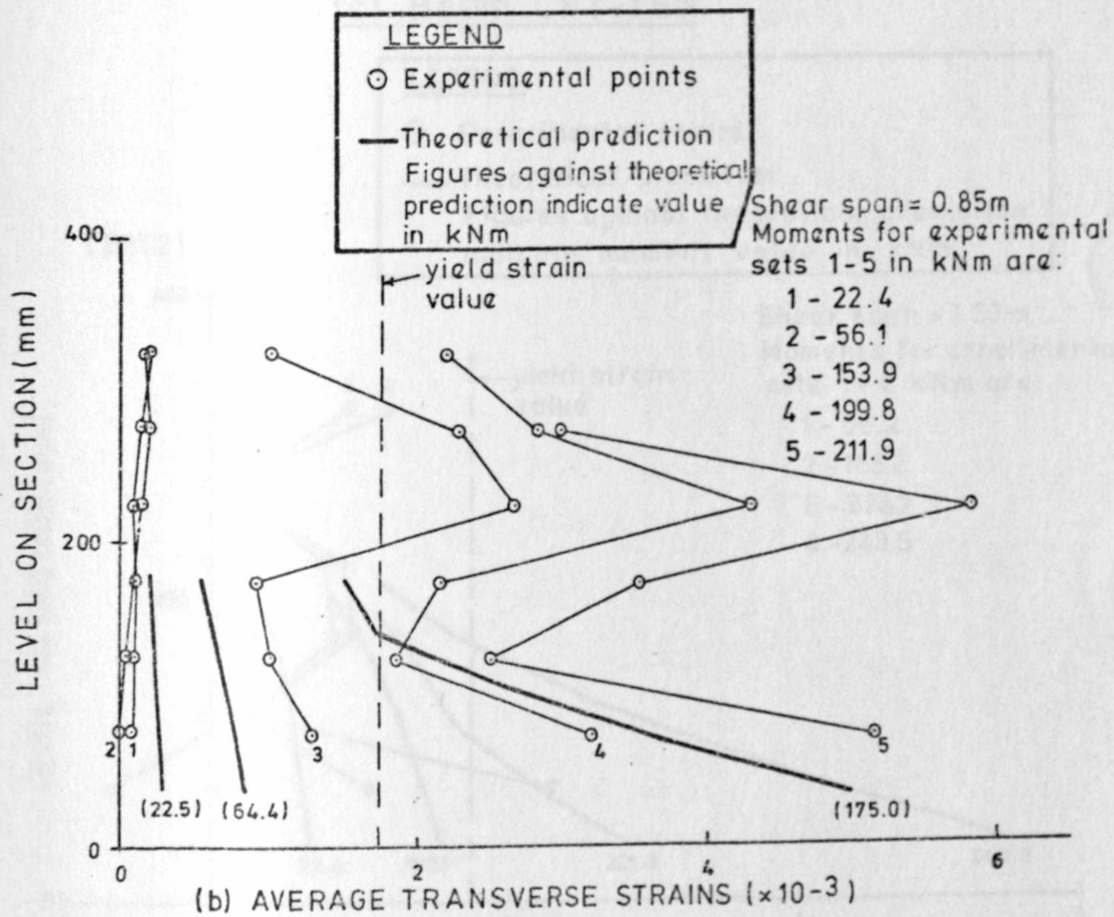


Fig. C.5: Transverse strain profiles



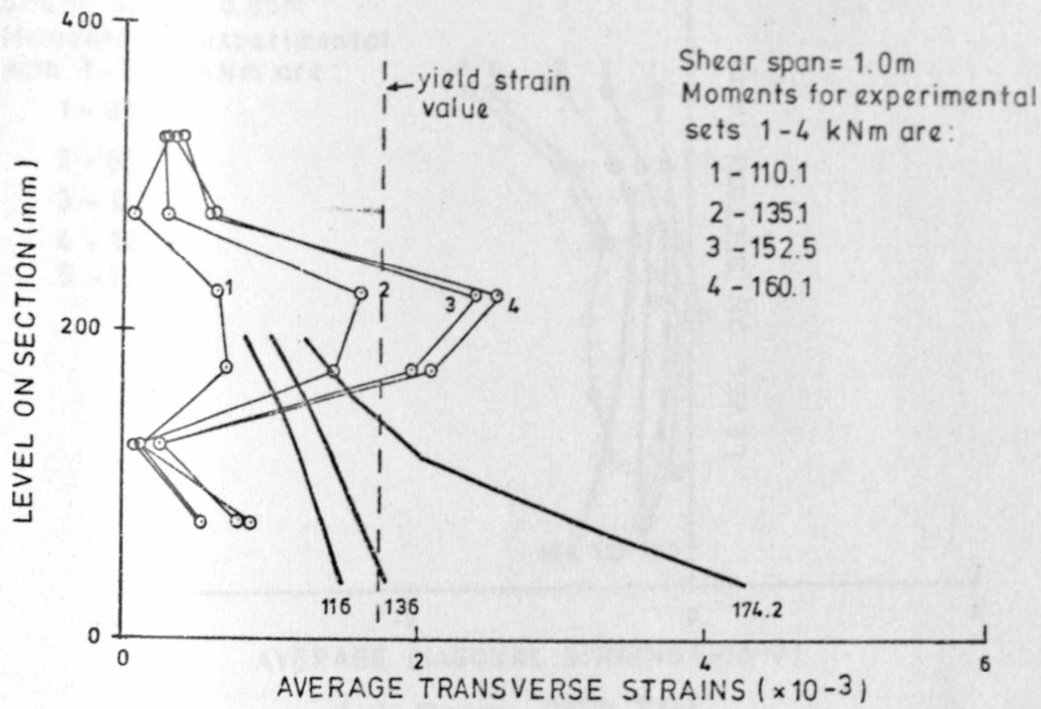
(a) Beam CFT-TB5



(b) Beam CFT-TB6

Fig. C.3 : Transverse strains profiles

TB8(1)

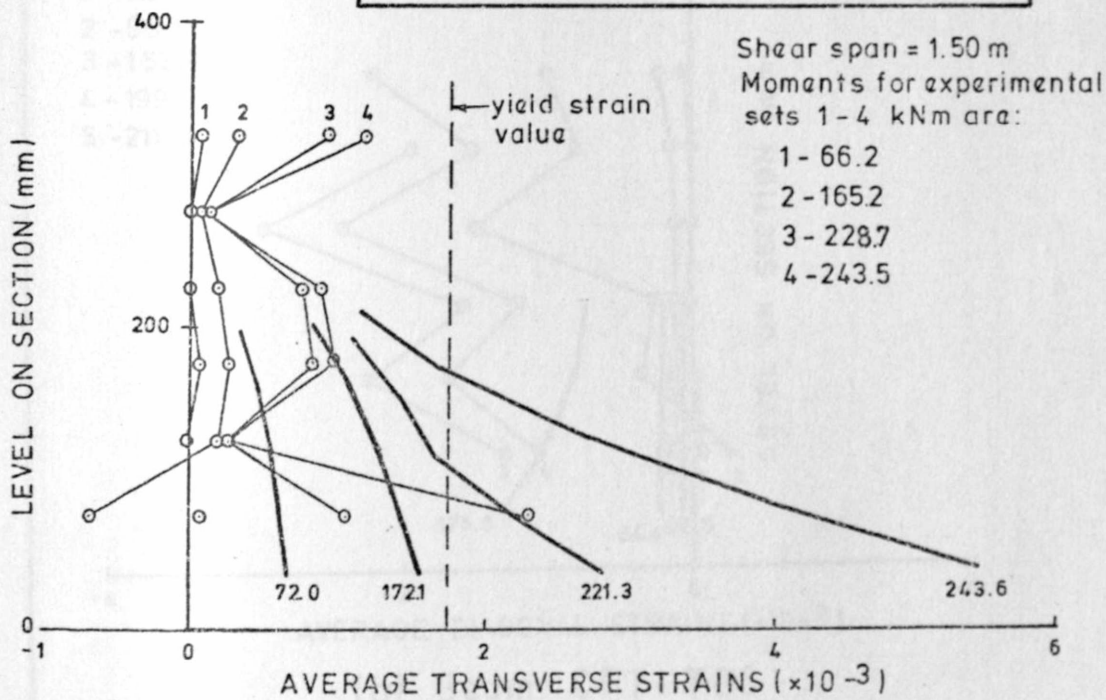


(c) Beam CFT-TB8

LEGEND

- Experimental points
- Theoretical prediction
- Figures against theoretical prediction indicate moment value in kNm

TB8(2)

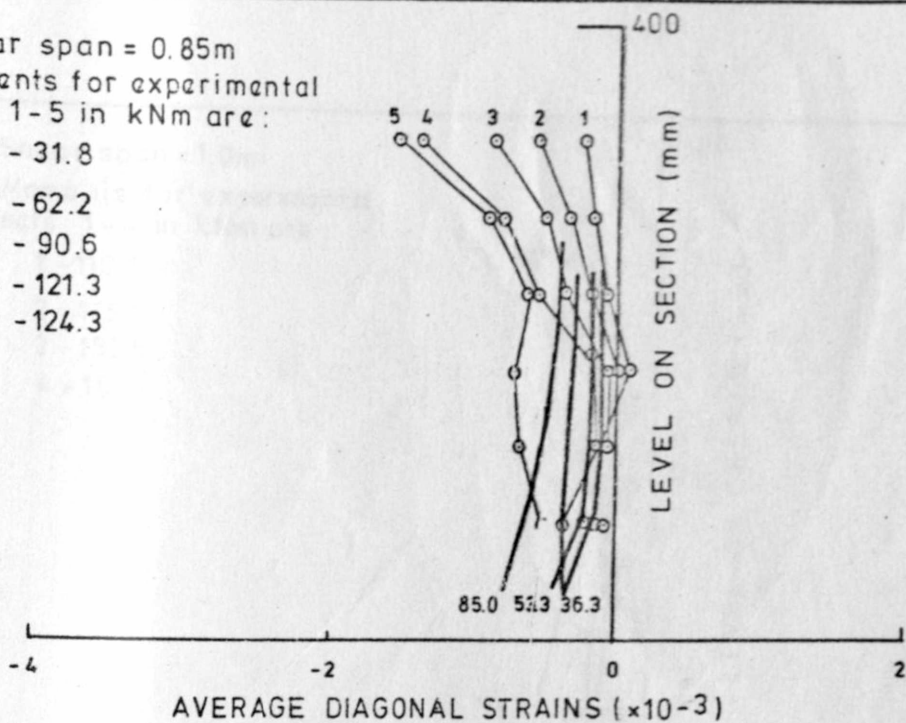


(d) Beam CFT-TB8

Fig. C.3 : Transverse strain profiles

Shear span = 0.85m
 Moments for experimental sets 1-5 in kNm are:

- 1 - 31.8
- 2 - 62.2
- 3 - 90.6
- 4 - 121.3
- 5 - 124.3



(a) Beam CFT-TB4

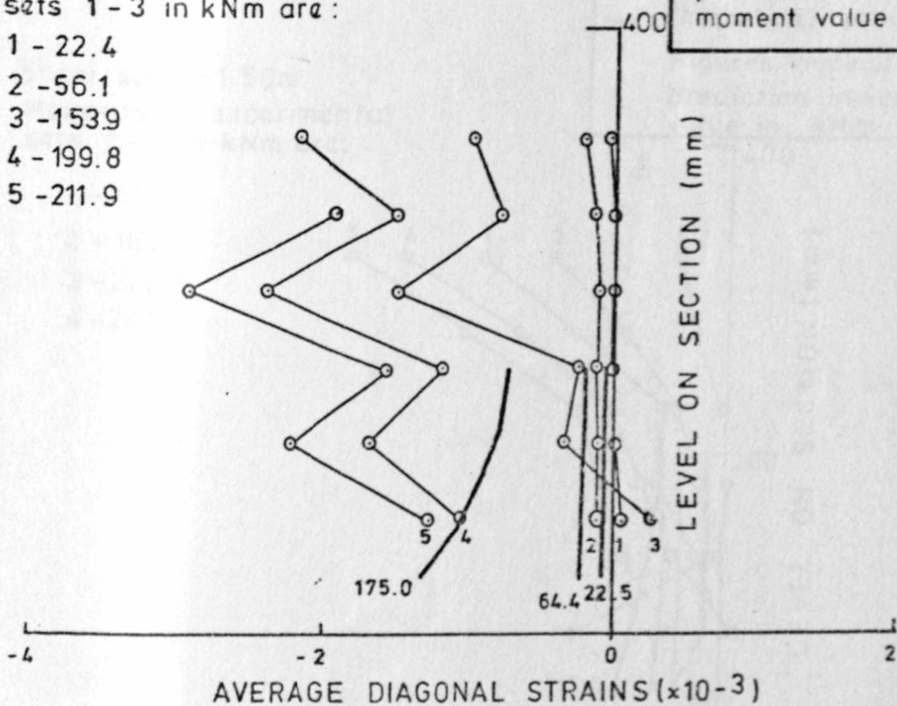
Shear span = 0.85m
 Moments for experimental sets 1-3 in kNm are:

- 1 - 22.4
- 2 - 56.1
- 3 - 153.9
- 4 - 199.8
- 5 - 211.9

LEGEND

- Experimental points
- Theoretical prediction

Figures against theoretical prediction indicate moment value in kNm

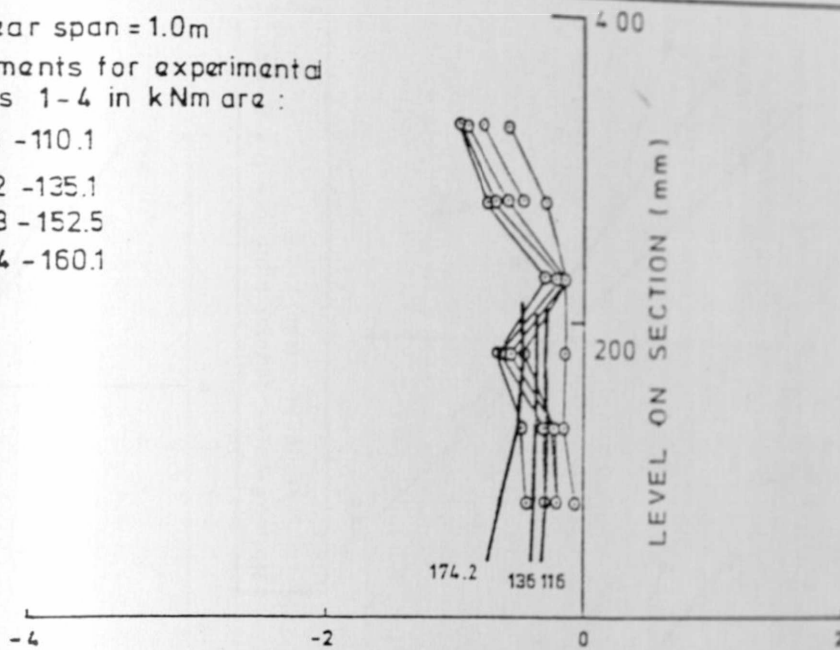


(b) Beam CFT-TB6

Fig. C.4: Principal compression strains profiles

Shear span = 1.0m
 Moments for experimental sets 1-4 in kNm are :

- 1 - 110.1
- 2 - 135.1
- 3 - 152.5
- 4 - 160.1



(a) AVERAGE DIAGONAL STRAINS ($\times 10^{-3}$)

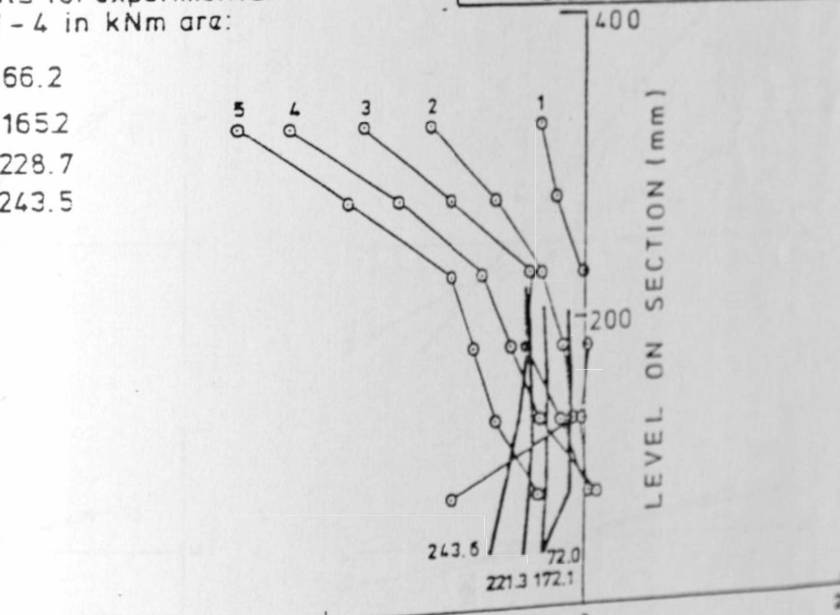
(c) Beam CFT-TB8

LEGEND

- Experimental points
- Theoretical predictions
- Figures against theoretical prediction indicate moment value in kNm

Shear span = 1.50m
 Moments for experimental sets 1-4 in kNm are :

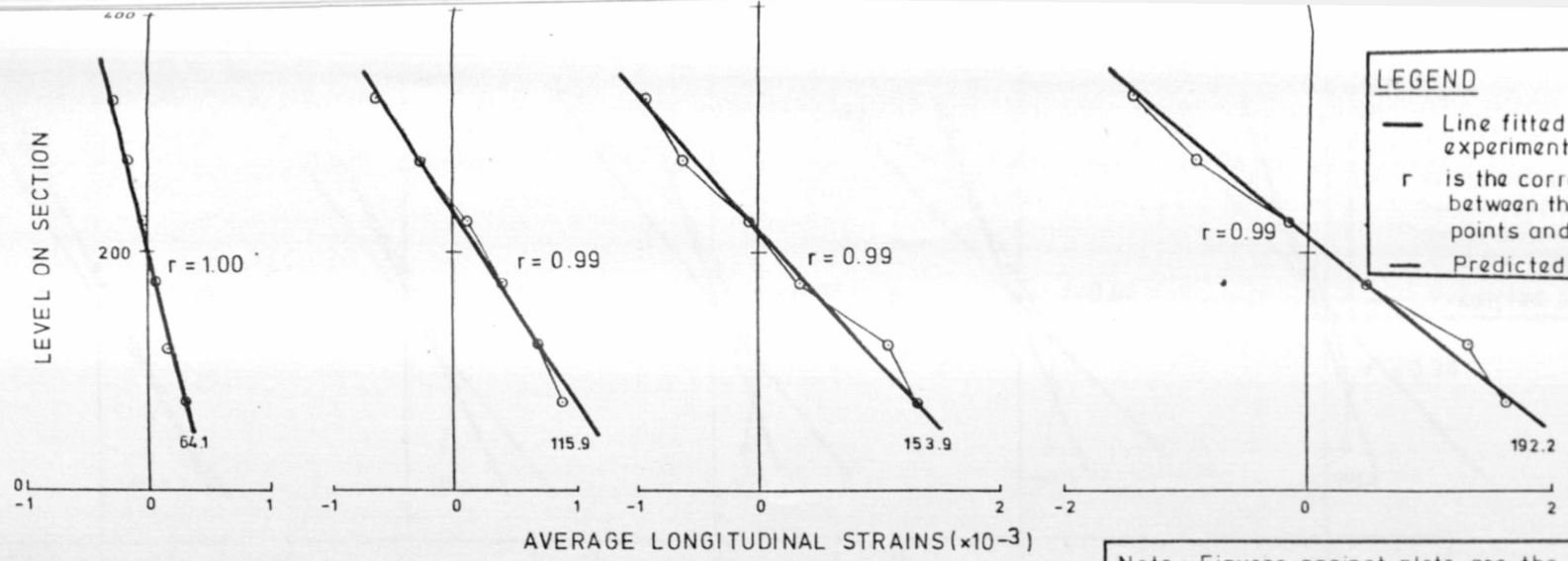
- 1 - 66.2
- 2 - 165.2
- 3 - 228.7
- 4 - 243.5



(b) AVERAGE DIAGONAL STRAINS ($\times 10^{-3}$)

(d) Beam CFT-TB8

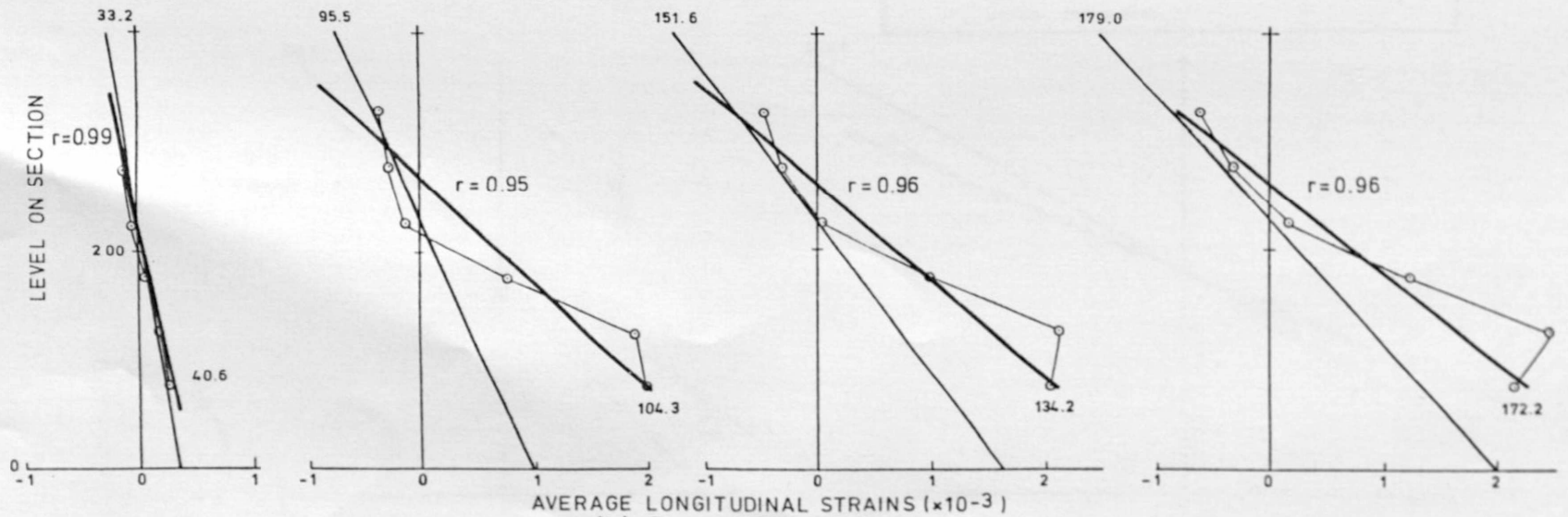
Figure C.4 : Principal Compression Strains Profiles



AVERAGE LONGITUDINAL STRAINS ($\times 10^{-3}$)

(a) Beam CFT-TB2

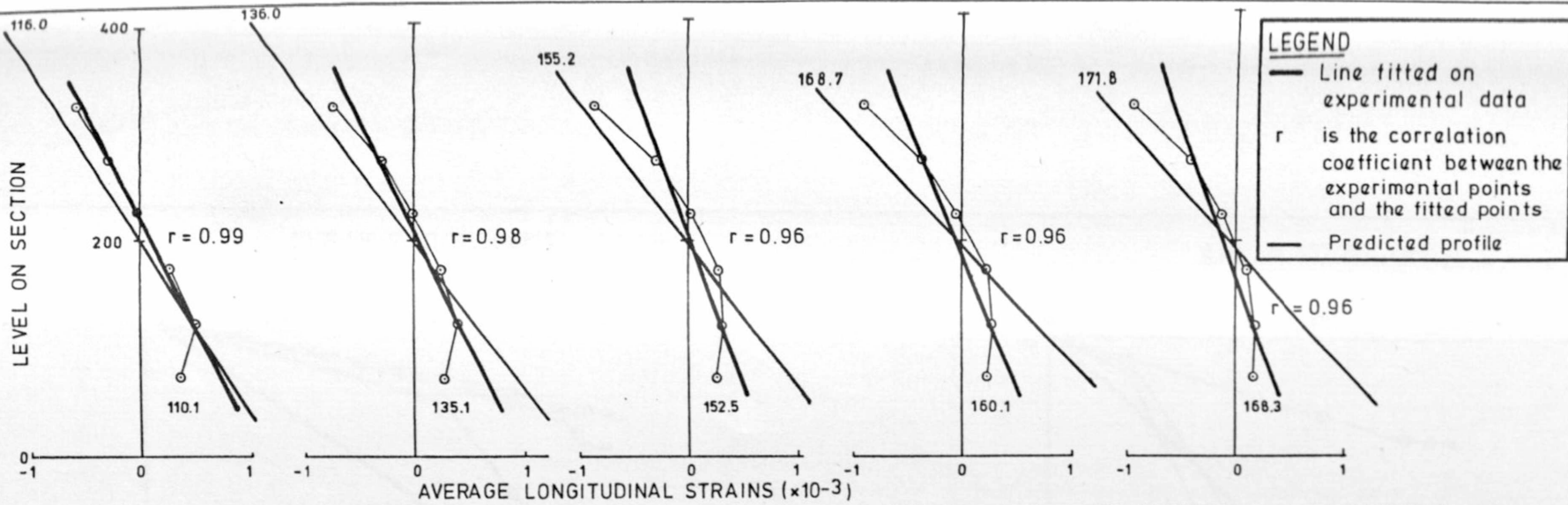
Note: Figures against plots are the moment value in kNm



AVERAGE LONGITUDINAL STRAINS ($\times 10^{-3}$)

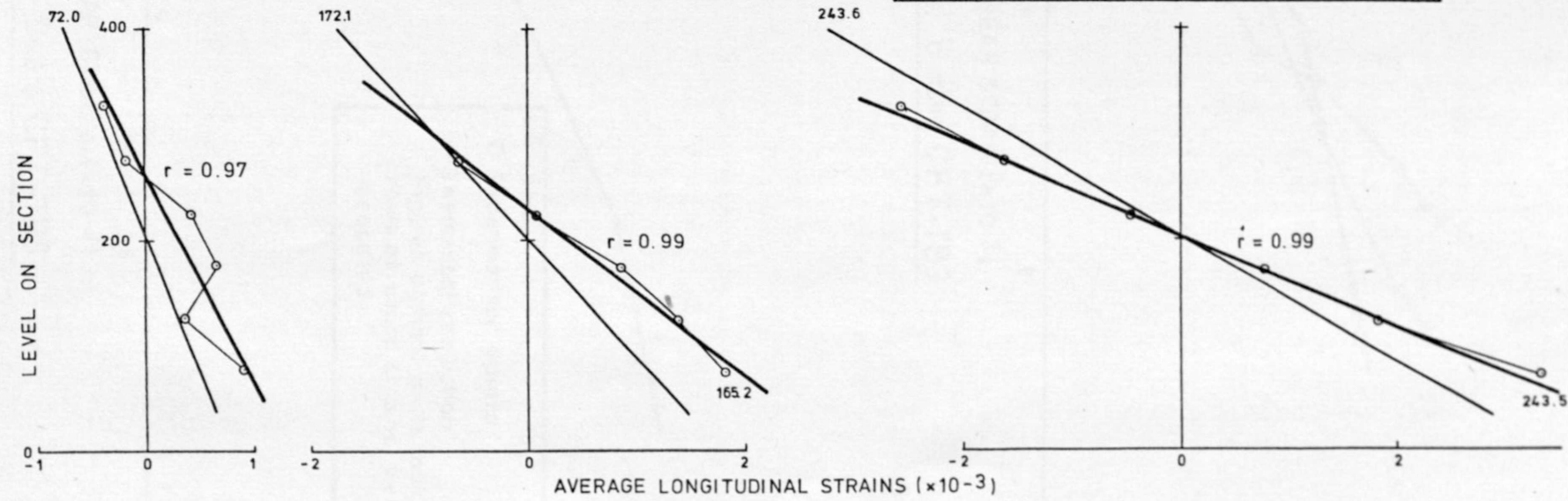
(b) Beam CFT-TB3

Figure C.5: Longitudinal strains profiles



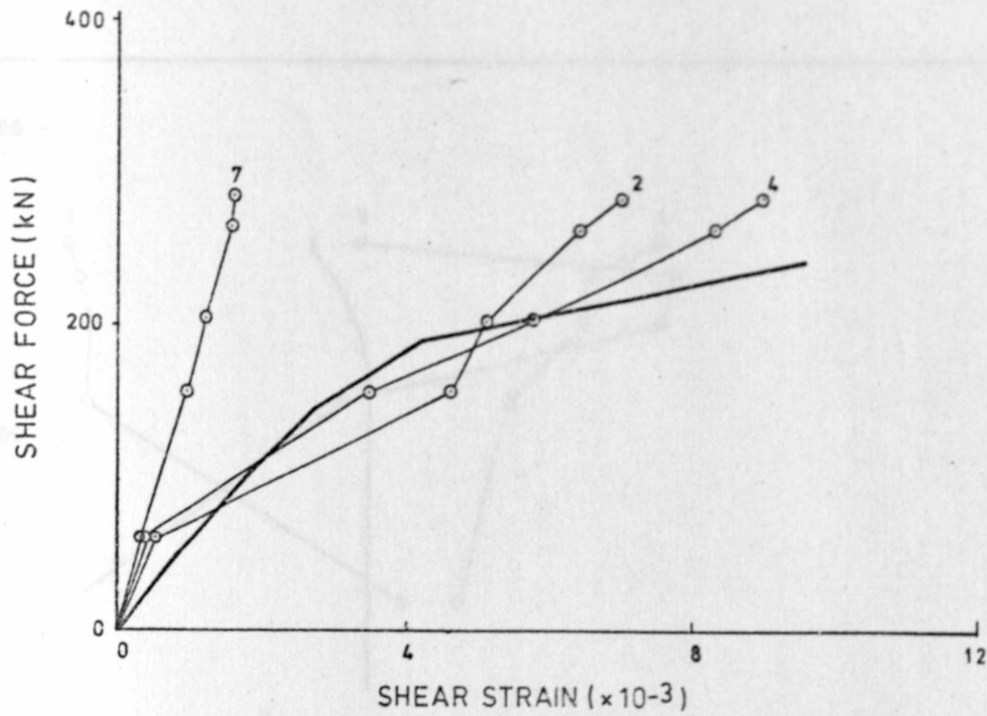
(c) Beam CFT-TB8

Note Figures against plots are the moment value in kNm

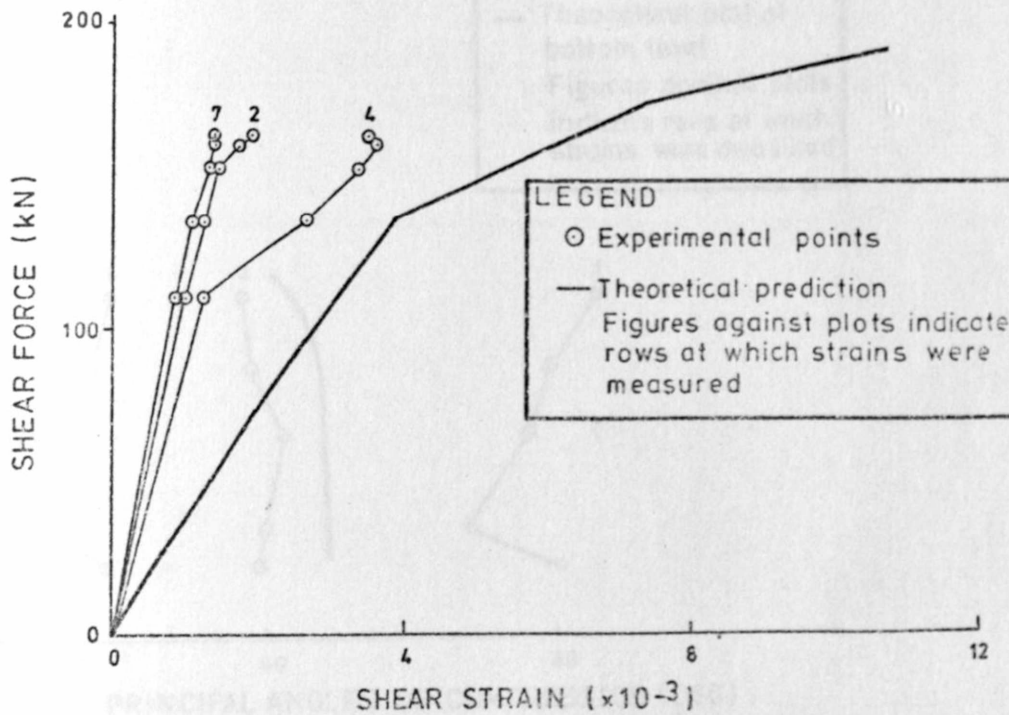


(d) Beam CFT-TB8

Figure C.5: Longitudinal strains profiles

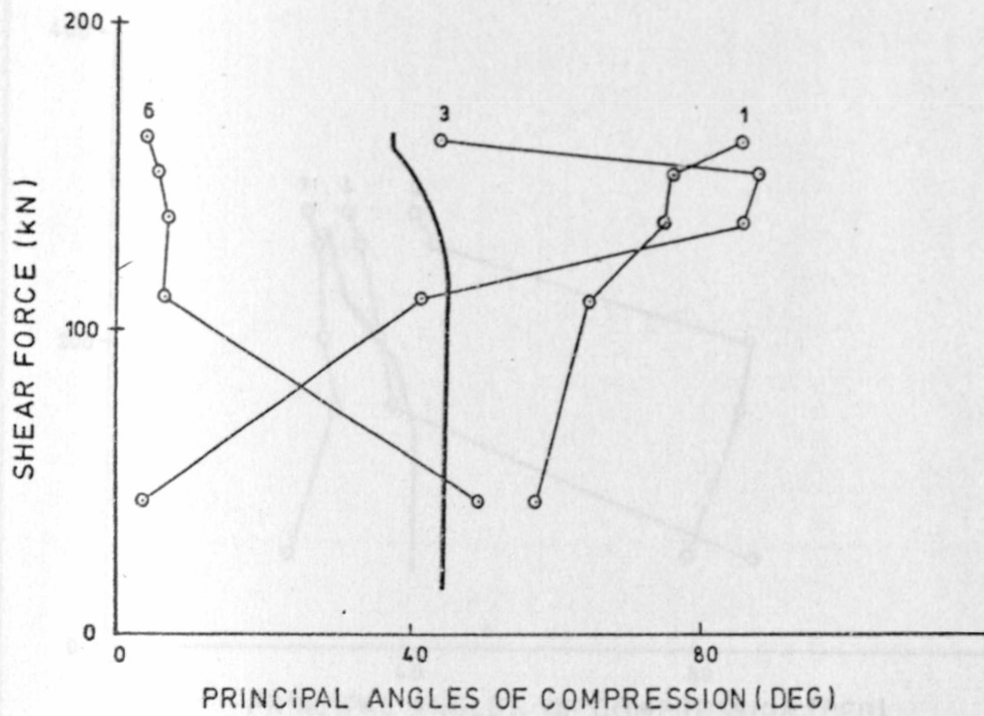


(a) Beam CFT-TB3



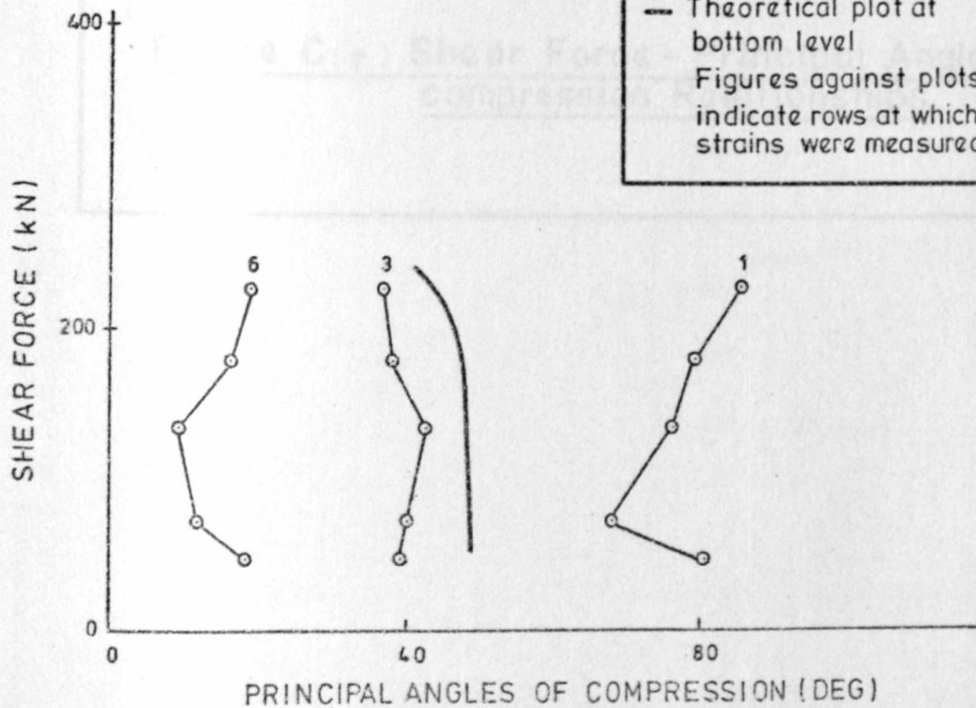
(b) Beam CFT-TB8

Figure C.6: Variation of Shear strain



(a) Beam CFT-TB8

LEGEND
○ Experimental points
— Theoretical plot at bottom level
Figures against plots indicate rows at which strains were measured



(b) Beam CFT-TB7

Figure C. 7: Shear Force - Principal Angles of compression Relationships

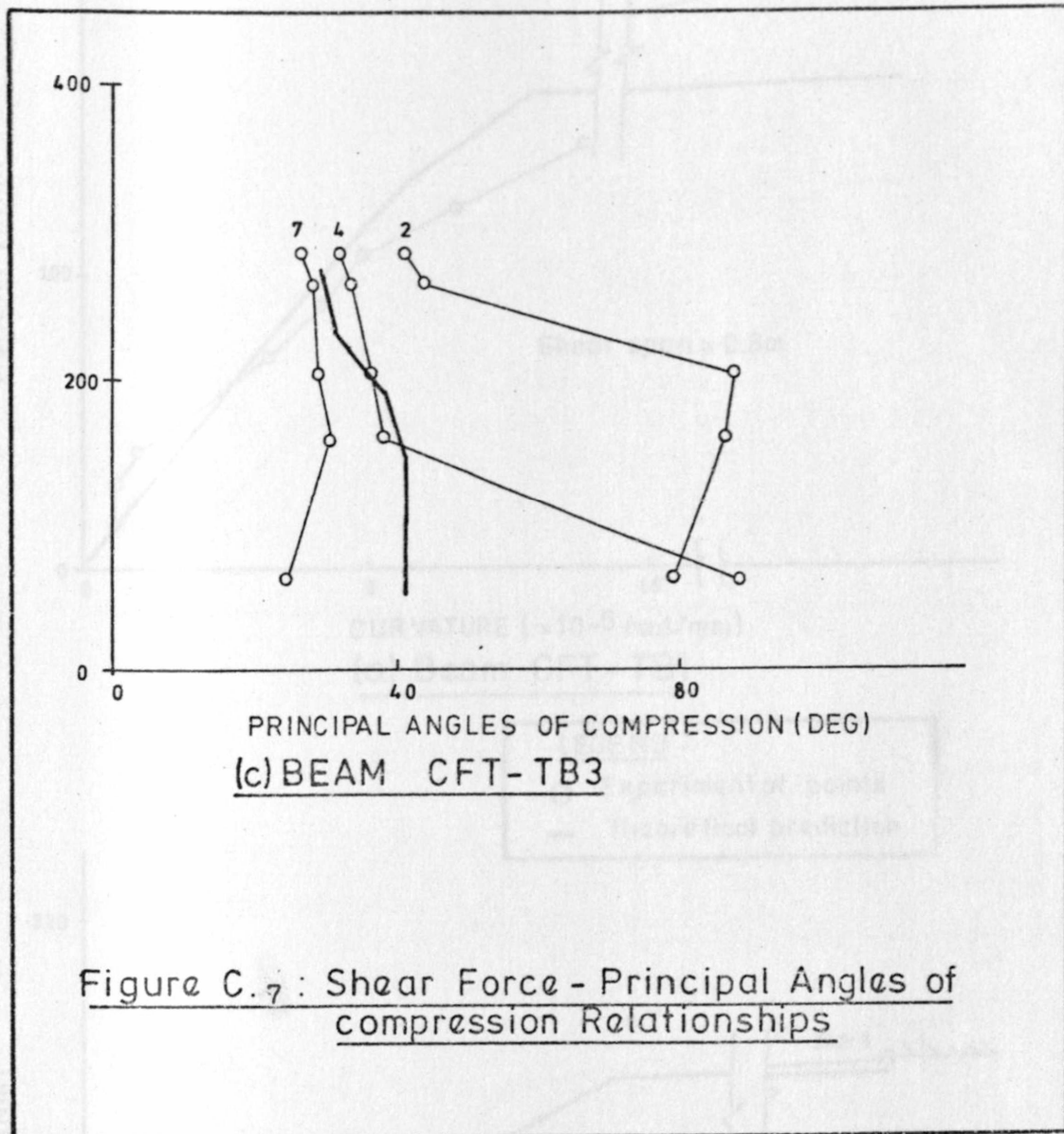
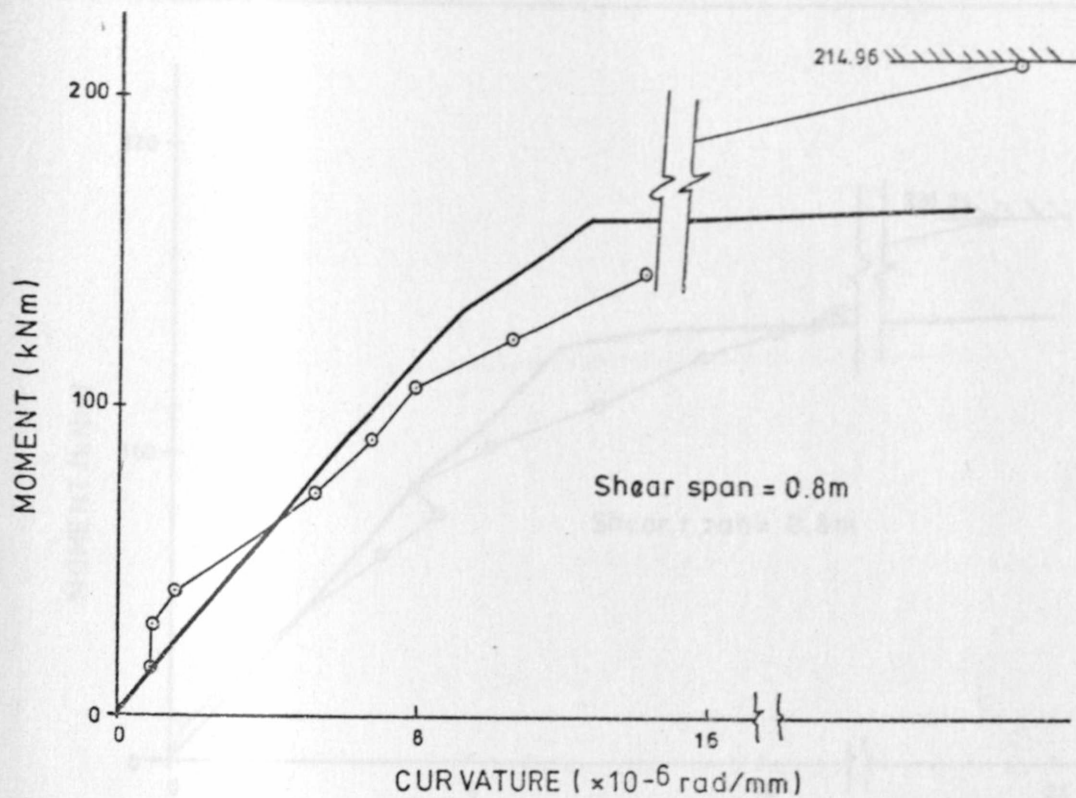


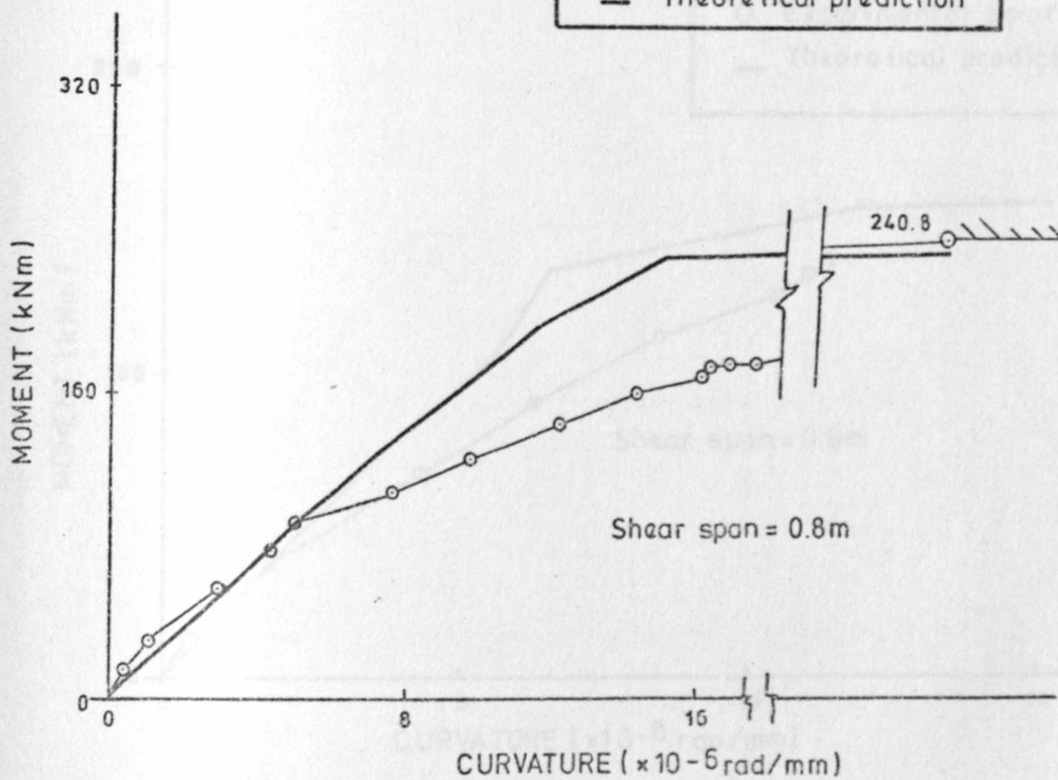
Figure C.7 : Shear Force - Principal Angles of compression Relationships



(a) Beam CFT-TB1

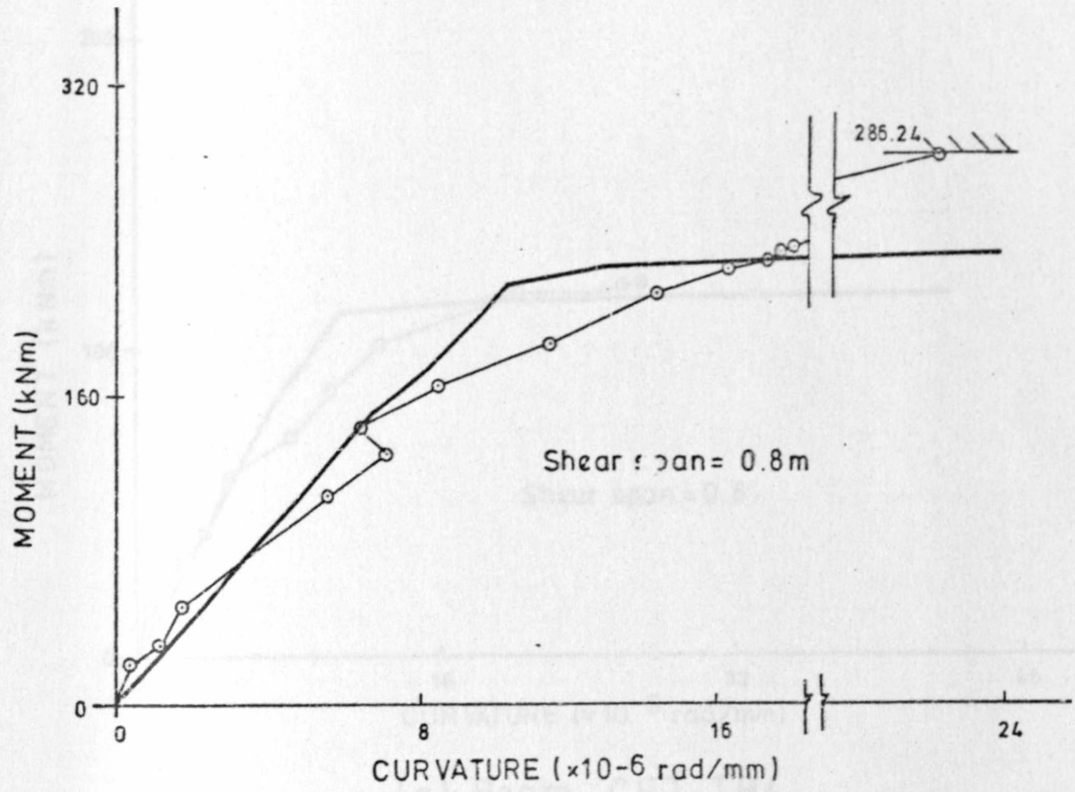
LEGEND

- Experimental points
- Theoretical prediction

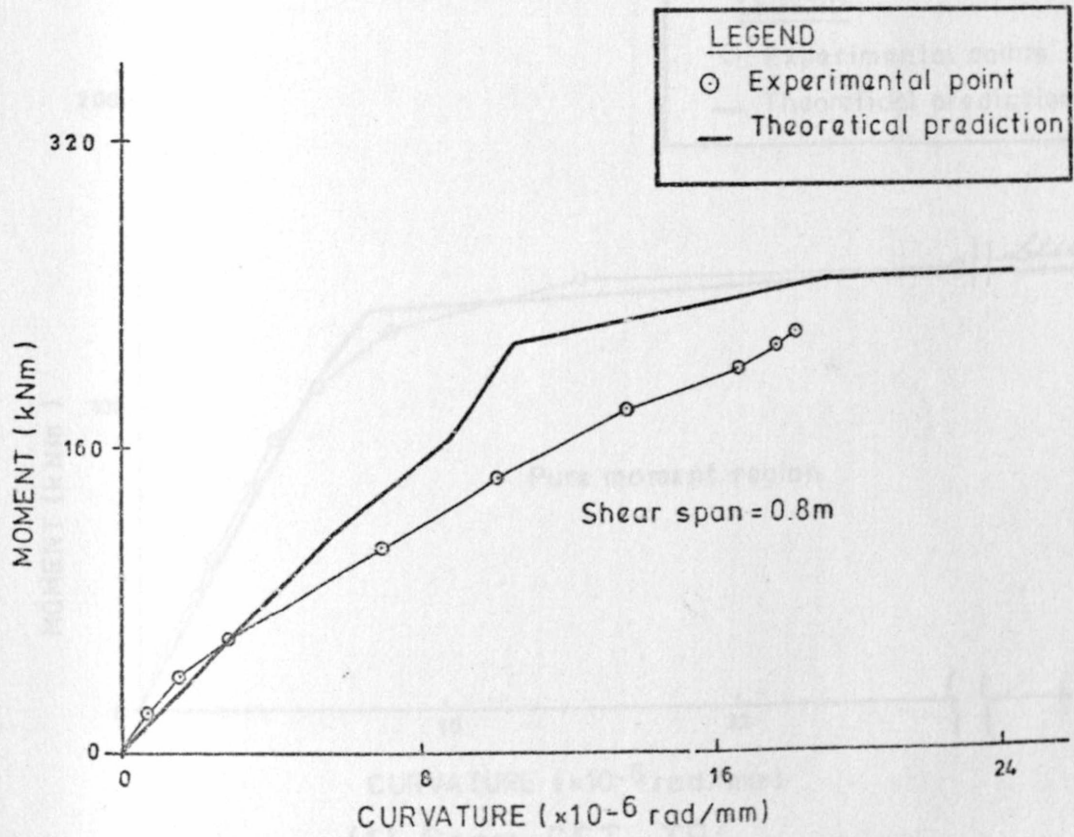


(b) Beam CFT-TB2

Figure C₈ : Moment - Curvature Relationships

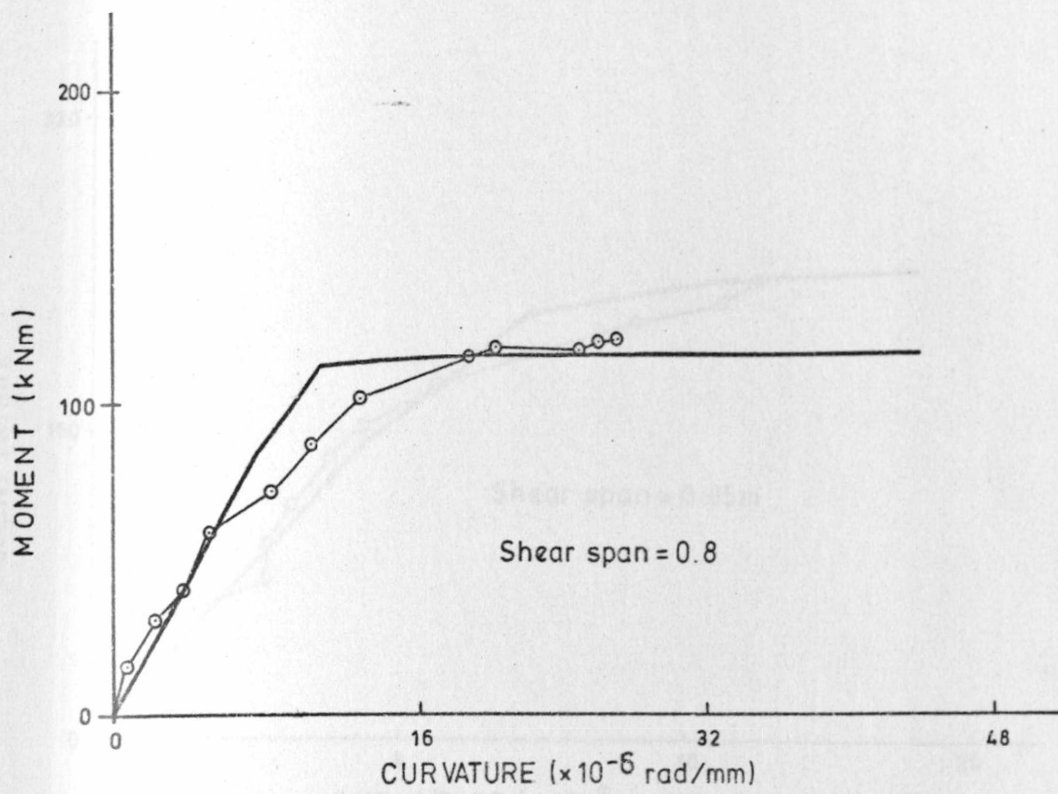


(c) Beam CFT-TB3

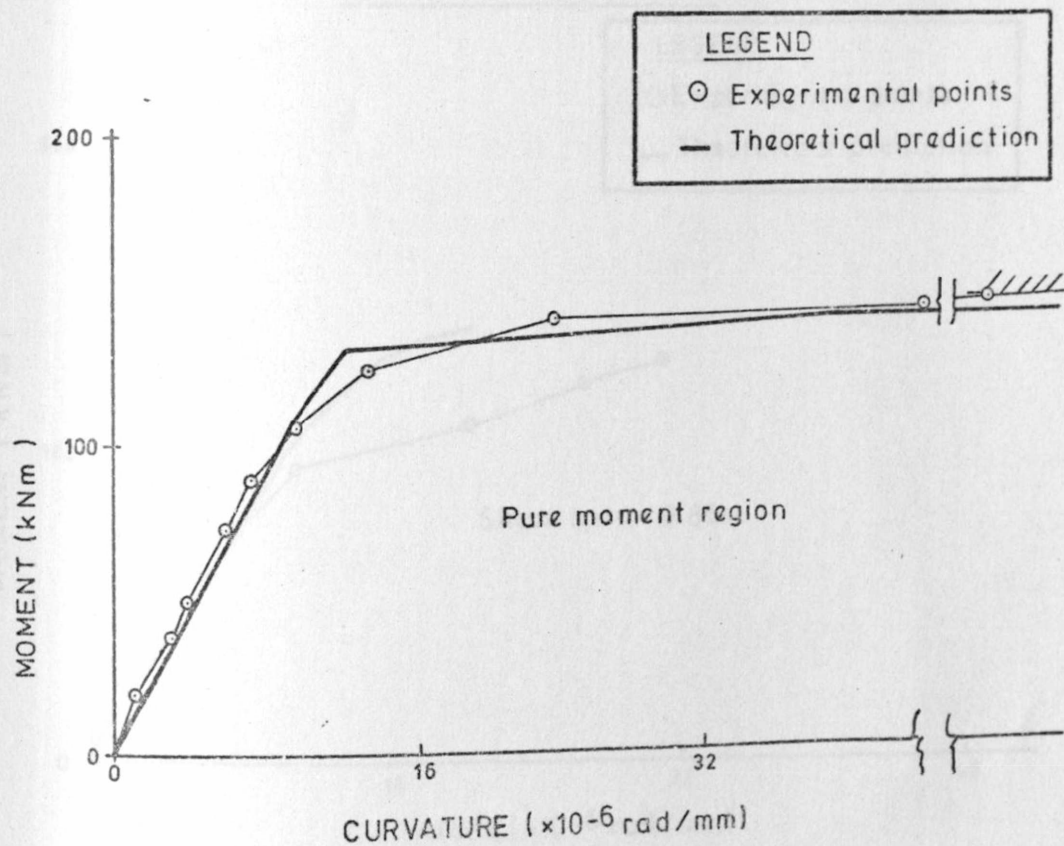


(d) Beam CFT-TB7

Figure C.8 : Moment - Curvature Relationships

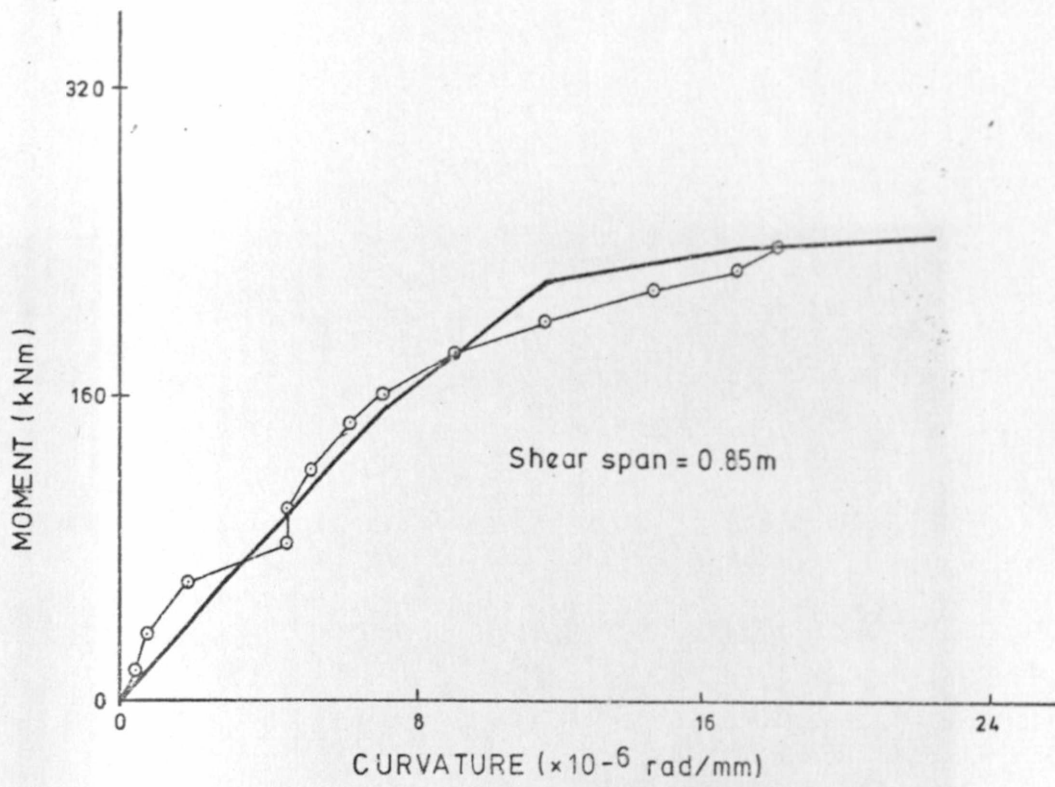


(e) Beam CFT-TB4



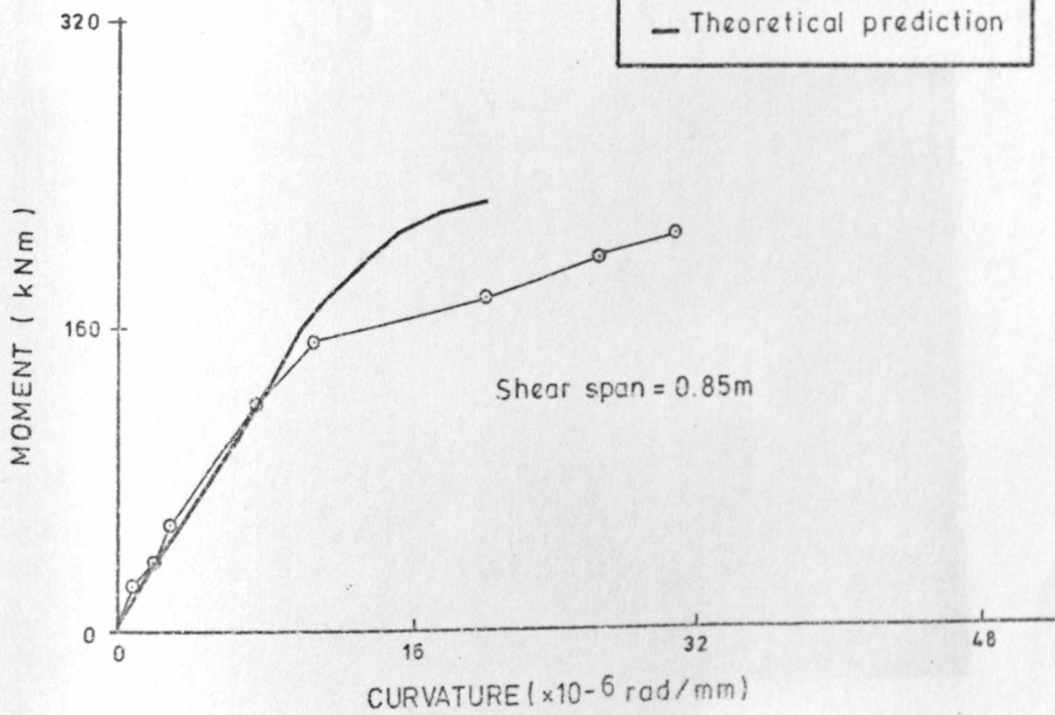
(f) Beam CFT-TB4

Figure C.8 : Moment-Curvature Relationships



(g) Beam CFT-TB5

LEGEND
○ Experimental points
— Theoretical prediction



(h) Beam CFT-TB6

Figure C.8: Moment - Curvature Relationships

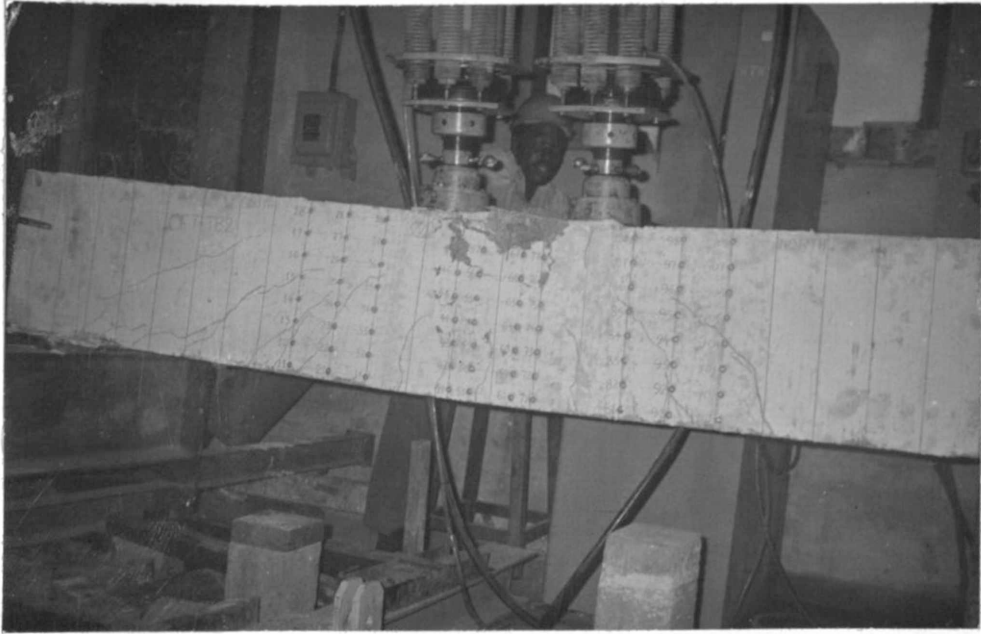


Plate C.1: Failure , Beam CFT-TB2

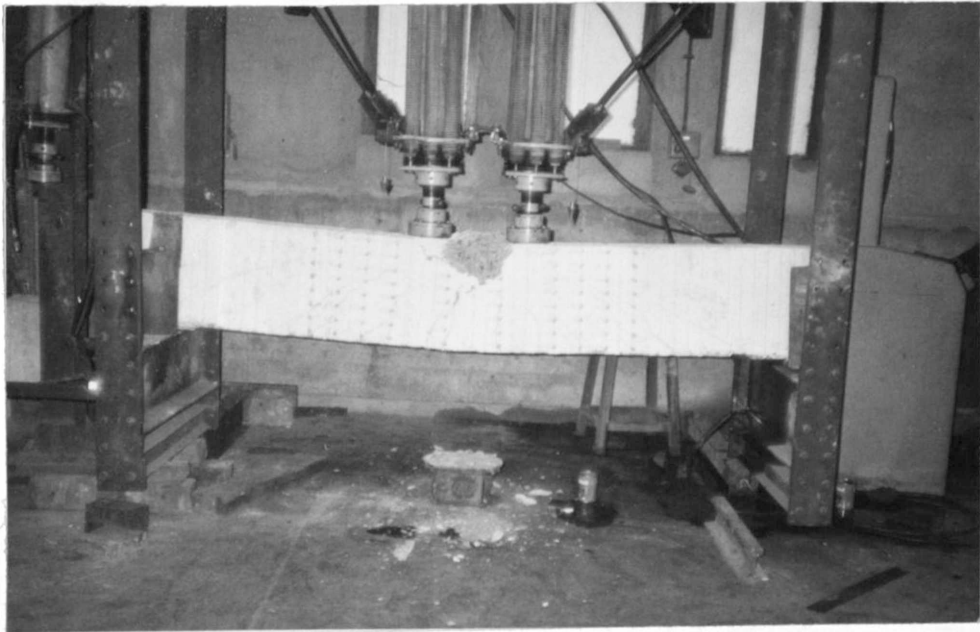


Plate C.2: Failure , Beam CFT-TB3

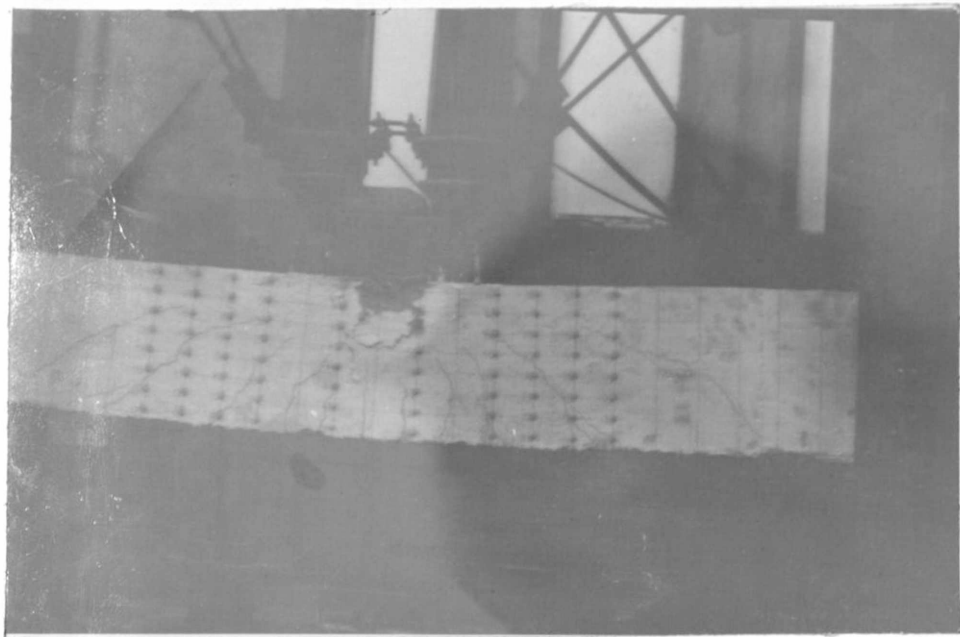


Plate C.3 : Failure , Beam CFT-TB7



Plate C.4 : Failure , Beam CFT-TB 8

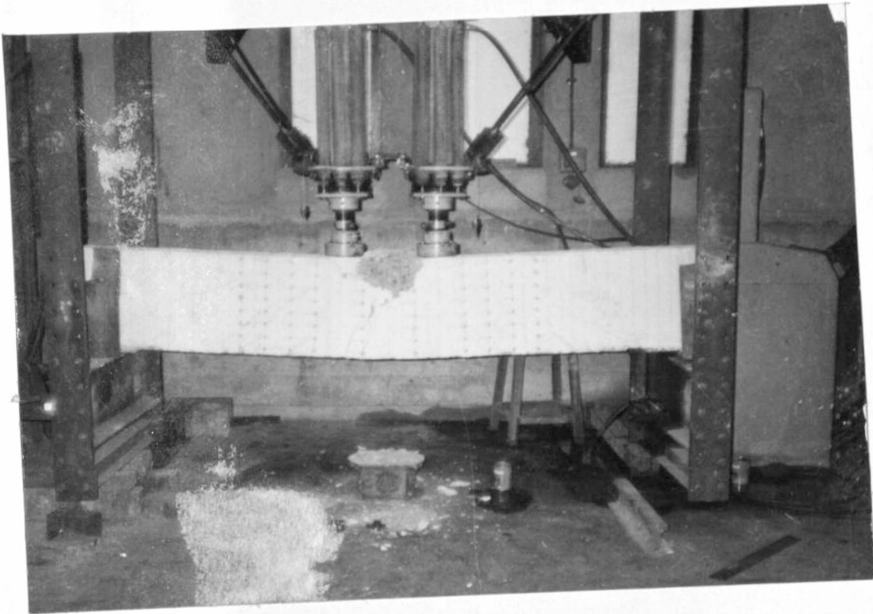


Plate C.5: Failure, Beam CFTTB5

APPENDIX D

EVALUATION OF SHEAR FLOW AT COMPRESSION STEEL LEVEL

D.1 Shear Flow Distribution for Sections with High Top Longitudinal Steel Content

As was pointed out in Chapter 3, the suggested shear flow distribution for the development of the theory applies only to cases with nominal longitudinal steel content in the compression zone. A high top longitudinal steel content will significantly affect the shear flow distribution. The shear flow value at the top steel level may be calculated in such cases by consideration of Figure D.1.

The compression force, C_t , on the element shown in Figure D.1(c) is balanced by the resultant, $T - C_{AB}$ of the compression force on the rest of the section and the tension force in the bottom steel. The distance of the point of action, $j_T d_1$, from the extreme compression fibre is given by:-

$$(T - C_{AB}) j_T d_1 + C_{AB} j_C d_1 - T d_1 = 0$$

$$j_T d_1 = \frac{T d_1 - C_{AB} j_C d_1}{T - C_{AB}} \dots \dots \dots (D.1)$$

The symbols are as defined on Figure D.1

The elemental moment on the section due to the force C_t is given by:-

$$M_t = C_t j_T d_1 \dots \dots \dots (D.2)$$

Differentiating,

$$\frac{\partial M_t}{\partial x} = \frac{\partial C_t}{\partial x} j_T d_1 + C_t d_1 \frac{\partial j_T}{\partial x} \dots (D.3)$$

But $\frac{\partial C_t}{\partial x} = q_t$ and $\frac{\partial M_t}{\partial x} = V_t$, the shear due to change in moment on the free body diagram of Figure D.1(c).

Hence using equation (D.3)

$$V_t = q_t j_T d_1 + C_t d_1 \frac{\partial j_T}{\partial x}$$

Assuming $C_t d_1 \frac{\partial j_T}{\partial x}$ is negligible,

$$q_t = \frac{V_t}{j_T d_1} \dots (D.4)$$

Now, the shear force, V, is proportional to the moment, M.

$$V = \frac{M}{a} \dots (D.5)$$

The compression force, C_t , on element is due to steel and the concrete over depth d_2 .

Denote contribution from steel C'_s and concrete C_{ct} . Then

$$C_t = C'_s + C_{ct}$$

$$C'_s = A'_l f'_l \text{ or } A'_l f'_l y \text{ for post yield range}$$

$$C_{ct} = \alpha \beta f'_c b d_2$$

For steel in elastic range

$$M_t = \alpha\beta f'_c b d_2 \left(j_T d_1 - \frac{d_2}{2} \right) + A'_l f'_l (j_T d_1 - d_2)$$

and from equation (D.5)

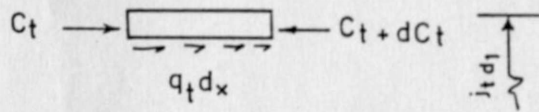
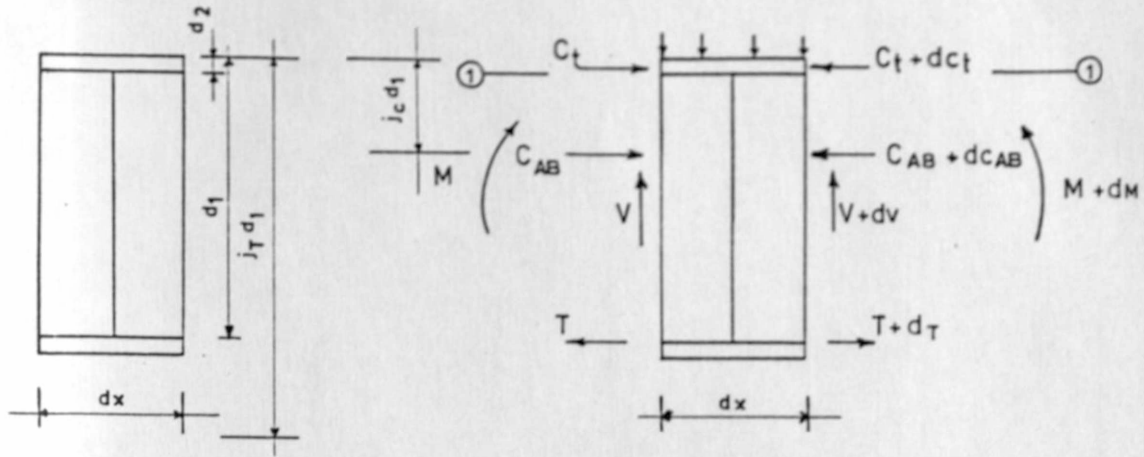
$$V_t = \frac{\alpha\beta f'_c b d_2 \left(j_T d_1 - \frac{d_2}{2} \right) + A'_l f'_l (j_T d_1 - d_2)}{a}$$

From equation (D.4)

$$q_t = \frac{\alpha\beta f'_c b d_2 (2j_T d_1 - d_2) + 2A'_l f'_l (j_T d_1 - d_2) \dots}{2aj_T d_1} \quad (D.6)$$

Hence q_t can be calculated, j_T being obtained from equation (D.1).

The bottom shear flow can now be determined in the manner illustrated in Figure 3.4 (d) and then proceeding as in section (3.2), the shear flow at the neutral axis is calculated by consideration of shear equilibrium leading to four ordinates between which linear variation is assumed. This is illustrated in Figure D.2.



(c) Determination of Shear Flow at ①-①

C_t = Compression Force over depth d_2

C_{AB} = Total compression Force on section less C_t

Figure D.1: Determination of Shear Flow

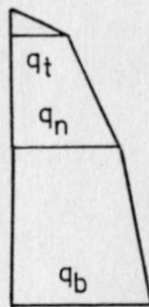


Figure D.2: Shear Flow Distribution